THE NEUROTOXIC EFFECTS OF ENZYME INHIBITORS AT THE NEUROMUSCULAR JUNCTION.

by

ANNA LAURA ROWBOTHAM

A thesis submitted for the
degree of
Doctor of Philosophy

THE UNIVERSITY OF ASTON IN BIRMINGHAM

September 1996

THE UNIVERSITY OF ASTON IN BIRMINGHAM

THE NEUROTOXIC EFFECTS OF ENZYME INHIBITORS AT THE NEUROMUSCULAR JUNCTION.

by

ANNA LAURA ROWBOTHAM

DOCTOR OF PHILOSOPHY - 1996

Summary

Current knowledge of the long-term, low dose effects of carbamate (CB) anti-cholinesterases on skeletal muscle or on the metabolism and regulation of the molecular forms of acetylcholinesterase (AChE) is limited. This is largely due to the reversible nature of these inhibitors and the subtle effects they induce which has generally made their study difficult and preliminary investigations were conducted to determine suitable study methods. A sequential extraction technique was used to rapidly analyse AChE molecular form activity at the mouse neuromuscular junction and also in peripheral parts of muscle fibres. AChE in the synaptic cleft involved in the termination of cholinergic transmission was successfully assessed by the assay method and by an alternative method using a correlation equation which represented the relationship between synaptic AChE and the prolongation of extra-cellular miniature endplate potentials. It was found that inhibition after *in vivo* CB dosing could not be maintained during tissue analysis because CB-inhibited enzyme complexes decarbamoylated very rapidly and could not be prevented even when maintained on ice. The methods employed did not therefore give a measure of inhibition but presented a profile of metabolic responses to continual, low dose CB treatment.

Repetitive and continual infusion with low doses of the CBs: pyridostigmine and physostigmine induced a variety of effects on mouse skeletal muscle. Both compounds induced a mild myopathy in the mouse diaphragm during continual infusion which was characterised by endplate deformation without necrosis; such deformation persisted on termination of treatment but had recovered slightly 14 days later. Endplate and non-endplate AChE molecular forms displayed selective responses to CB treatment. During treatment endplate AChE was reduced whereas non-endplate AChE was largely unaffected, and after treatment, endplate AChE recovered, whereas non-endplate AChE was up-regulated. The mechanisms by which these responses become manifest are unclear but may be due to CB-induced effects on nerve-mediated muscle activity, neurotrophic factors or morphological and physiological changes which arise at the neuromuscular junction. It was concluded that, as well as inhibiting AChE, CBs also influence the metabolism and regulation of the enzyme and induce persistent endplate deformation; possible detrimental effects of long-term, low-dose determination requires further investigation.

Keywords: Acetylcholinesterase, carbamates, skeletal muscle, myopathy, endplate.

ACKNOWLEDGEMENTS.

I would like to express my sincere thanks to Professor C. B. Ferry for his continual guidance and supervision and for the valuable advice, encouragement and inspiration he has contributed to the development of this work and to A. Crofts for her effort and assistance in our collaboration on this research project and overall contribution to its success.

This work has been carried out with the support of and was funded by Chemical and Biological Defence, Porton Down, U.K. I would like to thank our collaborators Dr. M. E. Smith and colleagues at Birmingham Medical School and Dr. D. Green and colleagues at CBD, Porton Down for many useful and critical discussions regarding the research.

I would also like to thank the academic and technical staff in the Department of Pharmaceutical and Biological Sciences for providing the facilities and equipment needed to undertake the experiments, to M. Gamble for his practical assistance and to colleagues in Lab. 442 for creating a friendly working environment.

Last, but not least, I wish to express my deepest gratitude to my family for their love and encouragement and a very special thanks to my husband, Mark, for his assistance and continuous support in the creation of this thesis.

CONTENTS.

LIST OF TABLES.

LIST OF FIGURES.

LIST OF FIGURES.

ABBREVIATIONS.

A	Readily-extractable asymmetric AChE
ACh	Acetylcholine
AChE	Acetylcholinesterase
AChE(eel)	Electric eel acetylcholinesterase
anti-ChE	Anti-cholinesterase
CB	Carbamate anti-cholinesterase
ChE	Cholinesterase
ECO	Ecothiopate
EPS	Endplate-specific
G	Globular AChE
H5	Homogenate 5 (5th sequential extraction fraction)
J	Junctional region
K-S	Kruskal-Wallis tests described by Seigel (1988)
L	Length (endplate)
MDFE	$(MEPP)_O$-derived functional AChE
$(MEPP)_O$	Extra-cellular miniature endplate potential
NE	Non-readily extractable asymmetric AChE
NF	Non-functional
NJ	Non-junctional
OP	Organophosphorous anti-cholinesterase
PHY	Physostigmine
PYR	Pyridostigmine
RER	Rough endoplasmic reticulum
S1	Supernatant 1 (1st sequential extraction fraction)
S2	Supernatant 2 (2nd sequential extraction fraction)
S3	Supernatant 3 (3rd sequential extraction fraction)
S4	Supernatant 4 (4th sequential extraction fraction)
$T_{50\%}$	Time to half amplitude of $(MEPP)_O$ decay phase
W	Width (endplate)
W/L	Width/length ratio

CHAPTER 1

INTRODUCTION

1.1 The biogenesis and regulation of acetylcholinesterase.

1.1.1 Background to AChE and its action.

1.1.1.1 The role of AChE in cholinergic transmission.

Cholinesterases have been a major topic of interest for many years because of their involvement in neuromuscular and other types of cholinergic transmission. They exist as a complex family of proteins differing in structure, properties and location and have a complex mode of regulation. A choline ester hydrolysing enzyme was first described by Dale in 1914 but was not linked to neuromuscular transmission. In the 1920s, Otto Loewi identified acetylcholine (ACh) as a neurotransmitter and when in 1938 Marney and Nachmansohn found that acetylcholinesterase (AChE) was present in high concentrations at points of nerve-muscle contact, it became apparent that this enzyme had a role in neuromuscular transmission. It is now known that AChE (acetylcholine acetylhydrolase: E.C. 3.1.1.7) rapidly hydrolyses ACh within 1 millisecond of its release from cholinergic synapses (Massoulie et al., 1993) and is located in the junctional cleft in association with the external surfaces of both pre- and post-synaptic membranes and basement membrane material (Koelle, 1963; Koelle et al., 1967; Salpeter, 1967, 1969; Csillik and Knyihar, 1968; Bowden and Duchen, 1976; Hobbiger, 1976). The enzyme was not found to be a structural component of endplate membranes, but merely coats them (Hall and Kelly, 1971). Quantitative investigations of the numbers and density of ACh receptors (Fambrough and Hartzell, 1972; Fertuck and Salpeter, 1976) and AChE (Salpeter, 1967; Rogers et al., 1969; Salpeter et al., 1978) using isotopically labelled ligands and light and electron microscope autoradiography have provided a detailed 'molecular map' of the neuromuscular junction.

1.1.1.2 Detection of AChE

In addition to AChE, pseudocholinesterases (ChE) are present in mammalian skeletal muscle (Vigny et al., 1978) which exist as low-salt soluble and insoluble molecules and share some properties with AChE. There are many methods available for detecting AChE and ChE in tissues. Common assays for AChE and ChE are the colorimetric method of Ellman et al., (1961) and the radiometric method of Johnson and Russell (1975). The latter is more sensitive but uses expensive radioactive isotopes. ChE can be located histochemically in tissue

sections or intact cells at the light and electron microscope level by adaptations of the staining techniques of Koelle and Freindenwald (1949) and Karnovsky and Roots (1964) and can also be located by autoradiographic techniques. Electron microscopic localisation revealed that AChE was located in the muscle sarcoplasm of rat diaphragms, closely related to the post-synaptic membrane and ChE was observed in the primary and secondary synaptic clefts between the axon and the teloglial cells (Teravainen, 1967). The irreversible inhibitor diisopropylfluorophosphate (DFP) was used by Salpeter (1967) to quantify the number and distribution of AChE molecules at an ultrastructural level and demonstrated that there were 0.9-1.2x10^7 molecules of AChE per rat diaphragm endplate (Rogers et al., 1969). More modern methods of locating AChE involve the use of a fluorescein-labelled antibody to AChE (Tsuji et al., 1973). AChE and ChE inhibitors have been extensively used to study the synthesis, assembly and processing of these enzymes in cells. Certain inhibitors such as BW 284c51 and iso-OMPA selectively inhibit AChE and ChE respectively whereas other less selective inhibitors such as DFP which can penetrate cell plasma membranes and ecothiopate which cannot, when used alone or in combination have enabled the study of the metabolic behaviour of intra- and extra-cellular pools of AChE (McIssac and Koelle, 1959; Rotundo, 1983).

1.1.1.3 Action of AChE.

The primary function of AChE is the termination of cholinergic transmission by the hydrolysis of ACh although the enzyme may have many other important roles. AChE is a serine protease which reacts with its substrate at a close to diffusion-controlled rate (Bazelyansky et al., 1986). Each molecule of AChE has binding and hydrolytic sites for ACh (Wright and Plummer, 1973). The number of active sites per motor endplate was determined by the use of radiolabelled DFP (Waser and Reller, 1965; Barnard, Rimazewska et al., 1971; Barnard, Wieckowski et al., 1971) and was found to be in the range 2x10^7 and 5x10^7 which corresponded to the number of ACh receptors. It was estimated that each active enzyme site could hydrolyse 1.6x10^5 to 8.3x10^5 molecules of ACh in one minute (Berry, 1951; Cohen et al., 1955; Wilson and Harrison, 1961). It took 80-100 μsecs to hydrolyse one molecule of ACh (Lawler, 1961; Wilson and Harrison, 1961) and Hobbiger in 1976 showed that there were at least ten ACh receptors and ten AChE active sites available for each molecule of ACh released by a nerve impulse. High concentrations of ACh were found to inhibit AChE activity and the graph relating the rate of ACh hydrolysis to concentration of substrate is bell-

shaped. Hobbiger in 1976 indicated that the concentration of ACh in the synapse immediately after release by a nerve impulse is in a mM range which partially inhibits AChE activity but considered that there was sufficient enzyme activity to lower the concentration of ACh to inactive levels within one millisecond which is well within the refractory period for the muscle fibre (Wilson, 1971). This rapid enzymatic activity combined with the physical diffusion of ACh from the receptor region ensures that there is no accumulation of ACh from one nerve impulse to the next even during very high physiological frequencies of nerve impulse traffic.

The function of AChE is therefore not only to terminate the interaction of transmitter with post-junctional receptors but also to prevent or control the interaction of diffused ACh with receptors on nerve endings. The existence of these is not disputed but there is controversy regarding whether these have a physiological role distinct from a mere pharmacological role in nervous transmission.

There is a good understanding of the kinetics of AChE activity and the composition of its active sites which has been summarised by Main (1976). Each active site consists of two subsites: the anionic site which attracts and holds the positively charged cationic nitrogen-containing trimethylammonium head group of ACh via the negatively charged oxygen of a dissociated carboxylate group of a glutamyl residue and the esteratic site which catalyses the hydrolysis and contains the side groups of histidine, tyrosine and serine. The hydrolysis of ACh occurs in two stages: choline is first cleaved off leaving an acetylated esteratic site on the enzyme which then reacts with water to release acetate and regenerate active enzyme (see Figure 1.1).

In recent years, cDNA cloning and sequencing has revealed the primary structure of various types of AChE (MacPhee-Quigley et al., 1985) and the three-dimensional atomic structure of the molecule has now been solved (Sussman et al., 1991). Site directed mutagenesis has been used to determine which residues are functionally important. The active site of AChE is now known to contain the typical catalytic triad of serine hydrolases with histidine as the intermediary charge relay residue (Wilson and Bergmann, 1950). In 1990 Gibney et al., identified serine-200 and histidine-440 to be active site residues in *Torpedo californica*.. Histidine residues were found to be conserved in most species at positions 425 and 400. The third residue in the triad is thought to be glutamate-327 in Torpedo and glutamate-334 in humans (Shafferman et al., 1992) but other surrounding residues were highlighted as having an important role. Residues involved in the catalytic triad may vary between species. Hence, AChE-driven hydrolysis, like protease-driven

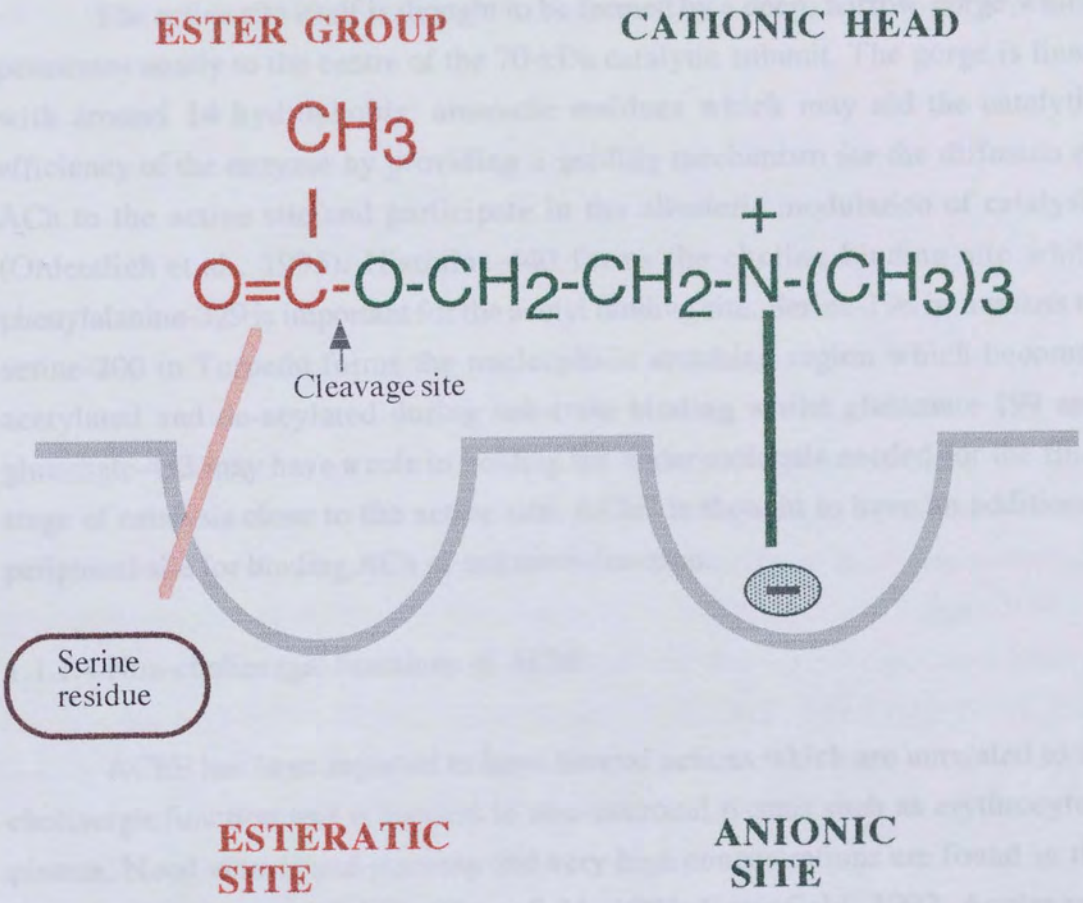

Figure 1.1: The active site of AChE. The esteratic site interacts with the acetyl head of acetylcholine and the choline tail interacts with the anionic site. ACh is then cleaved and choline is released. The acetylated enzyme then reacts with water to release acetic acid.

hydrolysis depends on a charge relay mechanism in which a carboxylic acid stabilises the tautomer of the imidazole necessary for proton transfer .

The active site itself is thought to be formed by a deep, narrow gorge which penetrates nearly to the centre of the 70-kDa catalytic subunit. The gorge is lined with around 14 hydrophobic, aromatic residues which may aid the catalytic efficiency of the enzyme by providing a guiding mechanism for the diffusion of ACh to the active site and participate in the allosteric modulation of catalysis (Ordentlich et al., 1995). Histidine-440 forms the choline binding site while phenylalanine-329 is important for the acetyl binding site. Serine-198 in humans or serine-200 in Torpedo forms the nucleophilic attacking region which becomes acetylated and de-acylated during substrate binding whilst glutamate-199 and glutamate-443 may have a role in holding the water molecule needed for the final stage of catalysis close to the active site. AChE is thought to have an additional peripheral site for binding ACh of unknown function.

1.1.1.4 Non-cholinergic functions of AChE.

AChE has been reported to have several actions which are unrelated to its cholinergic function and is located in non-neuronal tissues such as erythrocytes, plasma, blood vessels and placenta and very high concentrations are found in the brain in the absence of ACh (Greenfield, 1984; Greenfield, 1992; Appleyard, 1992).

Non-cholinergic roles are generally unclear but may include roles in neural development (Wolfgang and Forte, 1989; Massoulie et al., 1993) and neuromodulatory functions (Greenfield, 1984; Greenfield, 1992; Appleyard, 1992). AChE may also be a zymogen of neuropeptide processing enzymes due its location in neuropeptide-containing cells and its intrinsic protease activity and ability to hydrolyse neuropeptide precursors when activated by proteolysis (Small, 1989). The role of AChE as a zymogen may account for the polymorphism of the enzyme and its multi-cellular locations and may explain the existence of the secreted forms which are produced by a variety of cells including muscles. The role of AChE as a neuropeptide processing enzyme may be important in the understanding of neuropeptide regulation and is discussed in more depth in Section 1.1.6.3.

1.1.2 Structure and properties of AChE.

From 1969 onwards, Massoulie, Rosenberry and Silman produced many papers on the molecular forms of AChE and ChE, their solubility properties and

probable structure models. Early studies were carried out on eel and ray electric organs but were later generalised for rat, mouse, chicken and man (Bon et al., 1979; Rotundo and Fambrough, 1979; Fernandez et al., 1979; Carson et al., 1979).

1.1.2.1 Globular and asymmetric forms of AChE.

It was discovered that AChE existed not as one, but as several oligomeric forms, some which were anchored to membranes and others which were freely diffusible. A whole host of electrically excitable tissues as well as non-excitable cells were found to express any of the six different forms of AChE which could be separated and identified by a variety of methods such as velocity sedimentation on sucrose density gradients and gel filtration chromatography. In skeletal muscle, AChE displays a polymorphism which has been demonstrated in several vertebrate species (Massoulie and Reiger, 1969; Bon et al., 1979; Nicolet and Reiger, 1981).

AChE exists as two distinct classes: globular and asymmetric (Rosenberry, 1975, 1985; Massoulie, 1980; Massoulie and Bon, 1982; Brimijoin, 1993). The homomeric or globular forms are monomers, dimers and tetramers of a catalytic subunit of approximate weight 71,000 daltons with sedimentation co-efficients of around 5S, 7S and 11S respectively (which vary according to species). Massoulie referred to these as G1, G2 and G4 (see Figure 1.2). These can exist as soluble, hydrophilic forms or as amphiphilic forms which associate with membranes. The heteromeric or asymmetric forms consist of 1, 2 or 3 tetramers covalently linked by disulphide bonds to a three stranded collagen-like tail (Dubai et al., 1973; Bon et al., 1976; Lwega-Mukasa et al., 1976; Rosenberry and Richardson, 1977; Angister and Silman, 1978). The sedimentation co-efficients of these forms are around 12S, 15S and 16-17S and are called A4, A8 and A12 respectively (see Figure 1.2). The collagen-tail functions in anchoring asymmetric AChE to proteoglycans in the synaptic basal lamina of muscle fibres (Bon and Massoulie, 1978; Torres and Inestrosa, 1983; Torres et al., 1983, McMahan et al., 1987) and extra-cellular matrix of excitable cells. Collagen-tailed forms are highly concentrated in the neuromuscular junction and the A12 form which has a sedimentation co-efficient of 16S is believed to terminate cholinergic transmission (Hall, 1983).

Globular and asymmetric forms can be separated due to their different solubility characteristics in low and high ionic strength buffers. Globular forms are soluble in low ionic buffer (below 150mM) and asymmetric forms are soluble in high ionic buffer (0.5-1.0M). All tissues can synthesise and assemble all the forms of AChE but exhibit them in different proportions due to differences in rates of

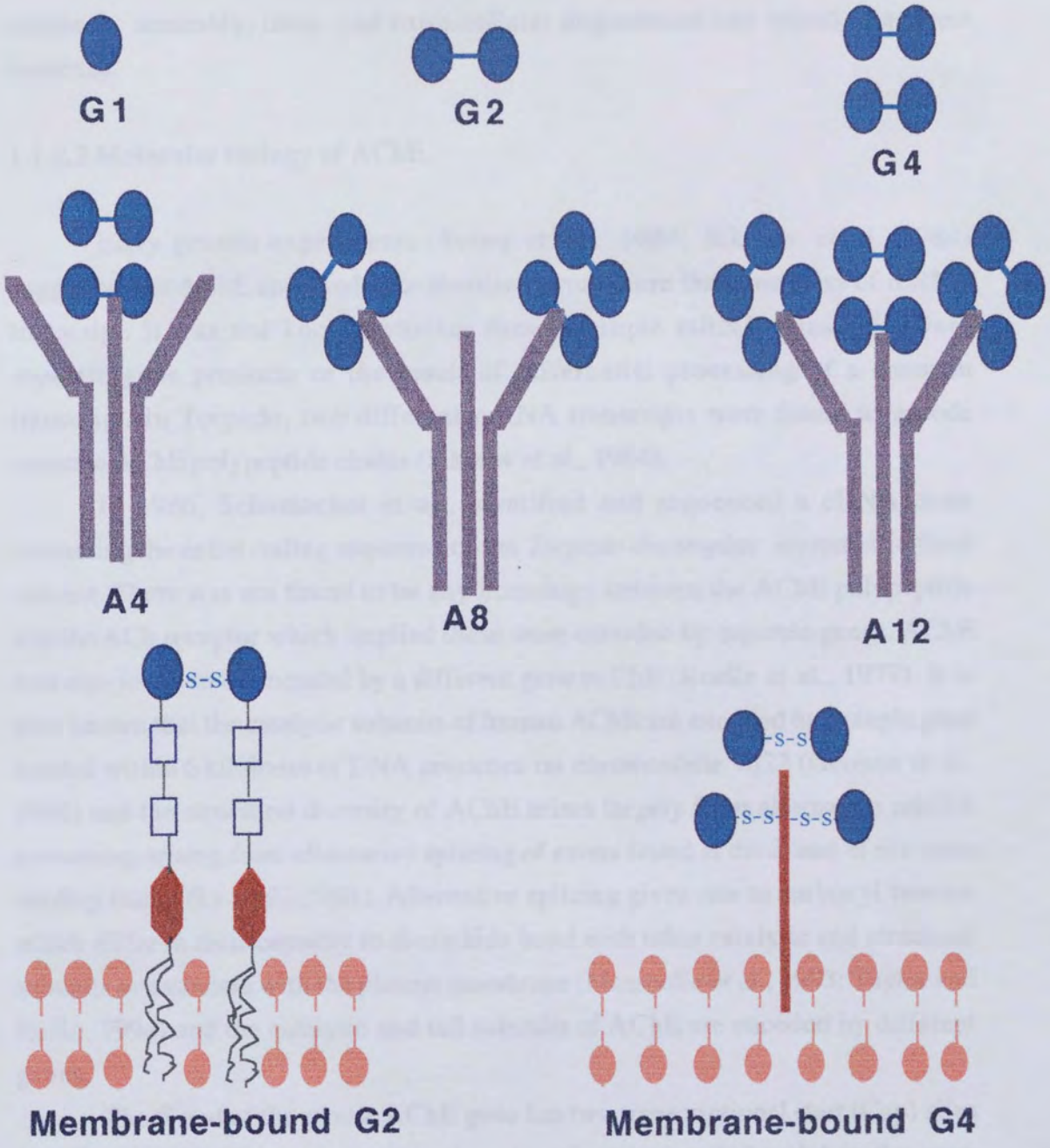

Figure 1.2: The molecular forms of AChE. Globular forms: G1 monomer, G2 dimer and G4 tetramer and asymmetric forms: A4, A8 and A12 consisting of one, two and three tetramers linked to a collagen-like tail. Also shown are the membrane-bound dimeric and tetrameric forms. The former inserts into the membrane via a glycophospholipid anchor and the latter via a 20kDa hydrophobic polypeptide anchor (modified from Inestrosa and Perelman, 1989).

synthesis, assembly, intra- and extra-cellular degradation and retention at their locations.

1.1.2.2 Molecular biology of AChE.

Early genetic experiments (Soreq et al., 1984; Sikorav et al, 1984) suggested that AChE appeared to be translated from more than one class of mRNA transcript. It was not known whether these multiple mRNA transcripts were separate gene products or the result of differential processing of a common transcript. In Torpedo, two different mRNA transcripts were found to encode separate AChE polypeptide chains (Sikorav et al., 1984).

In 1986, Schumacher et al., identified and sequenced a cDNA clone containing the entire coding sequence of the *Torpedo electroplax* asymmetric form subunit. There was not found to be any homology between the AChE polypeptide and the ACh receptor which implied these were encoded by separate genes. AChE was also found to be encoded by a different gene to ChE (Koelle et al., 1977). It is now known that the catalytic subunits of human AChE are encoded by a single gene located within 6 kilobases of DNA sequence on chromosome 7q22 (Getman et al., 1992) and the structural diversity of AChE arises largely from alternative mRNA processing arising from alternative splicing of exons found at the 3' end of the open reading frame (Li et al., 1991). Alternative splicing gives rise to carboxyl termini which differ in their capacity to disulphide bond with other catalytic and structural subunits or associate with the plasma membrane (Massoulie et al., 1993; Taylor and Radic, 1994) and the catalytic and tail subunits of AChE are encoded by different genes.

The 5' end of the mouse AChE gene has two transcriptional start (Cap) sites (see Figure 1.3). The gene contains three invariant exons; 2, 3 and 4 in the open reading frame which encode the signal peptide and 535 amino acids found in the primary sequence of both globular and asymmetric AChE and contain the genetic information for all essential catalytic residues and cysteines that form intra-subunit disulphide bonds. Alternative mRNA splicing from exon 4 to exons 5 and 6 dictates whether the type of AChE produced is destined to have a collagen-like tail or a glycophospholipid membrane anchor (Li et al., 1991). Splicing of exon 5 to exon 4 gives a hydrophobic sequence and leads to the addition of glycophospholipids. Subunits with the ability to form disulphide bonds with the collagen-tail subunit are encoded by the invariant exons 2-4 linked to exon 6.

Alternative polyadenylation signals (pA) are found in the 3'-untranslated region which may be important in influencing the stability of the mRNA. Promoter

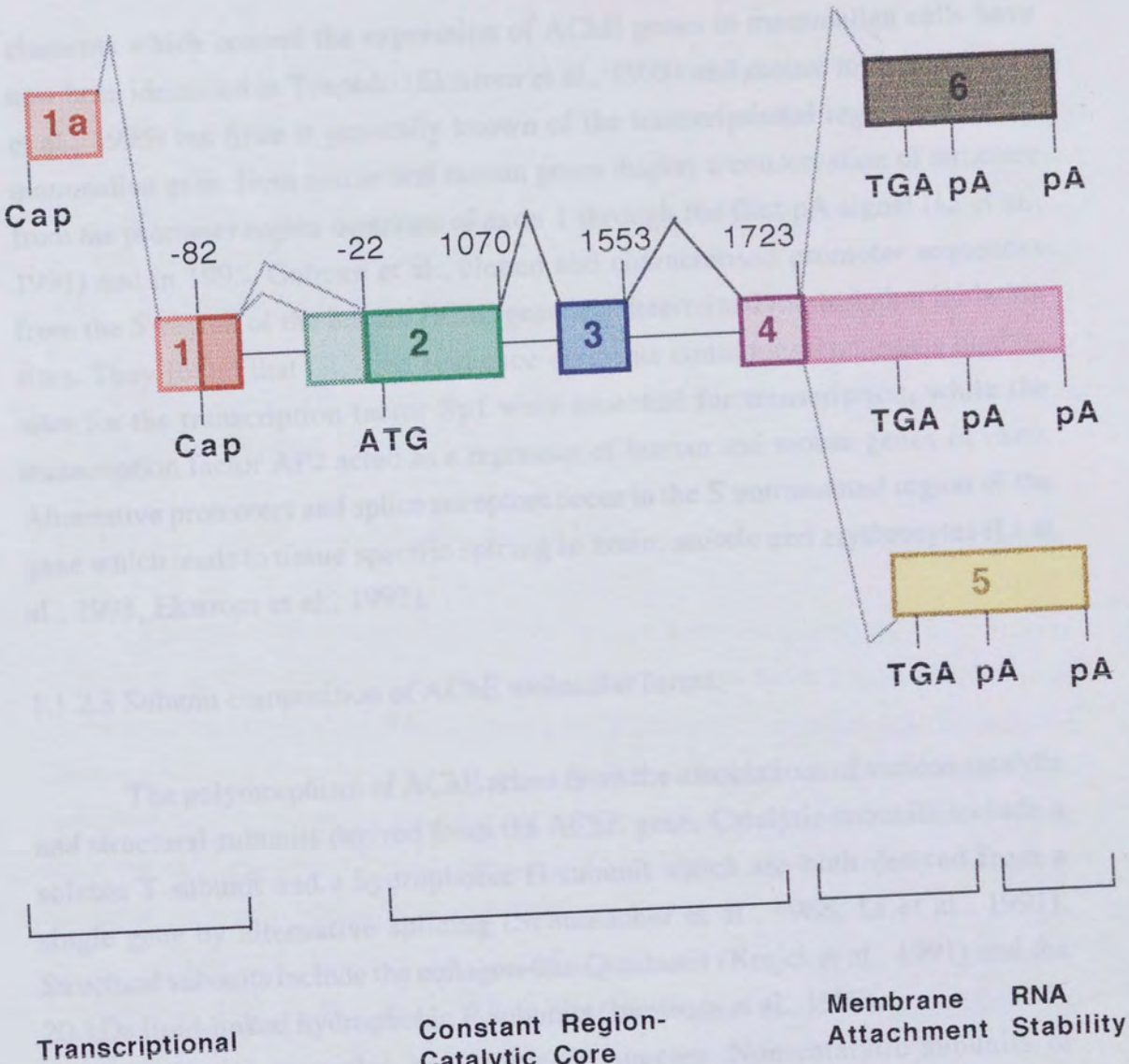

Figure 1.3: The mouse AChE gene. The gene consists of three invariant exons: 2, 3 and 4. Alternative splicing of exons 5 and 6 leads to differential expression of AChE (modified from Li et al., 1991).

elements which control the expression of AChE genes in mammalian cells have now been identified in Torpedo (Ekstrom et al., 1993) and mouse muscle (Mutero et al., 1995) but little is generally known of the transcriptional regulation of the mammalian gene. Both mouse and human genes display a conservation of structure from the promoter region upstream of exon 1 through the first pA signal (Li et al., 1991) and in 1995, Getman et al., cloned and characterised promoter sequences from the 5' region of the human AChE gene and determined transcription initiation sites. They found that GC-rich sequence elements containing consensus binding sites for the transcription factor Sp1 were essential for transcription, while the transcription factor AP2 acted as a repressor of human and mouse genes *in vitro*. Alternative promoters and splice acceptors occur in the 5' untranslated region of the gene which leads to tissue specific spicing in brain, muscle and erythrocytes (Li et al., 1993, Ekstrom et al., 1993).

1.1.2.3 Subunit composition of AChE molecular forms.

The polymorphism of AChE arises from the associations of various catalytic and structural subunits derived from the AChE gene. Catalytic subunits include a soluble T-subunit and a hydrophobic H-subunit which are both derived from a single gene by alternative splicing (Schumacher et al., 1988; Li et al., 1991). Structural subunits include the collagen-like Q-subunit (Krejci et al., 1991) and the 20-kDa lipid-linked hydrophobic P-subunits (Inestrosa et al., 1987).

Subunits may also vary between species. Non-catalytic subunits of unknown function were identified in electric ray asymmetric forms (Lee et al., 1982b) which were not present in electric eel. Also, membrane-bound globular forms differed to soluble globular forms and asymmetric forms with respect to covalent modifications and primary structure. For example, *Torpedo electroplax* asymmetric forms are associated with the basal lamina but the amphipathic dimeric globular forms are located exclusively on the pre-synaptic plasma membrane (Li and Bon, 1983). Some amphipathic dimeric globular forms are associated with vesicles (Bouma et al., 1977) and can be solubilised by treatment with phosphoinositol-specific phospholipase C (Futerman et al., 1984) suggesting that they may be associated with a phospholipid molecule which includes carbohydrate residues (Haas et al., 1986). Hence, membrane-bound and soluble globular forms can be differentiated by the presence or absence of covalently linked phospholipids and may have different primary structures (Lee and Taylor, 1982; Lee et al., 1982a).

Studies of mRNA suggest that in different species, different types of polypeptide chains may exist. Electric eel can translate one species of mRNA whereas electric ray can translate two separate species. G2 and G4 from chicken brain (Rotundo, 1984b) and muscle (Rotundo, 1984c) appear to contain two distinct polypeptide chains differing between 5000-10000 daltons which may be due to differences in primary structures of two distinct alleles (Randall et al., 1987). Hence, the general structures of AChE are conserved in various species but variations can occur with respect to catalytic subunit primary structure, size and covalent modifications.

1.1.2.4 Cell-bound and secreted forms of AChE.

The molecular forms of AChE can interact with cell membranes by a variety of inherent modifications found in dimers, tetramers and the collagen-tailed forms. (Inestrosa and Perelman, 1989). Globular AChE can exist as either soluble secreted forms, precursor forms or as detergent-soluble membrane associated forms. The differentiation between the globular forms arises from the T-subunit which forms secreted and cell-bound T-type dimers and tetramers attached to cell-associated structural subunits (Massoulie et al., 1992).

Cell-bound forms of AChE include dimeric enzyme found in human erythrocytes (Ott et al., 1975; Ott and Brodbeck, 1978; Dutta-Choudhury and Rosenberry, 1984; Rosenberry and Scoggin, 1984) and *Torpedo electroplax* (Bon and Massoulie, 1980; Viratelle and Bernhart, 1980; Lee et al., 1982a; Futerman et al., 1984) and tetrameric enzyme found in high concentrations in the brain (Reiger and Vigny, 1976; Grassi et al., 1981; Rotundo, 1984b). Extra-cellular AChE dimers attach to cell plasma membranes by the diacylglycerol moiety of a glycosylphosphatidylinositol glycolipid in the carboxy-terminus of the polypeptide (Richier et al., 1992) which can bind to one Triton X100 micelle (Dutta-Choudhury and Rosenberry, 1984) therefore rendering it detergent-soluble (see Figure 1.2). AChE tetramers attach to cell plasma membranes by a covalently attached 20kDa hydrophobic polypeptide anchor (see Figure 1.2). The G4 anchor contains three subdomains: a proximal subdomain containing disulphide bridges involved in the binding of the hydrophobic domain to the 68kDa catalytic subunit, a proteinase K-sensitive intermediate subdomain and a pronase-resistant 7kDa subdomain which contains fatty acids involved in binding the molecule to the membrane (Inestrosa and Perelman, 1989).

As well as G2 and G4 forms, asymmetric AChE has structural modifications enabling it to associate with the extra-cellular matrix. The tail subunit

of asymmetric forms contains a collagen-like composition and hydroxyproline, hydroxylysine, proline and glycine amino acids (Mays and Rosenberry, 1981). In addition, it also contains a non collagen-like domain due to the presence of amino acids not normally associated with collagen as well as a cleavage site for proteases that do not cleave collagen (Mays and Rosenberry, 1981) at a specific site by the amino-terminal end of the tail (Krejci et al., 1991). The collagen-tailed form can be removed by treatment with collagenase (Hall and Kelly, 1971; Betz and Sakmann, 1973). In muscle cell cultures, some asymmetric AChE was found to be covalently bound to muscle proteins by transglutaminase and suggested that these collagen-tailed AChE were crosslinked via one or more sites in the collagen-like subunits to transglutaminase substrates of fibronectin or other extra-cellular glycoproteins in a manner which directs the functional orientation of the catalytic subunits (Hand and Haynes, 1992). The primary structure of the tail subunit contains a signal peptide, an N-terminal proline-rich domain, a collagenic domain with periodic repetitions of glycine every three residues and a C-terminal domain containing a proline-rich region and a cysteine rich region. The collagenic domain is bracketed by two pairs of cysteines which lock the triple helical collagenic tail into a stable conformation. Collagen-tail formed AChE reversibly binds to heparin-like glycosaminoglycans present in extra-cellular matrix glycoproteins such as heparin or dermatan sulphate proteoglycans. Binding between AChE and proteoglycans is mediated by clusters of basic residues which form belts around the triple helix of the collagenic tail. (Deprez and Inestrosa, 1995).

Secretion of AChE from muscle cells was demonstrated by Wilson et al. (1973) and there was found to be a distinction between AChE targeted for the plasma membrane and for secretion (Rotundo and Fambrough 1980a,b). Secreted globular AChE may be unassembled T-subunits, degradation products of extra-cellular multimers or products of the recently identified mRNA species that encodes AChE subunits devoid of a COOH-terminal cysteine residue which is believed to be involved in the assembly of AChE into multimeric forms (Li et al., 1991). The role of secreted globular forms is unknown. They are secreted by a variety of cells including nerve and muscle (Linkhart and Wilson, 1975; Gisiger and Vigny, 1977; Oh et al., 1977) and are found in all body fluids including serum, cerebral spinal fluid and saliva.

1.1.3 Synthesis, assembly and processing of AChE.

1.1.3.1 Biogenesis of AChE.

Much of the study of the biogenesis of AChE has derived from tissue culture studies on nerve and muscle cells and a summary of the biogenesis process is shown in Figure 1.4. AChE mRNA transcribed from the AChE gene is transferred to the rough endoplasmic reticulum (RER) on ribosomes which bind to the membrane and translate AChE polypeptide chains into the lumen, as expected for secreted and membrane-associated proteins. In the RER the polypeptides are folded, disulphide bonds formed and core sugars are acquired before they are transferred to the Golgi apparatus for complex carbohydrate processing and targeting to specific cellular locations. Only about 20-30% of the AChE synthesised is transferred to the Golgi, the rest is degraded. All AChE polypeptides are glycoproteins containing approximately 15% asparagine-linked oligosaccharides by weight (Bon et al., 1976; Rotundo, 1983, 1984b). AChE polypeptides appear to contain only N-linked oligosaccharides which are added co-translationally.

Globular forms of AChE are assembled soon after synthesis in the lumen of the RER (Rotundo, 1984a). After assembly they are transported to the Golgi where further modification of their oligosaccharides occurs i.e. trimming of mannose residues and addition of N-acetylglucosamine and galactose. Finally sialic acid may be added depending on species (Bon et al., 1976). In tissue-cultured chicken and quail muscle cells processing of oligosaccharides during the journey of AChE polypeptides through the cell, takes about 2 hours. Only enzyme molecules with fully processed carbohydrate chains complete the journey through the cell and become externalised as secreted molecules or associated with the cell surface (Rotundo, 1984a). Cell-bound dimers acquire their glycophosphatidylinostiol anchors in the Golgi apparatus (Inestrosa and Perelman, 1989).

Asymmetric AChE is assembled late in the synthesis, processing and targeting pathway within muscle cells (Rotundo, 1984a; Inestrosa, 1984) from G4 tetrameric precursors (Rotundo, 1984; Lazar et al., 1984; Brockman et al., 1986) made 90 mins earlier in the RER by the addition of the collagen-tail. Intersubunit disulphide bonds involving the most COOH-terminal cysteine of the catalytic subunit have a key role in determining which globular molecules in the RER will be assembled into asymmetric forms (Lockridge et al., 1979; Roberts et al., 1991; Velan et al., 1991; Lockridge at al., 1979). It is possible that a cysteine-580 residue constitutes a RER retention signal for molecules destined to be assembled into higher forms and molecules without the residue are eventually secreted and form an

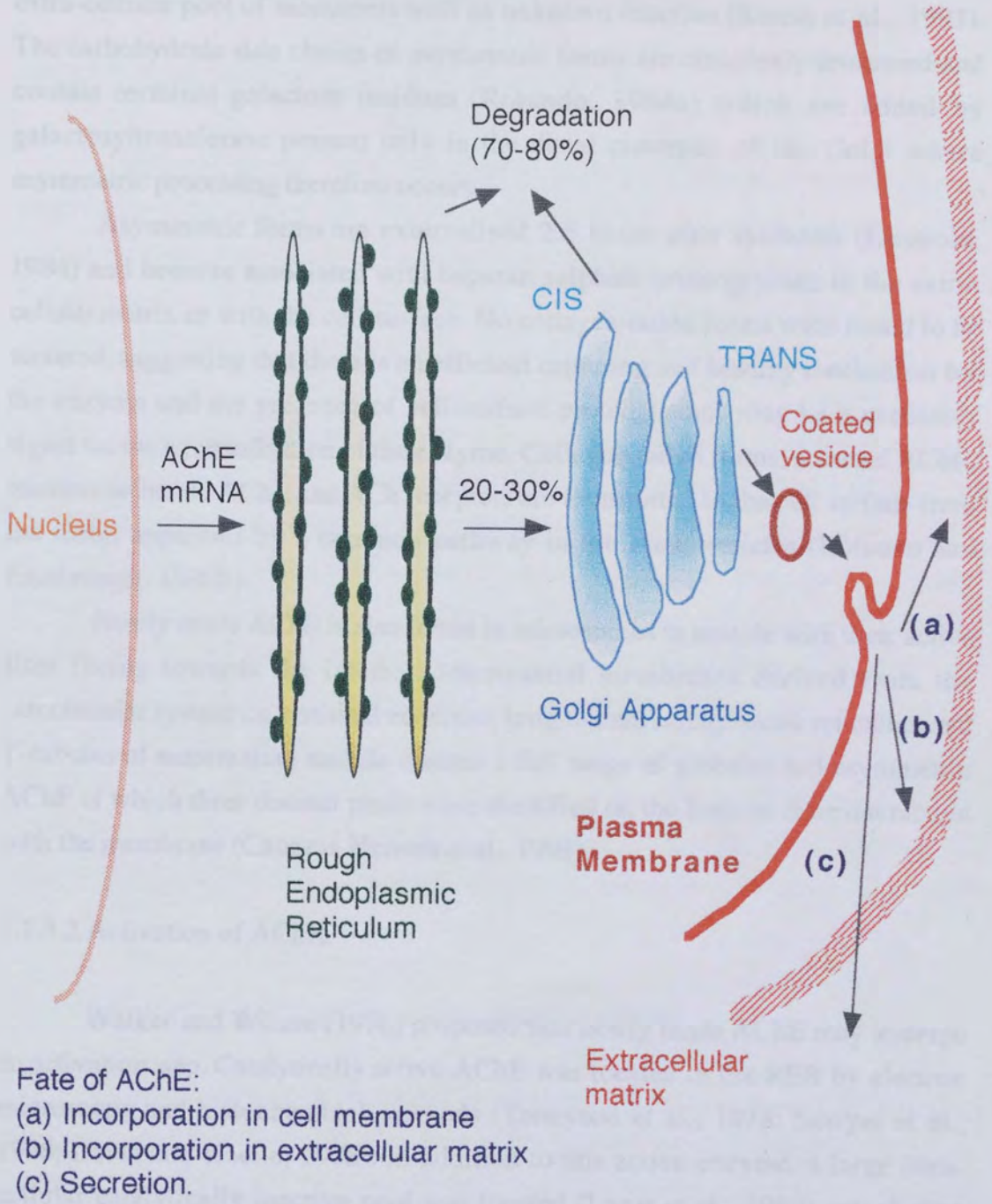

Figure 1.4: The biogenesis of AChE. Schematic representation of AChE mRNA transcription, processing in RER and Golgi and transport to cell surface. Also shown is the fate of AChE; new enzyme is (a) incorporated into the cell membrane, (b) incorporated into the extra-cellular matrix or (c) secreted (modified from Rotundo, 1987).

extra-cellular pool of monomers with an unknown function (Kerem et al., 1993). The carbohydrate side chains of asymmetric forms are complexly processed and contain terminal galactose residues (Rotundo, 1984a) which are added by galactosyltransferase present only in the distal cisternae of the Golgi where asymmetric processing therefore occurs.

Asymmetric forms are externalised 2.5 hours after synthesis (Inestrosa, 1984) and become associated with heparan sulphate proteoglycans in the extra-cellular matrix or with the cell surface. No collagen-tailed forms were found to be secreted, suggesting that there is an efficient capturing and binding mechanism for the enzyme and the presence of cell-surface proteoglycans may be a necessary signal for the externalisation of the enzyme. Collagen-tailed forms, secreted AChE, membrane-bound AChE and ACh receptors are transported to the cell surface from the Golgi apparatus by a common pathway in the same vesicles (Rotundo and Fambrough, 1980b).

Newly made AChE is also found in microsomes in muscle with their active sites facing towards the interior. Microsomal membranes derived from the sarcotubular system i.e. terminal cisternae, longitudinal sarcoplasmic reticulum and T-tubules of mammalian muscle contain a full range of globular and asymmetric AChE of which three distinct pools were identified on the basis of their interaction with the membrane (Cabezas-Herrera et al., 1993).

1.1.3.2 Activation of AChE.

Walker and Wilson (1976) proposed that newly made AChE may undergo an activation step. Catalytically active AChE was located in the RER by electron microscopy and histochemical methods (Tennyson et al., 1973; Sawyer et al., 1976; Davis and Koelle, 1978). In addition to this active enzyme, a large intra-cellular catalytically inactive pool was located (Lazar et al., 1984) which was approximately 40-80% of the total intra-cellular newly synthesised AChE and pulse-chase studies using radiolabelled amino acids showed that only a small fraction of this pool becomes activated and assembled into oligomeric forms whereas the rest is degraded. Studies proposed that the AChE activation mechanism is independent from AChE biosynthesis and largely unclear but maturation of the active site may involve a conformational change in the enzyme early in the processing of the molecule and may be analogous to that of the ACh receptor (Merlie and Sebbane, 1981; Merlie and Lindstrom 1983).

1.1.4 Transport and localisation of AChE in muscle.

1.1.4.1 Subcellular distribution of AChE.

Different forms of AChE appear to have different, but overlapping subcellular distributions. 65-75% of all active AChE is located in intra-cellular compartments (Rotundo and Famborough, 1980a,b; Brockman et al., 1982; Younkin et al., 1982) including organelles for synthesis and processing of exported proteins such as RER, the Golgi apparatus and vesicles involved in transport of proteins from one compartment to another. Newly made AChE is located in vesicles known to mediate intra-cellular transport of proteins to the plasma membrane (Porter-Jordan et al., 1986), lysosomes which mediate intra-cellular degradation of cell surface components, muscle sarcoplasmic reticulum (Tennyson et al., 1973), secretory granules (Wake, 1976; Sawyer et al., 1976) and the perinuclear space (Sawyer et al., 1976). In nerves, AChE molecules are transported from cell bodies to nerve terminals by rapid axoplasmic transport (Ranish and Ochs, 1972; Brimijoin and Wierma, 1978; DiGiamberardino and Couraud, 1978). Hence, based on the sequence of events during the synthesis and assembly of AChE molecular forms (Rotundo, 1984a) only globular forms are found in the RER of all cell types and all other forms are found in the late Golgi and post-Golgi organelles. The role of sequestered AChE in the sarcoplasmic reticulum of muscle is unknown (Tennyson et al., 1973).

1.1.4.2 Cell surface localisation of AChE molecular forms.

Cell surface AChE is important in neuromuscular transmission and acts as a marker for nerve-muscle contact. In muscle 30-50% of total cellular AChE is located externally on cell surfaces (Rotundo and Fambrough, 1980a,b; Brockman et al., 1982; Younkin et al., 1982; Donoso and Fernandez, 1985) and is predominantly asymmetric and membrane-bound G4 and G2 (Brockman et al., 1982; Inestrosa et al., 1982; Rotundo, 1983, 1984a).

Collagen-tailed AChE is present in higher amounts in innervated muscle (Hall, 1973) and is the predominant form in the neuromuscular junction where it inserts into the basal lamina (Inestrosa et al., 1982). The presence of the junctional form appears to be critically dependent on the integrity of neuromuscular transmission since interference by pharmacological means (Rubin et al., 1980) or surgical denervation (Hall, 1973) causes the activity to disappear. Although most junctional AChE is associated with the basal lamina and is located between the

nerve-ending and muscle plasma membranes (McMahan et al., 1978) some may be localised on the presynaptic plasma membrane (Salpeter et al., 1978). In some species, the collagen-tailed form has also been located in non-endplate regions but its function at these sites is unknown (Carson et al., 1979).

The compartmentalisation of cell surface asymmetric AChE with respect to function occurs due to the restricted expression of mRNA which encodes only enzyme destined for the synaptic membrane which overlies the nucleus of origin. However, transcripts encoding AChE are widely distributed in muscle fibres which can potentially be expressed by a majority of nuclei (Tsim et al., 1992). Rossi and Rotundo (1992) found that AChE molecules in multinucleated myotubes are preferentially transported and localised to regions of surface membrane overlying the nucleus from which they were expressed and this targeting could be important in maintaining specialised cell surface domains such as neuromuscular and myotendinous junctions.

1.1.5 Turnover of AChE.

1.1.5.1 Studies on tissue-cultured muscle.

The turnover of a molecule is a balance between the rate of synthesis and the rate of degradation. Little of known of the true turnover rate of AChE because it exists as a complex family with many subcellular locations and is difficult to study. Initial studies of AChE turnover involved inhibiting protein synthesis in cultured muscle cells and measuring the rate of disappearance of cell AChE (Wilson and Walker ,1974; Rotundo and Fambrough, 1980a). From these studies it was found that cell AChE is partially localised intra-cellularly and partially on the cell surface in the ratio 2:1 (Rotundo and Fambrough, 1980 a,b). The intra-cellular pool in cultured muscle had a rapid turnover and the half-life of catalytically active AChE is around 90mins (Lazar et al., 1984). The kinetics of the appearance of new catalytically active heavy AChE suggested the presence of a catalytically inactive precursor pool (Lazar et al., 1984). The turnover rate of the inactive pool is unclear. This inactive AChE probably never leaves the Golgi apparatus and cannot be easily detected by conventional methods.

Most of the intra-cellular pool is destined for secretion and some is destined for the cell surface where it becomes membrane-bound or associated with the basal lamina (Rotundo and Fambrough, 1980a; Brockman et al., 1982). Cell surface AChE accumulates at the rate of 3% of the total surface population of AChE per hour, and is degraded at the rate of 1% per hour (Rotundo and Fambrough, 1980a)

resulting in a net increase of surface AChE. Cell surface AChE has a half-life of approximately 40-50 hours (Lazar et al., 1984) whereas the half-life of ACh receptors is 20 hours, suggesting that cells can distinguish between AChE and receptors and degrade them at different rates. Cell surface AChE is degraded by a mechanism exhibiting first order decay kinetics which may be mediated by lysosomes (Devreotes and Fambrough, 1976).

1.1.5.2 Half-life of AChE at the neuromuscular junction.

Denervation studies of the turnover of synaptic AChE (Inestrosa and Fernandez, 1976, 1977) have under-estimated its duration in the synapse because injured nerve and muscle cells release proteases which may speed up the degradation of AChE (Fernandez and Duell, 1980). However McMahan et al. (1978) showed that after denervation a substantial amount of synaptic AChE could still be histochemically stained for several months suggesting that it had a slow turnover rate. Kasprzak and Salpeter (1985) estimated the half-life of mouse synaptic AChE to be around 20 days using radiolabelling and autoradiography and was longer than that predicted by denervation studies. The half-life of AChE was found to be nearly twice as long as that of the ACh receptor (Kasprzak and Salpeter 1985). Since, ACh receptors are integral membrane proteins and are degraded by internalisation of the cell surface and transport to lysosomes whereas AChE is located in the basal lamina which is at some distance from the plasma membrane (McMahan et al., 1978), it is unlikely that the same mechanism controls the turnover of these molecules. Non-endplate AChE, in contrast, has a shorter half-life than endplate AChE of around 26 hours (Newman et al., 1984)

1.1.6 Regulation of AChE synthesis and location.

1.1.6.1 Levels of regulation.

The regulation of appropriate AChE levels at their sites of function may occur at several different levels i.e. transcriptional, translational and post-translational and due to the development of molecular probes, this has recently become an active area of research. These probes include monoclonal and polyclonal antibodies to AChE polypeptides, enzymes which allow the study of associated oligosaccharides and cDNAs to several AChE mRNA allowing studies at the transcriptional level. However, much of the understanding of AChE regulation is still at an infant stage.

Little is known of the regulation of enzyme levels and expression of AChE at the transcriptional level. It is known that for ACh receptors transcription and presence of mRNA in the cytoplasm is insufficient for synthesis of subunit polypeptide chains (Merlie and Lindstrom, 1983; Merlie and Sebbane, 1981; Merlie 1984) which requires additional cellular signals. Post-translational control of AChE may therefore be important in determining how many functional AChE molecules are assembled into oligomeric forms and transit the cell to reach the plasma membrane.

AChE may also be regulated with respect to where it is located. New AChE which is externalised at the plasma membrane or synaptic basal lamina must be located at sites of function and control of localisation must therefore be dependent on interactions with other molecules in the plasma membrane, the cytoplasm or the extra-cellular matrix. For example, the location and attachment of junctional AChE to the basal lamina must depend on molecules in this region to which the enzyme can bind (McMahan et al., 1978). Since, asymmetric AChE can bind to (Bon and Massoulie, 1978) and be solubilised by heparin (Torres and Inestrosa, 1983; Torres et al., 1983) and a specific form of heparin sulphate proteoglycan is highly concentrated at sites of nerve-muscle contact (Anderson and Fambrough, 1983; Bayne et al., 1984), it follows that this molecule provides an anchorage site for junctional AChE. Hence, regulation of AChE in the cleft, is mediated by the presence of specific molecules in the cleft which provide binding sites.

It was previously thought that the nerve released trophic substances which alone regulated the functional integrity of muscle. This was found to be an oversimplification. Innervation has a profound influence on AChE activity as denervation effects both endplate and non-endplate AChE (Newman et al., 1984). Muscle function was found to be dependent on muscle activity as well as the contribution of factors from nerves which also function in the localisation and anchorage of other synaptic components of the neuromuscular junction (Guth, 1969; Drachman, 1972; Reiger et al., 1980; Lomo and Slater, 1980a,b; Rubin et al; 1980; Younkin et al; 1978; Davey et al., 1979; Fernandez et al; 1979a,b; Fernandez et al; 1980; Lentz et al, 1981). The influence of the nerve on mammalian skeletal muscle non-endplate AChE is mediated primarily by the activity (action potentials and contractions) exerted by the nerve on muscle and the influence of the nerve on endplate-specific AChE is mediated in part by muscle activity and a mechanism which is activity independent and possibly due to neurotrophic factors (Younkin and Younkin, 1988).

1.1.6.2 Influences of muscle activity.

Muscle activity refers to the occurrence and frequency of muscle contractions and all the associated electrical and ionic events at the plasma membrane and normal muscle activity is important for maintaining muscle integrity. If activity is abnormal, muscles may degenerate. The presence of nerve impulses to the muscle is important in determining the number and type of proteins made in the muscle. Weeds et al., (1974) showed that reinnervating slow muscles with fast muscle nerves switched off the synthesis of slow muscle myosin heavy chains and switched on the synthesis of fast muscle myosin heavy chains. The pattern of nerve impulses was also found to be an important variable in muscle function. When slow muscle was stimulated by electrodes at the rate that fast muscle is normally stimulated, the slow muscle began to make fast muscle myosin heavy chains (Salmons and Sreter, 1976; Rubenstein et al., 1978). Since fast and slow muscle myosin heavy chains are encoded by two distinct genes (Buckingham et al., 1984), the studies implied that the pattern of impulse activity could regulate which genes were transcribed and which mRNA was translated in the cell.

Muscle activity can also affect synthesis of synaptic components i.e. ACh and AChE. Several studies *in vivo* and in tissue cultures showed that the amount and pattern of muscle activity was important in determining AChE levels and the appearance of individual molecular forms. Reiger et al., (1980) and Rubin (1985) showed that when spontaneous contractions in cultured muscle cells were blocked by blocking voltage-dependent sodium channels with tetrodotoxin, asymmetric AChE disappeared but globular AChE was unaffected. Blockage of ACh receptors with curare (Rubin et al., 1980) also eliminated the appearance of asymmetric AChE but not of globular AChE. It was not known if the effects were due to inhibition of synthesis of polypeptides in the collagen-tailed subunit or due to prevention of the covalent association of various subunits in the asymmetric molecule.

Unlike ACh receptors which always increase after denervation, AChE molecular forms may increase or decrease. Denervation results in a decrease in total muscle activity in rat (Guth and Zalewsky, 1963; Lubinska, 1966; Hall, 1973) but an increase in muscle activity in chicken and rabbit (Sketelj et al., 1978; Bacou et al., 1982). Denervation of rat, rabbit or chicken muscle is always followed by a rapid decrease in the amount of asymmetric AChE to very low levels. (Hall, 1973; Collins and Younkin, 1982; Bacou et al., 1982; Sketelj et al., 1978; Silman et al., 1979; Fernandez et al., 1980). In adult mammalian skeletal muscle, denervation causes a rapid decrease in both endplate and non-endplate AChE and reinnervation

causes a reappearance these enzymes (Guth and Zalewski, 1963; Weinberg and Hall, 1979). Hence, unlike the regulation of ACh receptors which is similar between species, regulation of AChE between species may be different.

The contribution of muscle activity in the regulation of AChE was also studied by developing ectopic endplates. These were made by denervating muscles at the synapse and replanting the nerve at a different site along the muscle fibre (Guth and Zalewski, 1963; Lomo and Slater ,1980a,b; Weinberg and Hall, 1979; Weinberg et al., 1981). It was found that asymmetric AChE disappeared from the original synapse following denervation and reappeared at both the original and ectopic endplate following replanting of the nerve. This implied that the continual presence of the nerve was not necessary for localisation of AChE (Guth, 1968).

Recovery of AChE at the original synaptic site could also be induced by electrical stimulation (Lomo and Slater, 1980a,b) suggesting that muscle activity alone is sufficient for the accumulation of newly synthesised molecules at a denervated neuromuscular junction. Weinberg and Hall (1979) and Weinberg et al., (1981) showed that asymmetric forms developed at the original and ectopic sites, suggesting that muscle could express the correct form of AChE at a site in the absence of direct nerve contact when the muscle was active. However, expression of AChE at the former innervated site does require that the region of muscle, possibly via the basal lamina had been previously contacted by the nerve (Lomo and Salter, 1980a,b; Weinberg and Hall, 1979; Anglister and McMahan, 1985). The nerve is therefore capable of imprinting an enduring signal on the basal lamina that instructs the muscle fibre, when active to synthesise and insert AChE at a particular point (Anglister and McMahan, 1985). The normal expression of AChE at the endplate requires the presence of the motor nerve (Fernandez and Inestrosa, 1976) but the synthesis of asymmetric AChE is therefore an intrinsic property of muscles that does not require the presence of neurons (Vallette et al., 1990).

When rat soleus muscle (slow twitch type muscle) was denervated, total AChE decreased and asymmetric AChE disappeared (Lomo et al., 1985) and when the soleus was stimulated electrically at fast and slow muscle rates, AChE levels were increased to normal. Asymmetric AChE in denervated muscle was found to be increased by electrical stimulation and accumulated in junctional and extra-junctional regions of muscle. In some cases, innervation of denervated muscle increased asymmetric AChE to above normal levels (Lomo et al., 1985). Hence, muscle activity also has an important role in regulating the amounts of AChE expressed and the relative abundance of the different oligomeric forms.

Sveistrup et al., (1995) studied levels of AChE mRNA in muscle after 8 weeks of increased exercise in rats and found that in the fast extensor digitorum

longus muscle, total AChE increased by 72% due to a threefold increase in G4, whereas in the slow soleus muscle, total AChE increased by 33% but A12 was decreased by 30%. This suggested that increases in neuromuscular activity modulate the expression of the AChE gene and a pretranslational regulatory mechanism may be involved in the adaptive response of AChE to enhanced neuromuscular activation.

1.1.6.3 Role of nerve factors and hormones in the regulation of muscle AChE.

Little is known of the precise chemical nature of regulatory neurotrophic factors, their origin or the level at which they exert their effects. A variety of trophic factors, some which originate from the spinal cord have been implicated in regulating AChE in developing and mature systems, but their modes of action are unclear. Two classes of neural factors are important in regulating AChE: those acting on the level of biogenesis (these are generally hard to study) and those involved in localising molecules after externalisation or secretion - i.e. molecules which also act in aggregation of ACh receptors. Agrin, the molecule responsible for ACh receptor aggregation, but which has no role in receptor synthesis was also found to induce the synthesis and junctional accumulation of AChE (Leith and Fallon, 1993; Wallace, 1989). Agrin is probably made by the nerve and transported down the axon where it is released and attaches to the basal lamina.

Proopiomelanocortin is a common precursor for several pituitary peptides (POMC peptides) which in adult animals are restricted to the pituitary and brain but in immature animals are present in the spinal cord and motor neurones. ß-endorphin, a product of the POMC precursor is known to reversibly inhibit the A12 form of AChE in rat skeletal muscle (Haynes and Smith, 1982) and may be important in its regulation in developing systems (Haynes et al., 1984). Although POMC peptides disappear soon into the post-natal period, they are released into the circulation of adults in response to stress (Rosier et al., 1977) i.e. nerve damage, certain diseases such as muscular dystrophy and anti-ChE induced myopathy. POMC peptides are therefore obvious contenders for the role of maintaining the properties of the neuromuscular junction throughout life and for ensuring the responsiveness of skeletal muscle during stress. In addition to POMC peptides, their post-translationally modified derivatives may also have a role in the regulation of AChE expression and activity. Small, neurotrophic peptides such as triiodothyronine and glycyl-L-glutamine (Gly-Gln), a derivative of ß-endorphin, may up-regulate the transcription of AChE genes to mRNA in the superior cervical ganglion of cat through the mediation of a binding protein and its receptor (Koelle,

1988) and was also found to induce the production of A12 in cultured embryonic cells (Haynes and Smith, 1984, 1985).

Hormones may also have an important role in the regulation of AChE activity. Brank and Grubic (1993), found that after 10-15 days of chronic treatment with dexamethasone, glucocorticoid-mediated reduction of protein synthesis occurred and AChE levels in diaphragm endplate-free regions were reduced, whereas endplate-rich activity was not and suggested that these plasma-circulating glucocorticoids, which are known transcriptional controllers (Muller and Renkawitz, 1991), may regulate AChE activity in skeletal muscle and its metabolism according to environmental demands.

1.2 Anti-cholinesterase-induced myopathy

1.2.1 Background to anti-ChE and their action.

There are many compounds present in industrial chemicals, insecticides, medicines and warfare agents which have anti-cholinesterase (anti-ChE) properties. Since the last century there has been an interest in these compounds which as well as having beneficial purposes such as pest control and the treatment of various medical disorders, can also cause acute muscular disease and induce delayed neuropathy. In recent years, there has been a concern regarding these compounds as a risk to not only the environment but also to human health due to the extensive use of insecticides in agriculture which may threaten the food chain. There has also been much debate concerning the risk to the health of farmers who habitually come into contact with anti-ChE whilst handing sheep dip. Since, the incidence of human exposure to anti-ChE compounds in the last century has not been infrequent, research into this field is an on-going process. Perhaps the most striking event in recent times was the freak exposure of passengers on the Tokyo underground in 1995 to sarin released by terrorists.

The acute and selective toxicity of anti-ChE compounds can be very high (i.e. μg/kg) and results from the inhibition of AChE. There are two distinct groups of anti-ChE: organophosphorous (OP) compounds and carbamates (CB). Both types of anti-ChE agent inhibit the action of AChE by binding to its active site and taking the place of the normal substrate ACh. Unlike the acetylated intermediate formed in the hydrolysis of the normal substrate for AChE the phosphorylated and carbamoylated AChE complexes are stable. The inhibition of AChE by OPs is essentially irreversible and AChE activity can only be restored by *de novo*

synthesis or spontaneous reactivation. In contrast inhibition by CBs is less stable, lasting from 30 minutes to several hours after which AChE is regenerated intact.

The first OP anti-ChE produced was tetraethyl pyrophosphate by Phillipe de Clermont in 1854 although there was speculation regarding the purity and true identity of the compound. It was not until 90 years later that the toxicity of OPs was discovered by Lange who observed that inhalation of dimethyl or diethyl phosphoflouridate vapour produced choking and dimness of vision (miosis). Extensive investigations in the use of these compounds to produce insecticides was begun in 1936 by Schrader who by 1952 had synthesised in the region of 2000 OP compounds including the commonly known pesticides parathion and paraxon. Schrader's work was also used by governments of the time to create chemical warfare agents such as the nerve gas diisopropyl phosphorofluoridate (DFP) and more potent agents such as tabun, sarin and soman. In addition to use as insecticides and chemical warfare agents, OPs were found to have medicinal value and have been used as tranquillisers, to treat glaucoma, myasthenia gravis (Schaumann and Job, 1958), anticholinergic poisoning and paroxysmal atrial tachycardia.

The first CB, physostigmine was isolated from the Calabar bean which was isolated in the pure form in 1864 by Jobst and Hesse. In 1877 the drug was used therapeutically for the first time in the treatment of glaucoma. Physostigmine was found to produce miosis as well as other symptoms due to the urethane group of the drug. This lead to the preparation of a number of substituted urethanes such as neostigmine which was synthesised by Aeschliman and Reinert in 1931 which was initially used to stimulate the intestinal tract but was also found to be effective in the treatment of myasthenia gravis. Today, the CB pyridostigmine is also routinely used to treat this condition.

In the 1950's CB were first used as insecticides and in the manufacture of insect repellents and many analogues were tested and produced. Amongst the most common CBs used as insecticides are carbaryl and propoxur. The former is one of the most widely used insecticides whereas the latter is more commonly used for domestic pest control. Pyridostigmine bromide has prophylactic properties against nerve agent poisoning. Recently, during the Gulf War crisis, its protective use against chemical warfare was exploited on a grand scale during Operation Desert Storm. This was the first large-scale human use of pyridostigmine under field conditions in the anticipation of nerve agent attack (Keeler et al, 1991).

1.2.2 Organophosphorous compounds.

The general structure of an OP compound is shown in Figure 1.5(b). OPs are usually esters, amides or thiol derivatives of phosphoric acid. R_1 and R_2 are commonly aryl or alkyl groups which may be bonded directly or through an -O- or -S- bond. The structure of the OP ecothiopate (ECO), which is used throughout this study is shown in Figure 1.5(c). ECO, contains a quaternary nitrogen in its structure which limits its access to muscle and nerve cells because it cannot readily traverse the blood-brain barrier (except at high doses and possibly through ion channels) and mostly exerts its inhibitory effects on the peripheral nervous system.

The catalytic mechanism of AChE on its normal substrate, ACh, is shown in Figure 1.6. The catalytic site of AChE contains two active sites, the esteratic and the anionic site. Under normal circumstances, the ester group of ACh attaches to a serine residue in the esteratic site forming a strong covalent bond whilst the cationic head group of the molecule forms a less strong ionic bond with the anionic site. Hydrolysis of ACh occurs, choline is released and the enzyme is acetylated for a short time. It is then hydrolysed and the enzyme is reactivated. The interaction of a general OP compound with AChE is shown in Figure 1.7. The OP inhibits normal enzyme function by binding to the esteratic site. Hydrolysis of the inhibitor molecule then occurs leaving the esteratic site phosphorylated. Quaternary compounds such as ECO display some interaction with the anionic site due to the quaternary nitrogen. Dissociation of the phosphate group and reactivation of the enzyme can occur spontaneously or by the use of oximes. Some inhibitor-enzyme complexes undergo ageing where an R_1 group from the phosphorylated enzyme is hydrolysed. Once ageing has occurred, the enzyme cannot be reactivated. ECO displays some spontaneous reactivation with a half-life of between 44 and 64 hours and ages with a half-life of 41 hours (Hobbiger, 1976).

1.2.3 Carbamate compounds.

Prophylaxis with CB compounds such as pyridostigmine is known to prevent OP poisoning (Dirnhuber and Green, 1978; Gordon et al., 1978; Wecker et al., 1978a,b; Dirnhuber et al., 1979; French et al., 1979). CBs reversibly inhibit AChE such that in the event of OP intoxication, the enzyme is protected (Berry and Davies, 1970) and only a small portion of the enzyme, in the region of 25-30%, needs to be inhibited to maintain normal neuromuscular function (Hobbiger, 1976). The general structure of a CB is shown in Figure 1.5(d) and the structures of pyridostigmine and physostigmine which are used throughout this study are shown

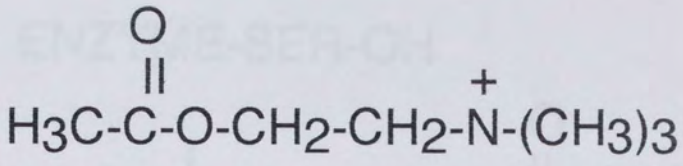

(a) Acetylcholine

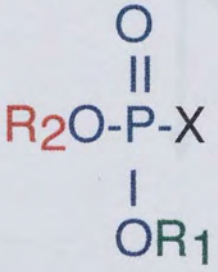

(b) Organophosphate

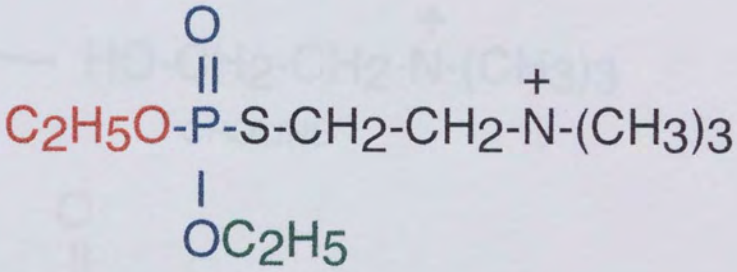

(c) Ecothiopate

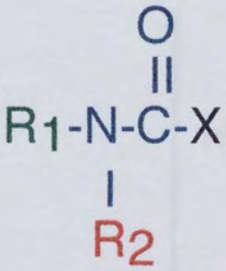

(d) Carbamate

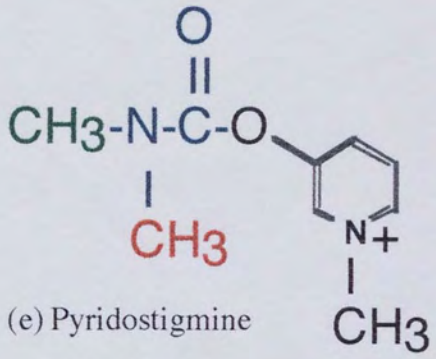

(e) Pyridostigmine

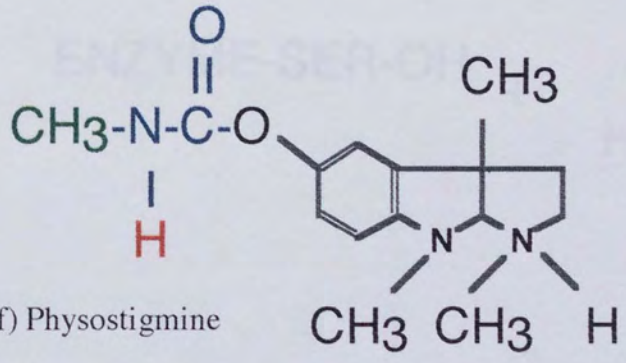

(f) Physostigmine

Figure 1.5: Structures of organophosphates and carbamates. Structures of (a) acetylcholine, (b) a general organophosphate, (c) ecothiopate, (d) a general carbamate, (e) pyridostigmine and (f) physostigmine.

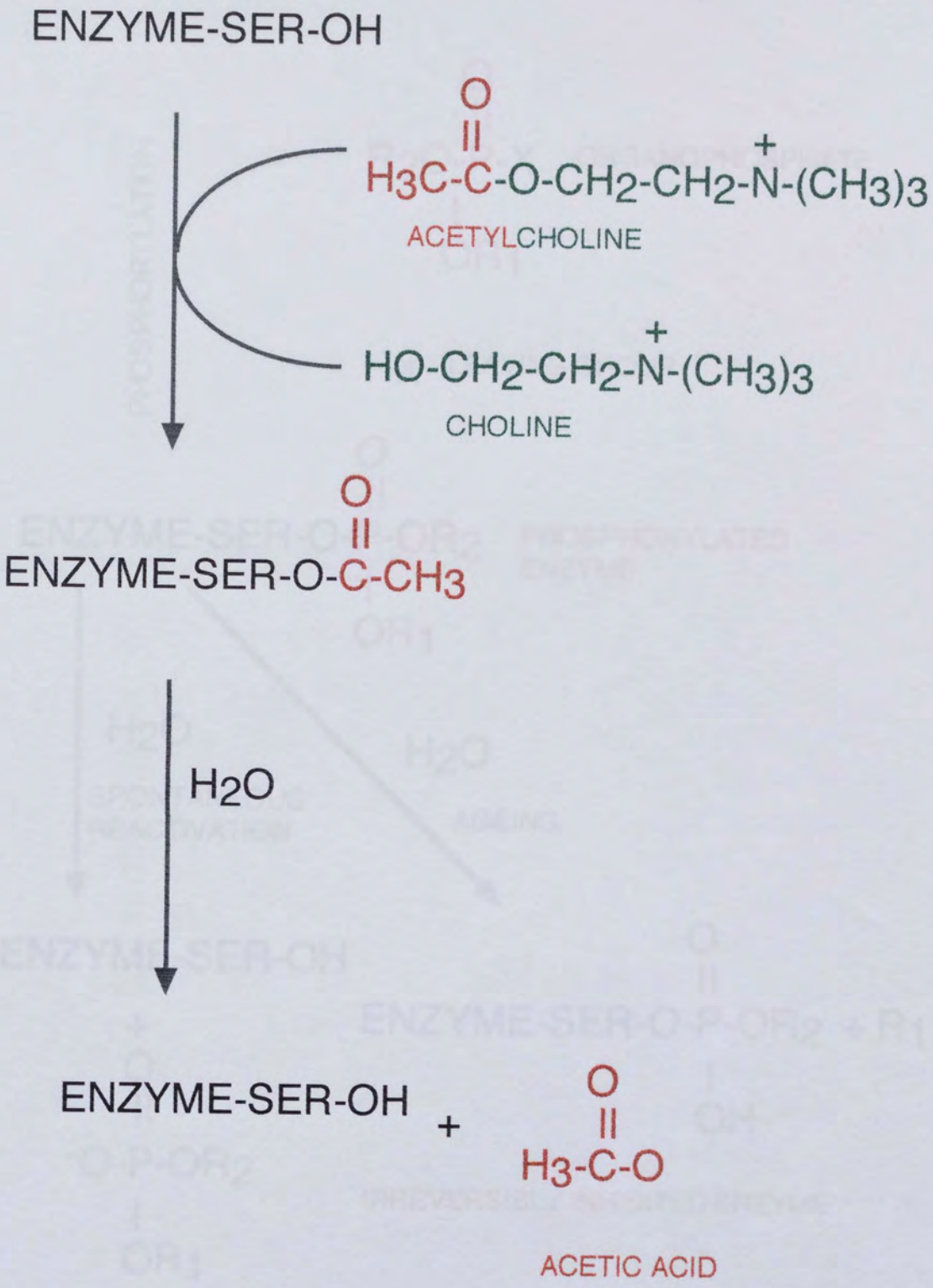

Figure 1.6: Interaction of ACh and AChE. ACh interacts with a serine residue of AChE, the molecule is cleaved, choline is released and AChE is acetylated. Acetylated AChE interacts with water and becomes de-acetylated.

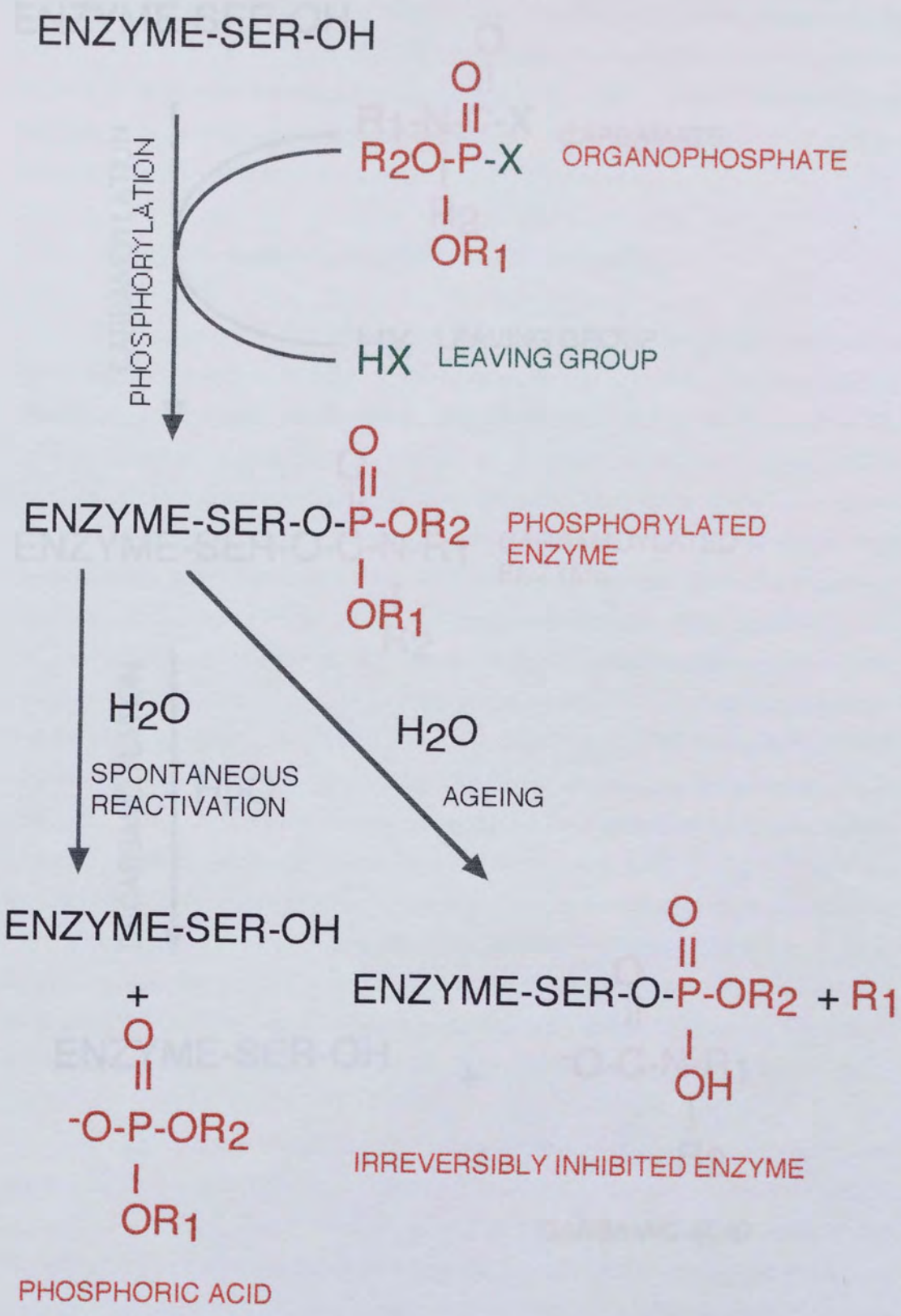

Figure 1.7: Inhibition of AChE by organophosphates. Schematic representation of the phosphorylation of AChE by a general OP, spontaneous reactivation and ageing.

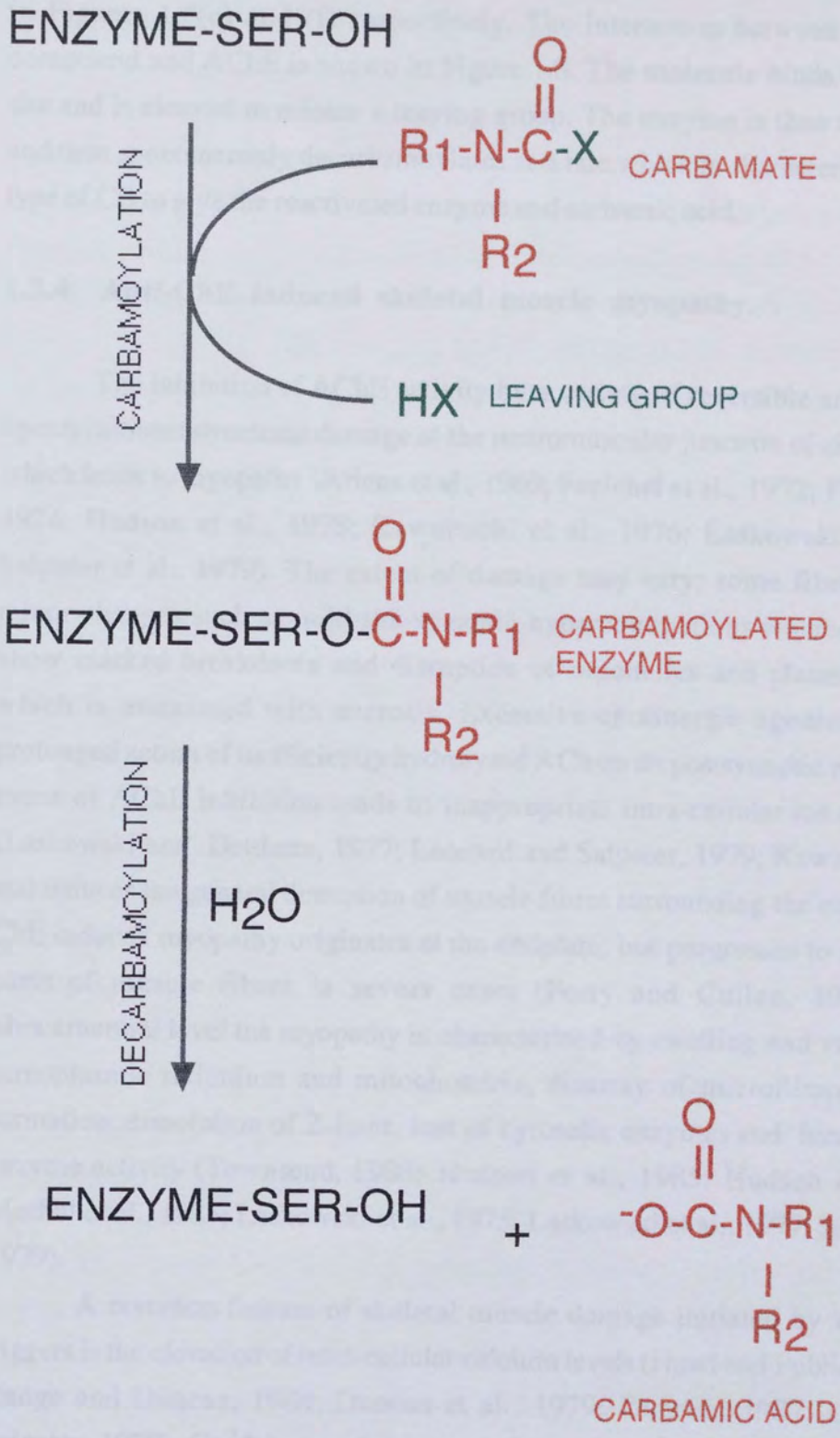

Figure 1.8: Inhibition of AChE by carbamates. Schematic representation of the carbamoylation of AChE by a general CB and spontaneous decarbamoylation.

in Figures 1.5(e) and (f) respectively. The interaction between a general CB compound and AChE is shown in Figure 1.8. The molecule binds to the esteratic site and is cleaved to release a leaving group. The enzyme is then carbamoylated and then spontaneously decarbamoylates at a rate which is characteristic to a given type of CB to give the reactivated enzyme and carbamic acid,

1.2.4 Anti-ChE induced skeletal muscle myopathy.

The inhibition of AChE activity by a variety of reversible and irreversible agents initiates structural damage at the neuromuscular junction of skeletal muscle which leads to myopathy (Ariens et al., 1969; Fenichel et al., 1972; Fenichel et al., 1974; Hudson et al., 1978; Kawabuchi et al., 1976; Laskowski et al., 1975; Salpeter et al., 1979). The extent of damage may vary; some fibres may show minor changes such as mild sub-synaptic hypercontractions whereas others may show marked breakdown and disruption of organelles and plasma membranes which is associated with necrosis. Excessive cholinergic agonism due to the prolonged action of inefficiently hydrolysed ACh on its postsynaptic receptor in the event of AChE inhibition leads to inappropriate intra-cellular ion accumulation (Laskowski and Dettbarn, 1977; Leonard and Salpeter, 1979; Kawabuchi, 1982) and induces the general disruption of muscle fibres surrounding the endplate. Anti-ChE induced myopathy originates at the endplate, but progresses to non-endplate parts of muscle fibres in severe cases (Ferry and Cullen, 1991). On an ultrastructural level the myopathy is characterised by swelling and vacuolation of sarcoplasmic reticulum and mitochondria, disarray of microfilaments, crystal formation, dissolution of Z-lines, loss of cytosolic enzymes and increased serum enzyme activity (Townsend, 1988; Hudson et al., 1985; Hudson et al., 1986; Meshul et al., 1985; Laskowski et al., 1975; Laskowski et al., 1977; Salpeter et al., 1979).

A common feature of skeletal muscle damage initiated by a variety of triggers is the elevation of intra-cellular calcium levels (Howl and Publicover, 1987; Rudge and Duncan, 1984; Duncan et al., 1979; Duncan, 1987; Leonard and Salpeter, 1979). Ca^{2+} has an important role in cells as transient rises in the ion from 10^{-7}M to 10^{-6}M triggers a variety of normal cellular processes including exocytosis, motility, enzyme activity and membrane conductance changes and any anti-ChE induced changes in Ca^{2+} homeostasis will invariably have a profound effect on cellular metabolism. The influx of Ca^{2+} after anti-ChE induced prolonged depolarisation of the sarcolemmal membrane due to the prolonged action of ACh has been shown to occur via endplate ion channels (Evans, 1974; Mideli et al,

1977; Takeuchi, 1963) However, increases in intra-cellular Ca^{2+} may also be calcium-induced (Duncan and Smith, 1980; Fabiato, 1982; Endo, 1977), depolarisation-induced from intra-cellular Ca^{2+} sequestering compartments such as the sarcoplasmic reticulum (Chandler et al., 1976; Schneider, 1986) or Na^{+}-induced from mitochondria (Carafoli and Zurini, 1982; Affolter and Carafoli, 1980). After cellular injury, calcification and overloading occurs in the sarcoplasmic reticulum and mitochondria possibly in an attempt to compensate for high intra-cellular Ca^{2+} levels, which exceed 10^{-6}M, and results in impaired function and damage to protein structure and phospholipids (Oberc and Engel, 1977).

The precise role of Ca^{2+} in the induction of skeletal muscle myopathy is not clear. It has been suggested that there are two phases in the development of the myopathy (Das, 1989). In the first step is was postulated that the disruption of the integrity of the sarcolemmal membrane was dependent on extra-cellular Ca^{2+} and possible leakage of proteins (Rudge and Duncan, 1984). In the second step Ca^{2+} influx was thought to occur across the damaged sarcolemmal membrane down a steep electrochemical gradient and contribute to the onset of cellular necrosis. Ca^{2+} alone, however, is probably insufficient to promote ultrastructural damage and probably requires a Ca^{2+}-activated cytoplasmic factor. Possible factors which may contribute to myofibril degradation include the calcium-activated neutral proteases (CANP) which dissolve Z-disks (Dayton et al., 1976; Kar and Pearson, 1976), lysosomes (Li, 1980; Gerard and Schneider, 1979), phospholipases (Knapp et al., 1977), free-radicals which mediate lipid peroxidation (Barker and Brin, 1975; Braughler et al., 1985) and Ca^{2+}-mediated mitochondrial overloading (Wrogemann and Pena, 1976).

Accumulation of intra-cellular Ca^{2+} occurs during the onset of myopathy after OP and CB intoxication. Non-necrotising doses of ECO (< 300 nmol kg^{-1}) result in a significant accumulation of Ca^{2+} and a proportion of the OP-induced increase in intra-cellular Ca^{2+} is due to the postsynaptic action of ACh released non-quantally from nerve terminals (Burd et al., 1989). Creatine kinase activity in the plasma is elevated after OP-intoxication suggesting that endplate membranes become leaky (Das, 1989). Elevation of intra-cellular Ca^{2+} levels was also shown to be associated with ultrastructural damage after sub-acute dosing with pyridostigmine (Hudson, 1986). The role of Ca^{2+} in anti-ChE intoxication is therefore an important one and may mediate the myopathy which occurs to varying degrees. Elevated Ca^{2+} levels may potentially effect AChE activity; proteases liberated by the ion may degrade the enzyme or effect its transport and exocytosis.

1.2.5. Recovery of AChE activity after anti-ChE.

The mechanism by which AChE activity returns to normal after inactivation by anti-ChE is poorly understood and the evidence provided by the literature is confusing. Following inactivation of AChE enzymes by irreversible anti-ChEs, recovery of normal activity can occur by *de novo* synthesis (Grubic et al., 1981; Fernandez and Stiles, 1984) or spontaneous reactivation depending on the rates at which the inhibitor-enzyme complexes age. Recovery of AChE activity after reversible inhibition depends largely on reactivation of existing enzymes. The time course of recovery depends on the rate of enzyme synthesis, assembly and transport to target sites and the action of regulatory factors.

The precise rate at which various molecular forms recover after inhibition is unclear. Grubic et al., (1981) found that the return of low molecular weight precursor forms in the rat diaphragm after soman intoxication occurred within 2 days whereas cytochemical methods showed that newly synthesised enzyme could be detected within 5-12 hours. Van Dongen et al., (1988) found that after a dose of soman which was three times the $LD_{50\%}$, new AChE was detectable within 180 minutes. Several studies suggested that AChE activity recovered by a bi-phasic mechanism. These included methyl-phosphorothiolate inactivation of mouse diaphragm AChE (Goudou and Reiger, 1983) and sarin inhibition of AChE in cat stellate and superior cervical ganglia (Koelle et al., 1982).The mechanism proposed that following an initial lag of 3-6 hours, there was an initial 'early rapid phase' which lasted for a period of 15 hours and corresponded to a period of rapid protein synthesis of predominately G1 precursors forms when 60% of AChE was restored. This was then followed by a 'slow recovery phase' which lasted for 2-3 days during which time a further 20% of AChE was restored and corresponded to the replenishment of asymmetric forms. The complete recovery of AChE after soman was found to take longer than 3 days and was also reported by Salpeter et al., (1979) who found that two weeks after DFP only 25% of total AChE sites present normally could be detected. The purpose of the initial lag is unclear but suggests that *de novo* synthesis may not have a role in the early hours after intoxication (Van Dongen et al., 1988) and existing intra-cellular pools may be activated prior to gene activation.

An early feature AChE recovery after anti-ChE is the rapid recovery of the G1 form (Reiger et al., 1976; Grubic et al., 1981; Goudou and Reiger, 1981) and supports the hypothesis that this is the precursor of the higher molecular weight forms. The recovery of asymmetric forms may be delayed because of the inability of these newly synthesised forms to attach to their locations (Grubic et al., 1981)

suggesting that they may be ineffectively processed or that a fault has occurred in the targeting of these forms to the cell membrane. Agrin is known to function in the accumulation of asymmetric AChE in the basal lamina (Leith and Fallon, 1993; Wallace, 1989) and its transport to target sites may be hindered in the event of prolonged cholinergic agonism.

An interesting feature of the recovery of AChE after inhibition is that endplate and non-endplate AChE recover at different rates. After OP intoxication, non-endplate AChE recovered at a faster rate of 2.9% hr^{-1} (Van Dongen et al., 1988) than endplate AChE which recovered at 1.5% hr^{-1} (Grubic et al., 1981; Fernandez and Stiles, 1984). Differences in recovery rates may arise from differences in the regulation of AChE in each region. Non-endplate is regulated primarily by muscle activity whereas endplate AChE is regulated by muscle activity and neurotrophic factors (Younkin and Younkin, 1988). It is possible that the delay in the recovery of endplate AChE is related to a delay in the effects of neurotrophic regulators caused by abnormal synaptic activity.

Grubic et al., 1981 found that a few hours after soman, AChE synthesis had been induced in the endoplasmic reticulum and perinuclear membrane of the Schwann cell and the sarcoplasmic reticulum and the special tubule structures located under motor-endplates. This location of AChE was analogous to that observed during the post-natal development of rats and suggested that a similar system of regulation operates in developing systems and after anti-ChE intoxication. Likely candidates for this role are the POMC derived peptides which are important in developing systems (Haynes et al., 1984) and may have an important function in regulating the proportions of AChE molecular forms after anti-ChE intoxication (Haynes et al., 1984).

Goudou and Reiger (1983) observed that after OP intoxication, biosynthesis of A12 occurred in non-endplate parts of muscle fibre as well as endplate regions. It was proposed that A12 could originate from any part of muscle fibres and be selectively accumulated in synaptic structures. The mechanism by which this occurs is unclear as is the relationship between endplate and non-endplate AChE. The recovery of AChE activity has largely been studied using OP anti-ChEs and little is known about the recovery after reversible inhibition. It is evident, that AChE recovers by a complex mechanism which is regulated and influenced by many factors.

1.3 Aims of the Investigations.

Sections of this thesis have been conducted as joint research carried out by myself and Amanda Crofts and have investigated the anti-ChE effects of OPs and CBs on mouse skeletal muscle using electrophysiological techniques to monitor endplate synaptic currents and biochemical methods to analyse responses of functional and non-functional molecular forms of AChE. Current knowledge of the long-term, low dose effects of CBs on mouse skeletal muscle is limited and the primary objective of this study was to investigate these effects. The study was conducted via a series of aims which are listed below:

(a) To rapidly extract AChE molecular forms from the mouse diaphragm, represent endplate-specific AChE and synaptic AChE activity and determine the distribution of AChE molecular forms.

(d) To investigate the effects on mouse skeletal muscle of acute OP dosing and monitor muscle recovery.

(e) To relate synaptic AChE activity determined by assay to the prolongation of extra-cellular miniature endplate potentials and determine the nature of the relationship between them.

(f) To determine whether CB-induced inhibition after *in vivo* dosing can be maintained for the duration of tissue preparation for the assay of molecular forms.

(g) To investigate effects on mouse skeletal muscle of 14 days of continual CB infusion, the recovery of muscle after 7 days of continual CB infusion and determine whether CB pre-treatment protects against the effects induced by an acute OP dose.

CHAPTER 2

METHODS

2.1 Animals.

Six month old male albino mice from Bantin and Kingman, usually exbreeders and weighing 40-50g were used for experimentation. The animals were given a pelleted breeding diet and water. At 6 months the mice are adult and a suitable study model as their neuromuscular junctions have stable characteristics for several months (Banker et al., 1982; Kelly, 1978).

2.2 Administration of drugs.

2.2.1 Ecothiopate.

Ecothiopate iodide (ECO) was obtained from Cusi (UK) Ltd. as Ecothiopate Eyedrops BNF (phospholine iodide) consisting of a dry powder of 12.5mg ecothiopate iodide and 40mg potassium acetate and a diluent containing 0.5% chlorobutanol, mannitol, boric acid and sodium phosphate. The dry powder was dissolved with 3.2ml of the diluent to give a solution of 10^{-2}M ECO. This was then diluted with distilled water to a 10^{-4}M stock solution which was stored at -20°C.

An injection solution was prepared by adding 1.4 x10^{-4}M atropine sulphate and 0.9% sodium chloride to the 10^{-4}M ECO stock solution. All injections were administered subcutaneously, between the shoulder blades of unanaethetised mice in a dose of 0.1ml per 20g of body weight (i.e. ECO 500 nmol kg^{-1} plus 700 nmol kg^{-1} atropine). Atropine was always given with ECO to prevent any muscarinic effects.

2.2.2 Pyridostigmine (repetitive dosing experiments).

A pyridostigmine (PYR) dosing solution was prepared by adding 1 mg ml^{-1} ampoules of PYR to 0.9% sodium chloride solution (PYR was obtained from Sigma). Mice were given PYR in sign-free doses of 100 μg kg^{-1} body weight in the form of a subcutaneous injection of volume 0.1 ml kg^{-1} twice daily at 9am and 5pm such that the total dose of drug received in 24 hours was 200 μg kg^{-1} (the molar equivalent of each dose was 383 nmol kg^{-1}). Diaphragms were removed for enzyme studies and blood samples were taken for analysis 3 hours after the first dose in the treatment and 3 hours after the morning dose on various days thereafter.

2.2.3 Pyridostigmine and physostigmine (continuous infusion experiments).

2.2.3.1 General procedure.

Mice were implanted with Alzet mini-osmotic pumps Model 200l (available from Charles River UK Ltd.) which had a nominal reservoir volume of 200μl, and pumped at a rate of 1.0 μl hr^{-1} for 7 days which had been filled with pyridostigmine (Sigma) or physostigmine salicylate (Sigma) prepared in 0.9% saline. Concentrations of each drug were prepared such that pyridostigmine was administered at the rate of 11.4 nmol hr^{-1} and physostigmine at the rate of 14 nmol hr^{-1}. Diaphragms were removed for analysis at various time points.

2.2.3.2 Principle of operation of the Alzet osmotic pump.

The Alzet osmotic pump is a miniature pump which can continuously deliver agents at controlled rates to laboratory animals and serve as a constant source for prolonged drug delivery when implanted subcutaneously or intraperitoneally.

The pump is composed of three concentric layers; the drug reservoir, the osmotic sleeve and the rate-controlling, semipermeable membrane (see Figure 2.1). An additional component called the flow modulator is a 21 gauge stainless steel tube with a plastic end-cap which is inserted into the pump after filling. The internal drug reservoir is made from a synthetic elastomer, is chemically inert to most aqueous drugs and is impermeable such that there is no exchange of material between the reservoir and the osmotic compartment. The osmotic sleeve contains a high concentration of sodium chloride and the difference in osmotic pressure between the sleeve and the site where the pump is implanted causes water to enter the sleeve along the osmotic gradient which compresses the flexible reservoir and displaces and releases the test drug through the flow modulator. The rate at which water enters the osmotic sleeve is regulated by the water permeability of the semi-permeable membrane, its dimensions and the osmotic pressure difference across the membrane. The pumps are designed to deliver at a constant rate due to the presence of a driving agent in the osmotic sleeve which maintains constant osmotic activity during the lifetime of the pump. The pumps were sterile and bubble packed.

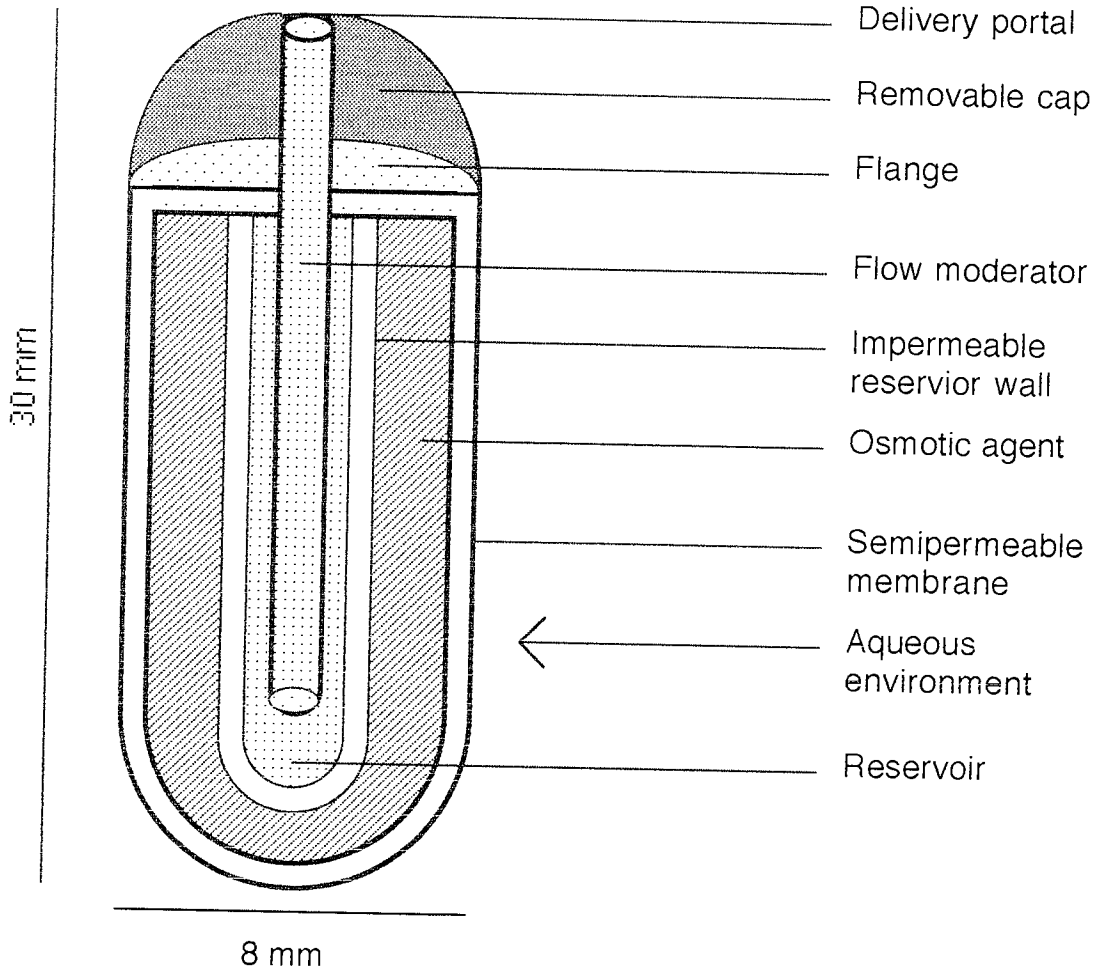

Figure 2.1: Alzet osmotic pump. Cross sectional representation of an Alzet osmotic pump showing design, components and mechanism of operation.

2.2.3.3 Filling Alzet osmotic pump.

During filling, the pumps were handled with surgical gloves as skin oils could interfere with the performance of the pump if allowed to accumulate on the surface. Prior to filling, the empty pump and flow modulator were weighed. The pump was then filled at room temperature with drug using a syringe and a blunt tipped filling tube. All drug solutions were sterilised prior to loading into pumps by filtering through a 0.22μm syringe-end filter (Millex Filter Unit, Millipore). After careful filling of the pump, the flow modulator was inserted and the entire unit was weighed. The total volume of drug in the reservoir was calculated by subtracting the two weights. Incorrectly filled pumps had potential to display unpredictable pumping rates and were therefore refilled. In order to ensure that pumps ready for animal implantation would operate at the correct pumping rate, filled pumps were placed in isotonic saline at 37°C for 4 hours to allow the pumping rate to reach steady state. This steady state pumping rate could be maintained until 95% of the contents have been delivered. There was a 5% reservoir residual volume which could not be displaced.

2.2.3.4 Surgical subcutaneous implantation and removal of Alzet osmotic pumps.

The most usual site for subcutaneous implantation of the pumps in mice is on the back, slightly posterior to the scapulae. Mice were shaved and the skin of the implantation site area was disinfected before anaesthesia was induced with 3% halothane/ 50% oxygen/ 50% nitrous oxide. During surgery, halothane administration was reduced to and maintained at 1.5%. A mid-scapular incision was then made adjacent to the site using a scalpel. Spencer Wells forceps were then inserted into the incision and the jaws were opened so as to spread the subcutaneous tissue to create a pocket for the pump. The pocket was made about 1cm larger than the pump to allow for some movement. The pump was never inserted directly below the incisional wound were it could interfere with correct healing of the incision. The pump was inserted into the pocket with the delivery portal end first and the wound was closed using suture stitching. The wound was treated with a centrimide-containing cream to prevent infection. Mice usually made a complete recovery from the procedure within 5 minutes.

In experiments where the removal of the pump was required, this was again performed under anaesthesia. An incision was made adjacent to the original incision and the pump was carefully removed. The new wound was then closed using suture stitching and mice allowed to recover as before.

2.2.3.5 In vitro assessment of pumping rate.

A simple *in vitro* test was carried out to verify that the pumping rate of the Alzet unit remained constant within the recommended time scale. A pump was filled with 0.01M Coomassie Brilliant Blue solution prepared in 0.9% saline and incubated in isotonic saline for the 4 hour priming period. The pump was then transferred to a clean vessel containing 4ml of fresh saline and incubated at 37°C for 24 hours. This procedure was repeated every 24 hours for a period of 9 days. For each day therefore, the total amount of coloured compound released in a given period of time was collected. The precise concentration of Coomassie Blue released was established by performing spectrophotometric scans of the samples collected each day. Coomassie Blue gives a distinctive peak at 595nm thus by using the Beer Lambert law (checks were made that the compound obeyed the law by calculating the molar extinction coefficient at a variety of concentrations), the concentration and hence, compound delivery rate was calculated per day.

Independent studies were also carried out to check that there was no leakage of osmotic agent from the pump by carrying out similar experiments using pumps filled with saline only. A spectrum was obtained for the osmotic agent using a solubilised sample obtained from a dissected pump. This agent was found to give a distinctive peak at 276nm, but was not found to leak from the pumps during experimentation. When the daily samples in these experiments were scanned, only a constant absorption profile was obtained corresponding to the background sodium chloride present in the collecting medium (peaks were recorded at 283nm). Although PYR gave a distinctive peak at 270nm, it could not be used in the experiments to monitor flow rate because it did not obey the Beer-Lambert law. Verification of the pumping rate of the osmotic pump is discussed in Appendix A.3.

2.3 Preparation of diaphragm.

Mice were killed by a blow to the head and section of the cervical spinal cord. Skin was removed from the chest area and the thorax was opened allowing the dissection and removal of the whole diaphragm. The isolated diaphragm was immediately placed in physiological saline which had been gassed with 95% O_2/ 5% CO_2 and divided into left and right hemidiaphragms by section of the central tendon where required.

2.4 Biochemical methods for the assay of ChE activity.

2.4.1 Estimation of ChE activity using a spectrophotometric assay technique.

A spectrophotometric assay technique based on the method of Ellman et al., (1961) was used to determine the activity of ChE in enzyme extracts from mouse diaphragm and blood. This method was chosen due to its simplicity, sensitivity and reproducibility and has been widely used for routine determination of ChE activity.

2.4.1.1 General principle.

The spectrophotometric enzyme assay to determine ChE activity follows the rate of production of thiocholine, a product of the ChE catalysed hydrolysis of the substrate acetylthiocholine. The thiocholine continuously reacts with 5,5,-dithiobis-2-nitrobenzoate ions present in the reagent DTNB to yield a yellow coloured anionic product, 5-thiol-2-nitro benzoic acid. This product absorbs UV light at 412nm hence the rate of change of absorbance at this wavelength can be linked to enzyme activity.

Acetylthiocholine ----------> thiocholine + acetate.
Thiocholine + DTNB----------->YELLOW COLOUR.

2.4.1.2 Instrumentation.

The rate of hydrolysis of acetylthiocholine by ChE present in enzyme extracts was determined using a Philips PU8700 Series UV/VIS fixed bandwidth spectrophotometer with a Philips colour plotter, PU8700 cell programmer with multi-cell holder and temperature control as accessories.

Using the scan programme option of the spectrophotometer, a profile of the Ellman reaction was obtained in the wavelength range 200-600nm. During the course of the reaction a peak developed at 412nm corresponding to the formation of coloured product. Using the cell programmer option, the absorbance of multiple samples at a fixed wavelength of 412nm was recorded continuously for periods of 5 seconds and measurements were repeated at pre-selected time intervals of 1 minute for 10 minutes.

2.4.1.2 General procedure.

Prior to assay of samples for enzyme activity, the spectrophotometer was blanked by running a cuvette containing extraction buffer through the instrument in the reference compartment. This restored the baseline to zero. It was sufficient to blank the spectrophotometer only once prior to assaying samples. Prior to mixing assay reagents, glass test tubes were warmed to 30°C in a water bath. The assay mixture was prepared by adding 1ml of enzyme sample to the test tube followed by 1ml of DTNB colour reagent (see Appendix A.1.1). To initiate the reaction, 1ml of a 1.5mM stock solution of acetylthiocholine iodide substrate (see Appendix A.1.2) was added to each tube to give a final assay substrate concentration of 0.5mM (enzyme kinetic studies using purified electric eel AChE were carried out to determine the K_m value for the enzyme: see Appendix A.2). The contents of each tube was then mixed and transferred to a plastic disposable cuvette in the spectrophotometer. The change in absorbance at 412nm was then recorded every minute over a 10 minute period.

2.4.2 Preparation of diaphragm for routine ChE determination.

Hemidiaphragms were pinned via the ribs and central tendon to Sylgard in a petri dish. Connective and adipose tissue was trimmed away, the phrenic nerve was cut close to the muscle and excess blood was removed by gently squeezing the blood vessels.

The central tendon and ribs were trimmed and a central strip, 3mm wide was cut containing nerve terminal branches. This region was designated the junctional region (J) and contained virtually all the endplates. The remainder of the hemidiaphragm, consisting of two strips adjacent to the central region was designated the non-junctional region (NJ). J and NJ regions were blotted dry and weighed. Typical J regions weighed 25mg.

2.4.3 Extraction of ChE from mouse diaphragm.

2.4.3.1 Conventional extraction method.

The method employed previously in the laboratory shall be referred to as the conventional extraction method. J and NJ regions were each placed in centrifuge tubes containing 2ml of ice-cold 0.1M phosphate buffer at pH8.0 and homogenised for 1 minute using an Ultra Turrax T25 homogeniser set to give an output of

24,000rpm. The homogeniser was washed with 3ml of ice-cold buffer to give a final sample volume of 5ml. All samples were kept on ice during homogenisation. The 5ml homogenate samples were then sonicated using a high intensity 50watt model ultrasonic processor (Jencons). Sonication programmes were varied according to experiment. The homogenate was finally centrifuged at 2700rpm for 15mins in a Beckmann T.J. bench centrifuge at 4°C. The supernatants were removed for assay of ChE activity and pellets were discarded. Samples were kept on ice till assay.

2.4.3.2 Sequential extraction of high and low molecular forms of AChE.

The sequential extraction technique of Younkin et al., (1982) was used to extract globular and asymmetric molecular forms of AChE from endplate and non-endplate regions of muscle fibres. Globular and asymmetric forms of AChE can be selectively extracted on the basis of their differential solubility in low and high ionic strength buffer. If a set of extractions are performed sequentially, then the majority of tissue AChE molecular forms can be extracted by this method and appear in various extraction fractions. At each stage in the process, a homogenate was prepared in the appropriate buffer. Low ionic strength buffer was used to preferentially extract globular forms and high ionic strength buffer was used to extract asymmetric forms. Samples were centrifuged for 30mins at 39,000g. The supernatant was removed and assayed spectrophotometrically by the Ellman method for enzyme activity. The pellet was re-suspended in buffer and homogenised for the next stage in the process (the process is summarised in Figure 2.2).

J and NJ regions from the left and right hemidiaphragm of each diaphragm were pooled together and sequential extraction was carried out on each region independently. Extracts were prepared in 4ml of appropriate buffer and were maintained at 4°C throughout the process. Extracts were homogenised for 1 minute using an Ultra Turrax T25 homogeniser which was washed thoroughly with 100ml of distilled water between extractions and centrifuged in a Beckmann J2-21 centrifuge with a temperature control unit set to 4°C.

The first extraction was carried out using low ionic strength 10mM phosphate buffer, pH7.0 containing 1% Triton X-100 (LIB) and was intended to extract globular forms of AChE. The supernatant rendered was called S1. A second extraction was also carried out in LIB which yielded supernatant S2 in the attempt to ensure that any residual globular forms in the tissue were removed. The third extraction was carried out in high ionic strength 10mM phosphate buffer at pH7.0 containing 1% Triton X-100 and 1.0M NaCl (HIB) to extract asymmetric forms.

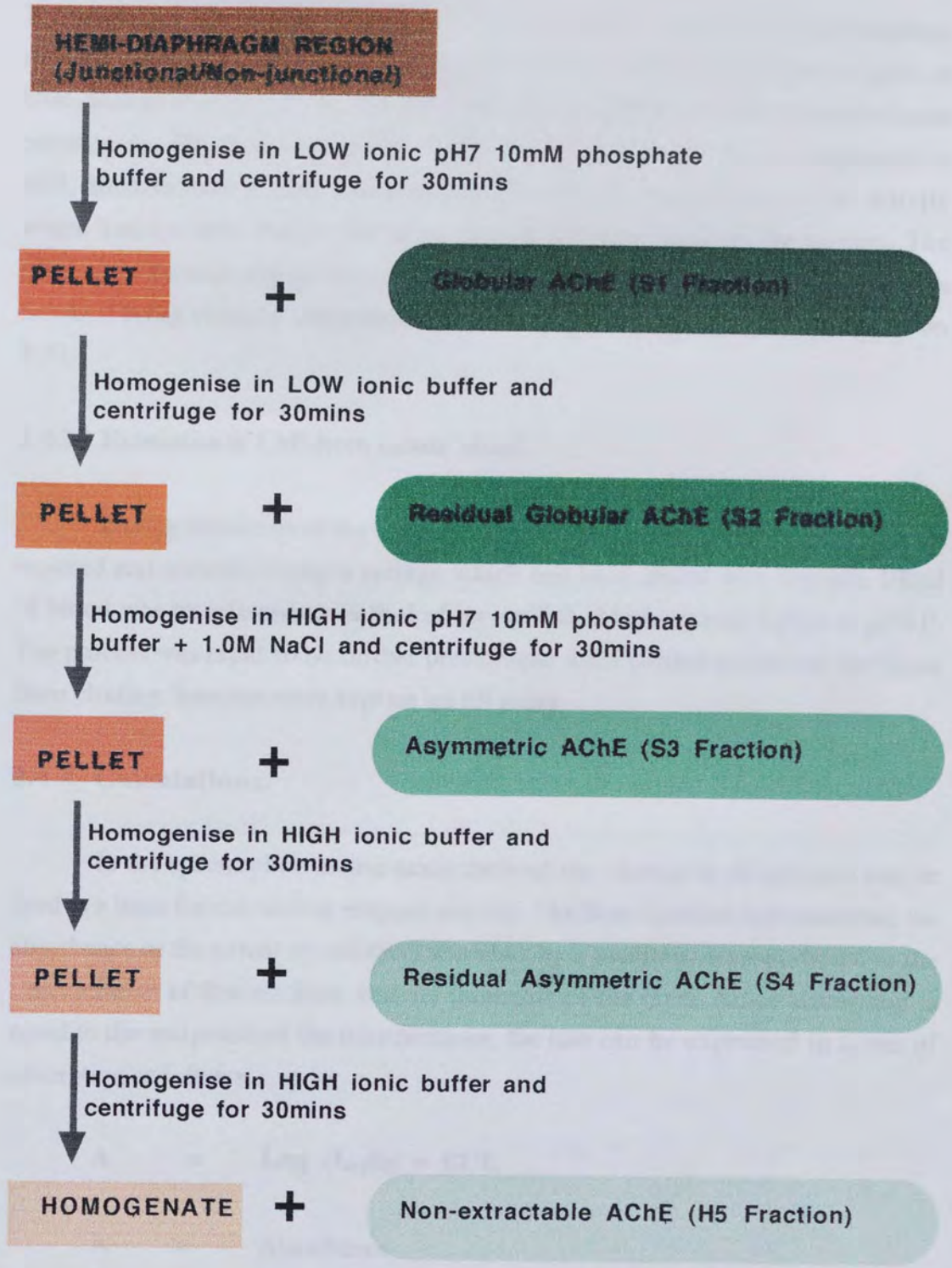

Figure 2.2: Sequential extraction of the molecular forms of AChE. Schematic representation of the sequential extraction technique for the separation of low and high molecular weight forms of AChE on the basis of their differential solubility in low ionic pH7.0, 10mM phosphate buffer and high pH7.0, 10mM phosphate buffer + 1.0M NaCl based on the method of Younkin et al., 1982.

The supernatant was called S3. Due to the structure of the asymmetric enzymes, they can only be solubilised in a high ionic media. The fourth extraction, again in HIB, was performed to remove any residual asymmetric forms from the tissue preparation. The pellet remaining following removal of S4 was re-suspended in HIB, homogenised to give a homogenate H5 and assayed for any AChE activity which had not been readily extracted during previous stages in the process. The precise molecular composition of each fraction; S1, S2, S3, S4 and H5 was checked using velocity sedimentation on sucrose density gradients (see Section 2.5).

2.4.3.3 Extraction of ChE from mouse blood.

During dissection of the diaphragm, the left or right limb femoral artery was exposed and severed. Using a syringe which had been rinsed with heparin, 100μl of blood was transferred to 19.9ml of ice-cold 0.1M phosphate buffer at pH8.0. The process was rapid so no further precautions were needed to prevent the blood from clotting. Samples were kept on ice till assay.

2.4.4 Calculations.

In the spectrophotometric assay method, the change in absorbance can be used as a basis for calculating enzyme activity. The Beer-Lambert law states that the absorbance or the extent of radiation absorbed by a medium, is proportional to the concentration of that medium and the thickness of the layer. Since absorption is equal to the reciprocal of the transmittance, the law can be expressed in terms of absorption as follows:

$$\mathbf{A = Log\ (I_o/I_t) = ECL}$$

A	=	Absorbance
I_o	=	Intensity of incident radiation
I_t	=	Intensity of transmitted radiation
E	=	Molar extinction coefficient for the absorbing medium (in units of litres mol^{-1} cm^{-1})
C	=	Concentration of the absorbing solution (molar)
L	=	Length of light path in the absorbing material (in cm)

Enzyme activity, expressed as the rate of hydrolysis of a given substrate, can be calculated from a general equation which applies to all spectrophotometric assays where the Beer-Lambert Law applies which is shown below:

$$\textbf{Enzyme activity} = \frac{\Delta A}{E\ L}$$

ΔA = Rate of change in absorbance at the experimental wavelength (min^{-1}).
E = Molar extinction coefficient for the absorbing medium (litres mol^{-1} cm^{-1}).
L = Length of light path in the cell (cm).

In the spectrophotometric assay of ChE activity, the above equation can be used as follows. The molar extinction coefficient for DTNB is 1.36×10^4 litres mol^{-1} cm^{-1}. Enzyme activity is usually in the order of nanomoles and for experimental purposes E is required in millilitres (i.e. small sample volumes were used) hence:

$$E_{(DTNB)} = 1.36 \times 10^4 \times 10^3 \times 10^{-9} \text{ ml nmol}^{-1} \text{ cm}^{-1}$$
$$= 1.36 \times 10^{-2} \text{ ml nmol}^{-1} \text{ cm}^{-1}$$

Since the length of the light path in the cuvette was 1cm, enzyme activity (i.e. the rate of hydrolysis of acetylthiocholine substrate) can be calculated from the following equation:

$$\text{Enzyme activity} = \frac{\Delta A_{(412nm)} \text{ min}^{-1}}{1.36 \times 10^{-2} \text{ml nmol}^{-1} \text{ cm}^{-1} \times 1\text{cm}}$$

In the routine determination of ChE activity if the concentration of tissue in a given sample was X mg ml^{-1} (determined from the weight of the tissue and the extraction buffer volume), the cuvette volume was 3 ml and the volume of tissue sample in the cuvette was 1 ml, then the activity can be expressed as follows:

$$\text{Enzyme activity} = \frac{\Delta A_{(412nm)} \text{ min}^{-1} \times 3\text{ml}}{1.36 \times 10^{-2} \text{ml nmol}^{-1} \text{cm}^{-1} \times 1\text{cm} \times X\text{mg ml}^{-1} \times 1\text{ml}}$$

$$= \frac{\Delta A_{(412nm)} \times 220.59}{X} \quad \text{nmol min}^{-1} \text{ mg}^{-1}$$

For the calculation of enzyme activity in the sequential extraction method, during the extraction process the molecular forms from a given tissue

region were extracted into a total volume of 20ml of buffer. The concentration of tissue in a given sample Xmg ml^{-1} was calculated by dividing the sample weight in mg by 20ml. Hence, in calculating the activity of molecular forms, although they were extracted sequentially, their overall activity was expressed with respect to the tissue of origin. The same calculations were then applied as for the routine ChE determination.

Since 0.1ml of whole blood was extracted into 19.9ml of phosphate buffer and hence diluted 1 in 200 times, in each 1ml of diluted sample there was $5x10^{-3}$ml of whole blood. In the calculation of whole blood activity the sample volume was $5x10^{-3}$ml, the cuvette volume was 3ml and the following equation was used:

$$\text{Enzyme activity} = \frac{\Delta A\ (412nm)\ min^{-1} \times 3ml}{1.36 \times 10^{-2}ml\ nmol^{-1}\ cm^{-1} \times 1cm \times 5x10^{-3}ml}$$

$$= \Delta A\ (412nm) \times 44118\ nmol\ min^{-1}\ ml^{-1}$$

Since the calculation tended to give large figures for whole blood ChE activity, a conversion to μmolar units from nmolar units was made and the activity was routinely calculated as:

Enzyme activity = $\Delta A\ (412nm) \times 44.118\ \mu mol\ min^{-1}\ ml^{-1}$

2.4.4.1 Expression of ChE activity.

ChE activities in tissue and the activity of AChE molecular forms were calculated and routinely expressed as nmol of acetylthiocholine hydrolysed min^{-1} mg^{-1} (abbreviated to nmol min^{-1} mg^{-1}). Whole blood ChE activity was expressed as μmol min^{-1} ml^{-1}.

2.4.5 Determination of endplate-specific activity.

Many attempts have been made in the past to give an accurate representation of AChE activity which is associated with the endplates of skeletal muscle fibres in isolation to the AChE which is found in the rest of the muscle. Since it is very difficult to extract the endplate enzyme without extracting enzyme found in other parts of the fibres and not very practical to use the complex methods available when rapid extraction is required, a more common way of assessing the endplate activity has involved the use of various calculations.

Previous attempts made by researchers to assess the endplate-specific enzyme activity by calculation have found it a daunting task. They have been faced with the question: which is the best way to investigate the activity of an enzyme which is part of a complex network of inter-related molecular forms which span the entire muscle? As yet, there are no hard and fast rules for calculating this activity. One of the more common ways to tackle this issue has been to make the following assumption. It was assumed that the J and NJ regions of each muscle fibre are similar except that a small portion (<1%) of each fibre in the J region is specialised as an endplate. Bearing this in mind it was therefore assumed that ChE activity per mg of J and NJ tissue was the same and ChE activity associated specifically with the endplate (EPS) was the difference between J and NJ ChE activity per mg of tissue. The following three equations represent different calculations commonly used to determine endplate-specific AChE activity (Das, 1989).

$$\mathbf{EPS_1 = J - NJ} \qquad \text{nmol min}^{-1}\text{ mg}^{-1} \qquad (1)$$

$$\mathbf{EPS_2 = W_J\ (J - NJ)} \qquad \text{nmol min}^{-1} \qquad (2)$$

$$\mathbf{EPS_3 = \frac{W_J\ (J - NJ)}{W_J + W_{NJ}}} \qquad \text{nmol min}^{-1} \qquad (3)$$

J = Junctional activity per mg of tissue.

NJ = Non-junctional activity per mg of tissue.

W_J = Weight of junctional region (mg).

W_{NJ} = Weight of non-junctional region (mg).

2.5 Separation of AChE molecular forms by differential centrifugation.

Differential centrifugation was used to separate the six molecular forms of AChE : G1, G2, G4, A4, A8 and A12 and was carried out to determine the precise molecular composition of each of the 5 enzyme fractions: S1, S2, S3, S4 and H5 obtained by the sequential extraction technique. This technique was not used routinely to determine AChE activity because the entire separation and analysis process could take around 24 hours to complete and was not appropriate for studies involving reversible inhibitors or irreversible inhibitors over longer time periods (Hobbiger, 1976).

2.5.1 General principle.

The molecular forms of AChE were separated by velocity sedimentation on a 5-20% linear sucrose density gradient of volume 12ml in a 13.5ml thin walled centrifuge tube. Sucrose gradients were prepared in enzyme extraction buffers. The gradient was made using a BioRad Econo Pump gradient former with a flow rate of 1ml min^{-1}. Enzyme extracts of sample size 1ml were carefully layered to the top of the gradient using a pipette. Gradients were centrifuged for 18.5 hours at 38,000rpm in a Beckman 18-M ultracentrifuge with a SW40Ti rotor. The centrifuge contained a refrigeration unit which was set to 4°C during the process.

2.5.2 Preparation of samples for velocity centrifugation.

Sequential extraction fractions were prepared at double the concentration required for routine enzyme determination. Due to the duration of the separation process a range of protease inhibitors : EGTA 3.8 mg ml^{-1}, benzamidine 0.3 mg ml^{-1}, aprotinin 0.2mg ml^{-1}, bacitracin 1 mg ml^{-1}, pepstatin 0.02 mg ml^{-1} and trypsin inhibitor 0.1 mg ml^{-1} were added to enzyme samples to ensure that there was minimal degradation of higher molecular forms during the period of separation.

2.5.3 Calibration of sucrose density gradient.

Sucrose gradients were calibrated using markers with known sedimentation coefficients: ß-galactosidase (16.14S), catalase (11.3S) and alcohol dehydrogenase (4.8S). These were added to samples prior to application to the gradient. The position of the markers on the gradient was determined by the appropriate assay shown below.

ß-galactosidase :	assay at 410nm by incubation at pH7.5 with 10nM p-nitrophenylgalactopyranoside in the presence of 1.5mM $MgCl_2$.
catalase :	assay at 210nm by incubation at pH7.5 with hydrogen peroxide.
alcohol dehydrogenase :	assay at 310nm by incubation at pH8.6 with 1.0M ethanol in the presence of ß-NAD.

2.5.4 Fraction collection and peak detection.

Fractions were collected from the gradients after centrifugation using the BioRad Econo Pump set in reverse mode. The pump tube was inserted into the bottom of the tube and fractions were collected in a carousel with a pre-set rotation time to collect fractions of volume 0.5ml. A total of 27 fractions were collected from each gradient. Fractions were assayed for AChE activity spectrophotometrically by the Ellman method. Sedimentation profiles were obtained for each sample by plotting fraction AChE activity against fraction number.

2.6 Histochemical methods.

2.6.1 Histochemical localisation of ChE.

The method of Karnovsky and Roots (1964) was used for the histochemical localisation of ChE. The method involves the hydrolysis of acetylthiocholine substrate by enzyme present in whole, fixed hemidiaphragms. Thiocholine liberated in the process reduces ferricyanide present in the stain medium to ferrocyanide which reacts with copper ions to form an insoluble copperferrocyanide precipitate (Hatchett's Brown). Copper ions present in the medium are complexed with citrate to prevent formation of copper ferricyanide.

The brown coloured precipitate is produced directly at sites of enzyme activity. The stain develops gradually and may be monitored to prevent over-staining by visualising tissues under a microscope. The staining procedure was carried out under controlled pH conditions. At stain pH greater than 5, the brown reaction product diffuses out of the endplate and gives and inaccurate definition of endplate shape.

2.6.2 Preparation of tissues for staining.

Hemidiaphragms were trimmed away from the ribs and connective tissue and the phrenic nerve was removed from them. Hemidiaphragms were then incubated in freshly prepared stain medium at room temperature. Staining of endplates could be seen after 20-30mins. The brown colour was allowed to develop until a large number of endplates were well defined and could be clearly visualised. Tissues were then removed from the stain, washed in distilled water and fixed in 4% formaldehyde in 0.2M acetate buffer at pH4 overnight before being mounted in glycerol jelly on glass microscope slides.

2.6.3 Measurement of endplate dimensions.

The widths and lengths of 30 endplates from each hemidiaphragm were measured in microns using a Zeiss microscope. All measurements were made using a graduated scale placed in the x10 eyepiece of the microscope and slides were viewed with a x40 objective. The microscope was calibrated using a stage micrometer and dimensions were measured in microns. Measurements were made by moving isolated endplates into the centre of the field of view (slides were always mounted so that muscles fibres appeared vertically across the field of view) and rotating the eyepiece so that the graticule scale was horizontal for width measurements and vertical for length measurements. The preparation was always moved in the same direction throughout the counting process and never moved backwards to ensure that the same endplate was not counted twice. Endplates were selected for measurement if they satisfied the following criteria:

(a) The endplate in focus must be located on a muscle fibre which could be clearly visualised and also be in focus.
(b) The outline of the endplate must be clearly defined so that all the stained product was retained within the boundary of the endplate and not diffused out.
(c) The endplate must be flat on the muscle fibre and be completely in focus. Endplates which were wrapped around fibres in focus or on fibres not in focus or overlapping other endplates were rejected.

It was found that despite the numerous endplates contained within each hemidiaphragm, few were ideally stained and satisfied the criteria discussed above. The ANOVA one-way test was applied to groups of 30 endplates measured from different hemidiaphragms which had received the same treatment to test the inter-mouse variation. The results of the test and the corresponding F-test values are shown in the appendix in Table A.9. In mice which had received the same treatment, an inter-hemidiaphragm variation was found which was independent of treatment and generally random. This may be due to differences in the staining of each hemidiaphragm or due to inter-mouse variation. In some cases: 8% of widths, 33% of lengths and 25% of width/length ratios the variation was significant (ANOVA, $P<0.0001$) but in the remaining cases the variation was not significant (each type of treatment w.r.t. drug and dose was taken to be one case). The between hemidiaphragm variation at each treatment was therefore taken into account in the overall analysis of endplate dimensions. The endplate data was analysed

using a multi-factor analysis of variance test (MANOVA) with a one-level nested design on the PC statistics package STATISTICA. The MANOVA model was designed to simultaneously test the between treatment variation and the within treatment variation.

2.7 Electrophysiological methods.

2.7.1 Recording of extra-cellular miniature endplate potentials .

The biochemical and histochemical assessment of mouse skeletal muscle responses to a range of anti-ChE treatments was carried out in collaboration with electrophysiological investigations of the mouse diaphragm conducted by A. Crofts. Throughout the thesis data obtained from analysis of extra-cellular miniature endplate potentials $(MEPPs)_o$ recorded by A. Crofts has been utilised and analysed in conjunction with corresponding biochemical data. A brief summary of the methods employed by A. Crofts is given below.

MEPPs were first characterised by Fatt and Katz (1950, 1952) who discovered spontaneous sub-threshold activity recorded from the surface of isolated muscle using an electrode near the nerve and an indifferent electrode at some distance away. These potentials varied in amplitude but had a consistent time course. They were localised at the neuromuscular junction and resembled endplate potentials in shape but had smaller amplitudes and were therefore aptly named 'miniature endplate potentials'. $(MEPPs)_o$ essentially resemble intra-cellular MEPPs in shape but represent different cellular events.

The recording of $(MEPPs)_o$ at the neuromuscular junction of mouse skeletal muscle was performed on hemidiaphragms which were dissected from mice and pinned out on Sylgard in a water-bath of volume 16ml which contained Liley's physiological saline gassed with carbogen (95% O_2/ 5% CO_2). Recordings were made with capillary micro-electrodes made from GC100TF-15 borosilicate glass (Clark Electromedical Instruments) with tip diameter 3-5μm pulled in two stages on a Kopf needle/pipette puller (model 750) and filled with Liley's saline. $(MEPPs)_o$ were recorded using a WPI duo 773 electrometer and Devices AC pre-amp 3160 with high and low frequency filters set at 10KHz and 0.8Hz respectively. Traces were displayed on a Tektronix dual beam oscilloscope D12 with a 5A81N dual trace amplifier and a 5B10N time base/amplifier. Recordings were analysed using an AD1N8 program or recorded onto Maxell 25-120 magnetic tape and analysed on a Northstar computer.

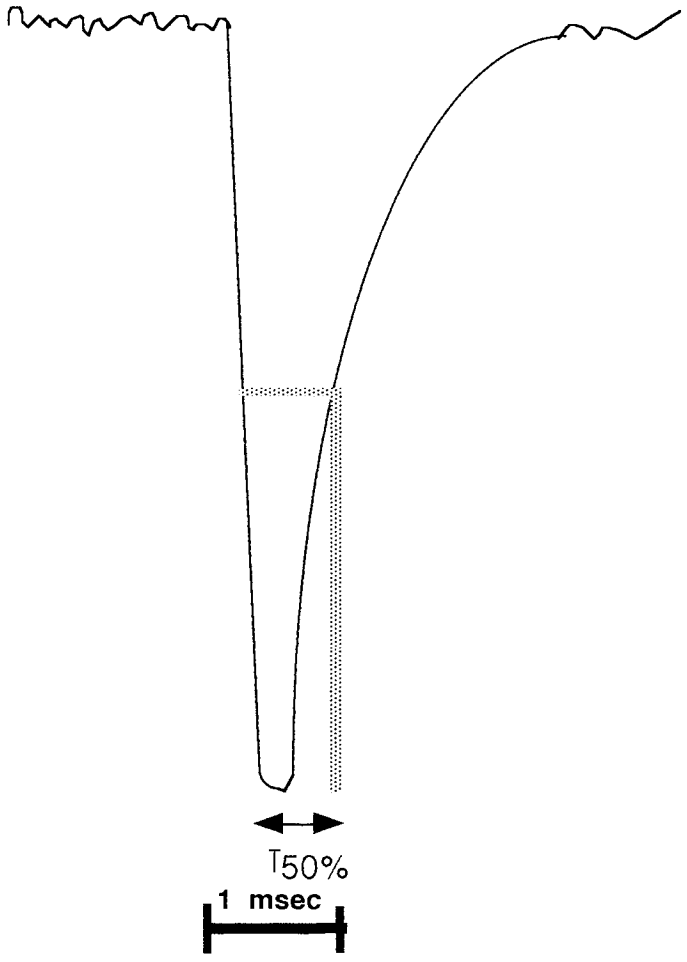

Figure 2.3: Extracellularly recorded miniature endplate potential. The $T_{50\%}$ is shown as the time from the peak amplitude to the half amplitude of the decay phase in milliseconds.

2.7.2 Measurement of time to half amplitude ($T_{50}\%$) of $(MEPPs)_o$.

The measurement of various parameters was carried out manually from traces of $(MEPPs)_o$ plotted on the Northstar computer which had been reproduced onto standard 80g A4 paper. Figure 2.3 shows a representation of a characteristic $(MEPPs)_o$ trace. The time to half amplitude ($T_{50}\%$) of $(MEPPs)_o$ was measured as the time from the peak amplitude of the trace to half the amplitude of the decay phase and was expressed in milliseconds.

The $(MEPPs)_o$ consists of two components: the rise phase and the decay phase. In electrophysiological studies related to the behaviour of anti-ChEs, the decay phase is important and is governed by the termination of transmitter action and its diffusion from the synaptic cleft .

In the event of inhibition or reduction of AChE, the action of transmitter on its receptor is prolonged and can be visualised by changes in the decay phase. These changes can be quantified by measurement of $T_{50}\%$ which is the time taken for the potential to decay to half amplitude. There is therefore a distinct relationship between the inhibition or reduction of synaptic AChE and the properties of $(MEPPs)_o$ decay phase.

2.8 Statistical tests.

The sample sizes of data from blood and diaphragm enzyme activity studies were too small to determine whether the data was normally distributed and the use of parametric tests was not appropriate. The Mann-Whitney non-parametric test was used were appropriate to compare two groups and the Spearman's rank non-parametric test was used to determine the correlation between data. In treatment studies the Kruskal-Wallis one-way analysis of variance by ranks test (K-S ANOVA) was initially used for groups in a treatment set for each enzyme to test the null hypothesis that the groups come from identical populations. When the test result was not significant, the null hypothesis of no difference between groups was accepted and no further analysis was performed on these groups. When the test result was significant, the null hypothesis of no difference between groups was rejected and the alternative hypothesis of differences between groups was accepted. These groups were analysed further using the Kruskal-Wallis multi-comparison test (Siegel and Castellan, 1988) to determine which groups were different within the treatment set for a given enzyme.

The samples sizes of hemidiaphragm endplate groups were large and found to be normal (STATISTICA normality tests) and parametric tests were therefore used. The one-way analysis of variance test (ANOVA) was initially used to test the null hypothesis that all groups in a given treatment set for a particular parameter are not different. When the ANOVA test was not significant the null hypothesis was accepted. When the result was significant the null hypothesis was rejected and the alternative hypothesis was accepted that there were differences between groups. The latter groups were further analysed using a one-level nested design model multi-factor analysis of variance test (MANOVA) and post-hoc comparison as described by Myers (1977) was performed to determine which groups in the treatment sets were different.

CHAPTER 3

THE EXTRACTION OF MOUSE DIAPHRAGM ACETYLCHOLINESTERASE

3.1 Introduction.

Prior to conducting any studies of inhibition, it was necessary to find a rapid and reproducible method for extracting the various molecular forms of AChE from mouse diaphragms which would be suitable for investigating the actions of irreversible and reversible inhibitors.

The conventional enzyme extraction method has been extensively used in the past for the routine determination of ChE activity. Due to its simplicity, this method, although rapid and reproducible, does not differentiate between ChE and AChE or between the six different molecular forms of AChE of which the A12 form is probably the most functionally important (Hall, 1973). In 1982, Younkin et al., adapted techniques used by Bon and Massoulie (1980) and Bon et al., (1979) to develop a sequential extraction method for selectively extracting AChE (in isolation to ChE) and distinguishing between globular and asymmetric forms due to their differential solubility in low and high ionic strength buffer respectively. In addition, the method gave the activity of non-readily extractable asymmetric AChE which was associated with the extra-cellular matrix. The precise molecular composition of the sequentially extracted fractions can be determined by velocity sedimentation on sucrose density gradients.

Neither method gives a direct measure of AChE which is associated with endplates alone. Hence, is this section an attempt was made to best represent endplate AChE and hence determine AChE activity likely to be associated with the synaptic cleft. The aims of this section can be summarised as follows:

(a) To rapidly extract AChE molecular forms from mouse diaphragms and identify fraction composition.
(b) To represent endplate-specific AChE.
(c) To determine the activity of AChE associated with the synapse.

3.2 Results and discussion.

3.2.1 Extraction of mouse diaphragm ChE by the conventional method.

Junctional (J) and non-junctional (NJ) ChE activities in left and right side hemidiaphragms are shown in Table 3.1. Statistical analysis using the Mann-Whitney non-parametric test showed that there was no significant difference between left and right hemidiaphragm ChE activity (see Figure 3.1) and data was

	J activity	NJ activity	EPS_1 activity (J-NJ)	EPS_2 activity $W_J(J-NJ)$	EPS_3 activity $\frac{W_J(J-NJ)}{W_J+W_{NJ}}$
Left HD	2.01	1.44	0.76	-	-
	±0.87	±0.59	±0.56		
	(21)	(21)	(21)		
Right HD	1.76	1.42	0.48	-	-
	±0.67	±0.55	±0.24		
	(24)	(24)	(24)		
Output 100	1.10	1.13	0.26	-	-
6 cycles	±0.30	±0.32	±0.26		
	(17)	(17)	(17)		
Output 60	2.08 ***	1.78 ***	0.52	-	-
6 cycles	±0.26	±0.38	±0.16		
	(6)	(6)	(6)		
Output 60	2.94 **	2.38 **	0.56	-	-
4 cycles	±0.24	±0.18	±0.29		
	(4)	(4)	(4)		
Output 60	2.84 **	2.09	0.75	-	-
3 cycles	±0.58	±0.49	±0.31		
	(5)	(5)	(5)		
	2.02	1.39	0.36	8.11	0.23
	±0.73	±0.58	±0.24	±5.32	±0.17
	(37)	(37)	(37)	(37)	(37)
CV	**36.1%**	**41.7%**	**66.7%**	**65.7%**	**73.9%**

Table 3.1: Conventional extraction method diaphragm ChE activity. The activity of junctional (J) and non-junctional (NJ) ChE in left and right hemidiaphragms (HD) and at different sonication programmes and EPS values calculated by three different methods: 1, 2 and 3 (See Section 2.4.5). Activities are in nmol min^{-1} mg^{-1}. Co-efficients of variation (CV) are in bold. N numbers are in parentheses and all values are means ± standard deviation (s.d.). ** and *** denote values significantly different from the first sonication programme values (Mann-Whitney, $P<0.02$ and $P<0.002$ respectively). Units:J,NJ,EPS_1(nmol min^{-1} mg^{-1}),EPS_2(nmol min^{-1}),EPS_3(nmol min^{-1}).

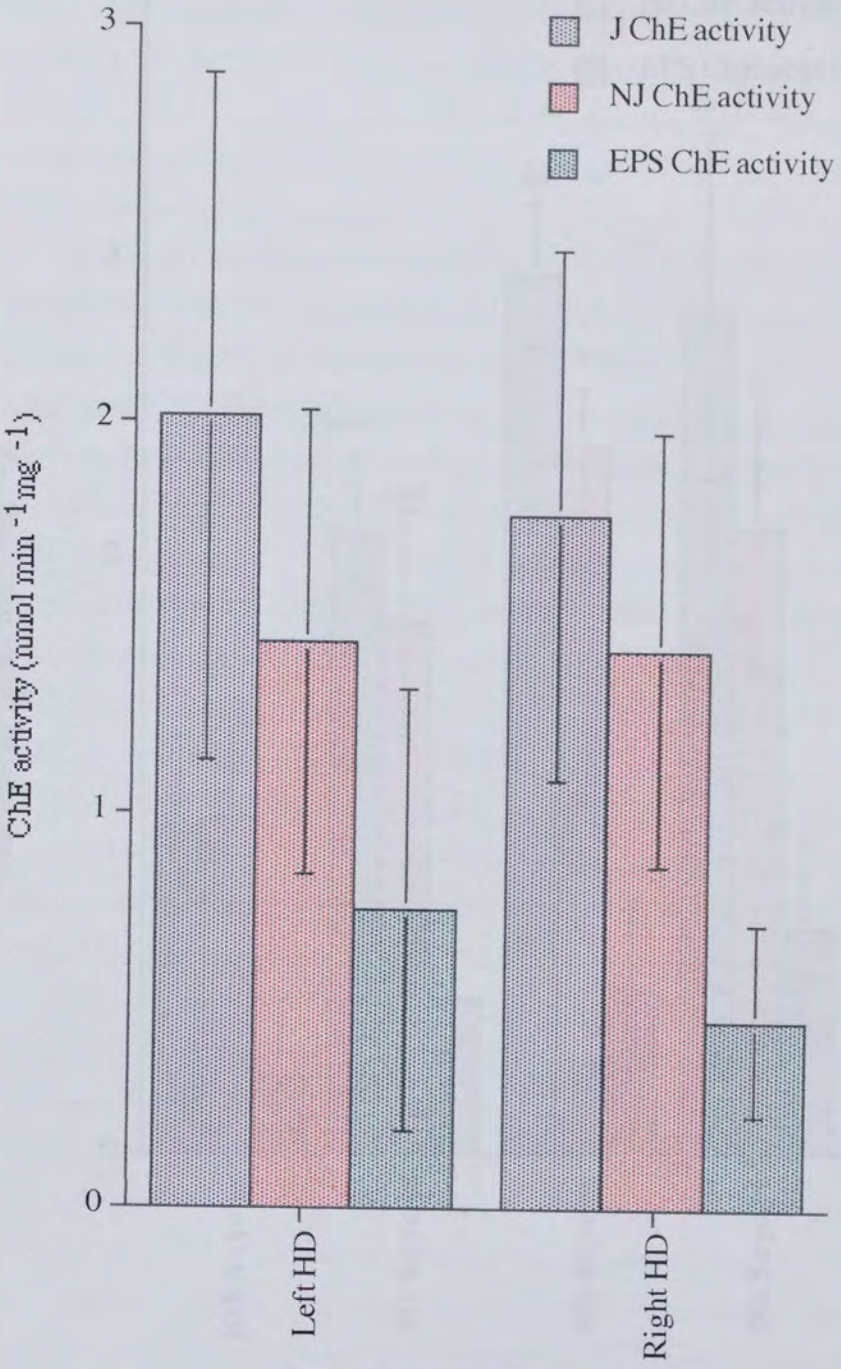

Figure 3.1: Left and right hemidiaphragm ChE. ChE activity in the junctional (J), non-junctional (NJ) and endplate-specific (EPS) regions of left and right mouse hemidiaphragms showing there are no significant differences between the enzyme activities.

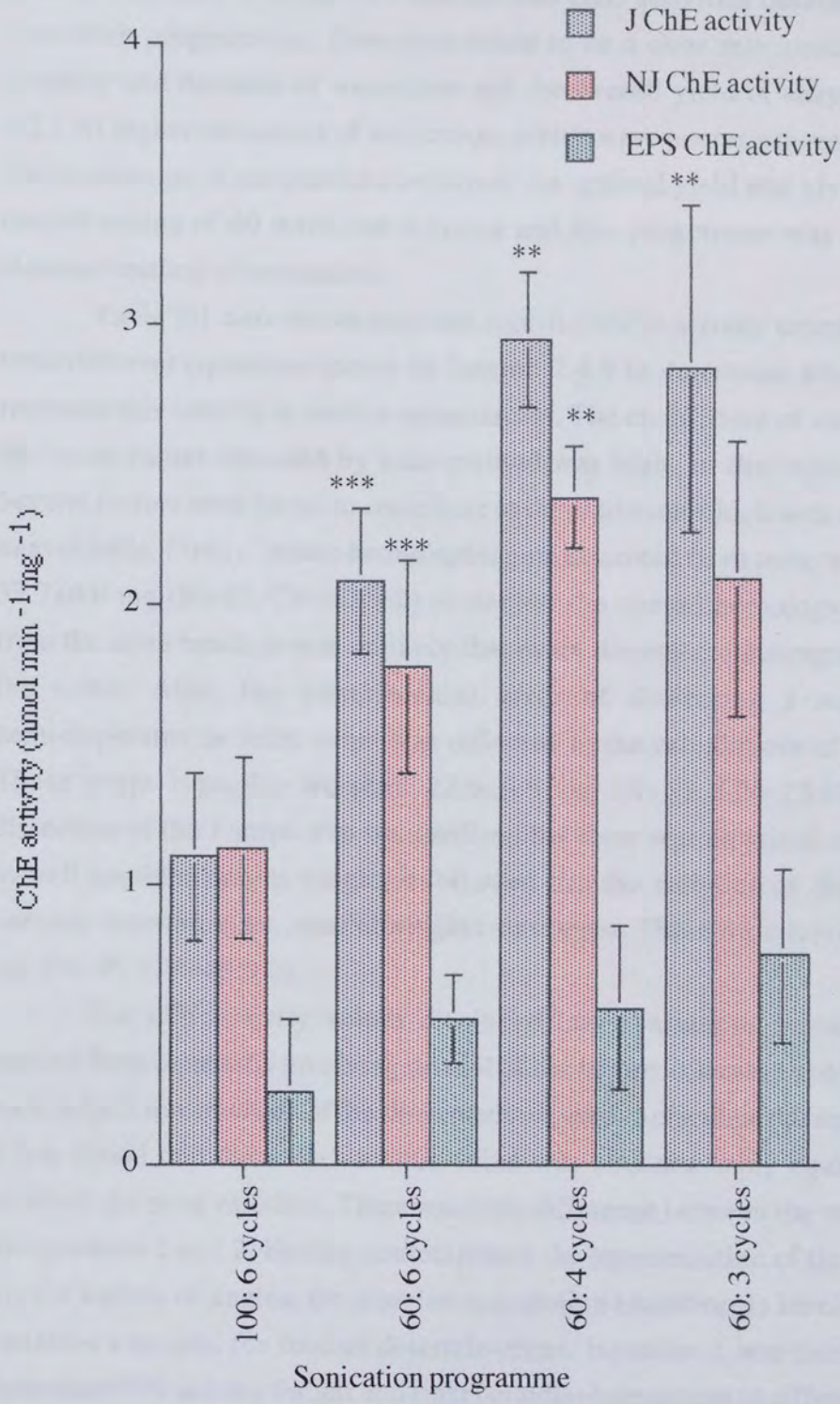

Figure 3.2: Variation of cholinesterase activity with sonication programme. ChE in the junctional (J), non-junctional (NJ) and endplate-specific (EPS) regions of mouse hemidiaphragm obtained at different sonication programmes.

pooled. Table 3.1 also shows J and NJ and ChE activities obtained by different sonication programmes. There was found to be a clear relationship between the intensity and duration of sonication and the overall yield of enzyme (see Figure 3.2.) At higher intensities of sonication, yields were poorer suggesting denaturing and destruction of enzyme had occurred. An optimal yield was given at an output control setting of 60 watts, for 4 cycles and this programme was adopted as the standard method of sonication.

Table 3.1 also shows endplate-specific (EPS) activity calculated using the three different equations shown in Section 2.4.5 to determine which would best represent this activity in routine experiments. The co-efficient of variation (CV) of the mean values obtained by each method was high, in the region of 60-70%. Several factors were found to contribute to this variation which were experimentally unavoidable. Firstly, whole hemidiaphragms dissected from mice weighed around 37.7±8.8 mg (N=45, CV=23.3%) so despite the overall homology between mice from the same batch, is was unlikely that every dissected diaphragm would weigh the same. Also, the experimental error of dissecting J regions out of hemidiaphrams as 3mm strips was reflected in the calculations of EPS activity. These strips typically weighed 22.9±5.8 mg (N=45, CV=25.3%). Since the dissection of the J strips was standardised but there was an initial variation in the overall hemidiaphragm weight, it followed that the variation of the sizes of the portions remaining, i.e., the NJ weights was larger. These were typically 14.8±7.1 mg (N=45, CV=48.0%).

The EPS activity values displayed large variations because they were derived from equations involving several of the factors discussed above which were each subject to variation. Of the three methods used to calculate the endplate values, it was found that the most variable value was obtained using equation 3 which involved the most variables. There was little difference between the values obtained by equations 1 and 2. Having contemplated the representation of the EPS activity from a variety of angles, the simplest calculation (equation 1) involving the least variables was used for routine determinations. Equation 1 was therefore used to determine EPS activity for left and right hemidiaphragms and at different sonication programmes (see Table 3.1).

3.2.2. Extraction of mouse diaphragm AChE by a sequential extraction method.

3.2.2.1. Activity of globular, asymmetric and non-extractable molecular forms and the representation of endplate-specific activity.

Table 3.2 and Figure 3.3 show AChE activities in sequential extraction fractions S1, S2, S3, S4 and H5 in junctional (J) and non-junctional (NJ) regions of mouse diaphragm. Previous work by Younkin et al., (1982) demonstrated that enzyme in fractions S1 and S2 was globular (G) in nature and enzyme in S3 and S4 was asymmetric (A) and a distinction between these forms could be made because A forms were only soluble in a high salt medium. Enzyme in H5 was non-extractable (NE) in nature. Enzyme in fractions S3, S4 and H5 was asymmetric but S3 and S4 corresponded to readily-extractable AChE (A) and H5 corresponded to non-readily extractable AChE (NE).

The first extract in each region, S1, was found to be the most enzyme rich fraction , followed by S3 and H5. A small proportion of G (S2) and A (S4) forms were residual and not extracted with the majority of G (S1) and A (S3) enzyme. It was important to carry out these residual extractions, to prevent contamination of A fractions with G enzyme and to maximise enzyme yields. Hence, for each extraction carried out, residual G and A forms were added to S1 and S3 activities respectively to give total G and A forms (see Table 3.3 and Figure 3.4).

Re-suspension of the pellet remaining at the end of the process into high ionic buffer and analysis for AChE activity showed that even after four previous extractions, enzymes were still present suggesting that they could not be readily extracted. AChE in the H5 fraction was digested with collagenase it was found to be asymmetric in nature and was identified as the collagen-tailed AChE associated with the extra-cellular matrix (Younkin et al, 1982).

In Section 3.2.1. an attempt was made to find the best way of representing the activity of enzyme which was associated with endplates using the conventional method and the simplest equation i.e. subtracting NJ from J activities was routinely applied because errors where minimised. To verify the criteria for this argument, EPS activities calculated from data obtained from the sequential extraction method were done so by the three different methods outlined in Section 2.4.5. These activities are shown in Table 3.3 and the corresponding variations are shown below them. Of the three calculation methods used, it was found that higher variations were obtained by methods 2 and 3, and the least variable EPS activities were

Fraction	Buffer	Molecular forms	J AChE activity	NJ AChE activity	EPS AChE activity
S1	Low ionic buffer (LIB)	Globular	3.06 ±0.48 (10)	1.67 ±0.35 (10)	1.40 ±0.53 (10)
S2	LIB	Residual globular	0.45 ±0.15 (10)	0.29 ±0.07 (10)	0.16 ±0.12 (10)
S3	High ionic buffer (HIB)	Asymmetric	0.98 ±0.21 (10)	0.55 ±0.19 (10)	0.42 ±0.16 (10)
S4	HIB	Residual asymmetric	0.34 ±0.06 (10)	0.20 ±0.09 (10)	0.14 ±0.11 (10)
H5	HIB	Non-extractable	0.80 ±0.20 (10)	0.29 ±0.15 (10)	0.50 ±0.13 (10)
Total			5.63 ±0.81 (10)	3.01 ±0.74 (10)	2.61 ±0.95 (10)

Table 3.2: Sequential extraction fraction AChE. Activity of junctional (J) and non-junctional (NJ) AChE extracted using low ionic strength buffer (LIB) and high ionic strength buffer (HIB) and calculated values of endplate-specific (EPS) activity for enzyme fractions: S1, S2, S3, S4 and H5. Activities are in nmol min^{-1} mg^{-1}. Values shown are means±s.d. N numbers are in parentheses. All NJ values are significantly different from J values in the corresponding fraction (Mann-Whitney, $P<0.02$).

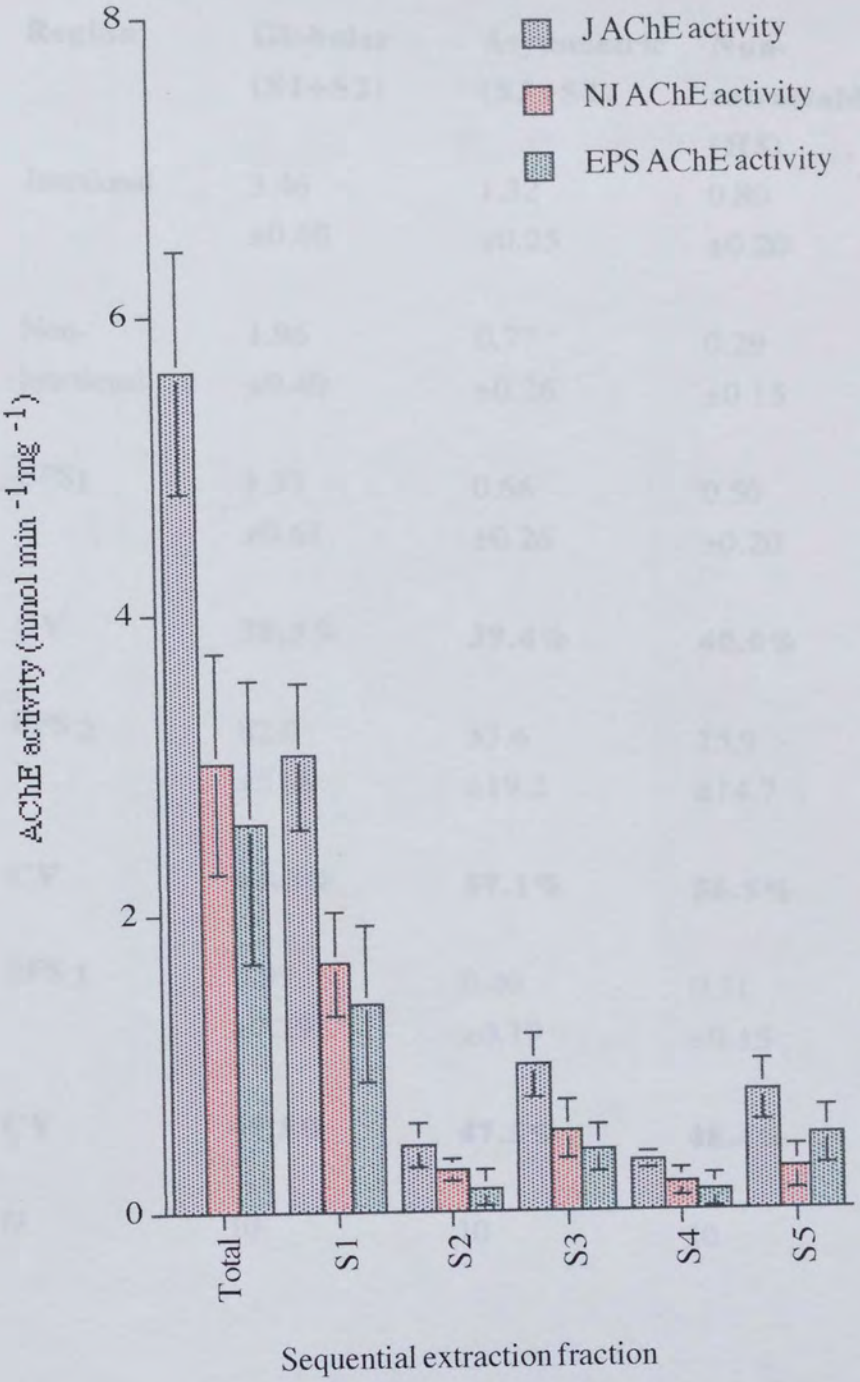

Figure 3.3: Sequential extraction fraction AChE activity. Total AChE activity and activity in sequential extraction fractions S1, S2, S3, S4 and H5 in the junctional (J), non-junctional (NJ) and endplate-specific (EPS) regions of mouse diaphragm.

Region	Globular (S1+S2)	Asymmetric (S3+S4)	Non-extractable (H5)	Total
Junctional	3.46 ±0.68	1.32 ±0.25	0.80 ±0.20	5.64 ±0.81
Non-junctional	1.96 ±0.40	0.77 ±0.26	0.29 ±0.15	3.01 ±0.81
EPS_1	1.57 ±0.61	0.66 ±0.26	0.50 ±0.20	2.61 ±0.95
CV	**38.9%**	**39.4%**	**40.0%**	
EPS_2	82.0 ±51.9	33.6 ±19.2	25.9 ±14.7	
CV	**63.3%**	**57.1%**	**56.8%**	
EPS_3	0.97 ±0.19	0.40 ±0.19	0.31 ±0.15	
CV	**49.5%**	**47.5%**	**48.4%**	
N	10	10	10	10

Table 3.3: Globular, asymmetric and non-extractable AChE activity. Total globular and asymmetric values were obtained by adding together S1 + S2 and S3 + S4 activities respectively. Non-extractable activity was obtained by assay of H5. Also shown are the mean values for endplate-specific activities calculated by three different methods and the corresponding co-efficients of variation (CV) for these values. J, NJ and EPS_1 and EPS_3 activity is in nmol $min^{-1}mg^{-1}$, EPS_2 activity is in nmol min^{-1}. All values are means±s.d.

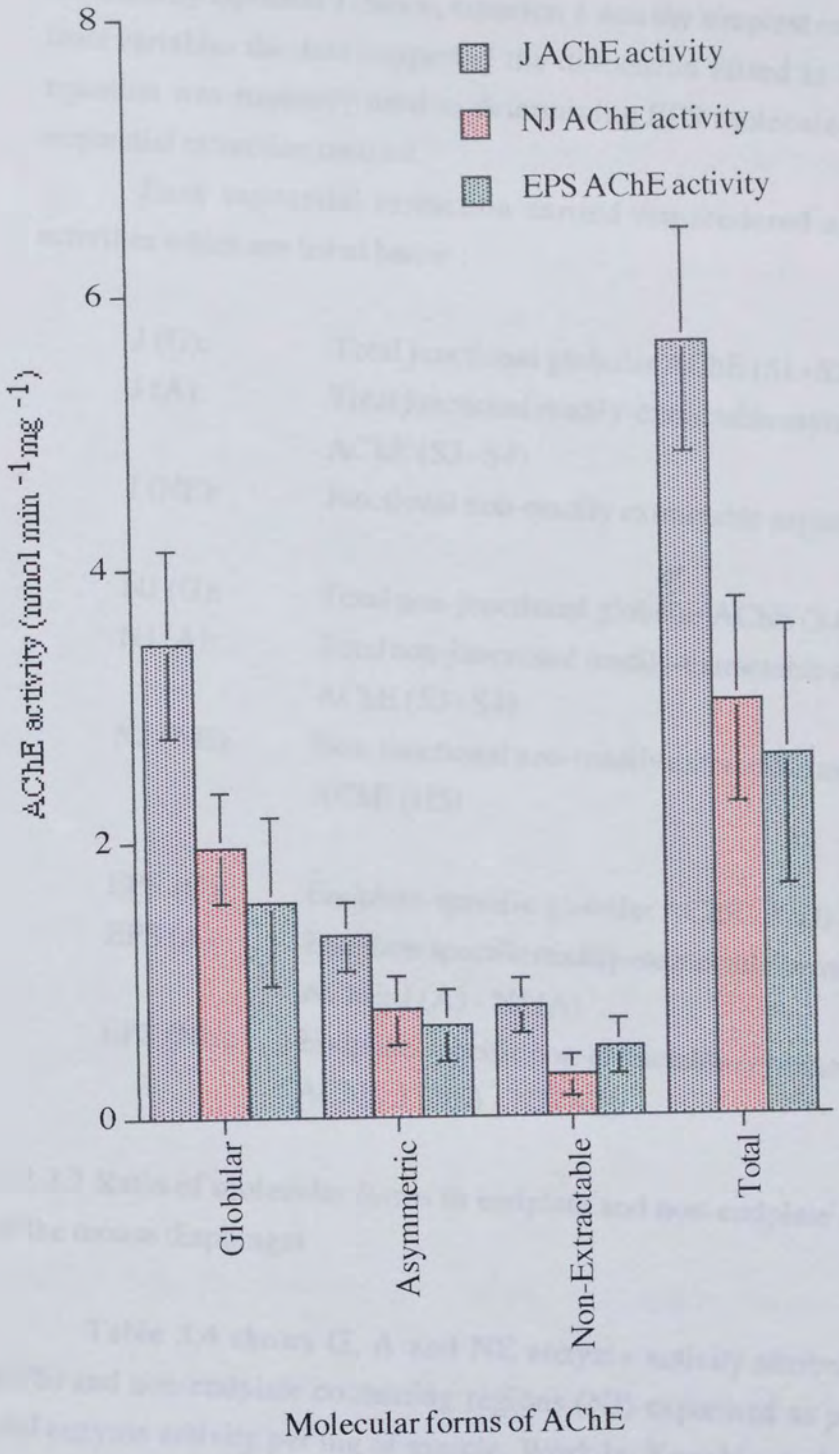

Figure 3.4: Globular, asymmetric and non-extractable AChE activity. Total AChE activity and activity of globular (S1+S2), asymmetric (S3+S4) and non-extractable (H5) AChE in junctional (J), non-junctional (NJ) and endplate-specific (EPS) regions of mouse diaphragm.

obtained by equation 1. Since, equation 1 was the simplest calculation involving the least variables the data supported the discussion raised in Section 3.2.1 and this equation was routinely used in determining EPS molecular form activity by the sequential extraction method.

Each sequential extraction carried out rendered a total of nine AChE activities which are listed below :

J (G):	Total junctional globular AChE (S1+S2).
J (A):	Total junctional readily-extractable asymmetric AChE (S3+S4)
J (NE):	Junctional non-readily extractable asymmetric AChE (H5)
NJ (G):	Total non-junctional globular AChE (S1+S2).
NJ (A):	Total non-junctional readily-extractable asymmetric AChE (S3+S4)
NJ (NE):	Non-junctional non-readily extractable asymmetric AChE (H5)
EPS (G):	Endplate-specific globular AChE : J (G) - NJ (G)
EPS (A):	Endplate-specific readily-extractable asymmetric AChE: J (A) - NJ (A)
EPS (NE):	Endplate-specific non-extractable asymmetric AChE: J (NE) - NJ (NE)

3.2.2.2 Ratio of molecular forms in endplate and non-endplate containing regions of the mouse diaphragm

Table 3.4 shows G, A and NE enzyme activity attributable to endplates (EPS) and non-endplate containing regions (NJ) expressed as percentages of the total enzyme activity per mg of muscle. Work by Younkin et al., (1982) indicated that in rat diaphragm 67.8% of whole muscle activity was due to G forms 22.7% due to readily extractable A forms and 9.4% due to NE forms. About 26% of enzyme activity was found to be in endplates whereas, 74% was associated with non-endplate regions. About 28% of enzyme activity in endplates was due to G forms, 45% to A forms and 27% was NE enzyme.

The enzyme distribution in mouse diaphragm was found to be similar. 61.4±12.1% of the total activity per mg of muscle was due to G forms, 56.5% of which were located in non-endplate containing regions of muscle fibres, and 43.5%

AChE	Non-endplate activity (NJ) as % of activity/mg tissue	Endplate activity (EPS) as % of activity/mg tissue	Total activity as % of activity/mg tissue
G	34.7 ±7.2	27.1 ±10.8	61.4 ±12.1
A	13.1 ±5.2	12.6 ±4.9	23.4 ±4.4
NE	5.2 ±2.6	8.9 ±3.6	14.1 ±3.6
Total	53.3 ±13.1	46.2 ±16.9	100

Table 3.4: Percentage of AChE molecular forms in diaphragm. Globular (G), asymmetric (A),non-extractable (NE) and total AChE in the non-endplate (NJ) and endplate (EPS) regions of mouse diaphragm expressed as percentages of the total activity per mg of muscle. Values shown are percentages±s.d. (N=10).

in endplates. Of the total activity per mg of muscle activity, 23.4±4.4% was due to A forms, again 53.8% which were in endplates and 46.2% were in non-endplate regions. Thus, neither G or A forms were exclusive to either endplate or non-endplate regions but were distributed between the two. Enzymes which were not readily extractable (NE) contributed to 14.1±3.6% of muscle activity and 70% of these are exclusive to endplates. About 30% of NE enzyme was not located in endplate regions but associated with peripheral parts of muscle fibres.

3.2.2.3 Determination of the precise molecular composition of the sequential extraction fractions.

The precise molecular composition of the sequential extraction fractions was determined by velocity sedimentation on sucrose density gradients. Figure 3.5 shows characteristic sedimentation profiles for J G, A and NE AChE fractions obtained by velocity sedimentation of extracts of S1+S2, S3+S4 and H5 obtained sequentially. J and NJ fractions had essentially similar compositions although NJ profiles were poor due to low enzyme levels and consequently profiles for EPS fractions (J-NJ) could not be obtained. The gradients were calibrated using markers with known sedimentation.

The predominant enzyme in the G fraction (S1+S2) sedimented around the 4S marker. Previous work showed that this enzyme corresponded to G1. The G2 form appeared as a hump on the G1 peak and sedimented around 6S. Also present in the G fraction was G4 which sedimented at the 10S marker. Globular forms are either low salt soluble intra-cellular precursors and secreted enzyme or detergent soluble integral membrane dimers and tetramers (Rotundo, 1984). Since the LIB extraction buffer used contained the detergent Triton-X100, the G fraction (S1+S2) represents AChE activity which is a combination of intra-cellular G precursors and extra-cellular integral membrane proteins.

The sedimentation profiles for the A fraction (S3+S4) and the NE (H5) fraction were similar with major sedimentation occurring around the 16S marker corresponding to the A12 form of AChE which has a functional role in the synaptic cleft (Hall, 1983). There was evidence in both A and NE fractions of sedimentation between 4S and 12S where the A4 and A8 forms were expected to appear but distinctive peaks could not be identified because an insufficient number of fractions was obtained by the method for better resolved peaks. Although A12 was present in both A (S3+S4) and NE (H5) fractions, the enzyme peak was better resolved in the NE (H5) fraction and constituted more than 60% of the activity. The A and NE fractions can be distinguished because the former contains readily-extractable

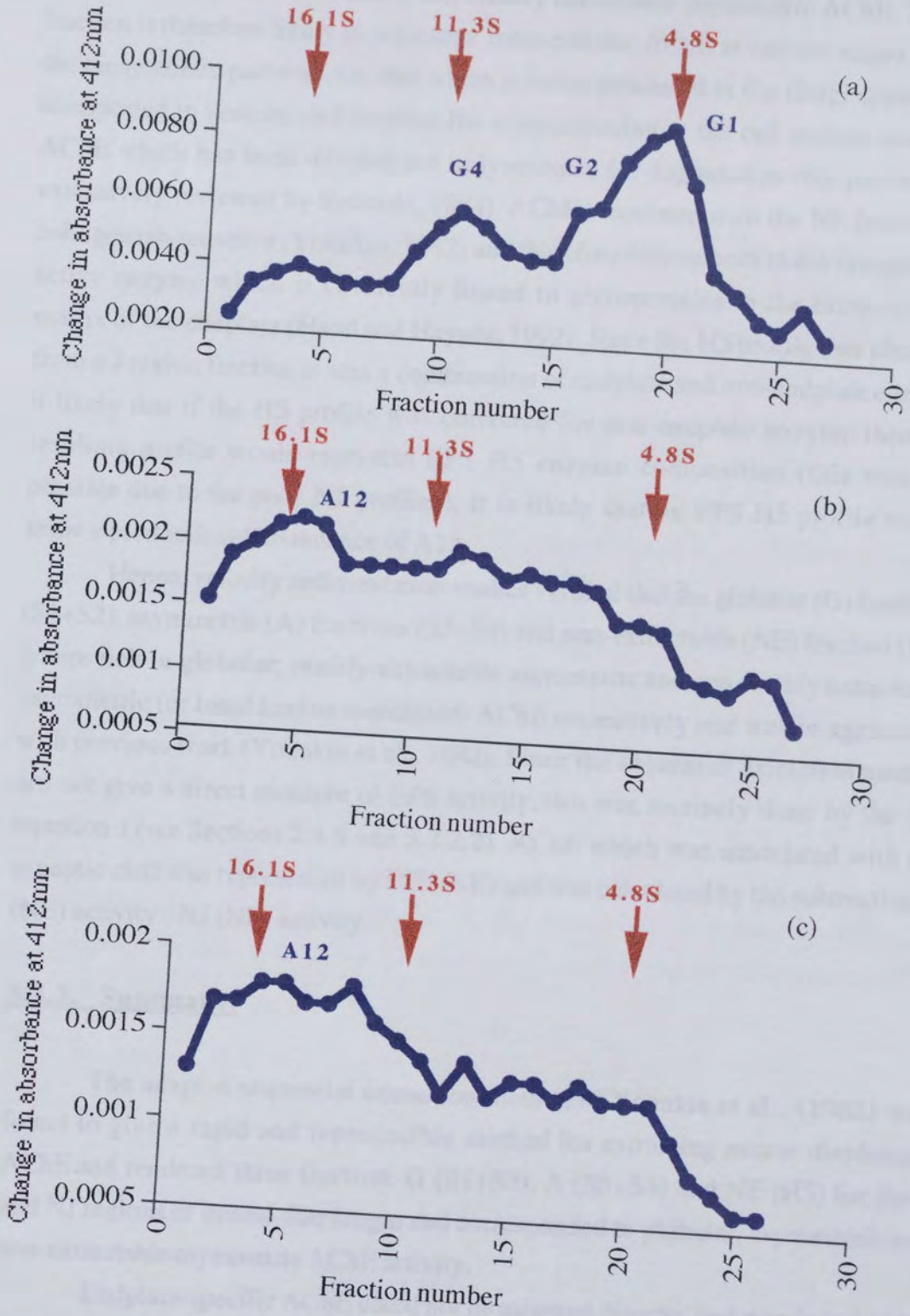

Figure 3.5: Sedimentation profiles of sequential extraction fractions. Profiles were obtained by velocity sedimentation on sucrose density gradients and show the predominant molecular forms of AChE in (a) globular fractions (S1+S2), (b) asymmetric fractions (S3+S4) and (c) non-extractable fraction (H5). Profiles for junctional and non-junctional regions were similar.

asymmetric AChE and the latter, non-readily extractable asymmetric AChE. The A fraction is therefore likely to represent intra-cellular AChE at various stages along the biosynthetic pathway, i.e. that which is being processed in the Golgi apparatus, transported in vesicles and targeted for externalisation at the cell surface and any AChE which has been internalised in lysosomes for degradation (the pathway is extensively reviewed by Rotundo, 1984). AChE associated with the NE fraction is collagenase-sensitive (Younkin, 1982) and therefore corresponds to the synaptically active enzyme which is covalently linked to glycoproteins in the extra-cellular matrix of the endplate (Hand and Haynes, 1992). Since the H5 profile was obtained from a J region fraction is was a combination of endplate and non-endplate enzyme it likely that if the H5 profile was corrected for non-endplate enzyme then the resulting profile would represent EPS H5 enzyme composition (this was not possible due to the poor NJ profiles). It is likely that an EPS H5 profile would show a predominant abundance of A12.

Hence, velocity sedimentation studies verified that the globular (G) fractions (S1+S2), asymmetric (A) fractions (S3+S4) and non-extractable (NE) fraction (H5) where rich in globular, readily-extractable asymmetric and non-readily extractable asymmetric (or basal lamina-associated) AChE respectively and was in agreement with previous work (Younkin et al., 1982). Since the sequential extraction method did not give a direct measure of EPS activity, this was routinely done by the use equation 1 (see Sections 2.4.5 and 3.2.2.2). AChE which was associated with the synaptic cleft was represented by EPS (NE) and was calculated by the subtraction: J (NE) activity - NJ (NE) activity.

3.2.3. Summary.

The adapted sequential extraction method of Younkin et al., (1982) was found to give a rapid and reproducible method for extracting mouse diaphragm AChE and rendered three fraction: G (S1+S2), A (S3+S4) and NE (H5) for the J and NJ regions of mouse diaphragm and corresponded to globular, asymmetric and non-extractable asymmetric AChE activity.

Endplate-specific AChE could not be assessed directly and was found to be best represented a simple calculation involving minimal variables. It was routinely calculated by subtracting NJ activity from J activity and was carried out for each sequential extraction fraction to determine molecular forms associated with the endplate (EPS (G), EPS (A) and EPS (NE)).

Molecular form localisation studies revealed that neither the G nor the A forms where exclusively located in the endplate or the non-endplate regions but

J/NJ AChE fraction	Sequential extraction fraction	Molecular form composition	Possible origin
G (Globular)	S1 + S2	G1, G2 and G4	Intracellular precursors, secreted soluble molecules, detergent-soluble membrane proteins
A (Asymmetric)	S3 + S4	A12 distinct peak A8, A4 detectable activity	Intracellular precursors, Golgi, vesicles, lysosomes
NE (Non-extractable)	H5	A12 distinct peak, A8, A4 detectable activity	Extracellular-matrix.

Table 3.5: Summary of sequential extraction fractions. The table shows the final J and NJ AChE fractions (G, A and NE), order of extraction (S1-H5), predominant molecular form composition identified by velocity sedimentation and possible cellular origin.

were found in both. The NE form was largely associated with the endplate, but a small proportion was also found in non-endplate regions.

Velocity sedimentation studies verified that the globular (G) fractions (S1+S2), asymmetric (A) fractions (S3+S4) and non-extractable (NE) fraction (H5) where rich in globular, readily extractable asymmetric and non-readily extractable asymmetric (or basal lamina-associated) AChE respectively. The fractions, their compositions and probable cellular origins are summarised in Table 3.5.

The NE fraction was found to be rich in A12 molecular form by velocity sedimentation and has previously been shown to be collagenase-sensitive and therefore associated with the basal lamina (Younkin et al., 1982). There was found to be a good abundance of A12 in the J (NE) profile and it is likely that correction of the J (NE) profile for non-endplate activity would indicate that most of the A12 is associated with the endplate. Functionally active AChE associated with the endplate was routinely calculated by subtracting NJ (NE) from J (NE) to obtain EPS (NE).

CHAPTER 4

THE EFFECTS OF ECOTHIOPATE ON MOUSE SKELETAL MUSCLE AND THE REPRESENTATION OF FUNCTIONAL ACETYLCHOLINESTERASE.

4.1 Introduction.

In Chapter 3, the molecular forms associated with endplate and non-endplate regions of mouse diaphragm were investigated and it was found that various globular and asymmetric forms were found in both regions in varying proportions. In this section, the distribution of AChE molecular forms in mouse skeletal muscle was investigated further and an attempt was made to determine internal and external cellular locations of the various molecular forms using the irreversible OP inhibitor, ecothiopate (ECO). ECO penetrates membranes very slowly and selectively inhibits extra-cellular AChE (Brimijoin et al., 1978; Wallace and Gillon, 1982). Due to its quaternary nature, ECO has been used in several studies (Younkin et al., 1982; McIssac and Koelle 1959; Rotundo, 1983) to distinguish between AChE with intra- and extra-cellular locations.

ECO was also used to study OP-induced myopathy by investigating the responses of AChE molecular forms, blood ChE and endplate dimensions to acute dosing. The recovery of AChE molecular forms and endplate shape was also monitored and attempt was made to determine various aspects of AChE biosynthesis and regulation after anti-ChEs.

When functional AChE in the synaptic cleft is inhibited, the action of ACh on its receptor is prolonged and there is a prolongation of extra-cellular miniature endplate potentials; $(MEPPs)_o$ (Boyd and Martin, 1956; Blaber and Christ, 1967). This suggests that there is a relationship between these endplate potentials and synaptic AChE activity which would apply under a variety of circumstances. Previous work carried out to explore dose and time dependent changes in AChE activity after treatment with anti-ChEs have concentrated on the use of a one step extraction method, which due to its simplicity, measured only the activity of low molecular weight globular forms of AChE which were probably not functionally relevant. When comparisons which were made between the effects of ECO on AChE measured by this method and the prolongation of $(MEPPs)_o$, a consistent correlation was not found (Bamforth, 1989) and suggested that the assay technique did not give a true indication of synaptic enzyme. In this section this hypothesis was investigated by examining the dose and time responses of a variety of AChE molecular forms to ECO and correlating these responses with electrophysiologically recorded data. An attempt was also made to determine the nature of the relationship between assayed synaptic AChE and the prolongation of $(MEPPs)_o$ and express the relationship in a reproducible form which could be applied to other experimental conditions. The aims of work in this section are summarised as follows:

(a) To determine the distribution of AChE molecular forms in mouse skeletal muscle.
(b) To investigate OP-induced myopathy with respect to muscle fibre morphology and molecular form activity.
(c) To investigate the recovery of skeletal muscle after OP intoxication and determine aspects of AChE metabolism.
(d) To relate synaptic AChE activity to the prolongation of $(MEPPs)_O$.

4.2 Results and discussion.

4.2.1 Response of mouse skeletal muscle to acute dosing with ECO.

4.2.1.1 Experimental design.

Mice were allocated into the following dosing groups and treated with a single subcutaneous injection of ECO with 700 nmol kg^{-1} atropine sulphate to prevent muscarinic effects.

Group 1 : 700 nmol kg^{-1} atropine sulphate only (untreated group).
Group 2 : 25 nmol kg^{-1} ECO + 700 nmol kg^{-1} atropine sulphate.
Group 3 : 50 nmol kg^{-1} ECO + " ".
Group 4 : 100 nmol kg^{-1} ECO + " ".
Group 5 : 300 nmol kg^{-1} ECO + " ".
Group 6 : 500 nmol kg^{-1} ECO + " ".

Three hours after the injection, mice were killed and a blood sample was removed from the femoral artery and assayed for ChE activity (see Section 2.4.3.3). Diaphragms were then dissected out and prepared for assay of molecular forms of AChE by the sequential extraction method (see Section 2.4.3.2). Hemidiaphragm endplates were also stained histochemically (see Section 2.6) and their dimensions were measured.

4.2.1.2 Whole blood ChE.

Table 4.1 and Figure 4.1 show the dose-response of whole blood ChE to ECO administered at doses in the range 25-300 nmol kg^{-1}. Whole blood ChE responded to ECO treatment in a dose-dependent manner. At low, non-necrotising

Dose ECO	Whole Blood ChE Activity (μmol min^{-1}ml^{-1})	% Inhibition
Untreated	3.58 ±0.84 (8)	0
25	1.85 * ±0.80 (4)	48.3
50	0.96 * ±0.31 (6)	73.2
100	0.79 * ±0.20 (4)	77.9
300	0.64 * ±0.25 (4)	82.1

Table 4.1: Whole blood ChE 3 hours after ECO (25-300 nmol kg^{-1}). The table shows blood ChE activities and the corresponding percentage inhibitions. Values are means±s.d. N values are shown in parentheses. Kruskal-Wallis one-way ANOVA: $P<0.05$, * denotes groups which differ from the untreated group:$P<0.05$ (Kruskal-Wallis multi-comparison test).

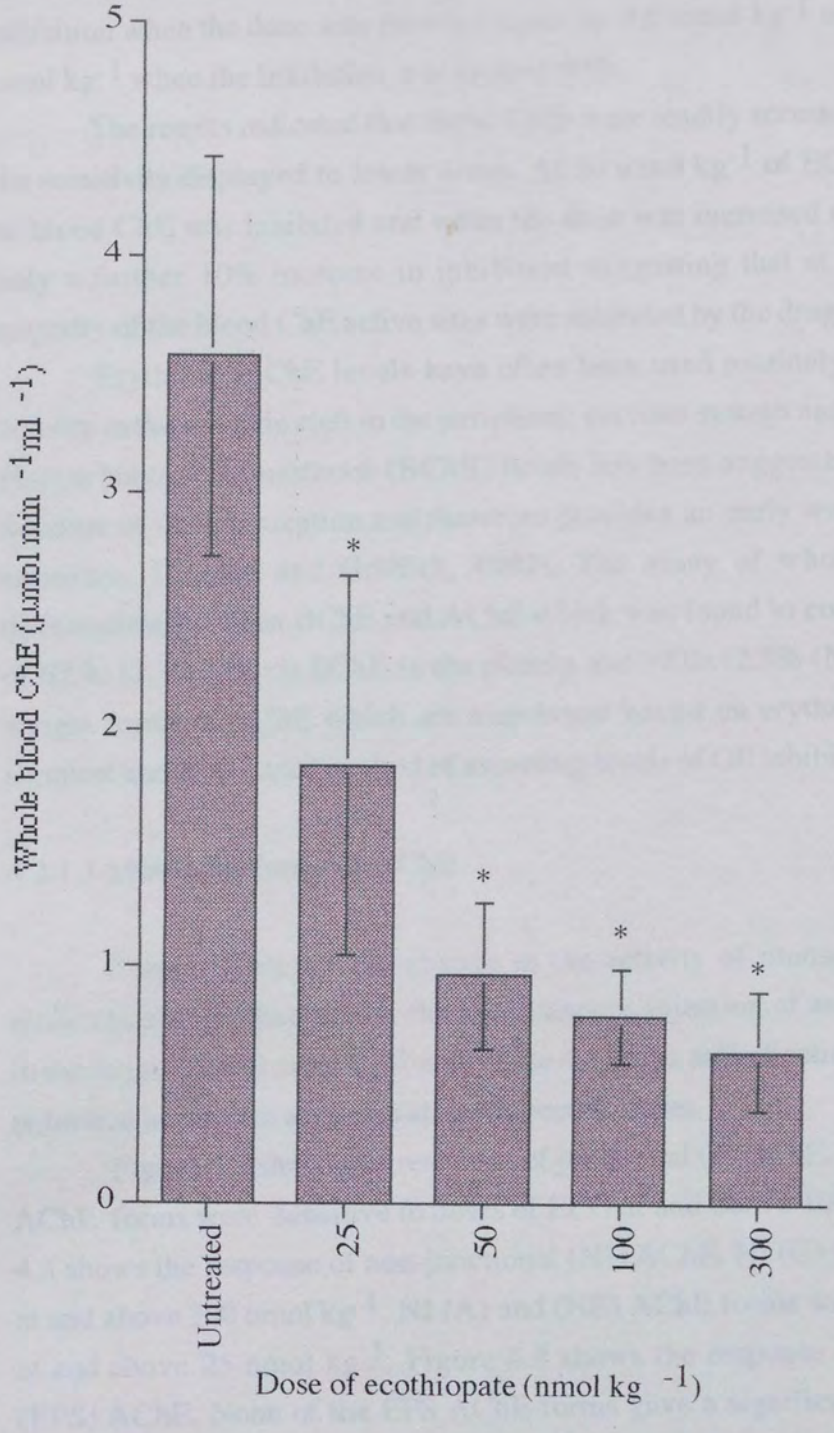

Figure 4.1: Whole blood ChE 3 hours after ECO (25-300 nmol kg^{-1}).
* denotes groups which differ from the untreated group: $P<0.05$ (Kruskal-Wallis multi-comparison test).

doses the inhibition of whole blood ChE was almost 50%. When the dose was doubled the inhibition increased to 70%. There was little change in the extent of inhibition when the dose was doubled again to 100 nmol kg^{-1} or increased to 300 nmol kg^{-1} when the inhibition was around 80%.

The results indicated that blood ChEs were readily accessible to ECO due to the sensitivity displayed to lower doses. At 50 nmol kg^{-1} of ECO more than 70% of blood ChE was inhibited and when the dose was increased 6 times, there was only a further 10% increase in inhibition suggesting that at the lower dose, a majority of the blood ChE active sites were saturated by the drug.

Erythrocyte ChE levels have often been used routinely to indicate AChE activity in the synaptic cleft in the peripheral nervous system and the assessment of plasma butyrylcholinesterase (BChE) levels has been suggested to be a sensitive measure of OP intoxication and therefore provides an early warning of excessive exposure (Duncan and Griffith, 1992). The assay of whole blood does not differentiate between BChE and AChE which was found to consist predominantly of 67.9±12.3% (N=5) BChE in the plasma and 32.0±12.3% (N=5) low molecular weight forms of AChE which are membrane bound on erythrocytes but was the simplest and most rapid method of assessing levels of OP inhibition.

4.2.1.3 Molecular forms of AChE.

Table 4.2 shows the change in the activity of mouse diaphragm AChE molecular forms 3 hours after the subcutaneous injection of an acute dose of ECO in the range 25-500 nmol kg^{-1} and Table 4.3 gives an indication of the percentage reduction in enzyme activities at the respective doses.

Figure 4.2 shows the response of junctional (J) AChE. J (G), (A) and (NE) AChE forms were sensitive to doses of ECO at and above 100 nmol kg^{-1}. Figure 4.3 shows the response of non-junctional (NJ) AChE. NJ (G) was senstive to ECO at and above 300 nmol kg^{-1}. NJ (A) and (NE) AChE forms were sensitive to ECO at and above 25 nmol kg^{-1}. Figure 4.4 shows the response of endplate-specific (EPS) AChE. None of the EPS AChE forms gave a significant response to ECO below the 300 nmol kg^{-1} dose. EPS (G) and EPS (NE) were sensitive to this dose, but EPS (A) was only sensitive to the 500 nmol kg^{-1} dose. EPS (NE) AChE displayed the most consistent dose-dependent variation.

None of the individual enzyme fractions displayed a good dose-response relationship as the percentage inhibitions were inconsistent and subject to large variations and the response of various endplate AChE molecular forms to ECO was different to that of the non-endplate molecular forms of AChE. Since the various

molecular forms of AChE do not differ significantly in their susceptibility to alkylphosphorylation by OP compounds (Madhukar and Matsumura, 1979) the different responses observed may be due to other influences.

The large variations in actual activities may be due to an inter-mouse difference in sensitivity to ECO. This variation was also observed in human blood AChE but is difficult to characterise (Duncan and Griffith, 1992). Since, portions of AChE in each region, are located internally and externally (Younkin, 1982), it is possible that the different responses to ECO arise from differences in the portions of enzyme which can be targeted by the drug in each region. The region with the higher portion of extra-cellular enzyme is more likely to display a response than the region which has a higher portion of intra-cellular AChE which is largely inaccessible to ECO. Also, intra-cellular AChE has a rapid turnover with a half-life of around 90 mins whereas extra-cellular AChE has a slower turnover with a half-life of around 40-50 hours (Lazar et al., 1984). It is possible therefore, that 3 hours after the administration of ECO, *de novo* synthesis of intra-cellular AChE has already increased enzyme levels such that the inhibitions recorded at this time do not truly reflect that which occurred soon after the drug was given. In addition, it was not known to what extent and at what dose ECO can penetrate the cell and inhibit intra-cellular pools of AChE.

Hence, the response of the molecular forms of AChE to ECO at a given dose and time was found to be selective and may depend on any one or a combination of factors i.e. cellular locations, enzyme turnover rates, inter-mouse variations and access to ECO. In addition, the response of whole blood to ECO was not found to closely parallel the response of any of the diaphragm forms of AChE which suggested that although the assay of whole blood gave a good indication of OP inhibition, it was not a good indicator of responses in peripheral nervous tissue.

Region	Un-treated	25 nmol kg^{-1} ECO	50 nmol kg^{-1} ECO	100 nmol kg^{-1} ECO	300 nmol kg^{-1} ECO	500 nmol kg^{-1} ECO
J (G) †	3.46	2.71	2.82	2.41*	2.06*	1.67*
	±0.68	±0.63	±0.28	±0.27	±0.02	±0.83
J (A) †	1.32+	0.86*	1.05	0.69*	0.61*	0.70*
	±0.25	±0.26	±0.21	±0.09	±0.12	±0.25
J (NE) †	0.80+	0.49	0.52	0.39*+	0.11*	0.18*
	±0.20	±0.31	±0.25	±0.10	±0.08	±0.11
NJ (G) †	1.96	1.54	1.50	1.56	1.28*	1.04*
	±0.40	±0.27	±0.31	±0.26	±0.24	±0.41
NJ (A) †	0.77+	0.22*	0.39*	0.33*	0.15*	0.40*
	±0.26	±0.12	±0.19	±0.34	±0.11	±0.21
NJ (NE) †	0.29+	0.01*	0.12*	0.08*	0.05*	0.14*
	±0.15	±0.01	±0.16	±0.09	±0.07	±0.14
EPS (G) †	1.57	1.17	1.32	0.85	0.78*	0.63*
	±0.61	±0.63	±0.18	±0.48	±0.46	±0.50
EPS (A) †	0.66	0.64	0.67	0.57	0.45	0.31*
	±0.26	±0.14	±0.14	±0.12	±0.22	±0.17
EPS(NE) †	0.50	0.48	0.41	0.32	0.09*	0.05*
	±0.20	±0.31	±0.20	±0.15	±0.26	±0.04
N	10	4	4	4	4	8

Table 4.2: Diaphragm AChE 3 hours after ECO (25-500 nmol kg^{-1}). Globular (G), asymmetric (A) and non-extractable (NE) enzyme activities in junctional (J), non-junctional (NJ) and endplate-specific (EPS) regions. All activities are in nmol min^{-1} mg^{-1}. † denotes sets with different groups (K-S ANOVA, $P<0.05$), * denotes groups which differ from the untreated group (K-S multi-comparison test, $P<0.05$) and + denotes different adjacent groups (K-S multi-comparison test, $P<0.05$).

Region	25nmol kg^{-1} ECO	50nmol kg^{-1} ECO	100nmol kg^{-1} ECO	300nmol kg^{-1} ECO	500nmol kg^{-1} ECO
J (G)	23.9	18.6	30.5	40.4	51.7
	±16.3	±6.9	±6.6	±9.0	±23.9
J (A)	34.9	20.8	48.1	54.2	46.9
	±17.1	±13.8	±5.8	±8.0	±19.0
J (NE)	39.4	35.0	51.2	86.6	77.9
	±33.2	±26.7	±10.4	±8.3	±14.2
NJ (G)	21.6	23.7	20.7	34.7	47.1
	±11.9	±13.8	±11.6	±6.9	±21.0
NJ (A)	71.4	50.0	57.8	80.2	48.7
	±13.4	±21.9	±38.6	±12.3	±26.9
NJ (NE)	97.4	60.4	74.2	84.5	50.4
	±4.5	±47.9	±26.3	±18.3	±47.8
EPS (G)	25.3	15.9	45.9	50.2	59.7
	±35.0	±9.7	±26.4	±13.1	±32.2
EPS (A)	1.2	4.6	45.5	31.5	53.2
	±18.4	±17.7	±26.6	±14.8	±25.6
EPS (NE)	4.5	19.0	37.0	87.5	90.3
	±54.1	±34.1	±26.6	±19.0	±8.7
N	10	4	4	4	8

Table 4.3: Percentage reduction of diaphragm AChE 3 hours after ECO (25-500 nmol kg^{-1}). Reduction in junctional (J), non-junctional and endplate-specific (EPS), globular (G), asymmetric (A) and non-extractable (NE) AChE. Values are mean percentage reduction ± s.d.

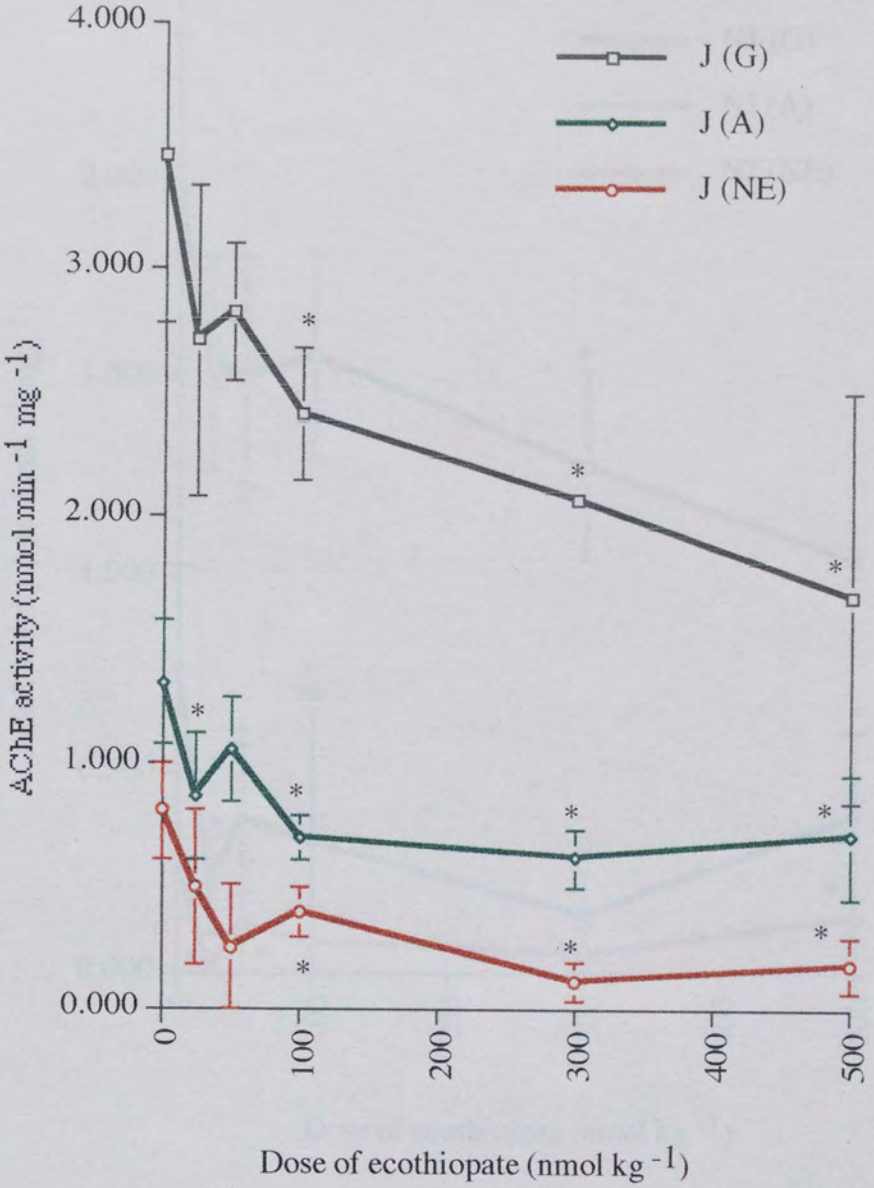

Figure 4.2: Junctional AChE 3 hours after ECO (25-500 nmol kg^{-1}). Globular (G), asymmetric (A), non-extractable (NE) and total AChE activity in the junctional (J) region of mouse diaphragm. * denotes groups which differ from untreated group: $P<0.05$ (Kruskal-Wallis mutli-comparison test).

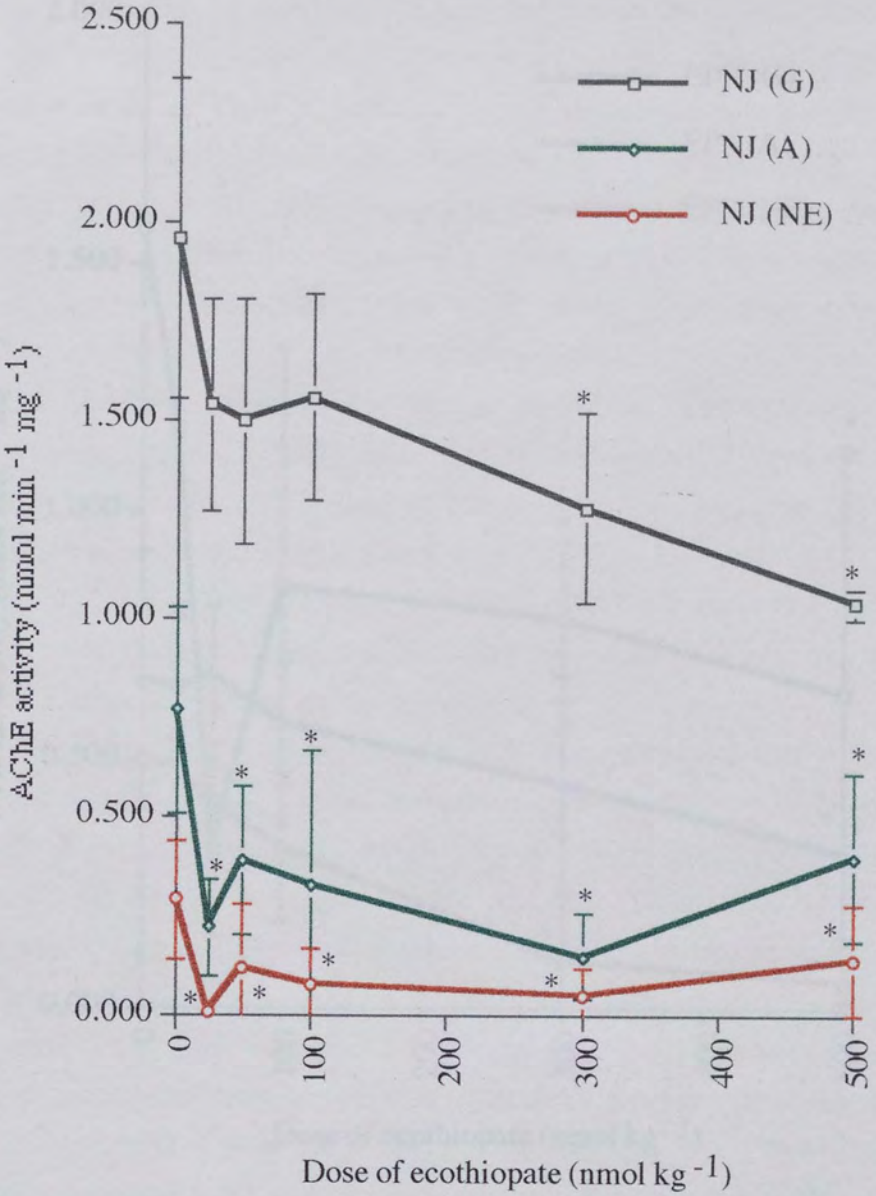

Figure 4.3: Non-junctional AChE 3 hours after ECO (25-500 nmol kg^{-1}). Globular (G), asymmetric (A), non-extractable (NE) and total AChE activity in the non-junctional (NJ) region of mouse diaphragm. * denotes groups which differ from the untreated group: $P<0.05$ (Kruskal-Wallis multi-comparison test).

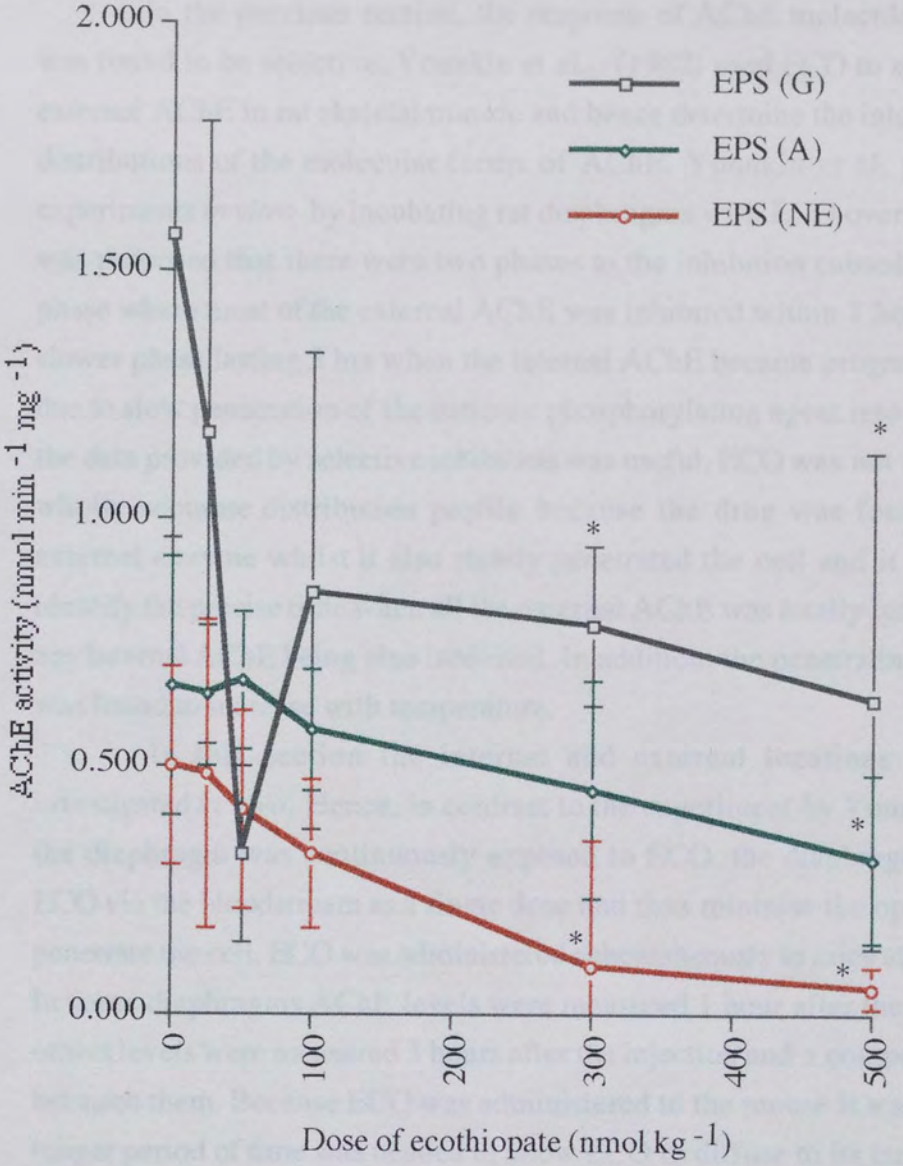

Figure 4.4: Endplate-specific AChE 3 hours after ECO (25-500 nmol kg^{-1}). Globular (G), asymmetric (A), non-extractable (NE) and total AChE activity in the endplate-specific (EPS) region of mouse diaphragm. * denotes groups which differ from the untreated group: $P<0.05$ (Kruskal-Wallis multi-comparison test).

4.2.1.4 Internal and external cellular locations of AChE.

In the previous section, the response of AChE molecular forms to ECO was found to be selective. Younkin et al., (1982) used ECO to selectively inhibit external AChE in rat skeletal muscle and hence determine the internal and external distributions of the molecular forms of AChE. Younkin et al. performed these experiments *in vitro* by incubating rat diaphragms with ECO over a time period. It was proposed that there were two phases to the inhibition caused by ECO: a slow phase where most of the external AChE was inhibited within 1 hour and a second, slower phase lasting 3 hrs when the internal AChE became progressively inhibited due to slow penetration of the cationic phosphorylating agent into fibres. Although the data provided by selective inhibition was useful, ECO was not found to give an wholly accurate distribution profile because the drug was found to inactivate external enzyme whilst it also slowly penetrated the cell and it was difficult to identify the precise time when all the external AChE was totally inactivated without any internal AChE being also inhibited. In addition, the penetrating ability of ECO was found to increase with temperature.

In this section the internal and external locations of AChE were investigated *in vivo*. Hence, in contrast to the experiment by Younkin et al. where the diaphragm was continuously exposed to ECO, the diaphragm would receive ECO via the bloodstream as a single dose and thus mininise the oportunity for it to penetrate the cell. ECO was administered subcutaneously to mice at 500 nmol kg^{-1}. In some diaphragms AChE levels were measured 1 hour after the injection and in others levels were measured 3 hours after the injection and a comparison was made between them. Because ECO was administered to the mouse it was assumed that a longer period of time was needed to allow ECO to diffuse to its target sites and the penetration of ECO into the cell would be minimal after 1 hour.

Table 4.4 shows the hypothesised percentage distribution of internal and external enzyme 1 hour and 3 hours after dosing with ECO. The actual AChE activities at the 2 time points was taken to represent internal enzyme and the difference between the untreated enzyme levels and the internal activity at each of the time points was taken to represent the external enzyme. Both the internal and external activities were expressed as percentages of the total activity per mg of untreated tissue. Table 4.4 shows that after 1 hour, NJ (G), NJ (A) and NJ (NE) were all predominately internal and EPS (G) and EPS (A) were equally distributed between the inside and outside of the cell but EPS (NE) was predominately external. When the activities were measured at 3 hours, there were only slight increases in the external proportions of all EPS forms and NJ (NE) whereas NJ (G)

	NJ (% activity / mg muscle)	EPS (% activity / mg muscle)	% activity/mg muscle
G	**34.7 ± 7.2**	**27.7 ± 10.8**	**61.4 ± 12.1**
Internal (1hr)	31.9 ± 3.6	13.4 ± 5.7	45.3 ± 5.4
External(1 hr)	2.8 ± 3.6	14.5 ± 5.3	16.1 ± 5.4
Internal (3 hrs)	18.4 ± 7.3	11.2 ± 8.9	26.6 ± 14.6
External (3 hrs)	16.4 ± 7.3	16.6 ± 8.9	31.8 ± 14.6
A	**13.1 ± 5.2**	**12.6 ± 4.9**	**23.4 ± 4.4**
Internal (1 hr)	12.0 ± 1.5	6.0 ± 2.4	18.0 ± 1.8
External (1 hr)	1.7 ± 1.5	5.7 ± 2.4	5.4 ± 1.8
Internal (3 hrs)	7.0 ± 3.7	5.5 ± 3.0	12.5 ± 4.4
External (3 hrs)	6.7 ± 3.6	6.2 ± 3.0	10.9 ± 4.4
NE	**5.2 ± 2.6**	**8.9 ± 3.6**	**14.1 ± 3.6**
Internal (1 hr)	3.9 ± 2.5	1.7 ± 1.8	5.6 ± 3.2
External (1 hr)	2.1 ± 1.8	7.3 ± 1.8	8.7 ± 3.2
Internal (3 hrs)	2.6 ± 2.5	0.9 ± 0.8	3.1 ± 2.0
External (3 hrs)	2.9 ± 2.1	8.0 ± 0.8	11.1 ± 2.0
Total/mg muscle	**53.3 ± 13.1**	**46.2 ± 16.9**	**100**
Internal (1 hr)	44.5 ± 6.5	19.6 ± 5.4	70.4 ± 9.5
External (1 hr)	8.9 ± 6.4	26.6 ± 5.4	29.6 ± 9.5
Internal (3 hrs)	27.9 ± 12.7	17.6 ± 10.7	45.2 ± 20.6
External (3 hrs)	25.4 ± 12.7	28.7 ± 10.7	54.8 ± 20.6

Table 4.4: The percentage distribution of diaphragm AChE. Activities are expressed as percentage of activity per mg of muscle (values in bold). Also shown are internal and external enzymes 1 hr and 3 hrs after a 500 nmol kg^{-1} injection of ECO. Internal and external percentages were also expressed by dividing the measured activities by the total activity per mg of tissue. N (1 hr) = 4, N (3hrs) = 8.

and NJ (A) external proportions increased by a greater extent. The reason for these observations is unclear. It is possible that at the 1 hour time point, ECO has only partially inhibited all the external AChE and at 3 hours it has inhibited all the external thus resulting in the observed decreases in internal AChE and increases in external AChE between the two time points. This would imply that the 3 hour distribution represents AChE location better than the 1 hour distribution. This however is unlikely because ECO is probably removed from the circulation quite quickly and the observation that the EPS (NE) enzyme is inhibited by around 90% at both the 1 hour and 3 hour time points suggests that the progressive inhibition of this enzyme does not occur. It is unlikely that the situation at 1 hour would be such that some enzymes are partially inhibited wherease others are completely inhibited. It is also possible that at 1 hour all the external enzyme is completely inhibited but after 3 hours some ECO penetrates the cell and additionally inhibits some internal NJ (A) and NJ (G) suggesting that at 1 hour the distribution gives a bettter representation of enzyme location that at 3 hours. Since it was unknown whether ECO is cleared from circulation between the two time points the possibility of progressive inhibition cannot completely be ruled out. It is unlikely that ECO can enter the cell across membranes which have been damaged due to anti-ChE action because cellular necrosis after only 3 hours is minimal (Townsend, 1988). Cell penetration may however occur by pinocytosis and the process of ECO injestion into the cell and subsequent inhibition of internal AChE by this method may occur slowly between the two time points and result in the decrease in internal NJ (G) and NJ (A) seen at 3 hours. Hence, in the absence of evidence to support or reject either of the possibilities disscused, both must be considered. In general, however, differences were observed in the extent to which the molecular forms where inhibited, irrespective of the time at which they were assessed, which suggested that they had been selectively inhibited by ECO on the basis of their cellular locations.

The percentages in Table 4.4 shown in bold type represent the total enzyme distribution in the diaphragm and was discussed in Section 3.2.2.2. It was found that 61.4±12.1% of the total activity per mg of muscle was G AChE, 23.4±4.4% was A AChE and 14.1±3.6% was NE AChE. Of the total activity per mg of muscle 53.3±13.1% was associated with NJ parts of muscle fibres (i.e. parts of the muscle which were not specialised as endplates) and 46.2±16.9% was associated with endplates (i.e. EPS AChE). Of the total G AChE in the diaphragm, 60% was associated with the NJ region and 40% with endplates. Of the total A AChE 60% was associated the NJ region and 40% with endplates and of total NE AChE 40% was associated with the NJ region and 60% with endplates. Hence, G, A and NE

AChE was associated with both endplate and non-endplate regions. In the mouse diaphragm there was only slightly more G AChE in the non-endplate region than in the endplate which was in contrast with the distribution found in rat (Younkin et al., 1982) where 82% was found in the non-endplate region and 18% in the endplate. In rat and mouse total asymmetric (A and NE) AChE was equally distributed between the non-endplate and endplate regions.

Of the total enzyme activity 45-70% was internal AChE and 30-55% was external suggesting that AChE was not exclusively internal or external. Of the total internal AChE about 60% was found in the NJ region and 40% was associated with endplates and of the total external AChE 30-50% was NJ and 50-70% in endplates.

G AChE accounted for 61.4±12.1% of the total activity per mg of muscle. Around 60% of G AChE was in the NJ region and 40% was in the endplates. About 40-70% of the total G AChE was located internally and 30-60% was external. Of the total internal G AChE 70% was in NJ parts and 30% in endplates. Of the total external G AChE 20-50% was in NJ parts and 50-80% in endplates. In the NJ region G AChE was 50-90% internal and 10-90% external. Since Younkin et al. determined that in the rat diaphragm G AChE was equally distributed between the inside and outside of the cell, this study proposes that the internal pool of NJ (G) enzyme may be larger that estimated and in the Younkin studies a lower estimate of internal NJ (G)was made because some of the internal enzyme had been inhibited by ECO which had penetrated the cell. However, Younkin et al., (1982) in their study, determined that of the non-endplate G AChE, the G1 form existed predominately internally whereas the G4 form was predominately external hence, individual G forms have different locations. In the endplates, however, 50% of G AChE was internal and 50% was external. The study suggested that both endplate and non-endplate regions contain intra- and extra-cellular pools of G forms. Intra-cellular forms are likely to be G1, G2 and G4 precursors in the RER and Golgi apparatus (Rotundo, 1984; Lazar et al., 1984; Brockman et al., 1986), processed G1, G2 and G4 forms in vesicles targeted for the cell membrane (Porter-Jordan et al., 1986) or molecules associated with the sarcoplasmic reticulum (Tennyson et al., 1973), lysosomes which mediate intra-cellular degradation of AChE and secretory granules (Wake, 1976; Sawyer et al., 1976). Studies have also indicated the existence of monomeric intra-cellular inactive pools which have an unknown function (Kerem et al., 1993; Lazar et al., 1984). Extra-cellular forms are likely to be secreted G1, G2 and G4 forms (Wilson et al., 1973) which may have a specific role or be degradation products of the multimetric forms or products of a recently identified mRNA devoid of an assembly signal (Li et al., 1991) or G1, G2 and G4

which are integral proteins of the sarcolemma (Rotundo, 1984a; Inestrosa and Perelman, 1989).

Readily-extractable asymmetric AChE (A) accounted for 23.4±4.4% of the total AChE activity per mg of muscle. About 60% of the total A AChE was in the NJ region and 40% in endplates. Of the total A AChE in the diaphragm about 50-70% was internal and 30-50% external. About 60% of the total internal A AChE was associated with the NJ region and 40% with endplates. Of the total external A AChE, about 30-60% was associated with the NJ region and 40-70% with endplates. In the NJ region 50-90% of A AChE was internal and 10-50% external. In the endplate region A AChE was equally distributed between the inside and outside of the cell. Readily-extractable asymmetric AChE was therefore equally distributed between the endplate and non-endplate regions and in each region was found internally and externally. This conflicted with the proposition in Chapter 3 that AChE in this fraction was totally intra-cellular because it is readily extractable and therefore not associated with the extra-cellular matrix. The collagen-tailed forms therefore exist as both intra- and extra-cellular pools in both regions. Intra-cellular A AChE is likely to be A4, A8 and A12 at various stages of processing and originating from various locations including the Golgi, vesicles, sarcoplasmic reticulum and lysosomes (Rotundo, 1984a; Inestrosa, 1984). Extra-cellular A AChE is possibly secreted A4, A8 and A12, or collagen-tailed AChE which has been externalised and failed to associate with the extra-cellular matrix although previous studies have suggested that no A forms are secreted and the capturing mechanism is largely effective. The origin of extra-cellular A AChE is therefore unclear. The occurrence of external A AChE in the non-endplate regions suggests that the enzyme have a non-cholinergic role because there are no endplates in this region.

The remainder of the total AChE activity per mg of muscle which accounted for 14.1±3.6% was due to NE AChE. About 40% of the total NE AChE was associated with the NJ region and 60% with endplates. Of the total NE AChE in the diaphragm, 20-40% was internal and 60-80% external. About 70-80% of the total internal NE AChE was located in non-endplate (i.e. NJ muscle regions) with the remaining 20-30% being located internally in the endplate. Of the external NE AChE, 80% was located at the endplate, with only a small portion, 20% found externally on non-specialised parts of muscle fibres. In the NJ region the NE forms were 50-75% internal and 25-50% external whereas in the endplates only about 10% was internal with the remaining 90% being external. Endplate NE AChE was therefore virtually all external and since the EPS (NE) fraction is predominately A12, this suggested that this enzyme was associated with the basal lamina of the

synaptic cleft and had a role in the termination of synaptic transmission (Inestrosa et al., 1982). Selective inhibition studies by Younkin et al., 1982, also identified endplate-associated A12 which was predominately external. NE AChE was also found to be associated with the non-endplate region in small amounts. Younkin et al., (1982) demonstrated using ^{125}I-alpha-bungarotoxin that this activity was not associated with stray endplates and therefore genuinely expressed high molecular weight forms at the cell surface of non-endplate regions. The function of or interaction with the cell membrane of these forms is unclear.

All the molecular forms of AChE were found in endplate and non-endplate parts of mouse skeletal muscle. The majority of these forms were distributed between the inside and outside of the cell with the exception of NE AChE in the endplate region which was predominantly external. It must be noted that the data provided in this section gives only an indication of enzyme distributions and not a precise map of the exact locations because the method used is based on assumptions about the movement of ECO through the tissue to the target areas. The cellular distribution of mouse molecular forms proposed by this study and for rat proposed by Younkin et al., (1982) support a hypothesis based on numerous studies and reviews of the metabolism of AChE. G1 appears to be a precursor for G4 and ultimately A12 (Koenig and Vigny, 1978). Globular and asymmetric forms arise from a single gene (Li et al, 1991) and extensive post-translational processing occurs to produce the secreted, cell-bound and basal lamina-associated molecular forms. The collagen-tailed forms of AChE are assembled internally and co-transported with enzyme targeted for secretion or membrane association in vesicles. External collagen-tailed AChE is predominately associated with the basal lamina, but some is associated with non-endplate regions whilst a portion appears to either secreted or unbound.

4.2.1.5 Endplate dimensions.

Table 4.5 shows endplate width (W), length (L) and width/length (W/L) ratio after various doses of ECO. At each dose the mean of averages of 30 endplates per hemi-diaphragm is given (in the statistical analysis of data the inter-hemidiaphragm variation was taken into account using a mixed-design MANOVA model as discussed in Section 2.6.3). Figures 4.5a and 4.5b show the changes in whole population W, L and W/L ratio respectively at each dose obtained by pooling together the ratios for all the endplates at that dose and the corresponding histograms for endplate ratios are shown in Figure 4.6.

Dose of ECO (nmol kg^{-1})	No. of HD No. of EP	Width of endplates (μm) †	Length of endplates (μm) †	W/L ratio †
Untreated	8 240	19.3±0.7	34.7±2.9	0.56±0.04
25	4 120	20.4±1.8	29.3±3.9 *	0.72±0.04 *
50	3 90	20.5±0.3 *	27.3±1.1 *	0.76±0.03 *
100	4 120	21.8±1.6 *	29.1±4.3 *	0.78±0.06 * +
300	2 60	22.8±1.4 * +	26.4±0.7 *	0.87±0.03 *
500	6 180	25.0±1.5 *	29.5±3.7 *	0.88±0.09 *

Table 4.5: Endplate dimensions 3 hours after ECO (25-500 nmol kg^{-1}) . Change in endplate width, length and width/length (W/L) ratio. HD gives the no. of hemidiaphragms and EP gives the total no. of endplates. Values are means±s.d. of averages of 30 EP per HD (300 nmol kg^{-1} dose value is ±min/max). † denotes sets with different groups (ANOVA, $P<0.05$), * denotes groups which differ from the untreated group (MANOVA, $P<0.05$) and + denotes different adjacent groups (MANOVA, $P<0.05$).

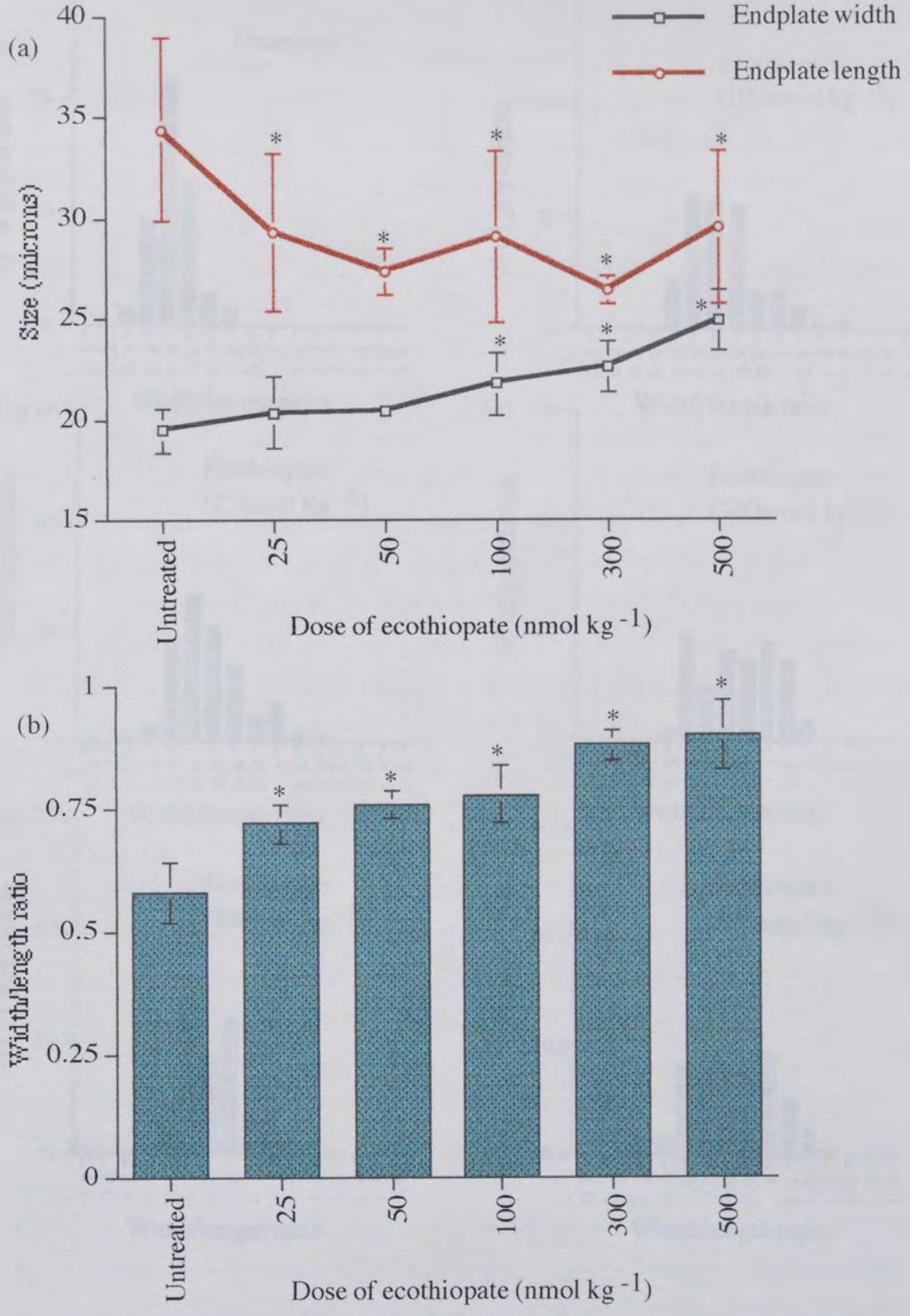

Figure 4.5: Width, length and width/length ratio of endplates 3 hours after ECO (25-500 nmol kg^{-1}). Variation in endplate population (a) widths and lengths and (b) width/length ratios. * denotes groups which differ from the untreated group: $P<0.05$ (MANOVA).

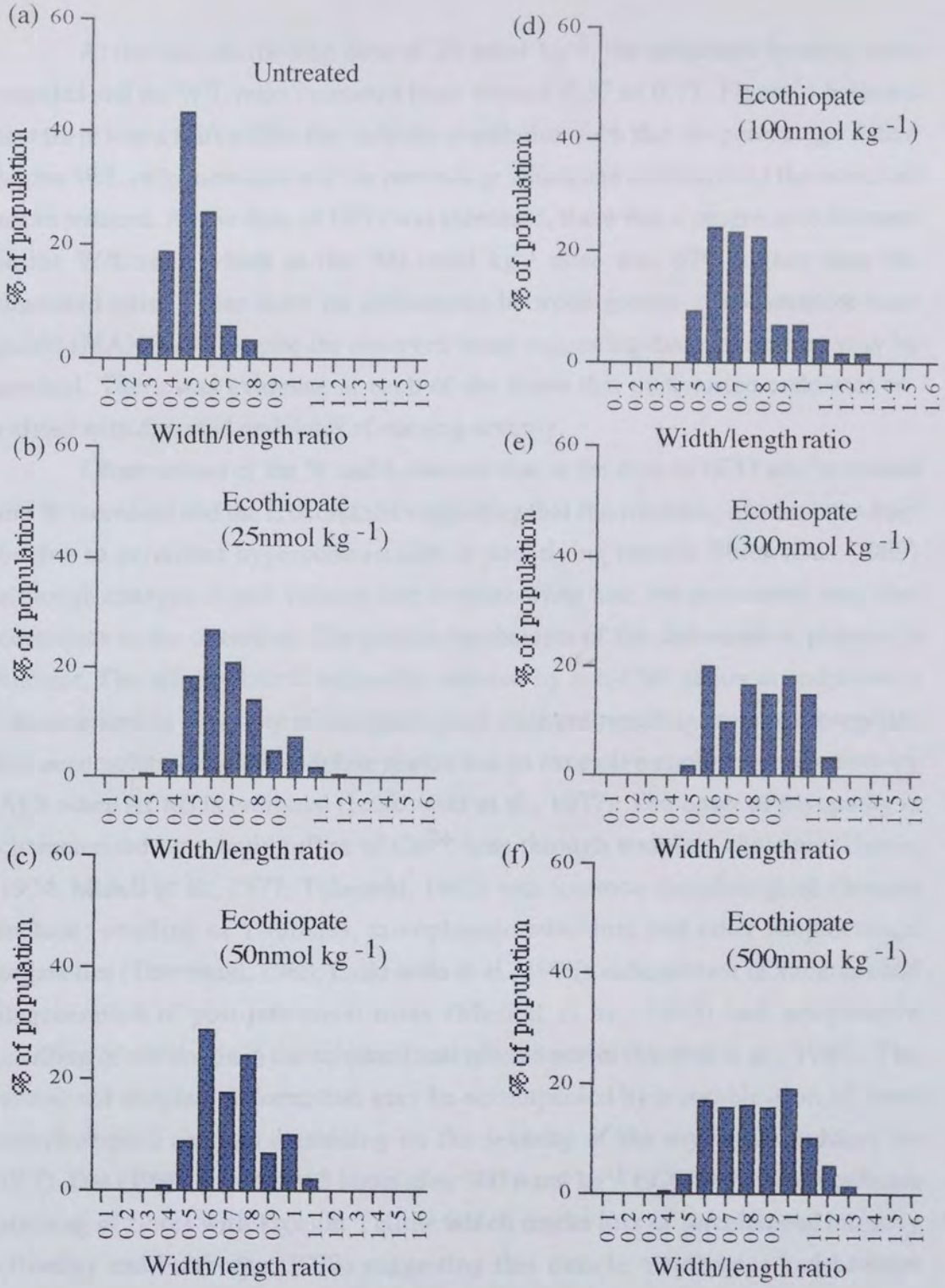

Figure 4.6: Histograms of endplates 3 hours after ECO (25-500 nmol kg^{-1}). Percentage of endplates per population at given width/length ratios for (a) untreated, (b) ECO 25 nmol kg^{-1}, (c) ECO 50 nmol kg^{-1}, (d) ECO 100 nmol kg^{-1}, (e) ECO 300 nmol kg^{-1} and (f) ECO 500 nmol kg^{-1}.

At the non-necrotising dose of 25 nmol kg^{-1}, the endplates became more rounded and the W/L ratio increased from around 0.57 to 0.72. Figure 4.6 shows that there was a shift within the endplate population such that the percentage with a higher W/L ratio increased and the percentage which had ratios around the untreated mean reduced. As the dose of ECO was increased, there was a progressive increase in the W/L ratio which at the 500 nmol kg^{-1} dose was 57% higher than the untreated ratio. There were no differences between groups at consecutive time points (MANOVA) despite the observed trend suggesting that the increase may be gradual. There was evidence at each of the doses that undistorted endplates co-existed with distorted endplates of varying severity.

Observations of the W and L showed that as the dose of ECO was increased the W increased and the L decreased suggesting that the rounding of endplates may be due to persistent hypercontractions in underlying muscle fibres (Das, 1989) although changes in cell volume due to proteolysis and ion movement may also contribute to the distortion. The precise mechanism of the deformation process is unclear. The ultrastructural myopathy induced by anti-ChE action at endplates is characterised by a variety of morphological changes resulting from inappropriate ion accumulations in the endplate region due to excessive cholinergic agonism by ACh when AChE is inhibited (Laskowski et al., 1977). The onset of myopathy is characterised by a rapid influx of Ca^{2+} ions through endplate channels (Evans, 1974; Mideli et al., 1977; Takeuchi, 1963) and common morphological changes include; swelling of T-tubules, sarcoplasmic reticulum and other subjunctional organelles (Townsend, 1988; Laskowski et al., 1975), enlargement of vacuoles and degeneration of post-junctional folds (Meshul et al., 1985) and progressive swelling of chromatin in the subjunctional muscle nuclei (Meshul et al., 1985). The visualised endplate deformation may be accompanied by a combination of these morphological changes depending on the severity of the myopathy induced by ECO. Das (1989) found that 3 hours after 300 nmol kg^{-1} ECO there was significant staining of fibres with Procion Yellow which marks loss of sarcolemmal integrity (Bradley and Fulthorpe, 1978) suggesting that muscle membranes had become leaky and contraction clumps were evident suggesting that the dose was potentially necrotising. In addition, these contraction clumps were localised in junctional regions and were not apparent in peripheral parts of the muscle (Das, 1989) indicating that the onset of damage originated close to the endplate and was therefore likely to be due to events at the endplate which were possibly instigated by Ca^{2+} influx. From the observations made by Das (1989), doses of ECO of and above 300 nmol kg^{-1} are defined as necrotising.

Endplate deformation was found to be an indicator of hypercontrations which are excessive and unphysiological contractions of myofibrils reflected by abnormally short sarcomeres (Das, 1989) induced by OPs. Due to the response observed at low doses of ECO, endplate deformation was therefore found to be a sensitive indicator of anti-ChE intoxication and a marker for mild myopathy.

4.2.2 Recovery of mouse skeletal muscle after a single acute dose of ECO.

4.2.2.1 Experimental design

Mice were given a single subcutaneous injection of 500 nmol kg^{-1} ECO with 700 nmol kg^{-1} atropine sulphate. At various time points after dosing (see below), a group of mice was killed and their diaphragms removed for analysis.

Group 1 : 3 hours after injection.
Group 2 : 1 day after injection.
Group 3 : 5 days after injection.
Group 4 : 7 days after injection.

4.2.2.2 Molecular forms of AChE.

Table 4.6 shows the activities of the various enzyme fractions 3 hours, 1 day, 5 days and 7 days after a 500 nmol kg^{-1} dose of ECO. Table 4.7 shows the percentage reductions in AChE activity. Three hours after a 500 nmol kg^{-1} dose of ECO, almost all the fractions of AChE measured were found to have reduced activities which remained so when measured after 1 day. Hence, ECO was found to locate its target enzymes rapidly and there was no change in the effects for at least 24 hours. The extent of reduction in enzyme activity, however, varied between enzyme type and location.

Figure 4.7 shows the responses of junctional (J) AChE. J (G), J (A) and J (NE) forms were reduced by 51.7±23.9%, 46.9±19.0% and 77.9±14.2% respectively 3 hours after ECO. One day later, the activities were still reduced (J (G) by 45.8±16.9%, J (A) by 52.6±14.2% and J (NE) by 65.7±16.3%). Five days after the initial dose, J (G) and J (A) AChE had completely recovered but J (NE) AChE was still reduced by 45.8±34.1%. Seven days after the initial dose, all the forms were at their normal level except J (A) AChE which was 23.3±31.3% lower than the untreated level.

Enzyme	Untreated	3 hrs	1 day	5 days	7 days
N	10	8	7	8	9
J (G) †	3.46+	1.67*	1.73*+	3.30	3.34
	±0.68	±0.83	±0.31	±0.61	±0.55
J (A) †	1.32+	0.70*	0.63 *+	1.05	0.97*
	±0.25	±0.25	±0.19	±0.37	±0.34
J (NE) †	0.80+	0.18*	0.27*+	0.51*	0.61*
	±0.20	±0.11	±0.13	±0.20	±0.27
NJ (G) †	1.96+	1.04*	1.23*+	1.95	1.94
	±0.40	±0.41	±0.31	±0.26	±0.39
NJ (A) †	0.77+	0.40*	0.39*+	0.65+	0.42*
	±0.26	±0.21	±0.17	±0.21	±0.13
NJ (NE) †	0.29	0.14	0.16	0.25	0.10
	±0.15	±0.14	±0.06	±0.12	±0.17
EPS (G) †	1.57+	0.63*	0.50*+	1.36	1.52
	±0.61	±0.50	±0.21	±0.70	±0.34
EPS (A) †	0.66+	0.31*	0.24*	0.40	0.54
	±0.26	±0.17	±0.20	±0.26	±0.30
EPS(NE) †	0.50+	0.05*	0.12*	0.26*	0.48
	±0.20	±0.04	±0.12	±0.14	±0.23

Table 4.6: Diaphragm AChE after 500 nmol kg^{-1} ECO (3 hrs-7 days). Globular (G), asymmetric (A) and non-extractable (NE) enzyme activities in junctional (J), non-junctional (NJ) and endplate-specific (EPS) regions are in nmol min^{-1} mg^{-1}. Values are means±s.d. † denotes sets with different groups (K-S ANOVA, $P<0.05$), * denotes groups which differ from the untreated group (K-S multi-comparison test, $P<0.05$) and + denotes different adjacent groups (K-S multi comparison test, $P<0.05$).

Region	3 hrs	1 day	5 days	7 days
J (G)	51.7 ±23.9	45.8 ±16.9	4.6 ±17.7	3.5 ±14.9
J (A)	46.9 ±19.0	52.6 ±14.2	20.3 ±27.7	27.6 ±22.6
J (NE)	77.9 ±14.2	65.7 ±16.3	45.8 ±34.1	23.3 ±31.3
NJ (G)	47.1 ±21.0	37.2 ±16.0	0.8 ±13.5	1.0 ±18.8
NJ (A)	48.7 ±26.9	49.3 ±22.3	15.3 ±26.8	44.6 ±16.0
NJ (NE)	50.4 ±47.8	46.3 ±20.9	12.5 ±42.2	66.6 ±53.5
EPS (G)	59.7 ±32.2	68.4 ±13.6	13.4 ±44.4	10.7 ±28.0
EPS (A)	53.2 ±25.6	64.3 ±29.9	39.4 ±40.1	17.5 ±42.2
EPS (NE)	90.3 ±8.7	76.3 ±23.1	48.8 ±27.8	4.5 ±42.8

Table 4.7: Percentage reduction of diaphragm AChE after 500 nmol kg^{-1} ECO (3 hrs-7 days). Percentage reduction in globular (G), asymmetric (A), non extractable (NE) AChE enzyme activity in junctional (J), non-junctional (NJ) and endplate-specific (EPS) regions. Values are mean percentage reductions±s.d.

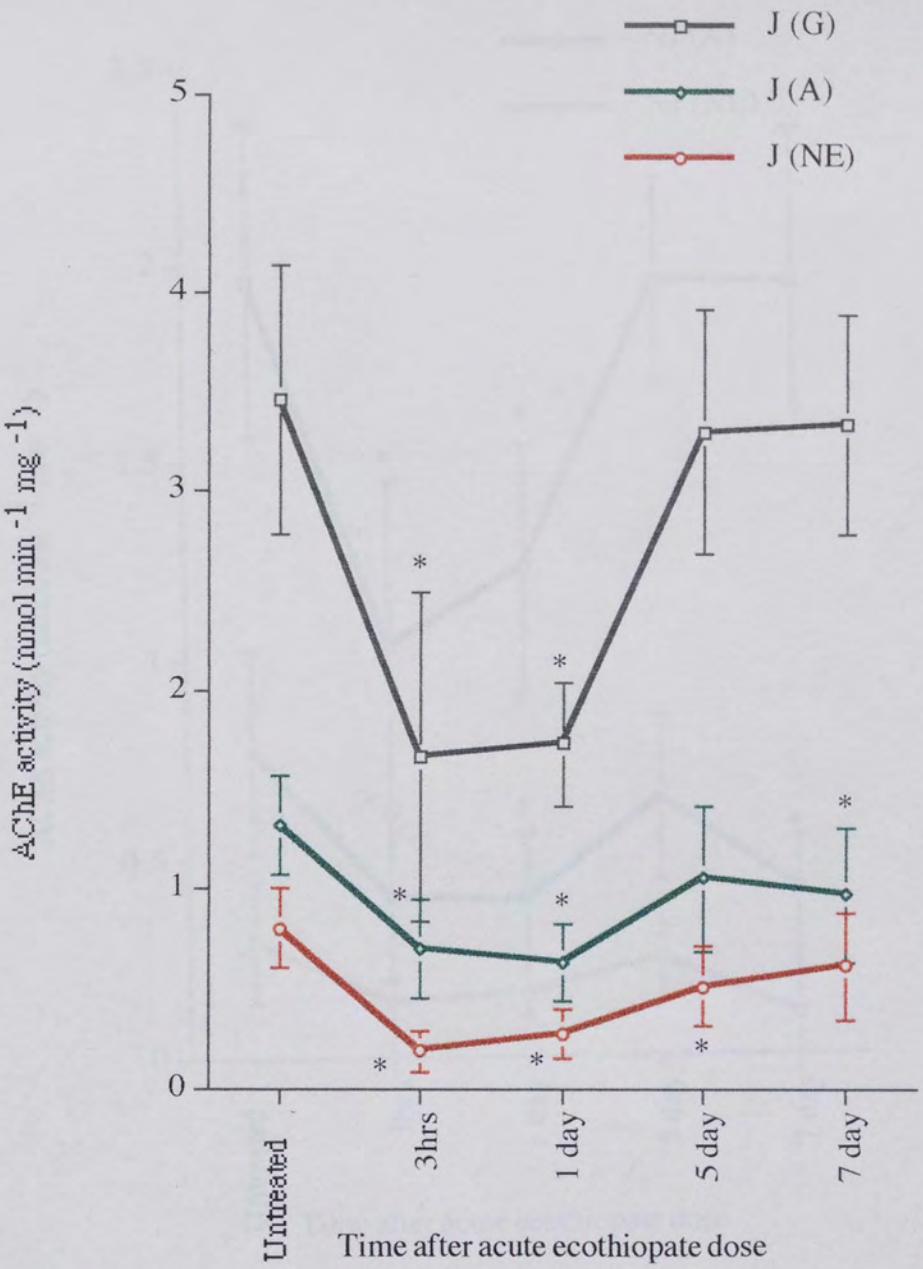

Figure 4.7: Junctional AChE after 500 nmol kg^{-1} ECO (3 hrs-7 days). Globular (G), asymmetric (A), non-extractable (NE) and total AChE activity in the junctional (J) region of mouse diaphragm. * denotes groups which differ from the untreated group: $P<0.05$ (Kruskal-Wallis multi-comparison test).

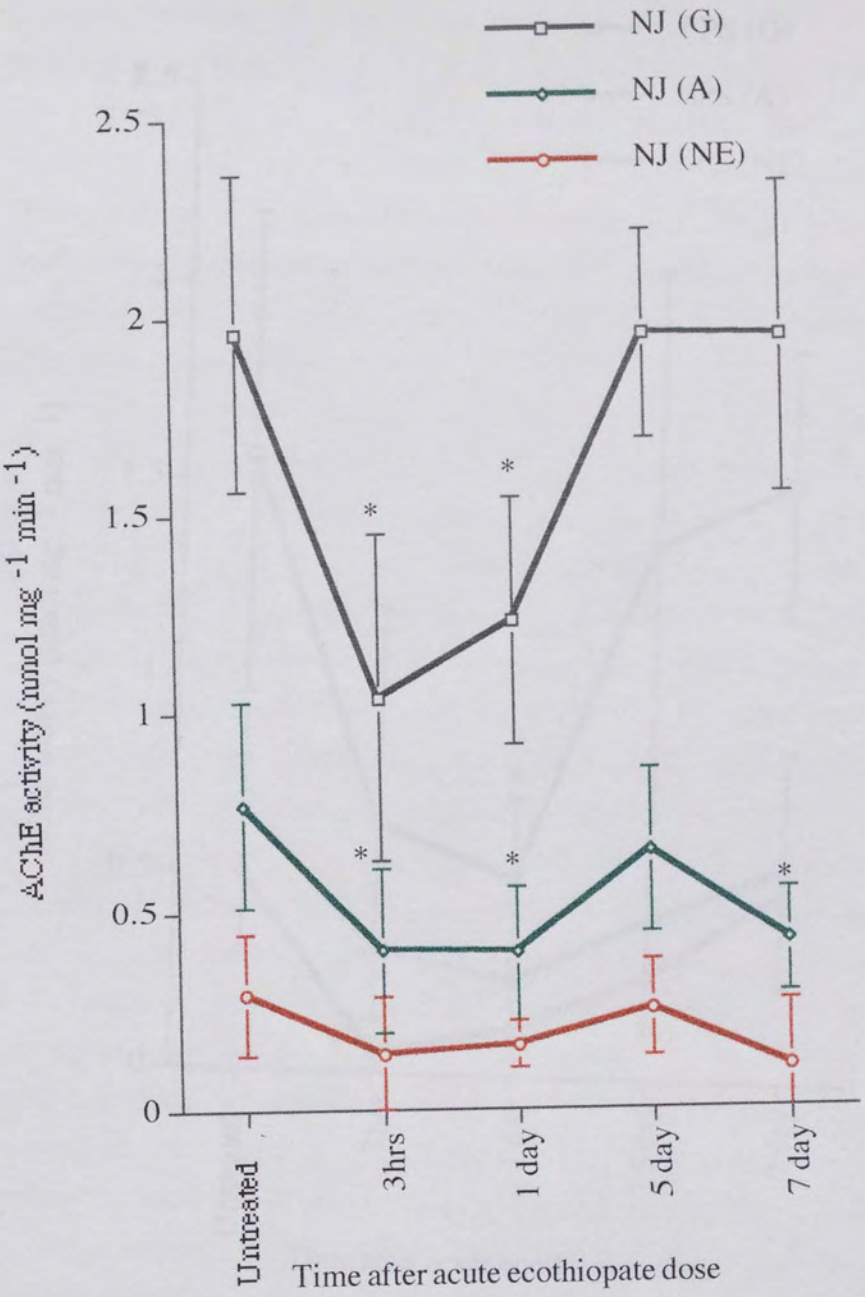

Figure 4.8: Non-junctional AChE after 500 nmol kg^{-1} ECO (3 hrs-7 days). Globular (G), asymmetric (A), non-extractable (NE) and total AChE activity in the non-junctional (NJ) region of mouse diaphragm. * denotes groups which differ from the untreated group: $P<0.05$ (Kruskal-Wallis multi-comparison test).

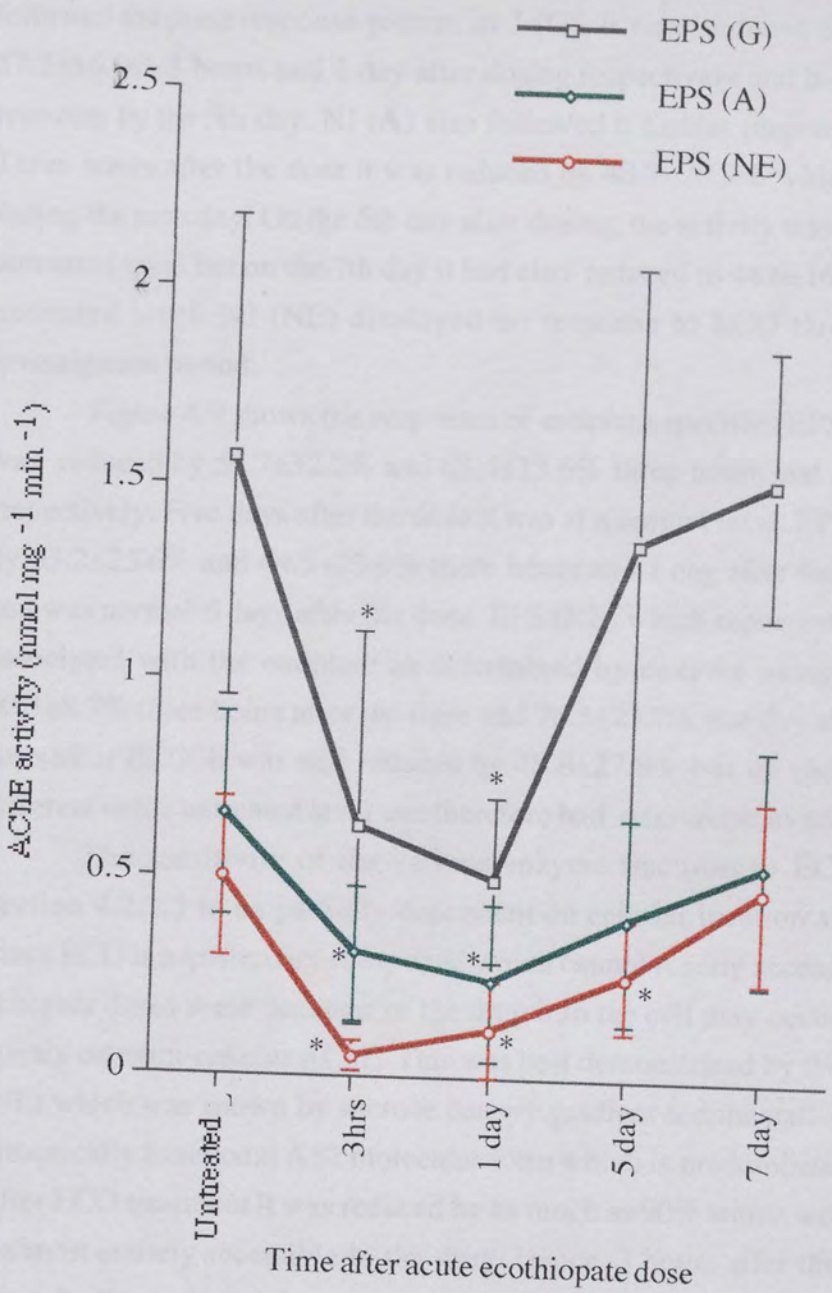

Figure 4.9: Endplate-specific AChE after 500 nmol kg^{-1} ECO (3 hrs-7 days). Globular (G), asymmetric (A), non-extractable (NE) and total AChE activity in the endplate-specific (EPS) region of mouse diaphragm. * denotes groups which differ from the untreated group: $P<0.05$ (Kruskal-Wallis multi-comparison test).

Figure 4.8 shows the responses of non-junctional (NJ) AChE. NJ (G) followed the same response pattern as J (G). It was reduced by 47.1±21.0% and 37.2±16.0% 3 hours and 1 day after dosing respectively and had made a complete recovery by the 5th day. NJ (A) also followed a similar response pattern to J (A). Three hours after the dose it was reduced by 48.7±26.9% which was maintained during the next day. On the 5th day after dosing, the activity was not different to the untreated level but on the 7th day it had also reduced to 44.6±16.0% lower than the untreated level. NJ (NE) displayed no response to ECO throughout the entire investigation period.

Figure 4.9 shows the responses of endplate-specific (EPS) AChE. EPS (G) was reduced by 59.7±32.2% and 68.4±13.6% three hours and 1 day after dosing respectively. Five days after the dose it was at a normal level. EPS (A) was reduced by 53.2±25.6% and 64.3±29.9% three hours and 1 day after the dose respectively and was normal 5 days after the dose. EPS (NE) which represented functional A12 associated with the endplate as determined by enzyme assay was reduced by 90.3±8.7% three hours after the dose and 76.3±23.1% one day after the dose. Five days after ECO, it was still reduced by 48.8±27.8% but on the 7th day was not different to the untreated level and therefore had returned to its normal level.

The sensitivity of the various enzyme fractions to ECO was found in Section 4.2.1.3 to be partially dependent on cellular location and turnover rates. Since ECO is a quaternary compound which cannot readily access the cell (although at higher doses some 'leakage' of the drug into the cell may occur) it therefore acts mainly on extra-cellular AChE. This was best demonstrated by the response of EPS (NE) which was shown by sucrose density gradient sedimentation to be rich in the synaptically functional A12 molecular form which is predominantly extra-cellular. After ECO treatment it was reduced by as much as 90% which would suggest that it is almost entirely accessible to the drug. Hence, 3 hours after the dose was given, the reductions observed were probably mainly due to the inactivation of external enzyme although as discussed in Section 4.2.1.4 some inactivation of internal AChE may have occured. The dose of ECO, however, inhibited the total diaphragm AChE only partially and not completely. Notably, the inactivation observed in all forms persisted for at least 24 hours, during which time there was no recovery. All molecular forms, with the exception of EPS (NE) completely recovered between the 1st and 5th days after treatment. Statistically, there was no significant difference between the activities of all the enzyme forms at this time point and their untreated level but there was a significant difference between all these activities and the previous time point implying that recovery may have taken place. An exception to this rule was displayed by EPS (NE) which was still reduced at 5 days. Since EPS

(NE) represents the A12 molecular form which has the highest molecular weight and is therefore at the end of the pathway, and by 5 days all the precursor forms had apparently reached normal levels, there may have been a delay in translocation of A12 to its synaptic target. Furthermore at 7 days, all the enzyme levels appeared to be as normal, including the A12 rich fractions, but the NJ (A) forms were lower that the untreated values, whereas previously, at 5 days, they were as normal. Since, these fractions contain predominantly lower molecular weight asymmetric enzymes i.e. A8 and A4 forms, they are most likely to be precursor pools for the A12 enzyme. A depletion of these forms, at 7 days was probably not due to the inhibitory effects of ECO, which was unlikely to persist in the system for such a length of time, and may be related to the increase in synaptic A12.

The rate of recovery of EPS (G) between the 1st and 5th days was more rapid (0.6% hr^{-1}) than the rate of recovery of the other forms (0.3-0.4% hr^{-1}). Since EPS (G) represents the combined activity of G1, G2 and G4 forms associated with the endplate region, this supports the hypothesis that these are precursors of the higher molecular forms. The rapid return of the G1 precursor is an established feature of recovery after OP-inactivation and has been observed after methyl-phosphorothiolate (Goudou and Reiger, 1983), soman (Grubic et al., 1981) and diisopropylflourophosphate (Reiger et al., 1976).

The precise mechanism by which the molecular forms of AChE recover after partial irreversible inactivation is unclear. In the literature, the recovery of AChE activity following OP inhibition is confusing with many conflicting views on recovery rates: after soman, low molecular AChE precursors recovered within 2 days (Grubic et al., 1981), cytochemical studies revealed that the recovery rate was much faster and the precursors could be seen within 5-12 hours and studies have show the appearance of precursors as early as 180 minutes after inactivation (Van Dongen et al., 1988). In this study, the onset of recovery was not rapid and did not occur until at least 24 hours after the dose of ECO had been administered.

Several studies have proposed a bi-phasic mechanism for the recovery of the molecular forms after methyl-phosphorothiolate (Goudou and Reiger, 1981) and sarin (Koelle et al., 1982). This involved an 'early rapid phase' which lasted for approximately 15 hours after dosing and corresponded to a period of increased protein synthesis when 60% of AChE activity recovered, followed by a 'slow recovery phase' which lasted for 2-3 days during which a further 20% of AChE activity recovered. It was proposed that the complete recovery of AChE took longer than 3 days (Salpeter et al., 1979). Grubic et al., (1981) found that the early phase corresponded to the synthesis of low molecular weight precursors and the slow phase corresponded to the slow reappearance of higher molecular weight AChE. It

is not clear whether the rapid recovery of precursors is due to OP-induced up-regulation or because they have a rapid turnover (Lazar et al., 1984) and the slow appearance of the higher forms is because they have a slower turnover rate (Lazar et al., 1984) or because there is an OP-induced delay in the biogenesis of these molecules. It is not known to what extent this model can be applied to recovery after ECO because there are several differences between the studies, although globular forms recovered rapidly and A12 recovered at a slower rate. The recovery model is based on administration of rapidly ageing OPs which inactivated almost all AChE such that recovery occurred predominantly by *de novo* synthesis (Grubic et al., 1981; Fernandez and Stiles; 1984). This was in contrast to the ECO study. ECO displays some spontaneous reactivation with a half-life between 44 and 64 hours and ages with a half-life of 41 hours (Hobbiger, 1976) and was administered at a dose which only partially inhibited all tissue AChE. It is proposed therefore that both *de novo* synthesis and spontaneous reactivation may contribute to the recovery of diaphragm AChE after ECO.

The failure of the system to adhere strictly to the bi-phasic recovery mechanism may be due to differences in effects on the regulation of AChE metabolism induced after severe and mild OP-intoxication. Knowledge of the exact regulation of AChE metabolism is limited; non-endplate AChE activity is regulated predominately by muscle activity whereas, endplate AChE activity is regulated by a combination of muscle activity and neurotrophic factors (Younkin and Younkin, 1988). After OP inhibition, the rate of recovery of non-endplate AChE was found to be more rapid than the rate of endplate recovery (Fernandez and Stiles, 1984) and may be because there is a delay in the transport of neurotrophic factors to target sites. Although a clear distinction was not evident in the ECO study between the recovery rates of endplate and non-endplate AChE, there was a delay in the recovery of the synaptic form. Grubic et al., (1981) found that after soman, there was a delay in the appearance of endplate-specific asymmetric AChE due to an inability of these forms to successfully attach to their subcellular structures. Since the nerve-derived molecule agrin has been associated with the accumulation of AChE in the basal lamina (Leith and Fallon, 1993; Wallace, 1989), it is possible that there may be some delay in its transport to the muscle in the event of prolonged cholinergic agonism.

After soman intoxication Grubic et al., (1981) observed the increased synthesis of AChE in the endoplasmic reticulum of the Schwann cell and the sarcoplasmic reticulum and special tubules located beneath the motor endplates. This was analogous to the accumulation of AChE during the postnatal development of rats (Brzin et al., 1980) and suggests that the induction of AChE synthesis at

these locations may be regulated by similar factors in developing systems and after anti-ChE intoxication. Likely candidates for this role are the POMC-derived peptides which are important in the regulation of developing system, (Haynes et al., 1984) and are released into the circulation in response to stress (Rosier et al., 1977). Amos et al. (1995) found that POMC-mRNA was up-regulated in the lumbar spinal cord 3-24 hours after ECO at 500 nmol kg^{-1} and returned to normal by the 5th day. Although there was no evidence of increased POMC peptide activity in the diaphragm and it is not known whether ECO induces the synthesis of AChE in the sarcoplasmic reticulum etc., POMC peptides after OP-intoxication may regulate the correct proportions of AChE molecular forms (Haynes et al, 1984). Hence, nerve-derived factors as well as muscle activity may determine the rate of recovery of AChE after OP inhibition which in turn may vary as a function of the degree of intoxication.

The recovery of AChE activity in mouse skeletal muscle after OP-intoxication occurs by a complex mechanism which is poorly understood and influenced by many factors.

4.2.2.3 Endplate dimensions.

Table 4.8 shows the variation in endplate W, L and W/L ratio 3 hours, 1 day, 5 days and 7 days after a single subcutaneous injection of 500 nmol kg^{-1} ECO. Figure 4.10a shows the variation in endplate W and L at the various time points and Figure 4.10b shows the corresponding variation in the W/L ratio. Figure 4.11 shows histograms of endplate W/L ratios at corresponding time points.

The W/L ratio of endplates was affected maximally after 3 hours and recovered to normal over the subsequent 7 day period. The rounding of endplates after 3 hours occurred due to a increase in W and a corresponding decrease in the L. Figure 4.11(b) shows that 3 hours after the dose there was a shift in the distribution of the histogram such that a higher percentage of endplates had a higher ratio and fewer endplates had ratios around the mean ratio in untreated tissues of around 0.5. Between 6 and 24 hours after the dose the ratio increased from 0.83 to 0.74. During the following 4 days there was little improvement in the ratio which persisited around 0.77 but between the 5th and 7th days a recovery was observed as the ratio reduced from 0.77 to 0.63 and endplate groups tested at these time points were different to each other. Observations of the histograms showed that during the 7 day period there was a progressive shift in the distribution such that a higher percentage of endplates had ratios around the untreated mean. There was no difference between the untreated W/L ratio population and the population at 7 days

Time after ECO 500 nmol kg^{-1}	**No. of HD No. of EP**	**Width of endplates (μm) †**	**Length of endplates (μm) †**	**W/L ratio †**
Untreated	8 240	19.3±0.7	34.8±2.9	0.56±0.04
3 hrs	6 180	25.0±1.5*	29.5±3.7*	0.88±0.09*
6 hrs	2 60	25.7±0.8*	31.6±1.3	0.83±0.01*
1 day	3 90	23.0±2.5* +	31.7±1.3	0.74±0.06*
5 days	5 150	22.2±1.1*	29.5±2.3* +	0.77±0.07* +
7 days	2 60	22.3±0.4*	36.5±0.9	0.63±0.04

Table 4.8: Endplate dimensions after 500 nmol kg^{-1} ECO (3 hrs-7 days). Change in endplate width, length and width/length (W/L) ratio. HD gives the no. of hemidiaphragms and EP gives the total no. of endplates. Values are means±s.d (7 day value is ±min/max). † denotes sets with different groups (ANOVA, $P<0.05$), * denotes groups which differ from the untreated group (MANOVA, $P<0.05$) and + denotes different adjacent groups (MANOVA, $P<0.05$).

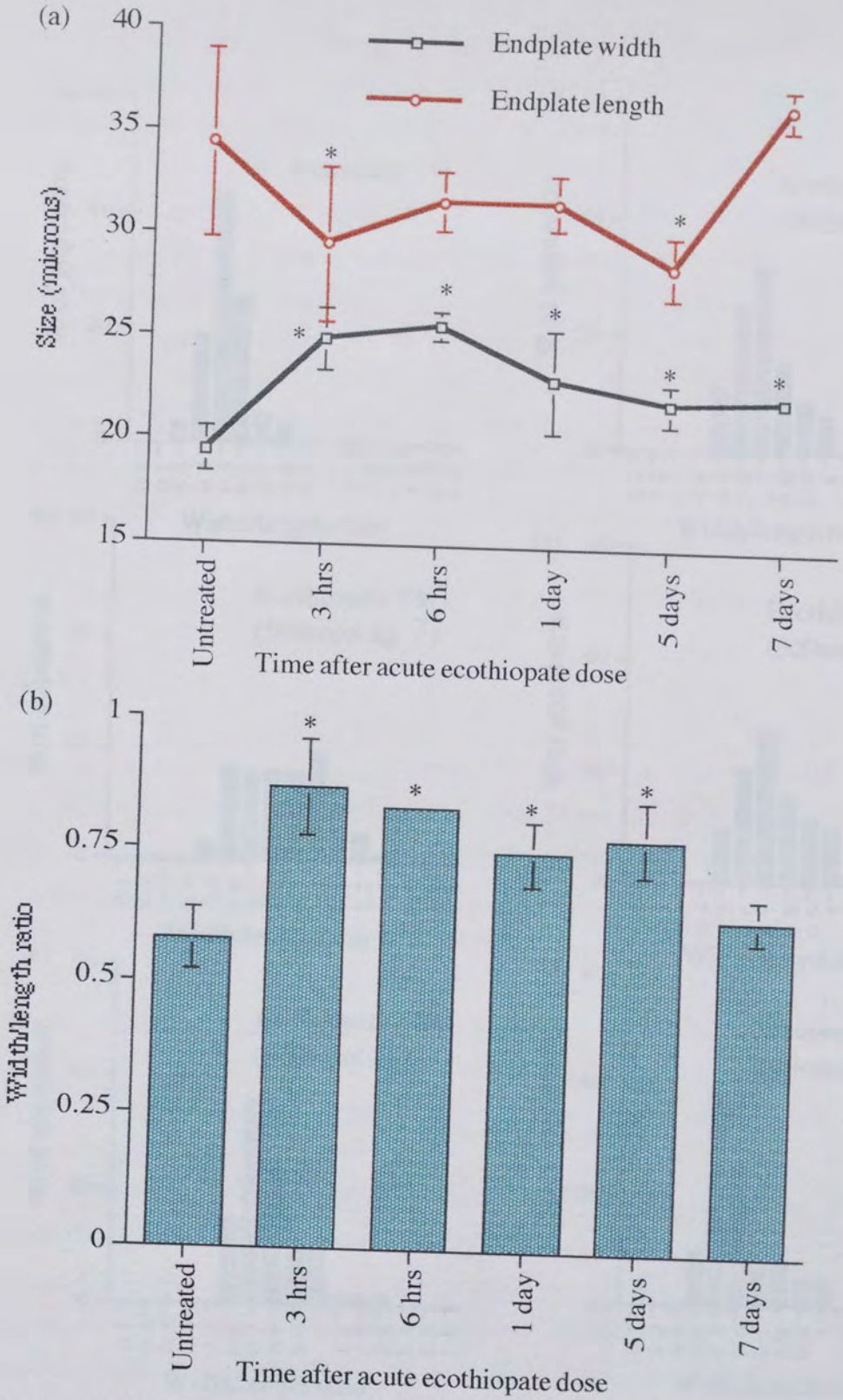

Figure 4.10: Width, length and width/length ratio of endplates after 500 nmol kg^{-1} ECO (3 hrs-7 days). Variation in endplate population (a) widths and lengths and (b) width/length ratios. * denotes groups which differ from the untreated group: $P<0.05$ (MANOVA).

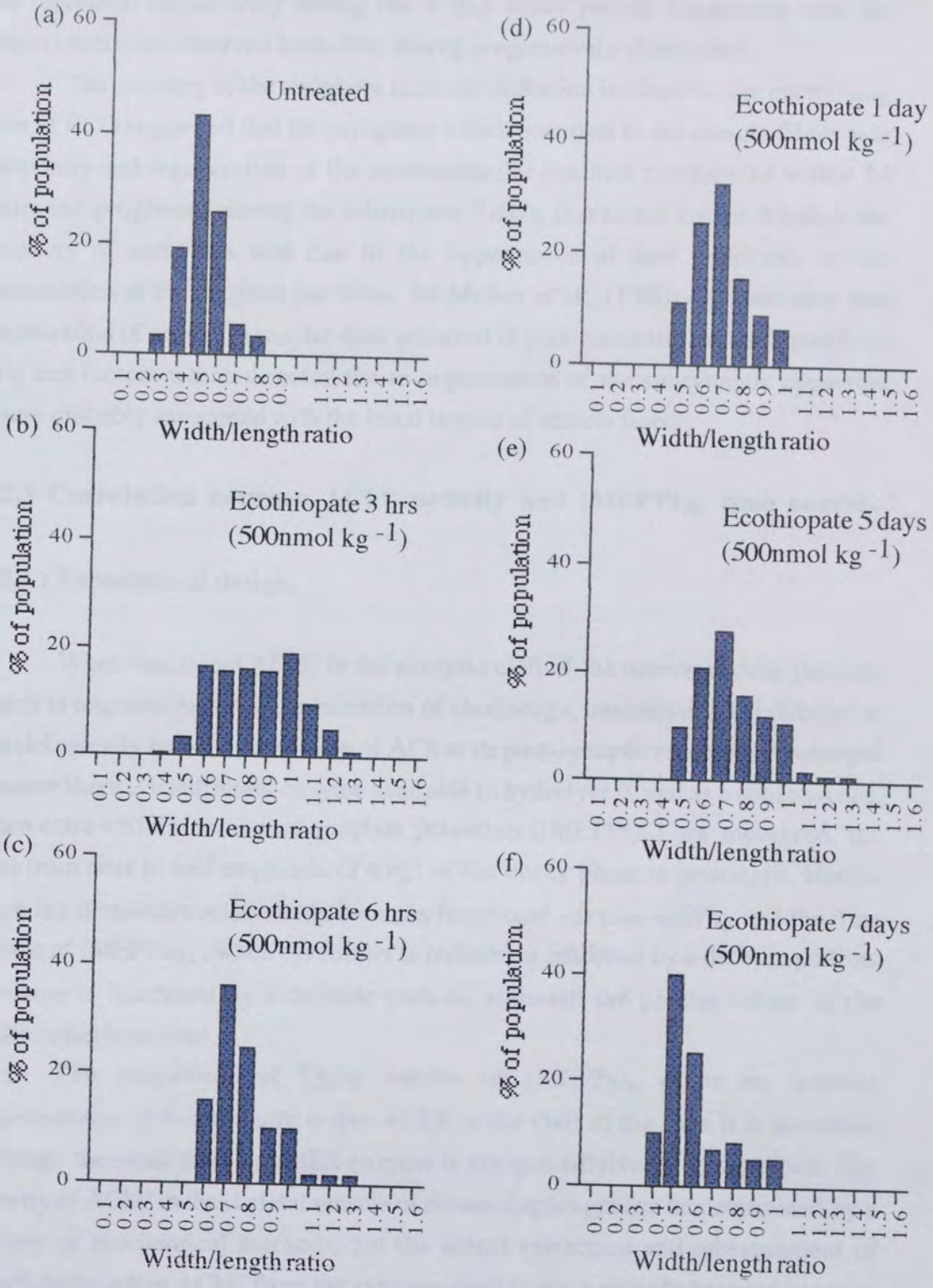

Figure 4.11: Histograms of endplates after 500 nmol kg^{-1} ECO (3 hrs-7 days). Percentage of endplates per population at given width/length ratios for (a) untreated, (b) after 3 hrs, (c) after 6 hrs, (d) after 1 day, (e) after 5 days and (f) after 7 days.

suggesting that complete recovery had occured. Both the W and the L decreased and increased respectively during the 7 day study period suggesting that the hypercontrations observed soon after dosing progressively diminished.

The recovery of the endplates from the distortion induced by the necrotising dose of ECO suggested that the myopathy which occurred in the muscle fibres was temporary and regeneration of the neuromuscular junction commenced within 24 hours and progressed during the subsequent 7 days. It was not known whether the recovery of endplates was due to the appearance of new endplates or the regeneration of the original junctions. McMahan et al., (1980) demonstrated that regeneration of original synaptic sites occurred in post-traumatic skeletal muscle in frog and factors which directed the re-organisation of the subsynaptic apparatus where probably associated with the basal lamina of muscle fibres.

4.2.3 Correlation between AChE activity and $(MEPPs)_o$ time course.

4.2.3.1 Experimental design.

When functional AChE in the synaptic cleft of the neuromuscular junction which is responsible for the termination of cholinergic transmission is inhibited or physiologically reduced, the action of ACh at its post-synaptic receptor is prolonged because there is insufficient enzyme available to hydrolyse it, and as a consequence, when extra-cellular miniature endplate potentials ($(MEPPs)_o$) are measured, the time from peak to half amplitude ($T_{50\%}$) of the decay phase is prolonged. Hence, there is a distinctive relationship between functional enzyme activity and the time course of $(MEPPs)_o$; when the former is reduced or inhibited by a definite portion, the latter is increased by a definite portion, although the precise nature of the relationship is unclear.

The magnitude of $T_{50\%}$ values of $(MEPPs)_o$ gives an indirect representation of functionally active AChE in the cleft at the time it is measured although the exact activity of this enzyme is not quantifiable by this method. The activity of AChE in the skeletal muscle of mouse diaphragm can be determined by a variety of biochemical methods, but the actual extraction and measurement of functionally active AChE from the synaptic cleft is not a straight-forward process. In this section, an attempt was made to correlate functionally active AChE represented by the response of $T_{50\%}$ of $(MEPPs)_o$ with the activity of functionally active AChE determined by the extraction and assay method.

The sequential extraction technique rendered a range of fractions containing molecular forms of AChE of which the NE fraction was shown to be the richest in

the A12 functional molecular form, thought to be active in the synaptic cleft, by velocity sedimentation on sucrose density gradients (see Section 3.2.2.3) and selective inhibition using ECO indicated that EPS (NE) most likely represented AChE activity associated with the synaptic cleft (see Section 4.2.1.4). If EPS (NE) truly represented the activity of functional synaptic enzyme then it was expected to correlate well with the time course of $(MEPPs)_o$ under the same experimental conditions; any reduction or inhibition of functional AChE in the cleft would be reflected by a corresponding increase in the $T50\%$ values irrespective of the type of drug used or the nature of the treatment. However, since the representation of A12 by calculation was not a direct measure of this enzyme but depended on the activity of other diaphragm enzymes, if these were subject to any metabolic regulatory effects or changes then the calculated EPS (NE) would no longer give a true indication of functionally active AChE in the cleft and the relationship would no longer apply. In the attempt to identify the relationship, it was necessary to use a suitable study model where fluctuations in the activities of these other diaphragm enzymes due to metabolic or other changes would not occur resulting in the miss-representation of synaptic AChE assessed by the assay method. The administration of the anti-ChE ECO at a range of doses was therefore considered a suitable study model to investigate the relationship for the following reasons:

(a) ECO is a known irreversible inhibitor of AChE. It forms stable complexes which are not likely to disassociate during the course of the study. Reductions in functional AChE activity due to inhibition would be complemented by a corresponding increase in $T50\%$ of $(MEPPs)_o$.
(b) ECO is a quaternary compound which does not readily traverse cell membranes such that intra-cellular precursor forms would be minimally affected and extra-cellular AChE i.e. the functional synaptic AChE will be preferentially inhibited.
(c) Data was collected 3 hours after dosing and since synaptic AChE has a slow turnover rate, any effects on the general metabolism of AChE were kept to a minimum preventing fluctuations in the enzyme activities which were important in the calculation of synaptic AChE.

It was proposed that in experiments where it was unclear if the functional AChE activity determined by the assay method truly represented functionally active enzyme in the cleft due to possible metabolic effects, the relationship could be used to predict functional A12 activity by substituting $T50\%$ values of $(MEPPs)_o$ into the relationship. The use of the relationship would therefore provide an alternative

method of determining the activity of functional synaptic AChE as well as distinguishing between functionally and non-functionally important AChE in the diaphragm (note: functional AChE refers only to that which is functionally active in the synaptic cleft and non-functional AChE represents enzyme which is not involved in cholinergic transmission). An attempt was made in this section to:

(a) Correlate the activity of various diaphragm forms of AChE with the time course of $(MEPPs)_o$ and identify which enzyme activity best represented functional enzyme after irreversible inhibition (Note: from inhibition studies alone it was not possible to precisely deduce the functional enzyme as all the molecular forms were expected to respond to the drug in a dose-dependent manner and therefore correlate well with $(MEPPs)_o$. Hence, in addition the cellular locations of the various enzymes was also taken into account.)
(b) Represent the relationship graphically and investigate the nature of the relationship.
(c) Use the relationship to predict functional AChE activity by an alternative method than the assay method, compare the methods and distinguish between functionally important and non-functional enzyme.

Initial studies were conducted where ECO was administered at a range of doses between 25 and 500 nmol kg^{-1}. Three hours after subcutaneous injection of the drug, the diaphragms were removed. These were assayed for AChE activity by the sequential extraction method and the $T_{50\%}$ of $(MEPPs)_o$ were recorded (all electrophysiological recordings were made by A. Crofts and all $T_{50\%}$ values quoted represent the time to half amplitude of the decay phase of extra-cellular miniature endplate potentials in milliseconds). In the second set of experiments, similar measurements were made, but only a single dose of 500 nmol kg^{-1} ECO was given and enzyme levels were recorded over a period of 7 days. The purpose of this second experiment was to investigate the relationship under a different set of conditions.

At each dose of ECO, assay of AChE activity and recordings of $(MEPPs)_o$ were carried out in parallel. Because the sequential extraction method needed two hemidiaphragms, $(MEPPs)_o$ were also recorded from two hemidiaphragms. To ensure that the prolongation of $(MEPPs)_o$ corresponded with the correct level of inhibition of functional AChE, two mice were dosed under identical conditions. One hemidiaphragm from each of these mice was then removed and pooled together for the extraction and assay of AChE and $T_{50\%}$ of $(MEPPs)_o$ were recorded from the two remaining hemidiaphragms. Each combined biochemical and

electrophysiological assessment thus made constituted an individual experiment and for each such experiment nine sets of data were obtained consisting of each AChE extraction fraction activity (i.e. J (G), J (A), J (NE), NJ (G), NJ (A), NJ (NE), EPS (G), EPS (A) and EPS (NE)) paired with the recorded $T_{50\%}$ of $(MEPPs)_o$. From the entire ECO dose study, a total of 35 experiments as described were performed. The AChE activities were correlated with the $T_{50\%}$ of $(MEPPs)_o$ using the following two procedures. Firstly, for each of the nine enzyme fractions, the AChE activity from each of the 35 experiments was correlated against the corresponding $T_{50\%}$ values. In the second analysis, data was grouped for a particular dose of ECO in the range 25-500 nmol kg^{-1} and means obtained for AChE activity and $T_{50\%}$ values. The mean AChE values were also correlated against the mean $T_{50\%}$ values. The latter was carried out because there was found to be a large variation in the actual data collected at the various experimental points and also provided an indication of the accuracy of the overall relationship determined. The data was then subjected to statistical analysis. Since, the data was not normally distributed, the Spearman's Rank non-parametric test was used to determine the correlation co-efficients and their significance.

To determine the nature of the relationship, a plot was made of the enzyme activities which best correlated with $T_{50\%}$ of $(MEPPS)_o$ versus the $T_{50\%}$. These were represented as scatter-grams and the line of best fit was applied Linear, exponential and logarithmic lines were fitted to the data and the equations of these lines were also determined. It was proposed that the relationship established would apply under all experimental conditions and was tested by applying it to a different set of experiment conditions (i.e. after a single dose of 500 nmol kg^{-1} ECO). It was proposed that any deviations from the relationship under different experimental conditions would be an indication that enzyme activities may be metabolically affected.

4.2.3.2 Correlation between AChE activity and $(MEPPs)_o$ and identification of functionally important AChE.

Figures 4.12-4.14 show scattergraph plots of the data for diaphragm AChE activity versus the corresponding $T_{50\%}$ of $(MEPPs)_o$ obtained during ECO dose studies. Each scattergraph for each of the nine diaphragm fractions consists of a plot of the activities versus $T_{50\%}$ values during each of the 35 experiments performed and also for mean values for each particular dose of ECO in the range 25-500 nmol kg^{-1} (N numbers for each $T_{50\%}$ and AChE mean at each dose of

ECO were : untreated:10; 25 nmol kg^{-1}:4; 50 nmol kg^{-1}:4; 100 nmol kg^{-1}:4; 300 nmol kg^{-1}:4 and 500 nmol kg^{-1}:9)

When correlation co-efficients using the Spearman's Rank non-parametric test (see Table 4.9) were obtained between the $T_{50\%}$ values and AChE activity and the significance of the relationship tested, it was found that AChE in some fractions correlated well whereas others did not. The relationship between assayed AChE activities and $T_{50\%}$ was negative as indicated by the sign of the co-efficient such that when AChE activities decreased, $T_{50\%}$ values increased. The significance of the correlations was also tested and it was found that as the co-efficients approached -1.00, the correlations became more significant. When measurements were made 3 hours after ECO a good correlation was obtained between all the J forms, but not with all the enzymes in the NJ region. Since the J AChE predominately originates from the endplates which are abundant in this region, this relationship was expected. However, by looking at the J enzymes only, no distinction could be made between functional and non-functional enzyme which was the primary objective of this study. For instance, J (G) displayed a significant correlation, but was not likely to be involved in the termination of synaptic transmission because the fraction was rich in precursor, secreted and cell-bound low molecular weight AChE. A good correlation was also obtained for the J (NE) enzyme fraction which was rich in A12. However, the NE fraction from the NJ region which contains trace levels of the A12 molecular form displayed a very poor correlation. A correction was therefore necessary for the non-functional enzymes present in the J region which arise from the non-endplate parts of muscle fibres present in this region by subtracting NJ activity from J activity in the calculation of endplate specific (EPS) activity.

EPS (G) and EPS (A) displayed only a moderately significant correlation with $(MEPPs)_o$ time course suggesting that they were probably not functionally important but had some other role in this region, probably as precursors. EPS (NE) gave a good significant correlation and probably represented synaptically functional AChE.

Despite displaying good correlations with the $(MEPPs)_o$ data, many of the enzymes could be eliminated from being functionally important because they either originated from non-endplate containing regions (i.e. the NJ enzymes), or where of low molecular weight such as the G form fractions. The enzymes which were important to the argument were the J (NE) fraction and the EPS enzymes. Both were measures of the A12 molecular form and displayed good correlations with $(MEPPs)_o$. However, the J enzyme fraction contained a non-functional component which may be subject to variation which would be reflected in the measurement of

AChE enzyme fraction	Co-efficient for ECO time studies (all points, N=35)	Co-efficient for ECO time studies (means)	Co-efficient for ECO dose studies (all points, N=35)	Co-efficient for ECO dose studies (means)
J (G)	-0.58 ***	-1.00	-0.77 ***	-0.94
J (A)	-0.57 ***	-0.80	-0.72 ***	-0.71
J (NE)	-0.57 ***	-1.00	-0.77 ***	-0.89
NJ (G)	-0.64 ***	-0.90	-0.71 ***	-0.83
NJ (A)	-0.30 ***	-0.80	-0.37 **	-0.26
NJ (NE)	-0.18	-0.40	-0.34	-0.09
EPS (G)	-0.38 ***	-0.90	-0.52 **	-0.66
EPS (A)	-0.49 *	-0.90	-0.54 **	-0.83
EPS (NE)	-0.42 **	-1.00	-0.77 ***	-1.00

Table 4.9: Correlation co-efficient values for the relationship between $T_{50}\%$ of $(MEPPs)_0$ and AChE fraction activity. RHO values were obtained by the Spearman's Rank test. The relationship is denoted by a negative sign because as AChE activity decreases, $T_{50}\%$ increases. Significance increases as values approach -1.00. Significant correlations are denoted by an asterix and *, **, *** denote significance ($P<0.05$, $P<0.02$ and $P<0.002$ respectively).

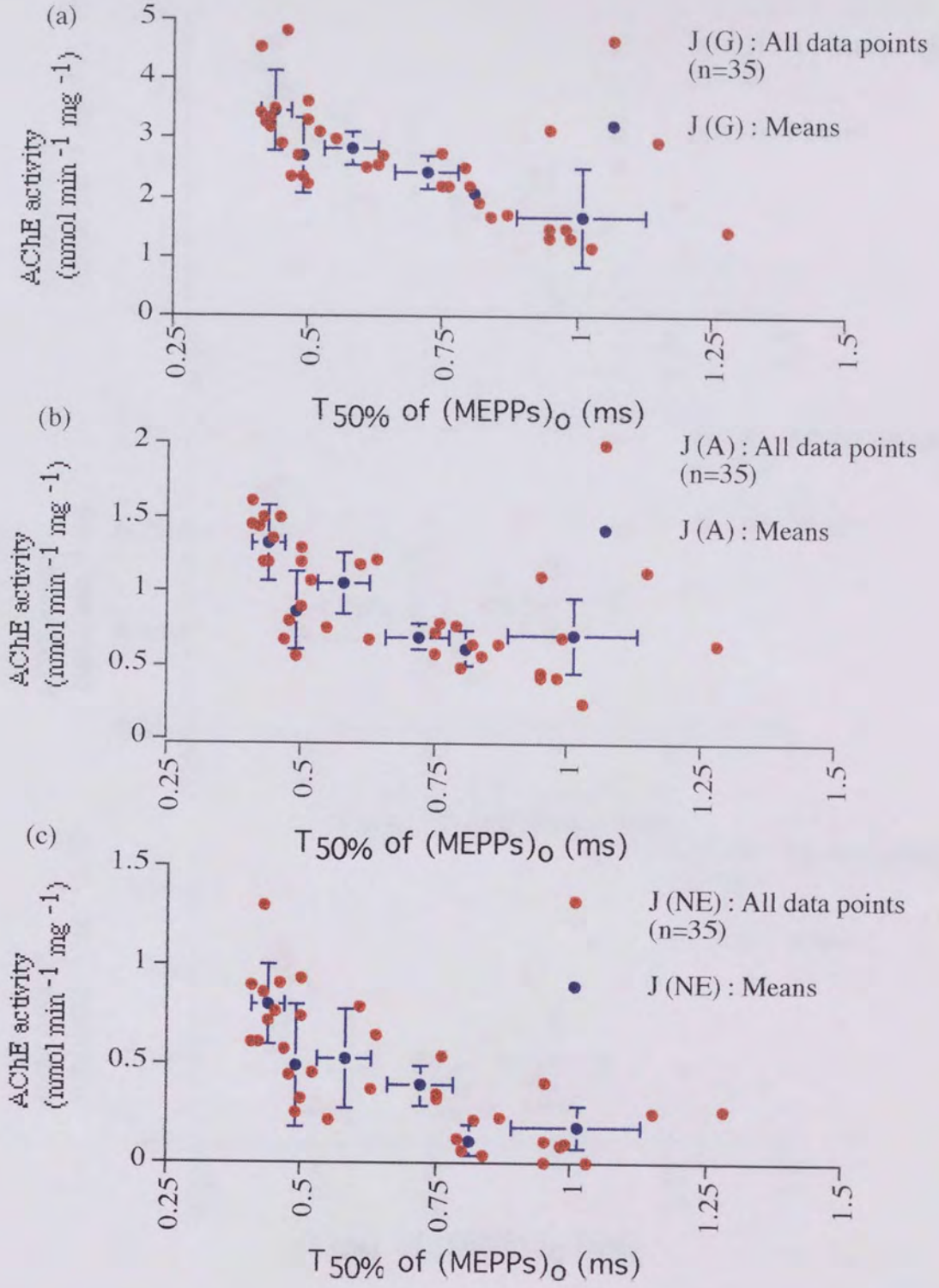

Figure 4.12: Correlation between junctional AChE and $T_{50\%}$ of $(MEPPs)_o$ 3 hours after ECO (25-500 nmol kg^{-1}). Scattergram plots of all data points (n=35) and means of junctional: (a) globular (G), (b) asymmetric (A) and (c) non-extractable (NE) AChE versus $T_{50\%}$ of $(MEPPs)_o$.

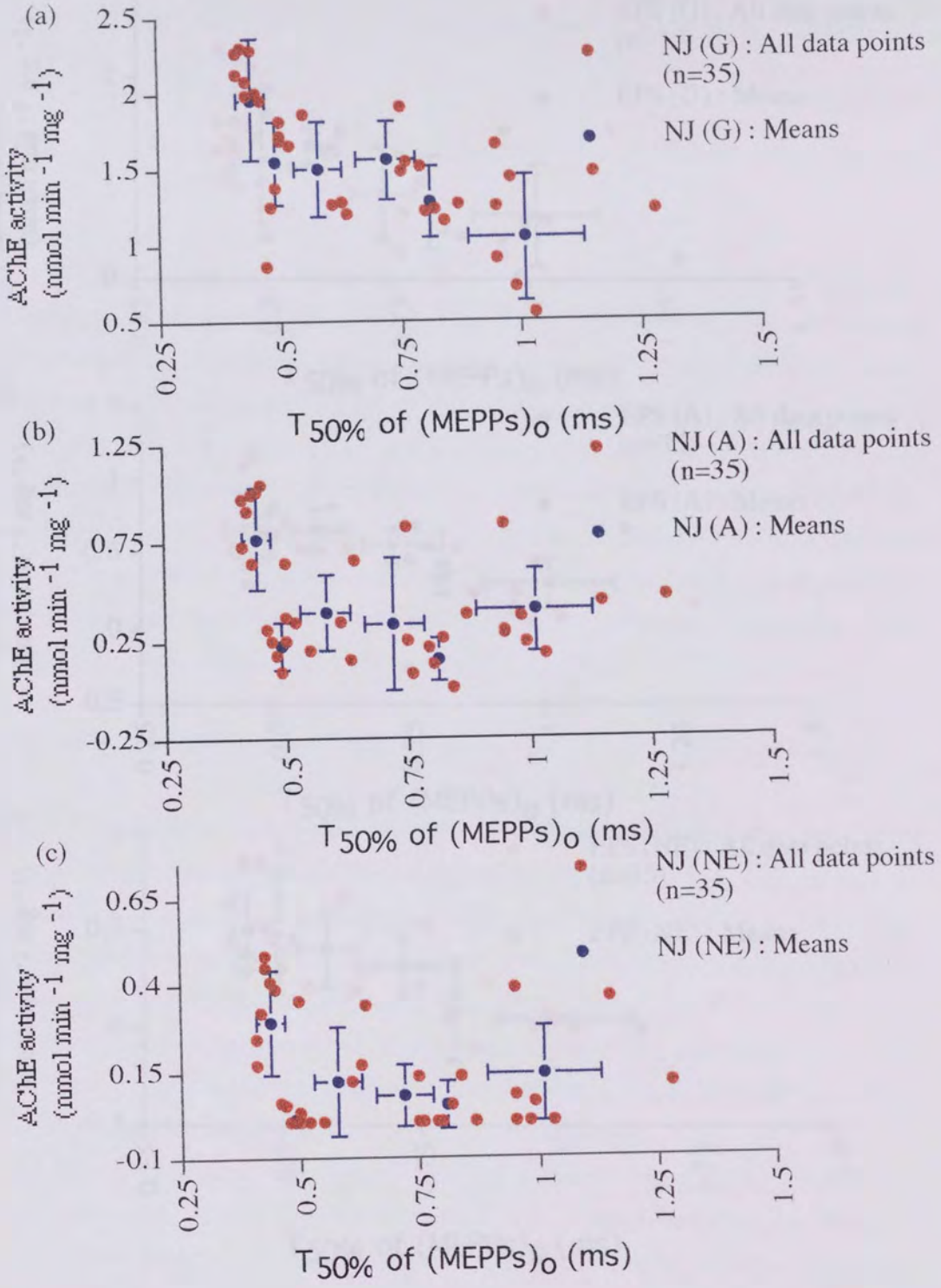

Figure 4.13: Correlation between non-junctional AChE and T50% of $(MEPPs)_o$ 3 hours after ECO (25-500 nmol kg^{-1}). Scattergram plots of all data points (n=35) and means of non-junctional: (a) globular (G), (b) asymmetric (A) and (c) non-extractable (NE) AChE versus T50% of $(MEPPs)_o$.

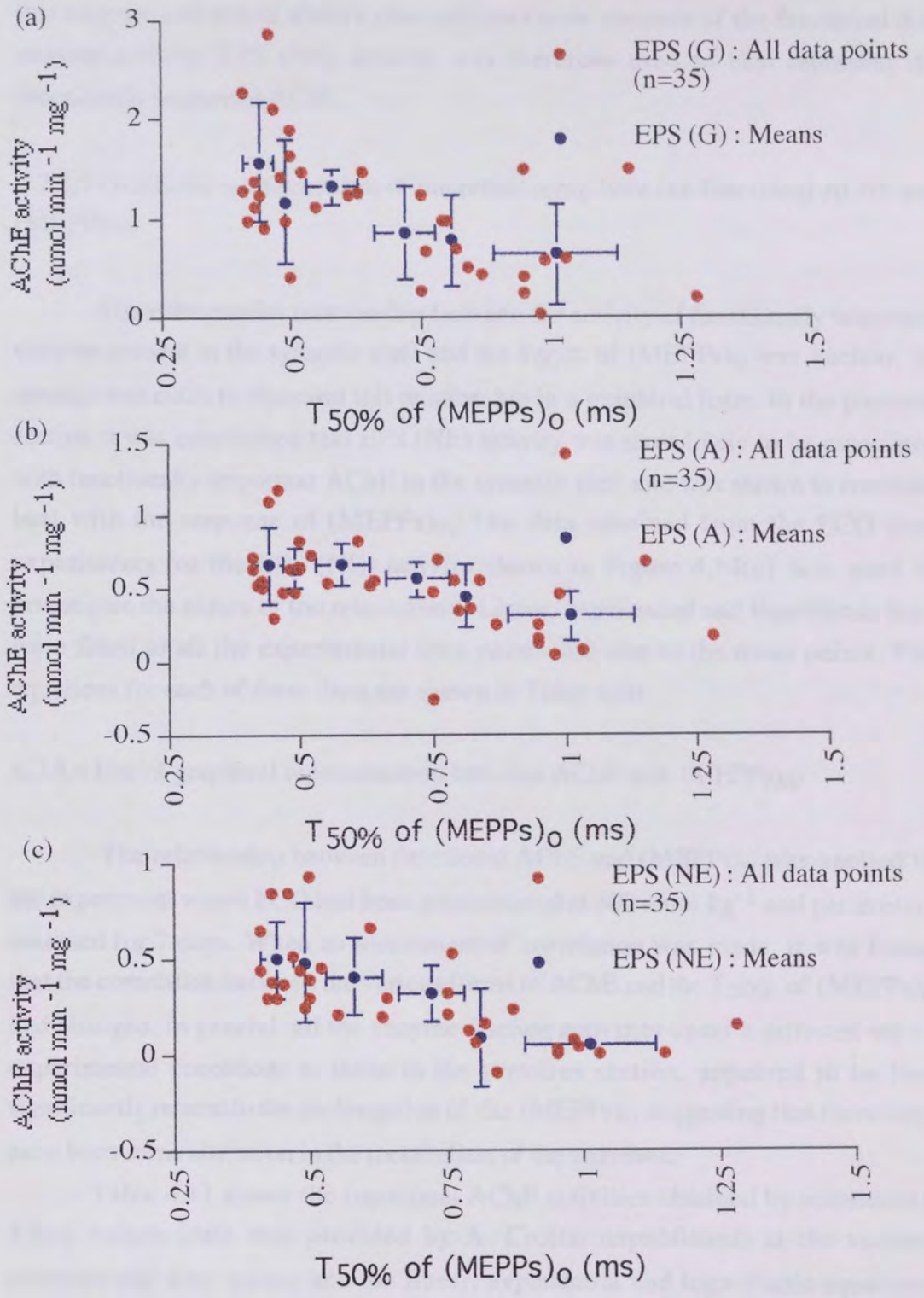

Figure 4.14: Correlation between endplate-specific AChE and $T_{50\%}$ of $(MEPPs)_o$ 3 hours after ECO (25-500 nmol kg^{-1}). Scattergram plots of all data points (n=35) and means of endplate-specific: (a) globular (G), (b) asymmetric (A) and (c) non-extractable (NE) AChE versus $T_{50\%}$ of $(MEPPs)_o$.

this enzyme and would always give and inaccurate measure of the functional A12 enzyme activity. EPS (NE) activity was therefore used to best represent the functionally important AChE.

4.2.3.3 Graphical representation of the relationship between functional AChE and $(MEPPs)_o$.

Since the precise relationship between the activity of functionally important enzyme present in the synaptic cleft and the $T_{50\%}$ of $(MEPPs)_o$ was unclear, an attempt was made to represent this relationship in a graphical form. In the previous section it was established that EPS (NE) activity was most likely to be associated with functionally important AChE in the synaptic cleft and was shown to correlate best with the response of $(MEPPs)_o$. The data obtained from the ECO dose experiments for the EPS (NE) activity shown in Figure 4.14(c) was used to investigate the nature of the relationship. Linear, exponential and logarithmic lines were fitted to all the experimental time points and also to the mean points. The equations for each of these lines are shown in Table 4.10.

4.2.3.4 Use of graphical representation between AChE and $(MEPPs)_o$.

The relationship between functional AChE and $(MEPPs)_o$ was applied to the experiment where ECO had been administered at 500 nmol kg^{-1} and parameters assessed for 7 days. When an assessment of correlation was made, it was found that the correlation between the various forms of AChE and the $T_{50\%}$ of $(MEPPs)_o$ had changed. In general, all the enzyme fraction activities under a different set of experimental conditions to those in the previous section, appeared to be less significantly related to the prolongation of the $(MEPPs)_o$ suggesting that there may have been some alteration in the metabolism of the enzymes.

Table 4.11 shows the functional AChE activities obtained by substituting $T_{50\%}$ values (data was provided by A. Crofts, unpublished) at the various experimental time points into the linear, exponential and logarithmic equations shown in Table 4.10 for the relationship between EPS (NE) and $(MEPP)_o$ time course. Functional enzyme activity obtained from the equations was called $(MEPP)_o$-derived functional enzyme (MDFE). At the 3 hour time point for both the linear and logarithmic substitutions, some derived enzyme values were found to be negative which was not possible suggesting that these equations were not appropriate for routine determination. The exponential equation therefore best

represented the relationship and was used in Table 4.11 to determine why the measured EPS activities in ECO time studies deviated from the correlation.

Figure 4.15 shows the activities of J (NE) and NJ (NE), MDFE (EXP) and junctional non-functional activity J (NF) which was obtained by subtracting the MDFE activities from J (NE) activities at corresponding time points. Initial observations showed that there was little difference between the functional activity values obtained from the correlation studies (MDFE) and experimentally (EPS (NE)) except there was a difference between the data sets at the 1 day time point (see data in Table 4.11). When the data sets were correlated against each other, there was found to be a good correlation which was improved if the 1 day data point was removed.

From the assay method, the J (NE) fraction gives the combined activities of A12 associated with the endplate and A12 associated with the non-endplate regions and endplate A12, EPS (NE), was obtained by correcting the J (NE) for the NJ (NE) component. From the correlation studies MDFE values represent functional AChE and when this is subtracted from the J (NE) value obtained from the assay, the remaining activity, termed junctional non-functional or J (NF), gives an indication of any AChE in the J fraction which is not involved in the termination of cholinergic transmission i.e. enzyme in the J strip which is located in parts of muscle fibres which are peripheral to the endplate and also any AChE in the cleft which does not participate in transmission termination. Hence the J (NF) and NJ (NE) both represent non-functional A12 which is either not located in the endplate or in the endplate but not involved in transmission termination. When J (NF) and NJ (NE) values were compared there was found to be a good correlation between these sets of data suggesting that both may represent the same enzyme since statistically there was no significant difference between them at each of the time points (Mann-Whitney, $P>0.1$). The similarity between J (NF) and NJ (NE) suggested that both activities were due to enzyme not located in the endplate. J (NF) was not higher that NJ (NE) suggesting that it was unlikely that very much A12 in the cleft was not involved in transmision termination. However, there was a deviation in the data sets at the 1 day time point when NJ (NE) was much higher J (NF). This explained why when NJ activity was subtracted from the J activity to give a routinely calculated assessment of EPS functional enzyme at the 1 day time point this deviated from the predicted level obtained by using the correlation equation. It followed therefore that non-functional high molecular forms of AChE along the length of the muscle fibre may not be subject to the same form of regulation and may fluctuate independently of each other.

Enzyme	Linear equation (all points) n=35	Exponential equation (all points) n=35	Logarithmic equation (all points) n=35
EPS (NE):y:	-0.747x + 0.816	1.865 X $10^{-1.358x}$	-1.230 log(x) + 0.071
Enzyme	**Linear equation (means)**	**Exponential equation (means)**	**Logarithmic equation (means)**
EPS (NE):y:	-0.846x + 0.882	3.508 X $10^{-1.734x}$	-1.334 log(x) + 0.059

Table 4.10: Linear, exponential and logarithmic equations for the relationship between EPS (NE) and T_{50}% of $(MEPPs)_o$. y represents AChE activity and x represents T_{50}% of $(MEPPs)_o$.

Time	T_{50}%	MDFE (LIN)	MDFE (LOG)	MDFE (EXP)	EPS (NE)	J (NE)	J (NF)	NJ (NE)
Un-	0.46	0.48	0.51	0.47	0.50	0.80	0.33	0.29
treated	±0.05	±0.02	±0.03	±0.04	±0.20	±0.20	±0.20	±0.15
	(10)	(10)	(10)	(10)	(10)	(10)	(10)	(10)
3 hrs	1.02	0.06	0.07	0.08***	0.06***	0.14***	0.08**	0.10
	±0.12	±0.09	±0.06	±0.03	±0.08	±0.12	±0.13	±0.13
	(9)	(9)	(9)	(9)	(12)	(12)	(9)	(12)
1 day	0.64	0.34	0.31	0.26***	0.12**	0.27***	0.02**	0.16
	±0.04	±0.03	±0.03	±0.03	±0.12	±0.13	±0.16	±0.06
	(6)	(6)	(6)	(6)	(7)	(7)	(6)	(7)
5 day	0.62	0.35	0.33	0.28***	0.26**	0.51**	0.25	0.25
	±0.10	±0.07	±0.08	±0.08	±0.14	±0.20	±0.26	±0.12
	(7)	(7)	(7)	(7)	(8)	(8)	(7)	(8)
7 day	0.49	0.45	0.46	0.42	0.48	0.61	0.16	0.10
	±0.10	±0.08	±0.10	±0.12	±0.23	±0.27	±0.22	±0.17
	(9)	(9)	(9)	(9)	(9)	(9)	(9)	(9)

Table 4.11: Derived functional AChE levels. AChE derived from linear (LIN), exponential (EXP) and logarithmic (LOG) equations obtained from ECO dose experiments for ECO time experiments. Also shown are corresponding $(MEPPs)_o$ values, EPS activity and J (NE) enzyme activities, J (NF) activity obtained by subtracting the EXP value from J and NJ activity. Activities are in nmol min^{-1} mg^{-1}) *, ** and *** denote significance from untreated levels ($P<0.05$, $P<0.02$ and $P<0.002$).

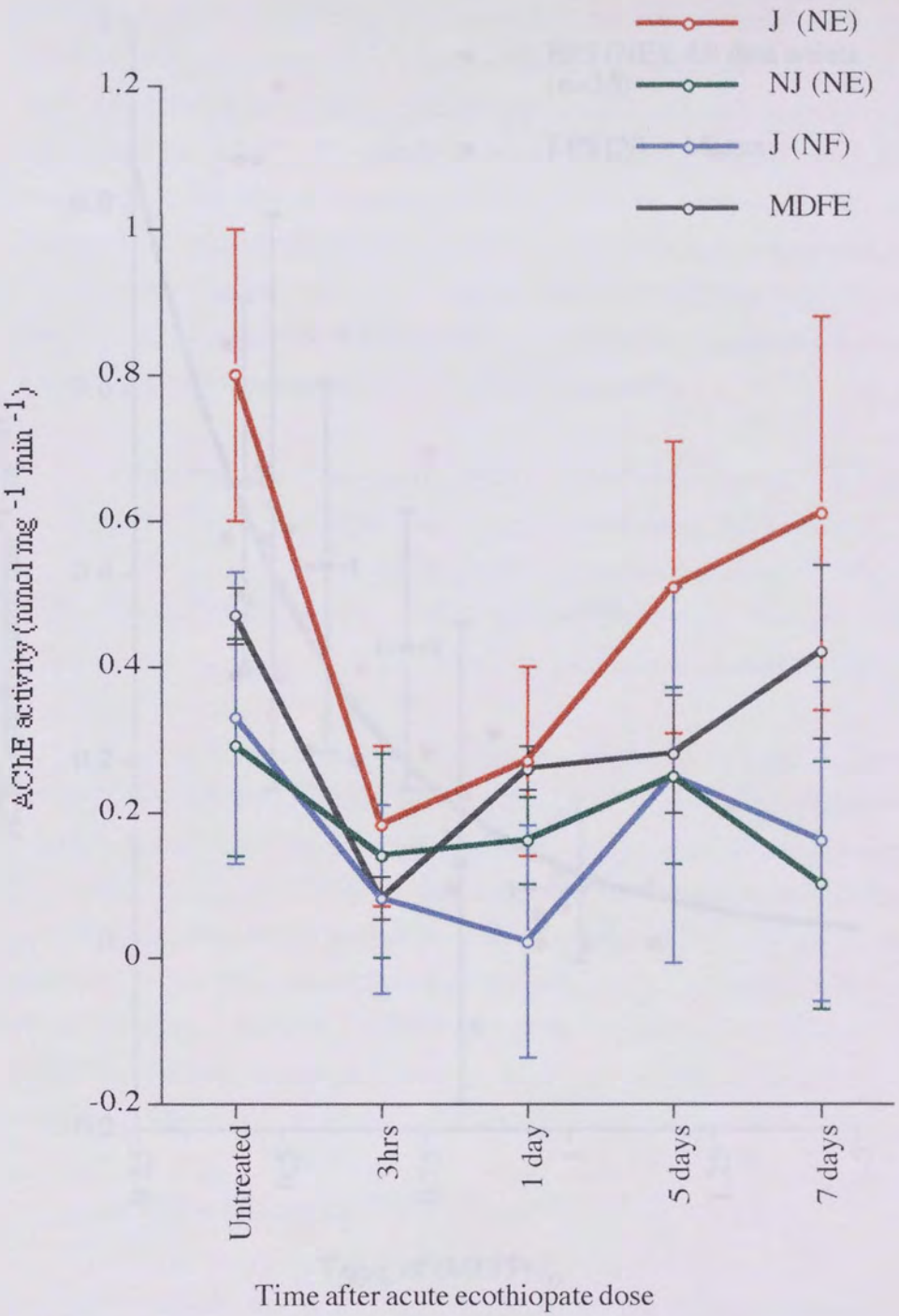

Figure 4.15: Functional and non-functional AChE after 500 nmol kg^{-1} ECO (3hrs-7days). Non-extractable AChE in the junctional region (J (NE)), non-junctional non-extractable AChE (NJ (NE)), junctional non-functional (J (NF)) and $(MEPP)_O$-derived (MDFE) AChE activity representing functionally important AChE associated with the synapse.

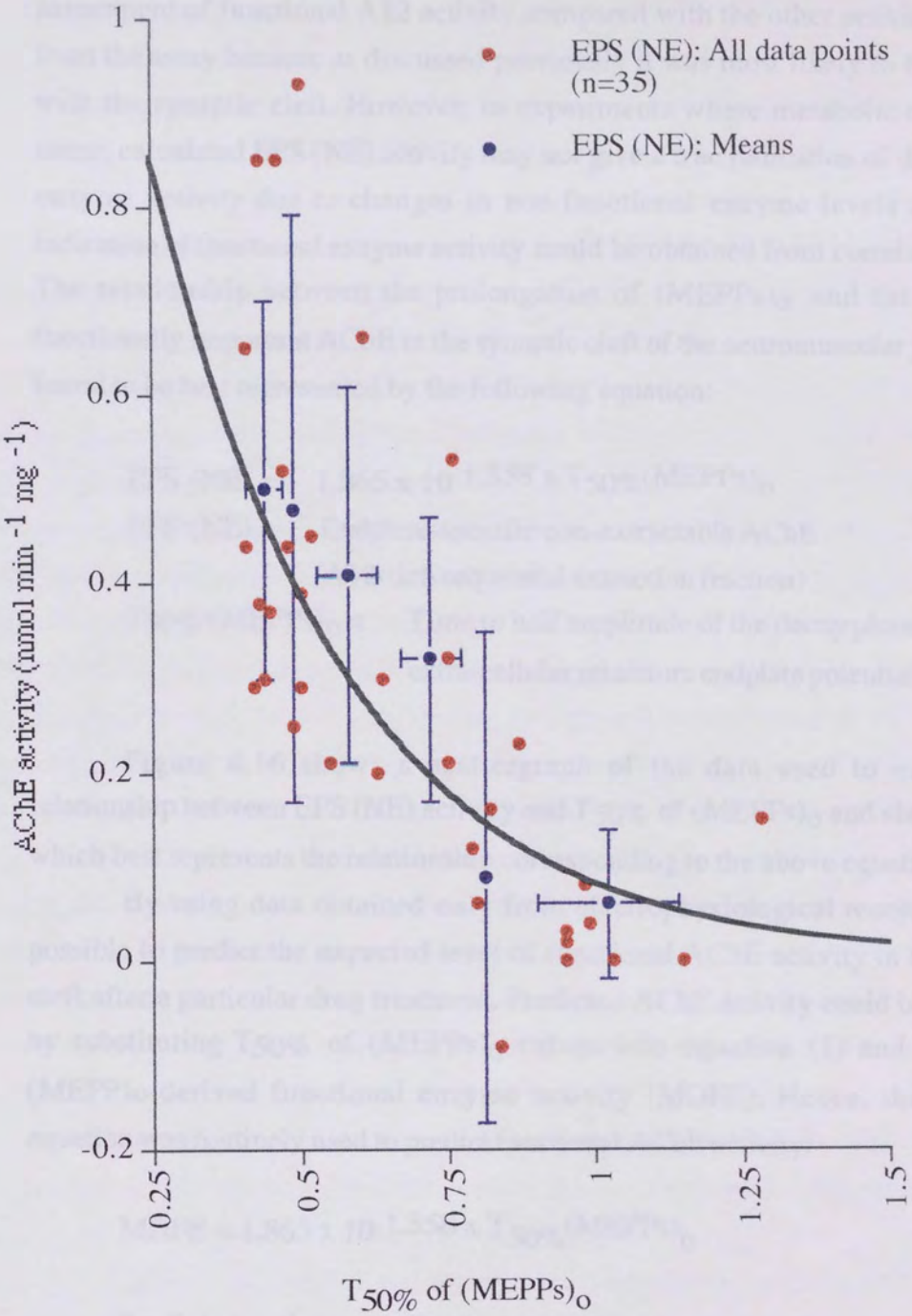

Figure 4.16: Correlation between functional AChE and $T_{50\%}$ of $(MEPPs)_o$ 3 hours after ECO (25-500 nmol kg^{-1}). Relationship between functionally important AChE determined by assay (EPS (NE)) and $T_{50\%}$ of $(MEPPs)_o$.

The results suggested that in general the EPS (NE) activity gave the best assessment of functional A12 activity compared with the other activities obtained from the assay because as discussed previously it was most likely to be associated with the synaptic cleft. However, in experiments where metabolic changes may occur, calculated EPS (NE) activity may not give a true indication of the functional enzyme activity due to changes in non-functional enzyme levels and a better indication of functional enzyme activity could be obtained from correlation studies. The relationship between the prolongation of $(MEPPs)_o$ and the activity of functionally important AChE in the synaptic cleft of the neuromuscular junction was found to be best represented by the following equation:

$$EPS\ (NE) = 1.865 \times 10^{-1.358 \times T_{50\%}(MEPPs)_o} \quad (1)$$

EPS (NE) = Endplate-specific non-extractable AChE (A12-rich sequential extraction fraction)

$T_{50\%}\ (MEPPs)_o$ = Time to half amplitude of the decay phase of extra-cellular miniature endplate potentials.

Figure 4.16 shows a scattergraph of the data used to establish the relationship between EPS (NE) activity and $T_{50\%}$ of $(MEPPs)_o$ and shows the line which best represents the relationship corresponding to the above equation.

By using data obtained only from electrophysiological recordings it was possible to predict the expected level of functional AChE activity in the synaptic cleft after a particular drug treatment. Predicted AChE activity could be calculated by substituting $T_{50\%}$ of $(MEPPs)_o$ values into equation (1) and was called (MEPP)o-derived functional enzyme activity (MDFE). Hence, the following equation was routinely used to predict functional AChE activity:

$$MDFE = 1.865 \times 10^{-1.358 \times T_{50\%}(MEPPs)_o} \quad (2)$$

Predicted activity levels obtained using the equation gave an alternative method of assessing the activity of functionally important AChE. These predicted activities could then be compared with the actual activity of EPS (NE) obtained after the same drug treatment. It was proposed that differences between activities obtained by the two methods would give an indication of the responses of other diaphragm enzymes.

4.3. Summary.

The assay of whole blood ChE was found to give a rapid assessment of OP inhibition. The response of AChE molecular forms to ECO was found to be selective and may depend on several factors including cellular location, turnover rate and intra-mouse variation. A comparison of the response of blood ChE and diaphragm AChE revealed that the former did not give a good indication of peripheral nervous tissue intoxication.

The use of ECO as a selective inhibitor was found to give a good indication of the internal and external cellular locations of diaphragm AChE. However, the distribution was not precise because of the nature of ECO which slowly inactivates external AChE whilst slowly penetrating the cell and the point at which all external AChE was inactivated without any internal enzyme being effected could not be determined. Total AChE was found to be equally distributed between endplate and non-endplate regions of mouse diaphragm. Around 61% of the total AChE was due to globular forms, 23% to readily-extractable asymmetric forms and 14% to non-readily extractable asymmetric forms. Endplate and non-endplate regions were found to have both intra- and extra-cellular pools of globular and readily-extractable asymmetric AChE. Intra-cellular G forms were probably precursors located in the RER, the Golgi, molecules in vesicles, secretory granules, the sarcoplasmic reticulum and lysosomes or inactive pools. Extra-cellular G forms were probably secreted enzymes, degradations products or cell-bound forms. Intra-cellular A forms were probably enzymes at various stages of processing whilst the role or origin of the external readily-extractable A AChE was largely unclear. The EPS (NE) form was 90% external and probably represented synaptically important A12. Some NE AChE was associated with non-endplate muscle which was probably not due to stray endplates and had an unknown function.

ECO-induced endplate-deformation was found to be a rapid and sensitive indicator of hypercontrations induced by OP-intoxication. The assessment of endplate dimensions therefore indicated abnormal cellular calcium levels and morphology and could be used as a marker for mild myopathy.

After a necrotising dose of ECO, all endplate and non-endplate AChE recovered within 5 days except EPS (NE) which recovered within 7 days. G forms, which have a rapid turnover rate, recovered more rapidly than A forms which have a slower turnover rate suggesting these were precursors. The recovery of diaphragm AChE after partial inhibition by ECO did not follow the bi-phasic model proposed by previous studies suggesting that AChE responses after mild and severe inhibition may be different. Recovery of AChE molecular forms therefore occurs by

a complex mechanism which is poorly understood but may depend on muscle activity, trophic factors and the regulation of AChE metabolism at various levels.

Abnormal cellular calcium and morphology after OP-intoxication was found to be temporary and substantial recovery in endplate shape occurred within 7 days after a necrotising dose of ECO. It was not known whether the recovery was due to the appearance of new endplates or the regeneration of old ones.

After various ECO doses, EPS (NE) consistently correlated well with the time to half amplitude of the decay phase of extra-cellular endplate potentials suggesting that the activity represented synaptically active AChE. The relationship was best represented by an exponential equation. Under certain experimental conditions, EPS (NE) gave a poor correlation suggesting that non-functional components of NJ (NE) and J (NE) used to calculate this activity were subject to regulation resulting in the mis-representation of synaptic AChE. To account for this, functional AChE was determined by two independent methods: by calculation of EPS (NE) and by use of the correlation equation.

CHAPTER 5

PRELIMINARY INVESTIGATIONS OF THE ANTICHOLINESTERASE EFFECTS OF CARBAMATES

5.1 Introduction.

Pyridostigmine (PYR) and physostigmine (PHY) are reversible CB inhibitors of AChE and the time elapsed since dosing *in vivo* is a crucial factor when investigating the inhibitory effects of these drugs on enzymes using assay techniques. In the case of both compounds, the carbamoylated enzyme complexes spontaneously decarbamoylate rapidly, regenerating the intact enzyme molecule. It was important therefore to investigate whether inhibition by PYR and PHY could be maintained during the time period required for preparation and assay of AChE such that during any subsequent experiments, it would be known whether the assay results would reflect any inhibition which had ocurred at the start of the process. The study of these effects was to some extent limited by the techniques available and the objective of work in this section was to investigate the rates of decarbamoylation during preparation of samples for assay by the methods discussed in Sections 3.2.1 and 3.2.2.

The conventional extraction process takes 1 hour to prepare but cannot distinguish between the various forms of AChE. The sequential extraction method gives a better indication of AChE molecular form and functional enzyme activity but takes 3-4 hours to prepare. In addition to these methods, velocity sedimentation of diaphragm homogenates on sucrose density gradients gives a good assessment of the activity of the molecular forms of AChE but takes longer than 24 hours to prepare by which time AChE would be completely decarbamoylated. Hence, in this section, some preliminary tests were conducted to determine the rates of decarbamoylation of CB-inhibited AChE molecular forms and synaptically functional AChE during the various methods which were intended to be used for the study of the long-term effects of CBs on mouse skeletal muscle AChE.

In the second part of this section, a set of experiments was conducted to investigate some of the long term effects of CBs on skeletal muscle and determine if any inhibition could be maintained after *in vivo* dosing. Mice were subcutaneously dosed twice daily at 9am and 5pm with 383 nmol kg^{-1} PYR and measurements of whole blood ChE, diaphragm AChE activity and endplate shapes were recorded over a three week period.

5.2 Results and discussion.

5.2.1 Investigation of the decarbamoylation rates of CB-inhibited ChE.

5.2.1.1 Dose-response curve for PYR and PHY on $(AChE)_{eel}$.

A dose-response curve was obtained for the inhibitory effects of PYR and PHY on purified electric eel AChE ($AChE_{(eel)}$ obtained from Sigma). $AChE_{(eel)}$ was incubated with either PYR or PHY in the dose range 10^{-9}M to 10^{-4}M in a water-bath at 37°C for 15 minutes. Samples were then taken and measured for $AChE_{(eel)}$ activity by the Ellman method. Table 5.1 shows the percentage inhibition of $AChE_{(eel)}$ activity at the various drug concentrations and Figure 5.1 shows the dose-response curves for each drug. It was found that the profiles for each drug were slightly different and that PHY was a more potent inhibitor of $AChE_{(eel)}$ than PYR. The $I_{50\%}$ value for PYR at 37°C at pH8.0 was 10^{-6}M and for PHY was 0.5×10^{-7}M.

5.2.1.2 Comparison of the decarbamoylation rates of CB-inhibited AChE at 37°C and on ice.

The process of extracting carbamoylated-AChE complexes by the sequential extraction method which is routinely used to study the effects of CBs on mouse skeletal muscle AChE takes around 3-4 hours and involves several processes where the complexes are diluted. Both PYR and PHY AChE complexes are known to have relatively short half-lives (Wetherall and French, 1991; Wilson et al., 1960) so there is a possibility that during the extraction process some spontaneous decarbamoylation may occur such that the levels of inhibition calculated from activities measured at the end of the extraction process may not give a true representation of the levels of inhibition which may have occurred *in vivo*. In this section, a set of experiments was conducted to predict if spontaneous decarbamoylation occurs during the extraction of carbamoylated-AChE compounds from mouse diaphragms.

The samples extracted during the sequential extraction process were small and not suitable for use in decarbamoylation studies hence $AChE_{(eel)}$ was used (one unit of pure enzyme hydrolysed 1.0 μmoles of substrate per minute at pH8.0 at 37°C) to investigate the rate of decarbamoylation of PHY and PYR-inhibited enzyme at 37°C and on ice. The primary objective of this study was to determine

Drug concentration (M)	% I ($AChE_{(eel)}$) PYR 37°C	% I ($AChE_{(eel)}$) PHY 37°C
10^{-9}	4.2 ±2.5 (4)	16.5 ±9.4 (6)
10^{-8}	4.4 ±8.3 (7)	21.5 ±10.9 (8)
10^{-7}	16.4 ±6.4 (7)	71.6 ±6.2 (7)
10^{-6}	50.6 ±7.6 (8)	81.4 ±8.5 (10)
10^{-5}	77.9 ±5.3 (7)	94.9 ±1.1 (7)
10^{-4}	92.3 ±1.8 (7)	98.5 ±0.5 (7)

Table 5.1: Percentage inhibition of purified electric eel AChE ($AChE_{(eel)}$) by PYR and PHY at pH8.0 at 37°C. Values shown are means±s.d. N numbers are shown in parentheses.

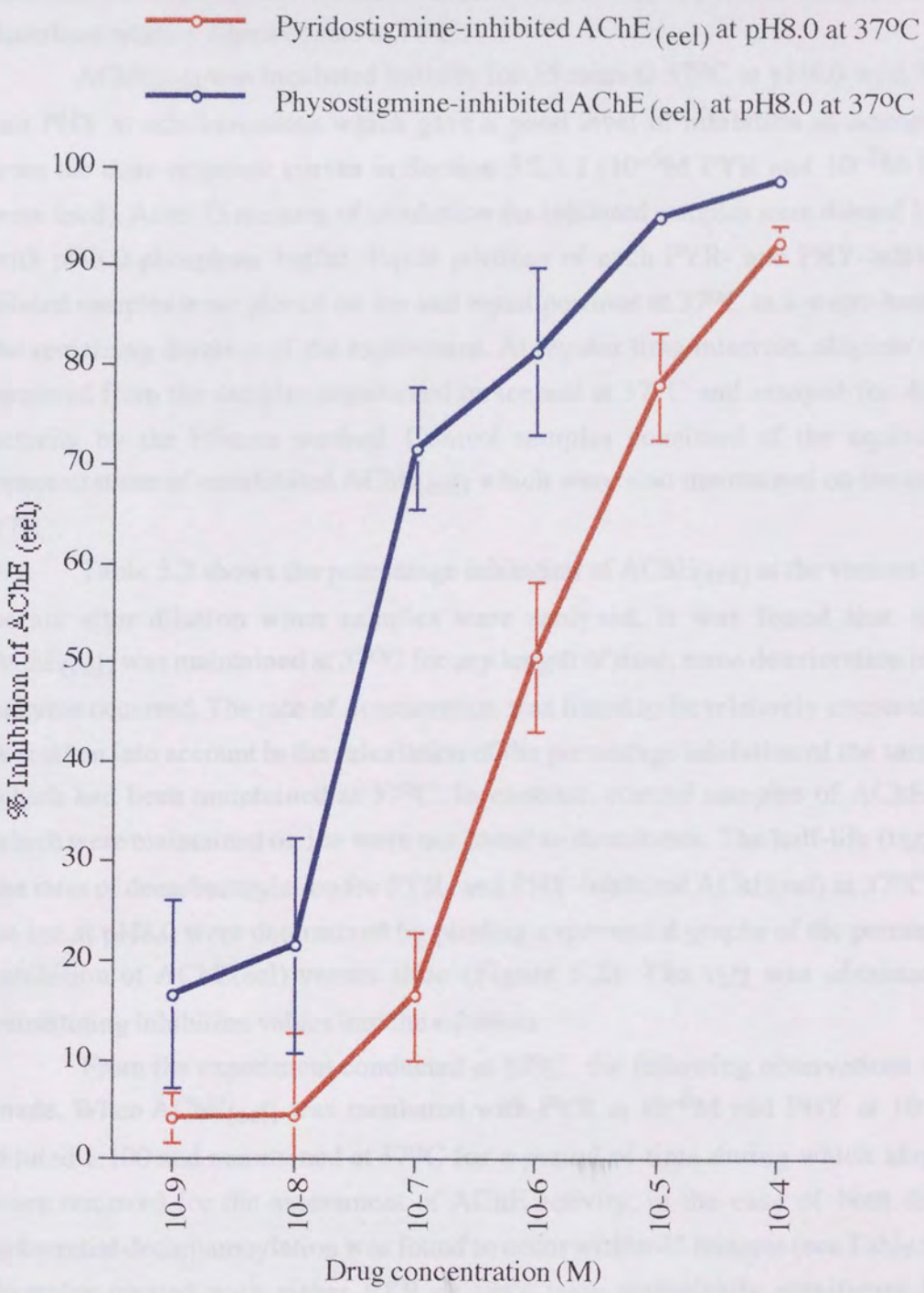

Figure 5.1: Dose-response curves of PYR-inhibited and PHY-inhibited AChE(eel) at pH8.0 and 37°C. Percentage inhibition of AChE (eel) at doses of PYR and PHY in the range 10^{-4}M to 10^{-9}M.

whether maintaining carbamoylated enzyme samples on ice, which was routinely performed during sequential extraction, prevented the rapid process of spontaneous decarbamoylation which occurs at 37°C.

$AChE_{(eel)}$ was incubated initially for 15 mins at 37°C at pH8.0 with PYR and PHY at concentrations which gave a good level of inhibition as determined from the dose-response curves in Section 5.2.1.1 (10^{-6}M PYR and 10^{-7}M PHY were used). After 15 minutes of incubation the inhibited samples were diluted 1:100 with pH8.0 phosphate buffer. Equal portions of each PYR- and PHY-inhibited diluted samples were placed on ice and equal portions at 37°C in a water-bath for the remaining duration of the experiment. At regular time intervals, aliquots were removed from the samples maintained on ice and at 37°C and assayed for AChE activity by the Ellman method. Control samples consisted of the equivalent concentrations of uninhibited $AChE_{(eel)}$ which were also maintained on ice and at 37°C.

Table 5.2 shows the percentage inhibition of $AChE_{(eel)}$ at the various time points after dilution when samples were analysed. It was found that when $AChE_{(eel)}$ was maintained at 37°C for any length of time, some deterioration of the enzyme occurred. The rate of deterioration was found to be relatively constant and was taken into account in the calculation of the percentage inhibition of the samples which had been maintained at 37°C. In contrast, control samples of $AChE_{(eel)}$ which were maintained on ice were not found to deteriorate. The half-life ($t_{1/2}$) of the rates of decarbamoylation for PYR- and PHY-inhibited AChE(eel) at 37°C and on ice at pH8.0 were determined by plotting exponential graphs of the percentage inhibition of AChE(eel) versus time (Figure 5.2). The $t_{1/2}$ was obtained by substituting inhibition values into the equation.

From the experiment conducted at 37°C, the following observations were made. When $AChE_{(eel)}$ was incubated with PYR at 10^{-6}M and PHY at 10^{-7}M, diluted 1:100 and maintained at 37°C for a period of time during which aliquots were removed for the assessment of AChE activity, in the case of both drugs, substantial decarbamoylation was found to occur within 45 minutes (see Table 5.2). Samples treated with either PYR or PHY were statistically significant from untreated values at each time point until 40 minutes when they were no longer statistically different. This suggested that when assayed after 40 minutes at 37°C, in the case of both drugs, the $AChE_{(eel)}$ was no longer inhibited. When statistical analysis was applied between consecutive time points, in the case of both drugs, the activities measured at each time point were found to be significantly higher than the previous time point (Mann-Whitney, $P<0.05$) suggesting that the drugs were dissociating from the enzyme with time. When graphs were plotted of the change in

Time (mins)	%I (AChE(eel)) PYR 37°C (N=8)	% I (AChE(eel)) PHY 37°C (N=4)	% I (AChE(eel)) PYR ice (N=8)	% I (AChE(eel)) PHY ice (N=8)
0	57.8±6.5 ***	70.2±0.8 *	60.9±1.2 ***	75.2±4.5 ***
5	41.2±1.7 ***	55.6±1.8 *	-	-
10	32.6±3.0 ***	37.0±2.0 *	53.6±3.0 **	64.5±0.4 **
15	29.9±0.5 ***	26.1±1.5 *	53.2±0.4 **	64.9±0.3 **
20	21.8±7.7 **	17.7±2.0 *	-	-
25	18.0±9.6 **	11.8±2.5 *	-	-
30	13.9±12.3 **	7.2±1.7 *	42.6±5.7 ***	58.1±0.1***
35	13.4±5.2 **	5.2±0.9 *	-	-
40	14.6±3.7	3.7±3.3	-	-
45	-	2.9±2.0	41.5±0.8 **	56.8±0.1 **
60	-	-	29.0±6.6 ***	49.5±4.7 ***
75	-	-	30.9±2.3 **	50.7±0.6 **
90	-	-	21.5±5.2 **	43.0±4.6 ***
120	-	-	6.6±1.9 **	33.2±0.7 **
150	-	-	2.7±5.2 **	25.0±1.2 ***
180	-	-	4.4±4.4 **	22.4±0.8 **
$t_{1/2}$ (mins)	**32.1±25.8**	**9.1±2.1**	**57.5±18.3 (+)**	**125.4±25.1 (++)**

Table 5.2: Percentage inhibition of purified (AChE(eel)) by PYR 10^{-6}M and PHY 10^{-7}M at pH8.0 at 37°C or on ice. Values shown are means ± s.d. *, ** and *** denote that the enzyme activities were significantly different from controls (Mann-Whitney, $P<0.05$, $P<0.02$ and $P<0.002$ respectively). Also shown are the half-lives ($t_{1/2}$) for the rates of decarbamoylation for PYR- and PHY-inhibited enzyme at 37°C and on ice. + and ++ denote that the $t_{1/2}$ of samples on ice were different from the $t_{1/2}$ of samples at 37°C (Mann-Whitney, $P<0.05$ and $P<0.02$).

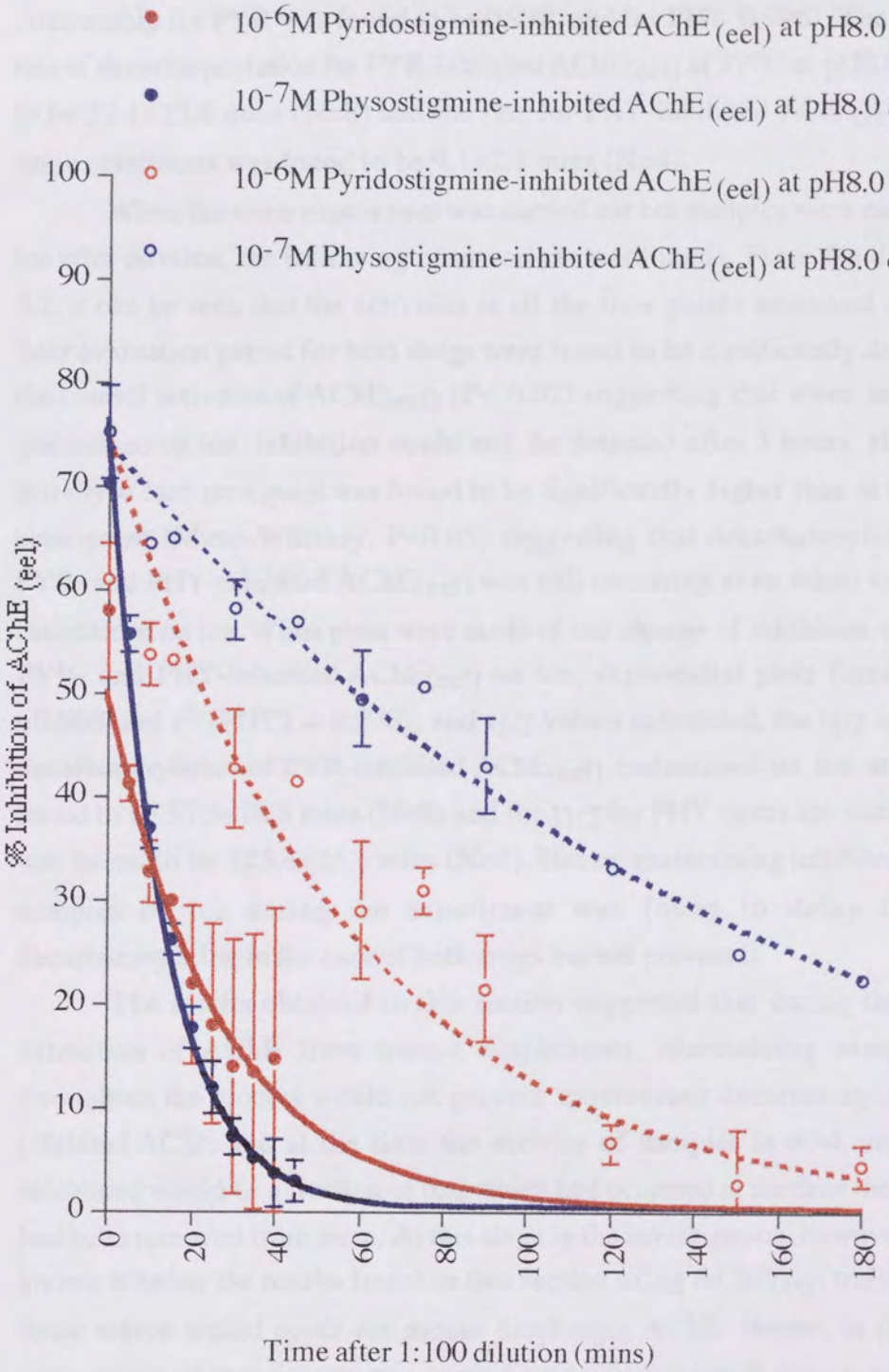

Figure 5.2: Decarbamoylation rates of PYR-inhibited and PHY-inhibited AChE(eel) at pH8.0 at 37°C and on ice. Percentage inhibition of AChE(eel) at various time intervals after 1:100 dilution of initial incubations with 10^{-6}M PYR and 37°C and on ice and 10^{-7}M PHY at 37°C and on ice.

inhibition with time for PYR and PHY treated AChE(eel), and lines were fitted to the graphs, the relationship between inhibition and time in the case of both drugs was found to follow an exponential decay curve (the correlation co-efficient for the relationship for PYR was found to be 0.938, and for PHY 0.996). The $t_{1/2}$ for the rate of decarbamoylation for PYR-inhibited AChE(eel) at 37°C at pH8.0 was found to be 32.1±25.8 mins (N=8) and the rate for PHY-inhibited AChE(eel) under the same conditions was found to be 9.1±2.1 mins (N=4).

When the same experiment was carried out but samples were maintained on ice after dilution, the following observations were made. From the data in Table 5.2, it can be seen that the activities at all the time points measured during the 3 hour evaluation period for both drugs were found to be significantly different from the control activities of AChE(eel) ($P< 0.02$) suggesting that when samples were maintained on ice, inhibition could still be detected after 3 hours. However, the activity at each time point was found to be significantly higher than at the previous time point (Mann-Whitney, $P<0.05$) suggesting that decarbamoylation of both PYR- and PHY-inhibited AChE(eel) was still occurring even when samples were maintained on ice. When plots were made of the change of inhibition with time for PYR- and PHY-inhibited AChE(eel) on ice, exponential plots fitted (r^2 (PYR) =0.908 and r^2 (PHY) = 0.978), and $t_{1/2}$ values calculated, the $t_{1/2}$ of the rate of decarbamoylation of PYR-inhibited AChE(eel) maintained on ice at pH8.0 was found to be 57.5±18.3 mins (N=8) and the $t_{1/2}$ for PHY under the same conditions was found to be 125.4±25.1 mins (N=8). Hence, maintaining inhibited AChE(eel) samples on ice during the experiment was found to delay the rate of decarbamoylation in the case of both drugs but not prevent it.

The results obtained in this section suggested that during the sequential extraction of AChE from mouse diaphragms, maintaining samples on ice throughout the process would not prevent spontaneous decarbamoylation of CB-inhibited AChE and at the time the activity of samples is read, any inhibition calculated would be a fraction of that which had occurred at the time the diaphragms had been removed from mice. At this stage in the investigation, however, it was not known whether the results found in this section using AChE(eel) truly represented those which would occur for mouse diaphragm AChE. Hence, in the following section a set of experiments was carried out to investigate if there is any similarity between the decarbamoylation rates of AChE(eel) and diaphragm AChE.

5.2.1.3 Decarbamoylation of PYR-inhibited functional AChE during the recording of $(MEPPs)_o$ and comparison of the rate of decarbamoylation of PYR-inhibited $AChE_{(eel)}$.

In Section 4.2.3 a relationship was established between the prolongation of miniature endplate potentials ($(MEPPs)_o$) and the activity of functional AChE and was found to be best represented by an exponential equation. In the previous section it was discussed that the rate of decarbamoylation during the sequential extraction of carbamoylated AChE could not be determined easily. However, since there was a relationship between the prolongation of $(MEPPs)_o$ and the activity of functional AChE present in the synaptic cleft of the mouse neuromuscular junction, it was possible to predict the activity of functional enzyme using this relationship and investigate the rate of decarbamoylation of diaphragm AChE by the recording and analysis of $(MEPPs)_o$.

The decarbamoylation rate of synaptically important AChE was investigated by recording $(MEPPs)_o$ after treatment with PYR under similar conditions used to determine the decarbamoylation rate of PYR-inhibited $AChE_{(eel)}$ at 37°C which had a half-life of around 30 mins (this experiment was conducted by A. Crofts). $T_{50\%}$ values were recorded from PYR-treated (10^{-6}M) mouse hemidiaphragms which were pinned out in a water-bath at 37°C at various times after the dose. The tissues were continuously bathed with fresh physiological saline to wash out any excess PYR from the system and prevent re-inhibition ($T_{50\%}$ data was provided by A. Crofts).

The $T_{50\%}$ values were used to obtain MDFE activities using equation (2) in Section 4.2.3.4 (see Table 5.3) which predicted the activity of functionally active AChE in the synaptic cleft of the neuromuscular junction at the various times that recordings were made. The percentage inhibition of AChE activity was calculated for the various time points and the half-life of the rate of decarbamoylation ($t_{1/2}$) was determined for 10^{-6}M PYR by the method used in Section 5.2.1.2. The $t_{1/2}$ of the rate of decarbamoylation of PYR-inhibited AChE during the recording of $(MEPPs)_o$ was found to be 42.1±20.7 mins and the rate of decarbamoylation of PYR-inhibited $AChE_{(eel)}$ after 10^{-6}M (also shown in Table 5.3) was found to be 32.1±25.8 mins. There was not found to be any significant difference between the $t_{1/2}$ of decarbamoylation at 37°C of PYR-inhibited AChE derived from $(MEPP)_o$ recordings or PYR-inhibited $AChE_{(eel)}$ (Mann-Whitney, $P>0.05$).

Since both assessments were made at a similar pH and both treatments were excessively diluted, it followed that the decarbamoylation of functional AChE in the synaptic region of the neuromuscular junction of mouse diaphragm which was

Time (mins)	T_{50}% $(MEPP)_o$ PYR 10^{-6}M (N=8)	MDFE PYR 10^{-6}M (N=8)	%I (MDFE) PYR 10^{-6}M (N=8)	%I ($AChE_{(eel)}$) PYR 10^{-6}M (N=8)
Untreated	0.41±0.14	0.55±0.15	-	-
0	-	-		57.8±6.5 ***
5	-	-	-	41.2±1.7 ***
10	-	-	-	32.6±3.0 ***
15	0.93±0.12 *	0.11±0.05 *	80.3±8.1	29.9±0.5 ***
20	-	-	-	21.8±7.7 **
25	-	-	-	18.0±9.6 **
30	0.85±0.19 *	0.15±0.07 *	72.8±13.1	13.9±12.3 **
35	-	-	-	13.4±13.3 **
40	-	-	-	14.6±14.6
45	0.71±0.14 *	0.23±0.11 *	58.8±20.3	
60	0.63±0.17 *	0.30±0.18 *	52.8±19.3	-
75	0.60±0.16	0.32±0.13	42.6±23.7	-
90	0.50±0.14	0.42±0.15	24.5±26.7	-
105	0.45±0.05	0.46±0.08	16.7±13.9	-
120	0.47±0.10	0.50±0.11	18.3±20.5	-
150	0.42±0.14	0.53±0.16	2.8±28.8	-
180	0.41±0.18	0.56±0.18	9.9±31.7	-
$t_{1/2}$ (mins)	-	-	**42.1±20.7**	**32.1±25.8**

Table 5.3: T_{50}% of $(MEPPs)_o$, MDFE and percentage inhibition of MDFE and $AChE_{(eel)}$ after 10^{-6}M PYR. Also shown are the half-lives ($t_{1/2}$) of the rates of decarbamoylation. All values shown are means ± s.d. *, ** and *** denote significant differences from untreated levels (Mann-Whitney, $P<0.05$, $P<0.02$ and $P<0.002$ respectively). T_{50}% values were provided by A. Crofts (unpublished).

indirectly assessed by the recording of $(MEPPs)_O$ and predicted by correlation studies, occurred at the same rate as purified $AChE_{(eel)}$. This suggested that the decarbamoylation of mouse diaphragm AChE maintained on ice would occur at the same rate as PYR-inhibited $AChE_{(eel)}$ maintained on ice as established in Section 5.2.1.2. Hence, it was predicted that during the extraction of AChE from the mouse diaphragm, decarbamoylation would still occur even if samples are maintained on ice. Since there was no method available which prevented spontaneous decarbamoylation, an accurate indication of the true levels of inhibition in all subsequent experiments were the 4 hour extraction method was used could not be obtained and it was highly likely that by the time samples were analysed, no inhibitor-enzyme complexes remained.

5.2.1.4 Dose-response curve for PYR on junctional and non-junctional ChE obtained by the conventional extraction method.

Table 5.4 and Figure 5.3 show the relationship between the dose of PYR and the activity of ChE which originated from either the junctional (J) or non-junctional (NJ) regions of the mouse diaphragm obtained by the conventional extraction method (see Section 2.4.3.1). Aquilots of tissue homogenates were incubated with various doses of PYR at 37°C prior to being assayed for ChE activity. The relationship was found to be sigmoidal for both ChE from J and NJ regions but PYR was found to have a more potent effect on the J enzymes than on the NJ enzymes. The activity of J ChE was found to be significantly different from the untreated level after 10^{-6}M PYR (Mann-Whitney test, $P<0.05$) and the activity of NJ ChE was found to be significantly different form the untreated level after 10^{-7}M PYR ($P<0.05$). $I_{50\%}$ for J ChE was found to be around 10^{-6}M and for NJ ChE around 10^{-5}M.

5.2.1.5 Decarbamoylation of PYR-inhibited ChE during extraction by the conventional method.

Tests in the previous sections predicted that during the preparation of PYR treated mouse diaphragms for the assay of AChE, spontaneous decarbamoylation of the carbamoylated-AChE may occur even if samples are maintained on ice during the preparation period. Since, it was not possible to use the actual samples obtained by the sequential method to investigate this prediction, a model was set up using the conventional extraction technique which rendered suitable portions of enzyme extracts. Mouse diaphragms were incubated with a known concentration of drug

Conc. of PYR (M)	J ChE	% I (J ChE)	NJ ChE	% I (NJ ChE)
N	**4**	**4**	**4**	**4**
Untreated	2.60 ±0.41	-	1.86 ±0.13	-
10^{-10}	2.42 ±0.38	6.8 ±3.0	1.74 ±0.13	7.2 ±6.0
10^{-9}	2.45 ±0.31	5.0 ±11.2	1.82 ±0.04	4.2 ±5.0
10^{-8}	2.03 ±0.35	11.2 ±1.5	1.76 ±0.08	6.0 ±3.0
10^{-7}	2.08 * ±0.26	19.7 ±5.2	1.62 * ±0.06	13.3 ±4.2
10^{-6}	1.19 * ±0.18	53.8 ±4.7	1.38 * ±0.10	26.3 ±3.8
10^{-5}	0.61 * ±0.18	76.1 ±3.5	0.98 * ±0.10	47.9 ±2.2
10^{-4}	0.46 * ±0.03	82.5 ±2.1	0.71 * ±0.08	61.3 ±3.7

Table 5.4: Junctional (J) and non-junctional (NJ) ChE and percentage inhibitions after PYR (10^{-4}-10^{-10}M). ChE activities are means ± s.d. in nmol min^{-1} mg^{-1}. * denotes significant difference from untreated ChE activity (Mann-Whitney, $P<0.05$).

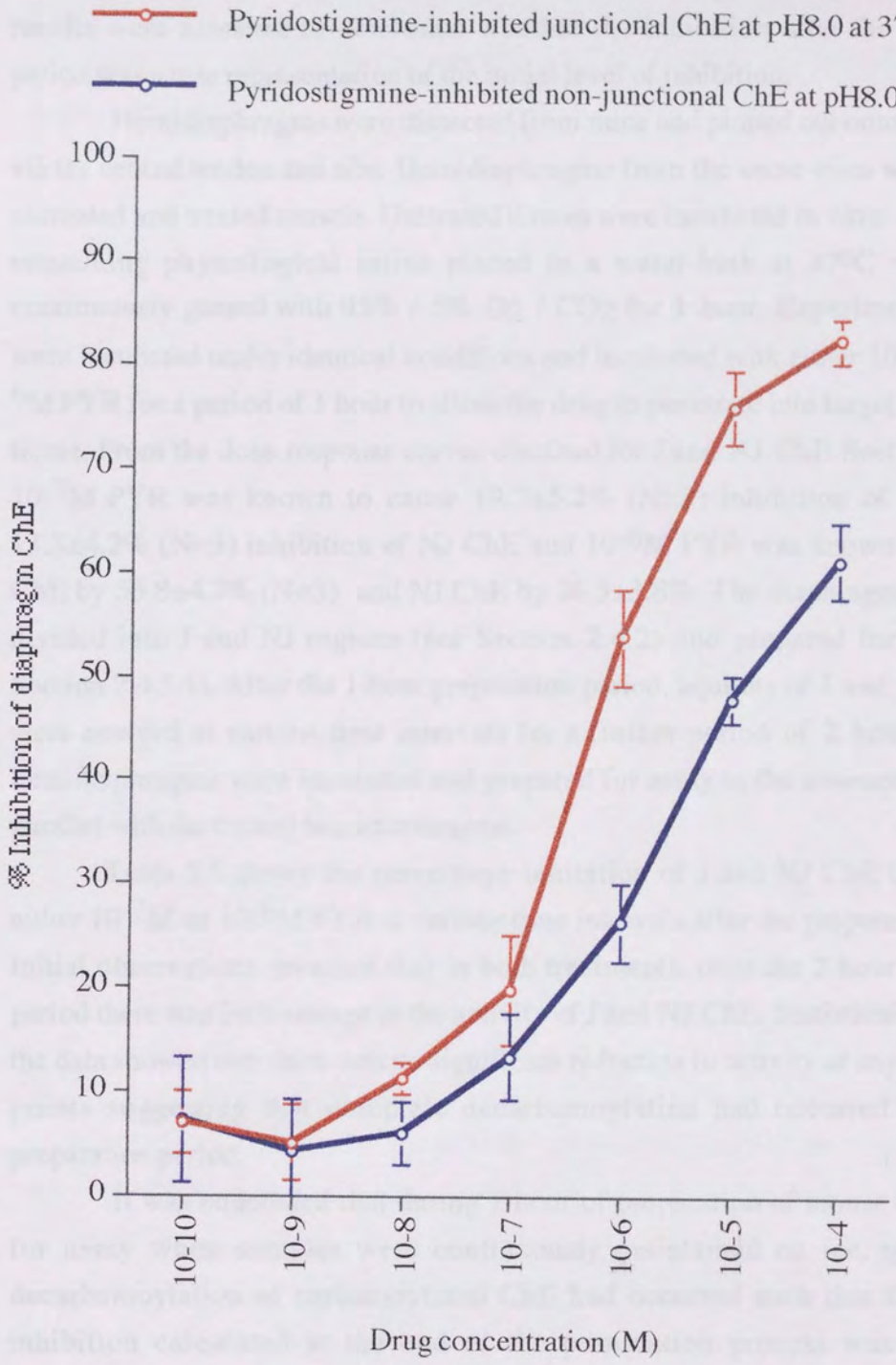

Figure 5.3: Dose-response curve of PYR-inhibited junctional and non-junctional ChE at pH8.0 at 37°C. Percentage inhibition of junctional and non-junctional ChE at doses of PYR in the range 10^{-4}M to 10^{-10}M.

which gave a known level of inhibition, then prepared for a period of 1 hour and any change in the level of inhibition after the preparation period was recorded. The results were assessed to determine whether the inhibition after the preparation period was a true representation of the initial level of inhibition.

Hemidiaphragms were dissected from mice and pinned out onto dental wax via the central tendon and ribs. Hemidiaphragms from the same mice were used as untreated and treated muscle. Untreated tissues were incubated *in vitro* in a beaker containing physiological saline placed in a water-bath at 37°C which was continuously gassed with 95% / 5% O_2 / CO_2 for 1 hour. Experimental tissues were incubated under identical conditions and incubated with either 10^{-7}M or 10^{-6}M PYR for a period of 1 hour to allow the drug to penetrate into target areas in the tissue. From the dose-response curves obtained for J and NJ ChE Section 5.2.1.4, 10^{-7}M PYR was known to cause 19.7±5.2% (N=3) inhibition of J ChE and 13.3±4.2% (N=3) inhibition of NJ ChE and 10^{-6}M PYR was known to inhibit J ChE by 53.8±4.7% (N=3) and NJ ChE by 26.3±3.8%. The diaphragms were then divided into J and NJ regions (see Section 2.4.2) and prepared for assay (see Section 2.4.3.1). After the 1 hour preparation period, aquilots of J and NJ samples were assayed at various time intervals for a further period of 2 hours. Control hemidiaphragms were incubated and prepared for assay in the absence of drug in parallel with the treated hemidiaphragms.

Table 5.5 shows the percentage inhibition of J and NJ ChE treated with either 10^{-7}M or 10^{-6}M PYR at various time intervals after the preparation period. Initial observations revealed that in both treatments, over the 2 hour assessment period there was little change in the activity of J and NJ ChE. Statistical analysis of the data showed that there was no significant reduction in activity at any of the time points suggesting that complete decarbamoylation had occurred during the preparation period.

It was concluded that during 1 hour of preparation of mouse diaphragms for assay when samples were continuously maintained on ice, spontaneous decarbamoylation of carbamoylated ChE had occurred such that the level of inhibition calculated at the end of the preparation process was not a true representation of the level of inhibition which had occurred during the incubation of samples with the CB at the start of preparation and the prediction made by tests performed in the previous sections was accurate. Hence, during the sequential extraction process which takes around 3-4 hours to obtain the various forms of AChE from the mouse diaphragm, complete decarbamoylation would be expected to occur and no measurable inhibition would be expected at the time the samples are assayed for AChE activity. Attempts were made to determine the rate of

Time after start of preparation	% I (J ChE) PYR 10^{-7}M	%I (NJ ChE) PYR 10^{-7}M	%I (J ChE) PYR 10^{-6}M	%I (NJ ChE) PYR 10^{-6}M
1 hr	19.1 ±9.2	14.1 ±15.6	32.6 ±11.2	23.6 ±17.6
1 hr 30 mins	23.6 ±6.5	10.8 ±14.0	32.6 ±13.3	19.6 ±18.5
2 hrs	20.1 ±10.3	11.3 ±18.6	32.2 ±12.5	19.0 ±18.4
2 hrs 30 mins	20.0 ±13.0	4.0 ±26.4	31.7 ±10.1	19.6 ±16.0
3 hrs	18.2 ±11.1	8.2 ±19.1	31.3 ±10.1	19.0 ±14.8

Table 5.5: Percentage inhibition of junctional (J) and non-junctional (NJ) ChE at regular time intervals after pre-incubation with 10^{-7}M or 10^{-6}M PYR. Samples were incubated at 37°C in a water-bath for 1 hr and prepared for assay for 1 hr (all samples were maintained on ice during the preparation period). Values shown are means±s.d based on N=3.

decarbamoylation during the sequential extraction method but proved to be unsuccessful as the molecular forms of AChE appeared to be sensitive to pre-incubation with drugs *in vitro* and were found to deteriorate (no significant deterioration of ChE samples was noted during the incubation of hemidiaphragms *in vitro* prior to preparation for the conventional extraction technique and sizeable pools of non-specific ChE were successfully extracted from these hemidiaphragms.).

In the absence of a suitable method for assessing the rate of decarbamoylation during the sequential extraction process, from the *in vitro* studies it is probable the process does occur even if samples are kept on ice and must therefore be accounted for in the assessment of the final data. Since the process of sequentially extracting the molecular forms is a lengthy one involving several hours of preparation and several dilutions of the originally treated tissues which accelerates decarbamoylation (Wilson et al., 1960), it was assumed that no carbamoylated-AChE can survive the process and any reductions in activity observed in the final readings may be due to actual AChE reduction.

5.2.2 The long-term effects of PYR on mouse skeletal muscle during repetitive dosing.

5.2.2.1 Whole blood ChE.

Figure 5.4 and Table 5.6 show whole blood ChE activity at various time intervals during a period of three weeks when mice were repetitively dosed with 383 nmol kg^{-1} PYR twice daily at 9am and 5pm. Blood ChE was assayed rapidly after removal from mice to avoid spontaneous decarbamoylation and reductions in activity were assumed to be due to inhibition.

During the first 24 hours of exposure to PYR, whole blood ChE was reduced by around 10% but was not significantly different from the untreated value. Between the 1st and 2nd day of the treatment, there was a reduction in the activity of blood ChE and the inhibition increased to 20%. In the following 2 days, there was a further reduction in activity with the inhibition increasing to more than 50%. This level of inhibition was maintained for a further 12 days and the activities measured at the relevant time points were found to differ from the untreated activities but there was not found to be any difference between consecutive time points suggesting that the level of inhibition had stabilised. It appeared therefore that after 4 days of consistent dosing, blood ChE gradually reached a stable level of inhibition. When the ChE activity was measured after 21 days of repetitive PYR

Time during treatment	N number	Whole Blood ChE †	% I (Whole blood ChE)
Untreated	15	3.03 ±0.97	-
3 hours	12	2.63 ±0.95	13.2
1 day	18	2.70 ±0.76 +	10.9
2 days	13	2.02* ±0.66 +	21.1
4 days	4	1.32* ±0.03	56.4
7 days	6	1.43* ±0.29	52.8
14 days	4	1.53* ±0.45	49.5
21 days	15	2.36 ±1.60	22.1

Table 5.6: Whole blood ChE after twice daily dosing with 383 nmol kg^{-1} PYR (3 hrs-21 days). ChE activities are in μmol min^{-1}ml^{-1}. All values shown are means ± s.d. † denotes the set has different groups (K-S ANOVA, $P<0.05$), * denotes groups with differ fron the untreated group (K-S multi-comparison test, $P<0.05$) and + denotes different adjacent groups (K-S multi-comparison test, $P<0.05$).

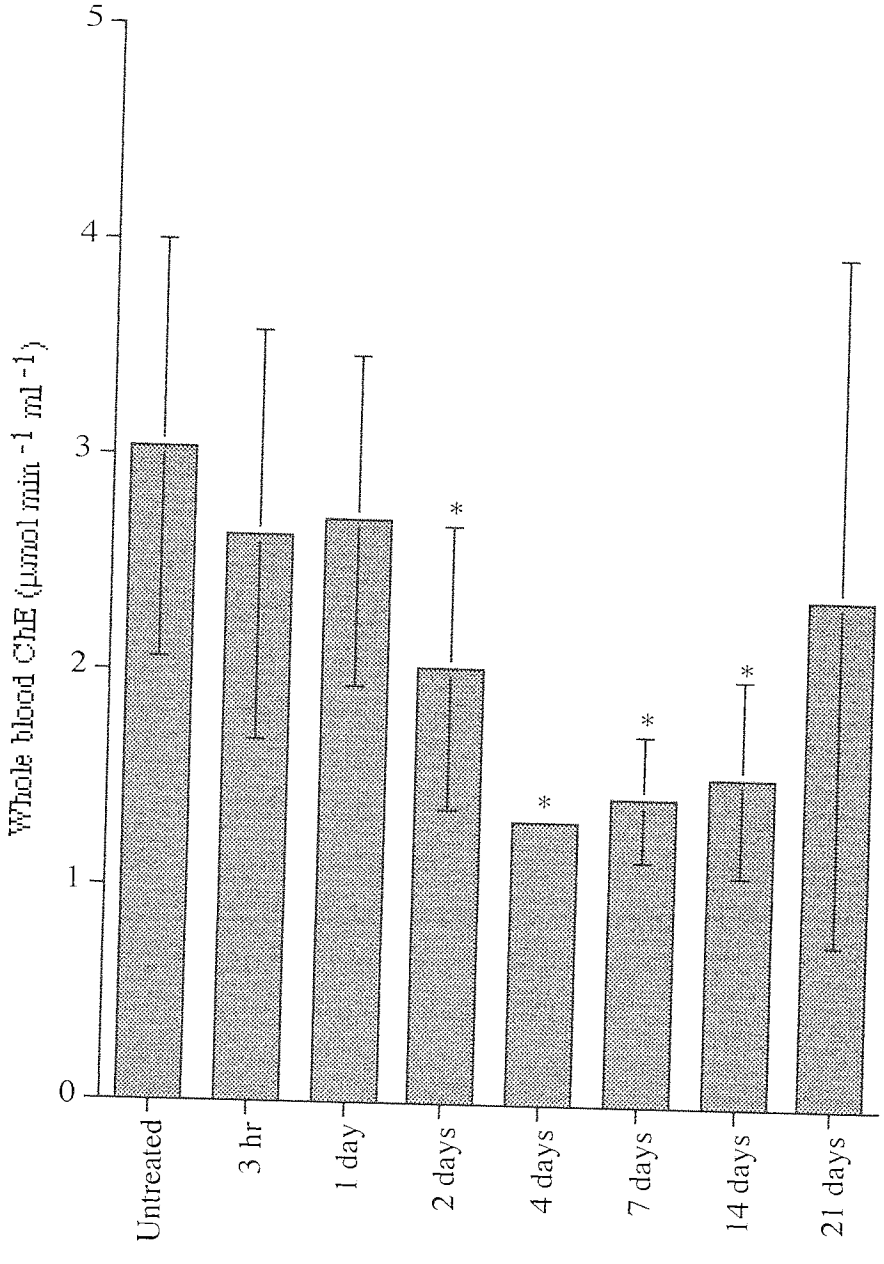

Figure 5.4: Whole blood ChE after twice daily dosing with 383 nmol kg^{-1} PYR (3 hrs-21 days). * denotes groups which differ from the untreated group: $P<0.05$ (Kruskal-Wallis multi-comparison test).

dosing, it was no longer found to be different from untreated values. This suggested that during the time period between 14 and 21 days of dosing, some adjustment may have occurred in the metabolism of the blood ChE in response to PYR resulting in increased enzyme synthesis.

Hence, during the entire dosing period, blood ChE was persistently reduced which was probably due to inhibition. The pattern of activity reduction suggested that there was an initial period of 4 days when activity gradually dropped followed by a period of at least 12 days when the reduction was stable and the level of inhibition was equivalent to that after a singe, low, non-necrotising dose of 25 nmol kg^{-1} ECO. After 3 weeks of dosing blood ChE no longer seemed to be affected by PYR. The assay of whole blood ChE gives the combined activity of AChE dimers bound to the membranes of erythrocytes (Ott et al., 1982; Rosenberry and Scoggin, 1984) and plasma BChE and it was unclear whether the changes in activity were attributable to the former or the latter. The function of blood ChE is unknown, but studies have suggested that the plasma form may function as a buffer for functional AChE because it binds to anti-ChE and excludes it from the nervous system (Wills, 1972; Ecobichon and Comeau, 1972; Jimmerson et al., 1989) and injection of exogenous AChE has successfully been demonstrated to protect against OP toxicity (Wolfe et al., 1987; Raveh et al., 1989; Doctor et al., 1991). It is possible that the response observed after 3 weeks of PYR dosing occurs due to increases in plasma ChE by up-regulation because the system has created its own biological scavengers to clear PYR from the circulation.

5.2.2.2 Molecular forms of AChE.

Table 5.7 shows the changes in activities of junctional (J), non-junctional (NJ) and endplate-specific (EPS): globular (G), asymmetric (A) and non-extractable (NE) forms of mouse diaphragm AChE after 9am and 5pm subcutaneous injections with 383 nmol kg^{-1} with PYR given daily for 3 weeks. On each of the days when enzyme level were measured, diaphragms were removed and prepared for assay 3 hours after the morning dose.

During the treatment, there was little overall variation in AChE molecular form activity. Some reduction in the activity of J (G) enzymes was observed 3 hours, 1 day and 4 days after dosing (see Figure 5.5a). J (A) and J (NE) enzymes were only reduced after 14 days of treatment as were the NJ (G) enzymes. The NJ (A) forms displayed some significant reduction at the 3 hour and 7 and 14 day time points (see Figure 5.5b). In contrast, The NJ (NE) enzymes appeared to be up-

Region	Untr-eated	3 hrs	1 day	2 days	4 days	7 days	14 days	21 days
N	10	8	8	8	4	4	4	6
J (G) †	3.46+ ±0.68	2.83* ±0.27	2.83* ±0.31	3.15+ ±0.26	2.15*+ ±0.10	4.00 ±1.21	3.52 ±0.25	3.03 ±0.29
J (A) †	1.32 ±0.25	1.12 ±0.29	1.11 ±0.27	1.22 ±0.20	1.05+ ±0.10	1.68+ ±0.57	0.58* ±0.15	0.99 ±0.35
J (NE) †	0.80 ±0.20	0.92 ±0.29	0.97 ±0.31	0.75 ±0.21	0.65+ ±0.01	1.24+ ±0.57	0.45*+ ±0.17	0.88 ±0.50
NJ (G) †	1.96 ±0.40	1.78 ±0.22	1.90+ ±0.20	2.35 ±0.48	2.31+ ±0.04	2.83* ±0.34	1.45*+ ±0.19	1.88 ±0.49
NJ (A) †	0.77 ±0.26	0.36* ±0.11	0.59 ±0.32	0.61+ ±0.19	1.03 ±0.09	1.21*+ ±0.35	0.15 * ±0.05	0.32 ±0.24
NJ(NE) †	0.29 ±0.15	0.17 ±0.09	0.34 ±0.33	0.29+ ±0.14	1.03* ±0.05	0.83*+ ±0.55	0.05* ±0.05	0.19 ±0.14
EPS(G) †	1.57 ±0.61	1.08 ±0.25	0.93* ±0.25	0.84*+ ±0.39	-0.17* ±0.14	1.18+ ±1.33	2.07 ±0.29	1.15 ±0.52
EPS (A)	0.66 ±0.26	0.76 ±0.22	0.48 ±0.28	0.62 ±0.21	0.01 ±0.01	0.48 ±0.80	0.43 ±0.13	0.65 ±0.24
EPS (NE)	0.50 ±0.20	0.76 ±0.24	0.63 ±0.35	0.46 ±0.27	-0.39 ±0.04	0.41 ±0.95	0.04 ±0.14	0.70 ±0.43
$T_{50\%}$ (ms)	0.40 ±0.02	0.42 ±0.02	0.43 ±0.03	0.42 ±0.02	0.42 ±0.02	-	-	0.42 ±0.2

Table 5.7: Diaphragm AChE after twice daily dosing with 383 nmol kg^{-1} PYR (3 hrs-21 days). The table shows junctional (J), non-junctional (NJ) and endplate-specific (EPS): globular (G), asymmetric (A) and non-extractable (NE) molecular form activities in nmol min^{-1} mg^{-1}. All values shown are means ± s.d. † denotes sets with different groups (K-S ANOVA, $P<0.05$), * denotes groups different from the untreated group and + denotes different adjacent groups (K-S multi-comparison test, $P<0.05$).Also shown are the times to half amplitude of the decay phase ($T_{50\%}$) of extra-cellular miniature endplate potentials (all data provided by A. Crofts, unpublished) which were assessed at the same time points.

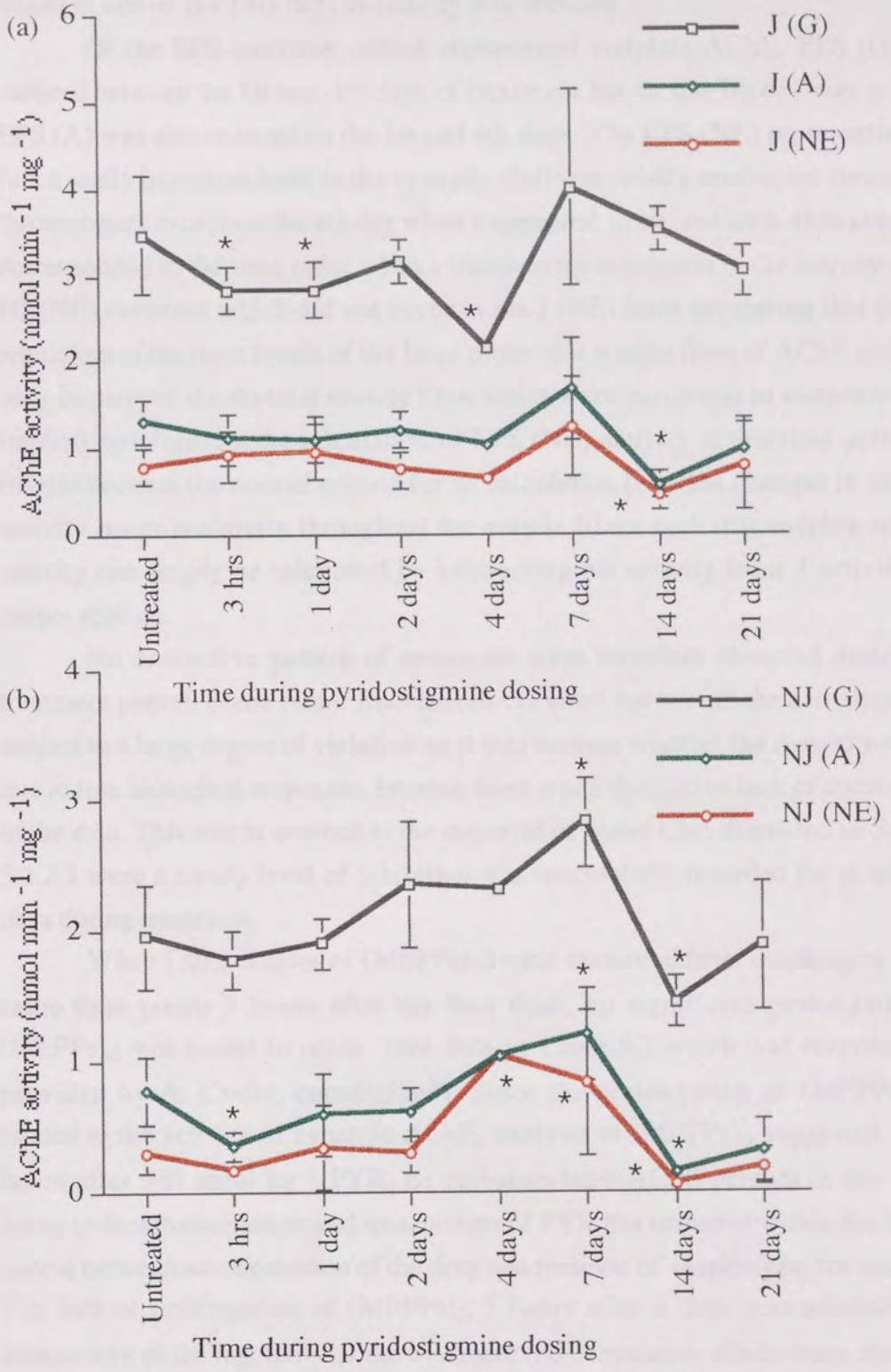

Figure 5.5: Junctional and non-junctional AChE after twice daily dosing with 383nmol kg^{-1} PYR (3hrs-21days). Globular (G), asymmetric (A) and non-extractable (NE) AChE in (a) junctional (J) and (b) non-junctional (NJ) regions. * denotes groups which differ from untreated group: $P<0.05$ (K-W).

regulated on the 4th and 7th days of treatment although this effect appeared to be transient and on the 14th day, its activity was reduced.

Of the EPS enzymes, which represented endplate AChE, EPS (G) was reduced between the 1st and 4th days of treatment but on the 7th day was normal. EPS (A) was also reduced on the 1st and 4th days. The EPS (NE) representing the functionally important form in the synaptic cleft was mostly unaffected throughout the treatment except on the 4th day when it appeared to be reduced. However, this corresponded to the time point when a transient up-regulation in the activity of the NJ (NE) occurred which did not occur in the J (NE) form suggesting that the up-regulation of the trace levels of the large molecular weight form of AChE occurred only in parts of the skeletal muscle fibre which were peripheral to endplates. This implied therefore that the calculation of EPS (NE) activity at this time point was invalid because the normal criteria for its calculation (i.e. that changes in enzyme activity occur uniformly throughout the muscle fibres such that endplate-specific activity can simply be calculated by subtracting NJ activity from J activity) no longer applied.

No distinctive pattern of responses were therefore observed during the treatment period. Some minor fluctuations occurred but overall the activities were subject to a large degree of variation so it was unclear whether the reductions were due to true biological responses because there was a distinctive lack of consistency in the data. This was in contrast to the response of blood ChE discussed in Section 5.2.2.1 were a steady level of inhibition was successfully recorded for at least 14 days during treatment.

When $T_{50\%}$ values of $(MEPPs)_o$) were measured from diaphragms at the same time points 3 hours after the 9am dose, no significant prolongation of $(MEPPs)_o$ was found to occur (see data in Table 5.7 which was recorded and provided by A. Crofts, unpublished). Since the prolongation of (MEPPs)o is related to the activity of synaptic AChE, analysis of $(MEPPs)_o$ suggested that 3 hours after 383 nmol kg^{-1} PYR, no carbamoylated AChE persists in the tissue because decarbamoylation and metabolism of PYR has occurred within the 3 hour period between administration of the drug and removal of diaphragms for analysis. The lack of prolongation of $(MEPPs)_o$ 3 hours after a dose was administered irrespective of the regularity of the treatment (no cumulative effects were observed during the monitoring of $(MEPPs)_o$ which were clearly unaffected on all the days of treatment) suggested that during the assessment of AChE activity by the assay technique no inhibition would be expected.

When diaphragms were removed 1 hour after 383 nmol kg^{-1} PYR $(MEPPs)_o$ were significantly prolonged (Mann-Whitney, $P<0.05$) and $T_{50\%}$ was

0.68±0.03 ms (this experiment was conducted by A. Crofts). When $T_{50\%}$ values were substituted into the correlation equation (See Section 4.3.5) the predicted level of AChE inhibition 1 hour after dosing was in the region of 50%. This suggested that 383 nmol kg^{-1} PYR effectively inhibited diaphragm AChE *in vivo* which could be recorded soon after dose administration but 3 hours later, complete recovery of AChE activity occurred due to the rapid decarbamoylation of inhibitor-enzyme complexes and metabolism of drug within the system. When drug administration is repeated the same process occurs: target enzyme is re-inhibited, and rapidly recovers within 3 hours. The effectiveness of dosing was supported by the results obtained from the studies on whole blood ChE which showed that if blood was analysed soon after removal, good levels of inhibition could be measured. The process of repetitive drug dosing can be continued for at least 3 weeks without a significant accumulation of effects being observed due to the build up of PYR in the system or a delay in the clearance of the drug out of the system.

In Sections 5.2.1.2 and 5.2.1.4 the rate of decarbamoylation of carbamoylated AChE during enzyme extraction processes was discussed and it was suggested that it was unlikely that at the end of sample preparation any inhibition which had occurred in the tissue would still be detected. If during the repetitive dosing experiment, the inhibited enzyme rapidly recovers during the 3 hour period between dosing and tissue removal and the total time elapsed between drug administration and measurement of AChE activity is approximately 7-8 hours it is unlikely that the reductions observed in AChE activity are due to inhibition.

Hence, within 3 hours of a PYR dose which initially caused at least 50% inhibition of functionally active AChE, complete recovery of inhibited AChE occurs either by spontaneous decarbamoylation or the metabolism of inhibitor-enzyme complexes. Effects on the activity of diaphragm AChE were not observed to accumulate during the treatment but there was a possible transient up-regulation of non-endplate A and NE forms between 4 and 7 days and some reduction in EPS AChE during the first 4 days of treatment.

5.2.2.3 Endplate dimensions.

Table 5.8 shows the changes in mouse diaphragm endplate width (W), length (L) and width/length ratio (W/L) ratio during 3 weeks of twice daily administration of 383 nmol kg^{-1} PYR. Three hours after the start of treatment, the W/L ratio had ncreased by 47% (Figure 5.6b). Analysis of endplate W and L showed that 3 hours after dosing, W had increased and L had reduced (Figure 5.6a)

Time	Width (μm) †	Length (μm) †	Width/length ratio †	No. of HD No. of EP
Untreated	19.3±0.7	34.8±2.9	0.56±0.04	8
	+	+	+	240
3 hours	23.8±1.3*	29.0±1.0*	0.84±0.03*	4
				120
1 day	23.8±0.5*	29.0±1.0*	0.84±0.02*	4
				120
2 days	22.1±1.4*	30.0±2.1*	0.75±0.08*	4
				120
3 days	20.1±1.3	27.4±0.6*	0.75±0.02*	4
	+	+		120
4 days	21.4±0.4*	28.8±2.2*	0.76±0.05*	4
	+			120
7 days	22.3±2.0*	27.1±3.2*	0.85±0.16*	4
	+			120
14 days	22.1±0.9*	29.5±2.7*	0.79±0.11*	4
	+			120
21 days	21.7±1.8*	26.3±2.3*	0.87±0.15*	4
				120

Table 5.8: Endplate dimensions after twice daily dosing with 383 nmol kg^{-1} PYR (3 hrs-21 days). Shown are variations endplate width, length and width/length ratio. HD gives the no. of hemidiaphragms and EP gives the total no. of endplates. Values are means±s.d. † denotes sets with different groups (ANOVA, $P<0.05$), * denotes groups which differ from the untreated group (MANOVA, $P<0.05$) and + denotes different adjacent groups (MANOVA, $P<0.05$)

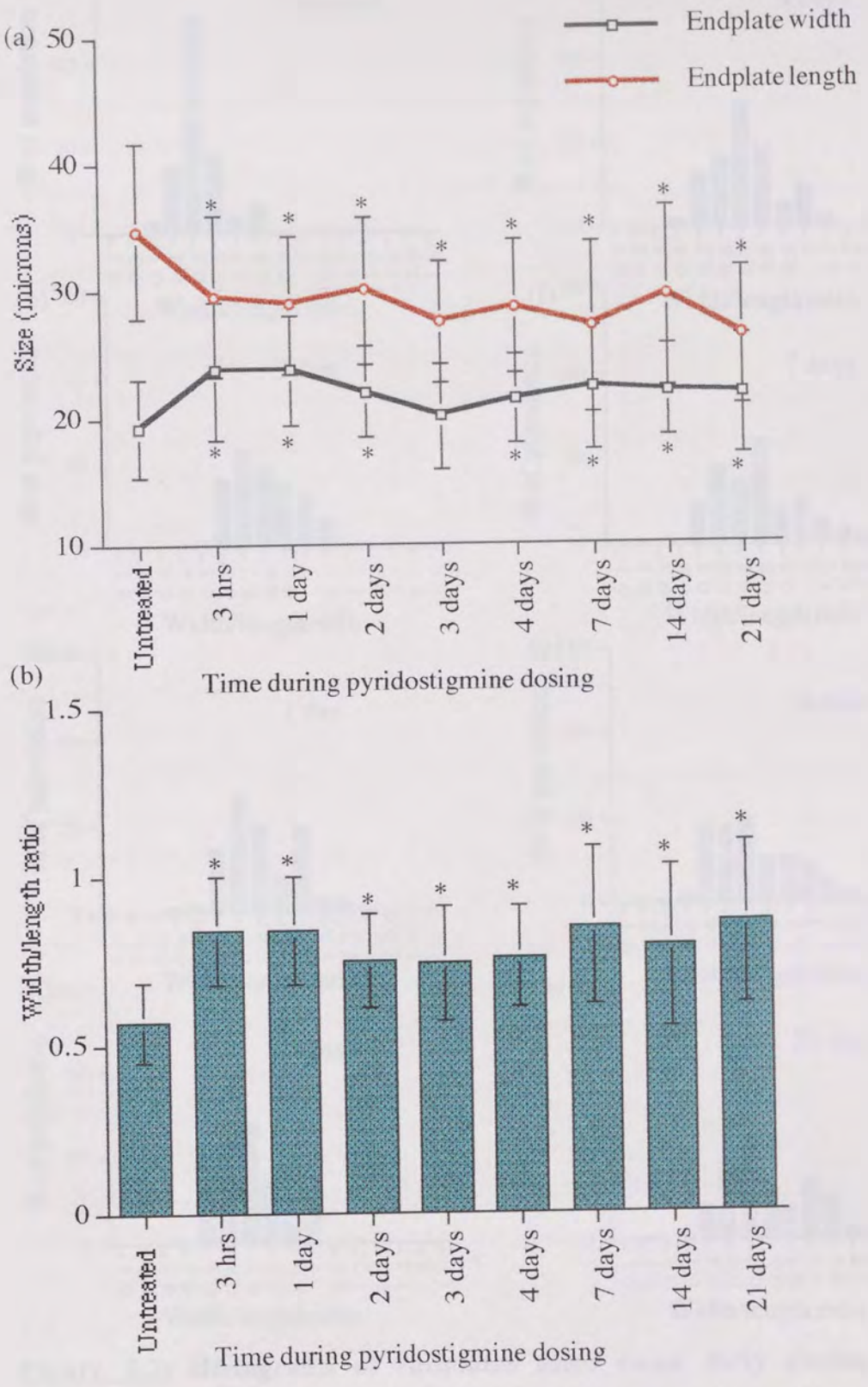

Figure 5.6: Width, length and W/L ratio of endplates after twice daily dosing with 383 nmol kg^{-1} PYR (3hrs-21days). * denotes groups which differ from untreated group: $P<0.05$(MANOVA).

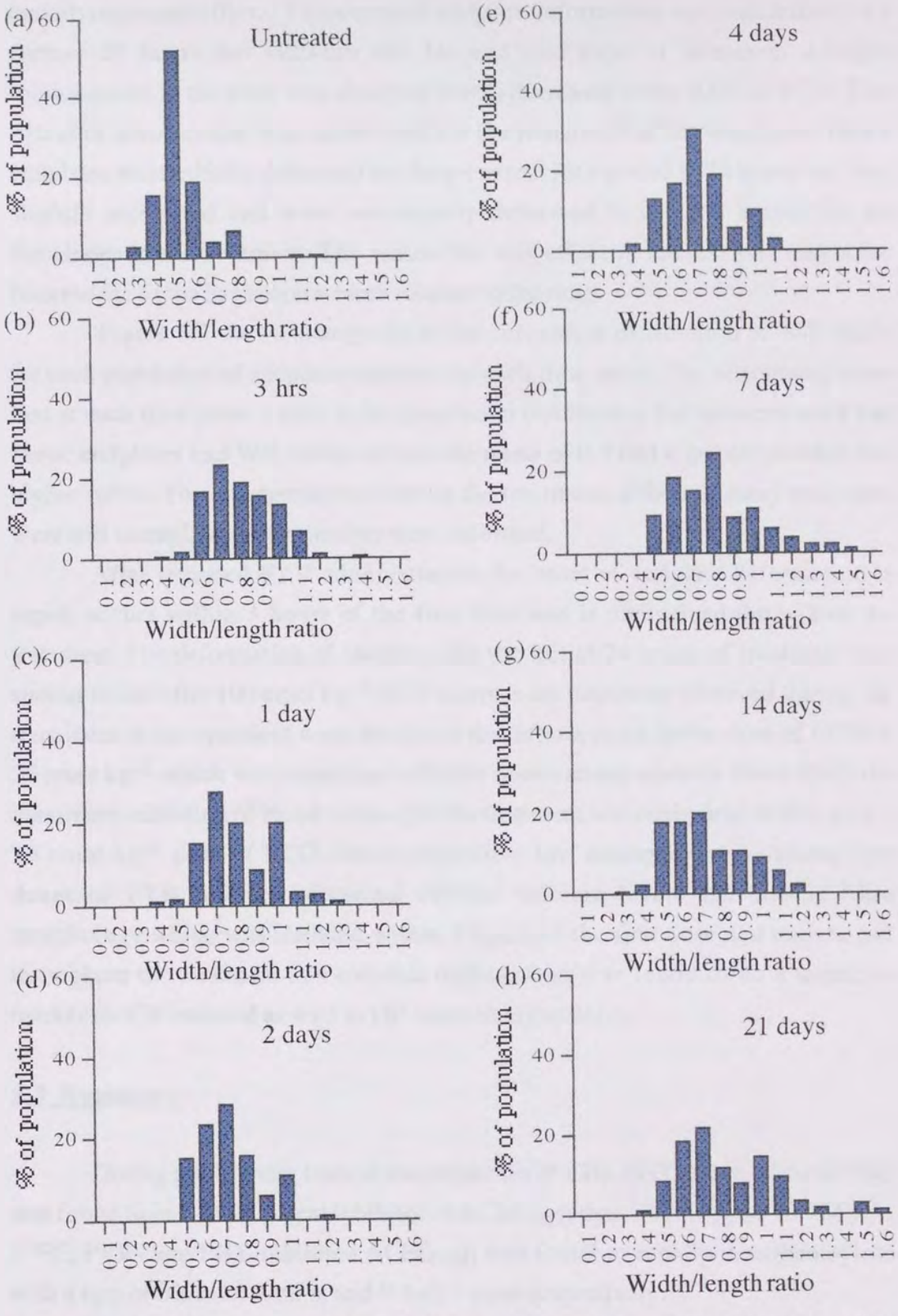

Figure 5.7: Histograms of endplates after twice daily dosing with 383 nmol kg^{-1} PYR (3hrs-21days). Percentage of endplates per population at given width/length ratios for (a) untreated, (b) 3 hrs, (c) 1 day, (d) 2 days, (e) 4 days, (f) 7 days, (g) 14 days and (h) 21 days.

indicating that endplates had become rounder due to hypercontractions in underlying muscle fibres. This extent of endplate deformation was maintained for a further 21 hours but between the 1st and 2nd days of treatment a slight improvement in the ratio was observed which decreased from 0.84 to 0.75. This extent of deformation was maintained for the remainder of the treatment. Hence endplates were initially deformed to a larger extent for a period of 24 hours but then slightly recovered and were consistently deformed to a lesser extent for the remainder of the treatment. The reason for this effect is unclear but may arise because the tissue has become more tolerant to the drug.

Figure 5.7 shows histograms of the percentage distribution of W/L ratios for each population of endplates analysed at each time point. The histograms show that at each time point a shift in the population distribution had occurred such that fewer endplates had W/L ratios around the mean of 0.5 and a greater number had higher ratios. This suggested that during the treatment, although many endplates were still normal, a greater number were deformed.

After repeated PYR administration the onset of endplate deformation is rapid, occurs within 3 hours of the first dose and is maintained throughout the treatment. The deformation of endplates for the initial 24 hours of treatment was similar to that after 100 nmol kg^{-1} ECO whereas the responses observed during the remainder of the treatment were similar to that after a much lower dose of ECO of 25 nmol kg^{-1} which was consistent with the observations made in blood ChE: the maximum inhibition of blood 4 days into the treatment was equivalent to that after a 25 nmol kg^{-1} dose of ECO. Hence, repetitive low dosing with non-necrotising doses of PYR induced abnormal cellular calcium levels and muscle fibre morphology which was initiated within 3 hours of the first dose and maintained throughout the treatment and endplate deformation was found to be a sensitive marker for CB-induced as well as OP-induced myopathies.

5.3 Summary

During preliminary tests of the properties of CBs, PHY ($I_{50\%}$: 0.5×10^{-6}M) was found to be a more potent inhibitor of $AChE_{(eel)}$ than PYR ($I_{50\%}$: 10^{-6}M). At 37°C, PYR- and PHY-inhibited $AChE_{(eel)}$ was found to rapidly decarbamoylate with a $t_{1/2}$ of 32.1±25.8 mins and 9.1±2.1 mins respectively.

The lack of stability of carbamoylated AChE was a potential problem in the investigation of the inhibitory effects of CBs on mouse diaphragm AChE. It was demonstrated that maintaining samples on ice delayed, but not prevented the rate of

decarbamoylation of PYR and PHY-inhibited AChE which occurred with a $t_{1/2}$ of 57.5±18.3 mins and 125.4±25.1 mins respectively.

Because decarbamoylation rates of mouse diaphragm AChE molecular forms could not be studied directly, the decarbamoylation rate of MDFE was determined from electrophysiological studies. The rate of MDFE decarbamoylation after 10^{-6}M PYR was 42.1±20.7 mins which was not significantly different from the rate of decarbamoylation of $AChE_{(eel)}$. Hence, diaphragm AChE and $AChE_{(eel)}$ have similar decarbamoylation properties and it was proposed that diaphragm AChE would decarbamoylate at the same rate on ice as $AChE_{(eel)}$.

After a minimal preparation period of 1 hour, substantial decarbamoylation of diaphragm ChE extracted conventionally was found to occur. It was predicted therefore, that the sequential extraction method which takes 3-4 hours to prepare would not successfully indicate the extent of inhibition of diaphragm AChE caused by CBs and assayed AChE activity would reflect uninhibited AChE.

Repetitive PYR dosing reduced whole blood ChE by 10-20% 3 hours to 2 days into the treatment and by 50% from 4 days to 14 days. After 21 days of dosing, there was less inhibition suggesting that blood ChE may have been up-regulated possibly to act as a biological scavenger for anti-ChEs. Effects on diaphragm AChE were minimal during the treatment: non-endplate A and NE forms were transiently up-regulated between 4 and 14 days and EPS AChE was transiently reduced between 1 and 4 days. Three hours after the 9 am PYR dose on each assessment day $(MEPPs)_o$ were not prolonged and hence, AChE was not inhibited suggesting that complete decarbamoylation of AChE had already occurred *in vivo*. However, 1 hour after the dose, $(MEPPs)_o$ were prolonged and AChE was inhibited by around 50%. The changes observed in AChE molecular forms 3 hours after the 9 am dose were probably therefore due to up- or down-regulation and not due to inhibition because decarbamoylation had occurred *in vivo* and *in vitro*.

Repetitive low doses of 383 nmol kg^{-1} PYR induced abnormal cellular calcium levels and muscle fibre morphology which had a rapid onset and persisted throughout the treatment. Endplate deformation during the first 24 hours of treatment was more severe than during the remainder of the treatment. During the initial period, the extent of deformation was similar to that after a 100 nmol kg^{-1} dose of ECO and for the remaining time corresponded to the deformation after a 25 nmol kg^{-1} dose. Endplate deformation was therefore a highly sensitive marker for both CB and OP-induced myopathy.

CHAPTER 6

LONG-TERM EFFECTS OF LOW DOSES OF PYRIDOSTIGMINE ON MOUSE SKELETAL MUSCLE

6.1 Introduction.

Carbamate (CB) anti-ChEs are commonly used in the therapy of myasthenia gravis and potentially in the treatment of Alzheimer's disease. They also have a function as prophylactics against OP poisoning because they are reversible AChE inhibitors. A CB compound administered at a dose which inhibits around 30% AChE can be successfully protective because it rapidly disassociates from the enzyme and provides some level of cholinergic transmission.

There is at this stage, only a limited insight into the long-term, low-dose effects of CBs on cellular function because only subtle toxic effects may be produced which are undetectable by many conventional methods. An investigation was carried out to study possible long-term effects of PYR on skeletal muscle AChE activity, functional synaptic AChE, blood ChE and endplate shape when administered by an osmotic pump. A parallel investigation of electrophysiological effects on the endplate was carried out by A. Crofts. Experimental protocols were designed with the following objectives in mind:

(a) To investigate the effects 1 day, 2 days, 4 days, 7 days and 14 days after the implantation of an osmotic pump which continually administered PYR at the rate of 11.4 nmol hr^{-1} during a 2 week period.
(b) To investigate whether there was any recovery 2 days, 7 days and 14 days after a pump which had administered drug for 7 days was removed and the treatment was terminated.
(c) To investigate whether PYR administered at 11.4 nmol hr^{-1} for a period of 4 days by the osmotic pump successfully protected against the inhibitory effects of a 500 nmol kg^{-1} dose of ECO which was administered after 4 days of pre-treatment and an assessment made 5 days later.

6.2 Results and discussion.

6.2.1 Long-term effects of PYR administered for 14 days on mouse skeletal muscle.

6.2.1.1 Whole blood ChE.

Table 6.1 and Figure 6.1 show whole blood ChE during 2 weeks of treatment with PYR administered by an osmotic pump at the rate of 11.4 nmol hr^{-1}.

Time after implant of pump	N number	Whole blood ChE † (μmol $min^{1}ml^{-1}$)	% I (Whole blood ChE
Untreated	15	3.03 ±0.97 +	-
1 day	5	2.20* ±0.50	27.4
2 days	5	2.07* ±0.51	31.7
4 days	4	2.10* ±0.42	30.7
7 days	13	1.69* ±0.36	44.2
14 days	4	1.47* ±0.57	51.5

Table 6.1: Whole blood ChE after 11.4 nmol hr^{-1} PYR (1-14 days). ChE activities are in μmol $min^{-1}ml^{-1}$ and the values shown are means ± s.d. † denotes the set has different groups (K-S ANOVA, $P<0.05$), * denotes groups which differ from the untreated group (K-S multi-comparison test, $P<0.05$) and + denotes diferent adjacent groups (K-S multi-comparison test, $P<0.05$).

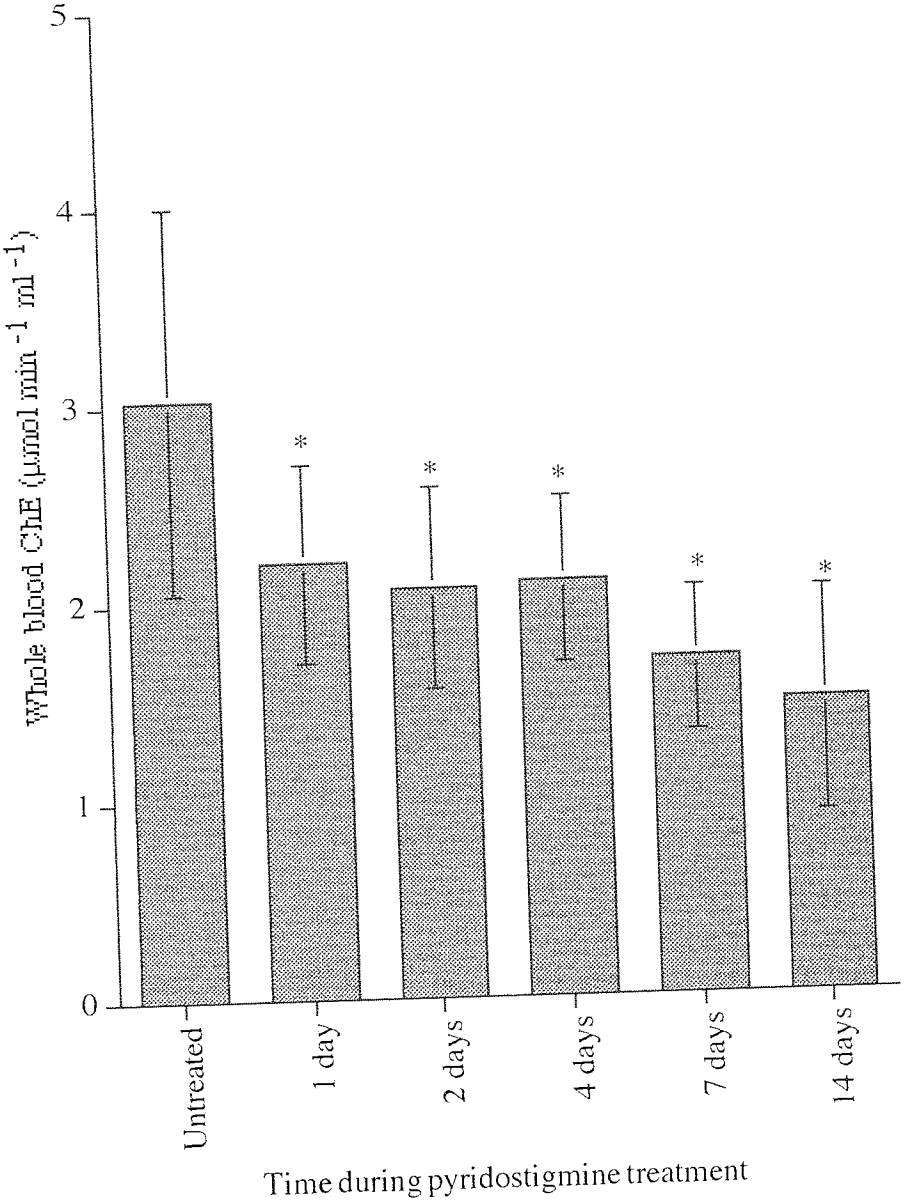

Figure 6.1: Whole blood ChE after 11.4 nmol hr^{-1} PYR (1-14 days). * denotes groups which differ from the untreated group: $P<0.05$ (Kruskal-Wallis multi-comparison test).

Blood ChE was assessed soon after samples were taken from mice and kept on ice for the short time before assay hence very little spontaneous decarbamoylation of PYR-inhibited ChE was expected and reductions in ChE activity were probably due to inhibition. All treated ChE activities were found to be different from the untreated level at all the time points investigated. The inhibition after 1 day of treatment was found to be around 30%. There were no differences between the treated groups at each time point suggesting that there was no progressive increase in the inhibition of blood ChE during the treatment. Hence blood ChE inhibition was between 30-50% during the 2 week dosing period.

The range of PYR inhibition was below that after 25 nmol kg^{-1} ECO suggesting that PYR was constantly administered at low doses. The responses of blood ChE gave a useful indication of *in vivo* inhibition by PYR at various time points during treatment.

6.2.1.2 Molecular forms of AChE.

Table 6.2 shows the activities of diaphragm AChE in junctional (J) and non-junctional (NJ) regions and endplate-specific (EPS) activity calculated by the standard method (see Section 2.4.5) measured at various time intervals during 14 days of continual infusion of mice with 11.4 nmol hr^{-1} PYR. Osmotic pumps filled with only 0.9% saline were initally implanted in mice and molecular form activities were measured after 24 hours to investigate whether pump implantation affected AChE levels. There were not found to be any significant differences between the activities of any of the molecular forms which had been given saline and molecular form activites in untreated mice (Mann-Whitney, $P>0.1$ in all cases) hence the activities were pooled together (see Appendix A.6 for the relevant data).

NJ (G) and NJ (A) (Figure 6.2b) activities were measured at normal levels throughout PYR treatment. Had any actual inhibition occurred prior to extraction of the enzymes from the mice is unclear as it is possible that this may have occurred but that during the process of preparing the enzymes for assay the drug may have become dissociated due to spontaneous decarbamoylation (tests carried out in Chapter 5 suggested that this is possible even if samples are maintained on ice). The minor A12 element (NJ (NE)) normally present in the NJ parts of untreated tissue was found to be in excess of the untreated level by around 200% on the 2nd day of treatment suggesting that at this time point it may been transiently up-regulated by a considerable amount. During the remainder of the treatment, the NJ (NE) enzyme level was not found to be different from the untreated level.

Enzyme	Un-treated	1 day	2 days	4 days	7 days	14 days
N	13	5	4	5	9	4
J (G) †	3.48	2.86	2.59*	2.31*	2.48*	3.08
	±0.80	±0.46	±0.79	±0.49	±0.48	±0.48
J (A) †	1.29	1.24	1.46+	0.91*	0.79*	1.09
	±0.31	±0.35	±0.23	±0.23	±0.18	±0.20
J (NE) †	0.79	0.58	0.84	0.64	0.59*	0.69
	±0.20	±0.14	±0.30	±0.27	±0.21	±0.21
NJ (G)	1.9	1.95	1.78	1.46	1.81	2.32
	±0.49	±0.66	±0.84	±0.37	±0.32	±0.41
NJ (A)	0.73	1.17	1.13	0.58	0.60	0.64
	±0.30	±1.01	±0.56	±0.30	±0.32	±0.17
NJ (NE)†	0.29	0.47	0.84*	0.47	0.29	0.22
	±0.16	±0.35	±0.43	±0.24	±0.25	±0.11
EPS (G)†	1.63+	0.91*	0.81*	0.85*	0.68*	0.77
	±0.62	±0.48	±0.24	±0.47	±0.48	±0.64
EPS (A)†	0.62+	0.07*	0.33	0.36*	0.19*	0.45
	±0.26	±0.85	±0.38	±0.13	±0.28	±0.27
EPS(NE)	0.50+	0.11*	0.03*	0.11*	0.30*	0.47
†	±0.18	±0.48	±0.40	±0.07	±0.17	±0.26
MDFE †	0.47+	0.28*	0.25*	0.20*	0.22*	0.13*
	±0.04	±0.07	±0.03	±0.01	±0.11	±0.00
	(NS)	(NS)	(NS)	(NS)	(NS)	(NS)
J (NF)	0.33	0.30	0.59	0.44	0.25+	0.59
	±0.20	±0.16	±0.25	±0.27	±0.28	±0.19
	(NS)	(NS)	(NS)	(NS)	(NS)	(NS)

Table 6.2: Diaphragm AChE after 11.4 nmol hr^{-1} PYR (1-14 days). The table shows junctional (J) and non-junctional (NJ) globular (G), asymmetric (A), and non-extractable (NE) and endplate specific (EPS) activities in nmol min^{-1} mg^{-1}. Also shown are the $(MEPP)_o$-derived functional enzyme activities (MDFE) and the activity of non-functional enzyme in the junctional region (J (NF)). Values are means±s.d. † denotes sets with different groups (K-S ANOVA, $P<0.05$), * denotes groups which differ from the untreated group and + denotes different adjacent groups (K-S multi-comparison test, $P<0.05$). (NS) denotes that there was no significant difference between MDFE and EPS (NE) and J (NF) and NJ (NE).

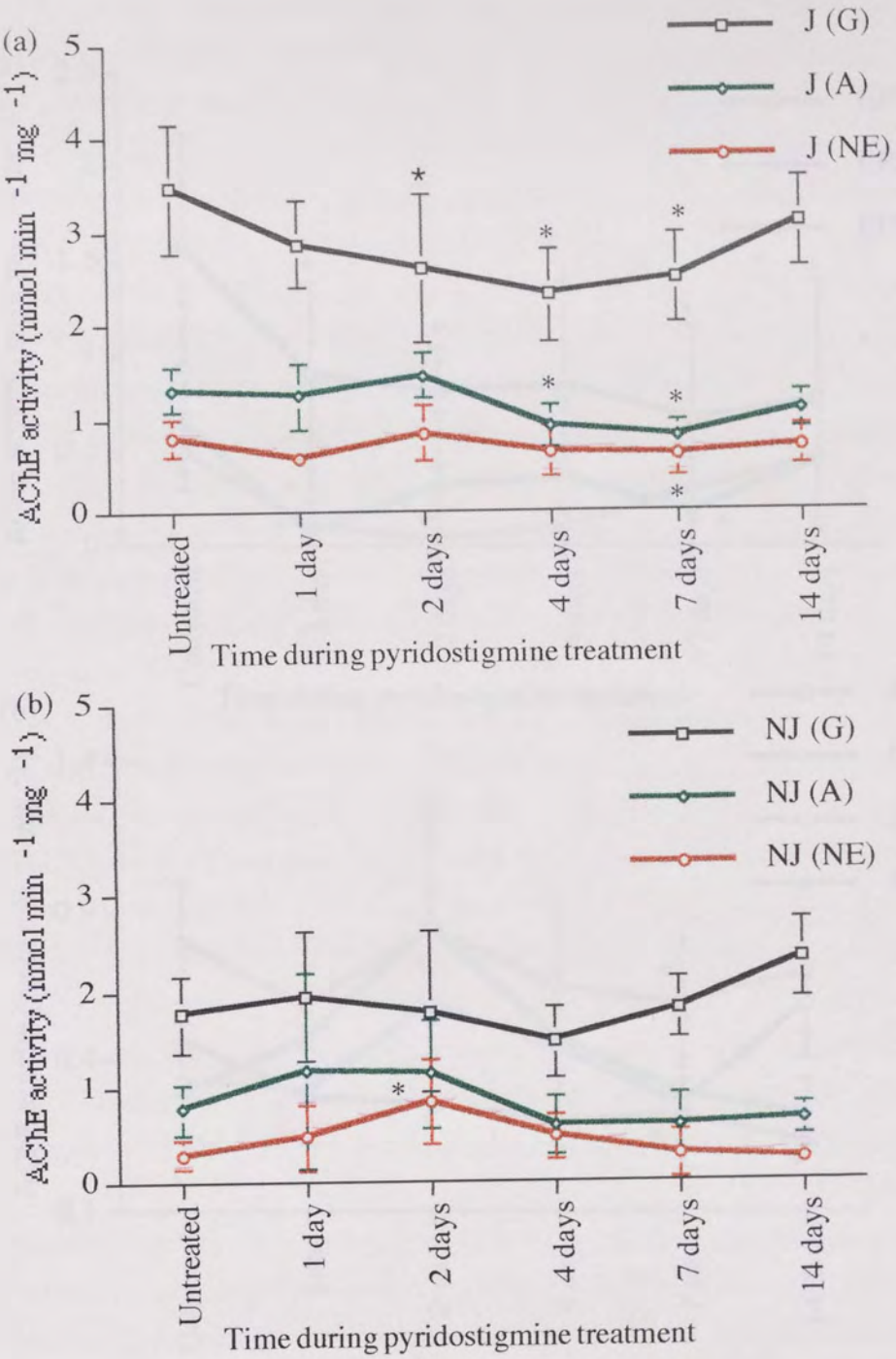

Figure 6.2: Junctional and non-junctional AChE after 11.4 nmol hr^{-1} PYR (1-14 days). Globular (G), asymmetric (A) and non-extractable (NE) AChE activity in (a) junctional (J) and (b) non-junctional (NJ) regions of mouse diaphragm. * denotes groups which differ from the untreated group: $P<0.05$ (Kruskal-Wallis multi-comparison test).

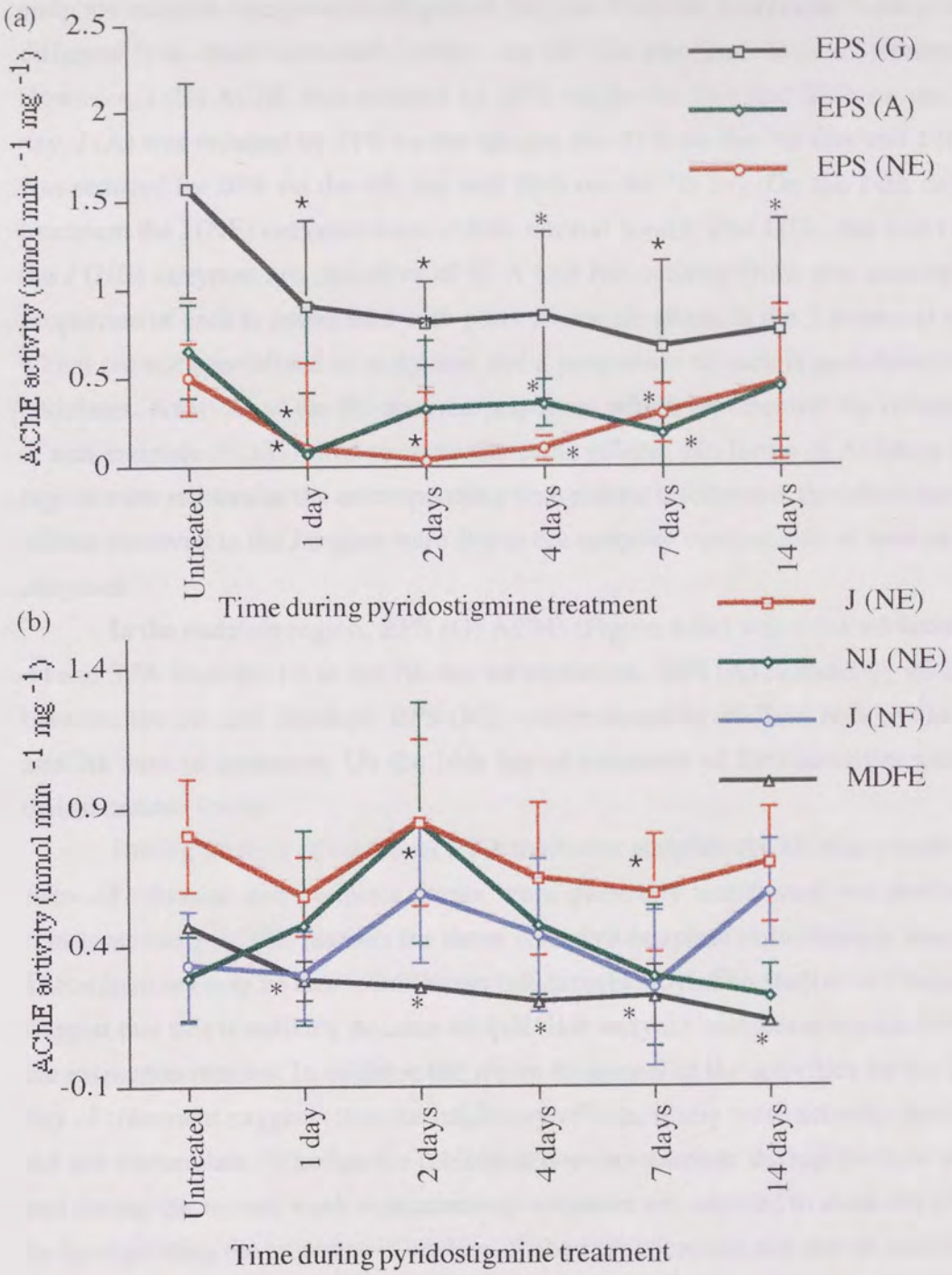

Figure 6.3: Endplate-specific AChE after 11.4 nmol hr^{-1} PYR (1-14 days). (a) Endplate-specific (EPS) globular (G), asymmetric (A) and non-extractable (NE) AChE determined by assay and (b) junctional non-extractable (J (NE)), non-junctional non-functional (NJ (NE)), junctional non-functional (J NF)) and $(MEPP)_O$-derived functional AChE (MDFE) associated with the synapse. * denote groups which differ from the untreated group: $P<0.05$ (Kruskal-Wallis multi-comparison test).

In the J region of the diaphragm, which consisted of both endplate and non-endplate enzyme components (Figure 6.2a), no J AChE molecular forms were different from their untreated levels on the 1st and 2nd days of treatment. However, J (G) AChE was reduced by 33% on the 4th day and 28% on the 7th day, J (A) was reduced by 31% on the 4th day and 31% on the 7th day and J (NE) was reduced by 20% on the 4th day and 26% on the 7th day. On the 14th day of treatment the J (NE) enzymes were at their normal levels. The J (G), the J (A) and the J (NE) enzymes are measures of G, A and NE activity from two sources : a proportion of each is associated with parts of muscle fibres in the J dissected strip which are not specialised as endplates and a proportion of each is associated with endplates. Analysis of the NJ enzyme responses which represented the responses of non-endplate AChE failed to show the same effects. No forms of AChE in this region were reduced at the corresponding time points. It followed, therefore that the effects observed in the J region were due to the endplate components of each of the enzymes.

In the endplate region, EPS (G) AChE (Figure 6.3a) was reduced between 44 and 57% from the 1st to the 7th day sof treatment. EPS (A) reduced by 45-88% between the 1st and 7th days. EPS (NE) was reduced by 40-78% betwen the 1st and 7th days of treatment. On the 14th day of treatment all EPS activities were at their untreated levels.

During 14 days of continual PYR treatment endplate AChE was selectively reduced whereas non-endplate forms were generally unaffected but displayed transient changes. The reasons for these selective endplate reductions is unclear. The reductions may be due to inhibition but decarbamoylation studies in Chapter 5 suggest that this is unlikely because no inhibitor-enzyme complexes would survive the extraction process. In addition the return to normal of the activities by the 14th day of treatment suggests that the inhibitory effects, if any were actually detected did not accumulate. Whether the inhibition does accumulate during the first week and during the second week compensatory measures are initiated to mask the effect by up-regulating the enzymes is unclear. If the reductions are not due to inhibition then alternative explanations are necessary. Localisation studies in Chapter 4 suggested that G and A forms were located in both endplate and non-endplate regions and portions in each region existed as intra- and extra-cellular pools. About 60% of each form was associated with NJ regions and 40% was EPS. Portions of NJ (G) and NJ (A) were internal and external and around half of EPS (G) and EPS (A) were internal and external. Hence, it was unlikely that PYR would selectively target and inhibit only endplate enzyme when NJ AChE is equally accessible to the drug. Also, in the event that both NJ and EPS had been inhibited but at the time the

activities were measured the drug had dissociated from the enzymes it would be unlikely that PYR would only dissociate from the NJ AChE but not from EPS AChE form due to selective binding characteristics because the EPS AChE is not known to be distinct from the NJ AChE. Further evidence against the selective inhibition theory was provided by the decarbamoylation studies in Chapter 5 which proposed that no inhibition would be detected during such studies. In addition, EPS (NE) was reduced between the 1st and 7th days of treatment but NJ (NE) was generally unaffected but transiently up-regulated on the 2nd day suggesting that the response of these enzymes to PYR was distinct.

The response of EPS AChE to PYR is therefore distinct from the response of non-endplate AChE possibly because AChE associated with endplates and non-endplates are biologically distinct and subject to different modes of regulation. The differential regulation of endplate and non-endplate AChE activity has been previously demonstrated by Younkin and Younkin (1988) who suggested that non-endplate activity was regulated by nerve-mediated muscle activity whereas endplate AChE was regulated by both nerve-mediated muscle activity and neurotrophic factors. Since PYR appears to predominantly affect endplate AChE, these effects may become manifest through the actions of neurotrophic factors although the possible involvement of muscle activity in these responses cannot completely be ruled out. The differential responses may be due to the actions of different components of muscle activity which may have been effected by PYR. As many of the structural and physiological changes after anti-ChEs originate at the neuromuscular junction (Ariens et al., 1969; Fenichel et al., 1972; Fenichel et al., 1974; Hudson et al., 1978; Kawabuchi et al., 1976; Laskowski et al., 1975; Salpeter et al., 1979), nerve-mediated muscle activity associated with these changes may mediate the effects in endplate AChE and explain the absence of a corresponding response in muscle fibres parts which are peripheral to the endplate. Also, the importance of the transient up-regulation of non-endplate AChE cannot be over-looked. Previous studies have shown that increased muscle activity is associated with increased AChE synthesis (Barnard et al., 1984) and the PYR-induced effects on muscle fibres which originate at the endplate also become manifest in other parts of muscle fibres (Ferry and Cullen, 1991). If consequences of these PYR-induced effects on muscle fibres become manifest as transient increases in muscle activity, then signals may be sent to up-regulate non-endplate AChE.

EPS (G) was demonstrated in Chapter 3 to be 40% internal precursory and processed forms (Rotundo, 1984; Lazar et al., 1984; Brockman et al., 1986) and 60% external secreted (Wilson et al., 1984) and integral sarcolemma membrane

proteins (Younkin et al., 1982). EPS (A) were 50% internal precursory and processed forms (Rotundo, 1984a; Inestrosa, 1984) and 50% external of unknown function and EPS (NE) was 90% functional A12 located in the synaptic cleft. A common feature of endplate AChE reduction was that the effect applied to all the forms, was in the region of 50-60% and occurred at some point between the 2nd and 7th day of treatment. Studies of the metabolism of AChE suggest that G1 is a precursor for higher molecular weight forms (Koenig and Vigny, 1978) and the reduction of endplate AChE may occur at the transcriptional level due to the PYR-induced down-regulation of the AChE gene associated with endplate nuclei. The origin of factors which mediate between PYR action and endplate AChE reduction is unclear. Possible mediators may include muscle activity itself (Younkin and Younkin, 1988; Newman et al., 1984) or trophic regulators; POMC peptides which are known to be released into the circulation after muscle damage and toxic stress (Rosier at al., 1977), glucocorticoids (Brank and Grubic, 1993) which are known transcriptional controllers (Muller and Renkawitz, 1991), ACh itself (Drachman et al., 1982) or a host of other substances including: diffusible substances produced by the spinal cord, brain and sciatic nerve, transferrin and neural peptides (reviewed by Oh et al., 1988).

6.2.1.3 Functionally-active AChE.

In Section 4.2.3, a relationship between the time to half amplitude of the decay phase of extra-cellular miniature endplate potentials ($T_{50\%}$ of $(MEPPs)_O$) and functionally active AChE in the synaptic cleft was established and represented as an exponential equation. It was found that this relationship could be used to predict the activity of functional AChE in the synapse by substituting $T_{50\%}$ values determined electrophysiologically into the equation. This provided an alternative assessment of functional AChE which could be compared with the functional AChE activity determined by the assay method. In addition, the relationship could also be used to make a distinction between AChE in the mouse diaphragm which was functionally and non-functionally important. Table 6.2 shows $(MEPP)_O$-derived functional enzyme (MDFE) activities which represent the predicted functional AChE activities determined electrophysiologically. Values representing the non-functional activity in the junctional region (J (NF)) are shown in Table 6.2 below the MDFE activities. These parameters are also shown graphically in Fig. 6.3b.

The MDFE activities were significantly reduced by about 40% between the 1st and 7th days of treatment. On the 14th day, the MDFE activity was reduced by 72% but this activity did not differ from the activities at any other time point during

the treatment. This suggested that the reduction in the activity of MDFE due to exposure of the system to PYR was constant from one time point to the next and there was no evidence that effects accumulate.

Despite the superficial differences, there were not found to be any significant differences between MDFE and EPS (NE) AChE at any of the time points suggesting that both represented the same AChE activity. The superficial differences were attributed to EPS (NE) activities which were found to have a high co-efficient of variation. It followed that EPS (NE) gave an indication that functional enzyme was affected by PYR treatment but the assessment of MDFE activity which was in part related to the consequences of functional enzyme reduction i.e. prolonged action of ACh on its receptor, provided a more sensitive indication of the response of functional AChE activity. The response of MDFE to PYR suggested that the reduction in synaptic AChE may last longer than predicted by EPS (NE).

The prolongation of the time course of $(MEPPs)_o$ observed during the treatment resulting from the delayed action of the ACh on its receptor suggested also that there was insufficient AChE available in the cleft to hydrolyse the neurotransmitter. At the time recordings of $(MEPPS)_o$ were made it was unlikely that any AChE-inhibitor complexes were still intact. Evidence for this was provided by experiments conducted by A. Crofts to investigate whether the prolongation of $(MEPPs)_o$ was due to the inhibition or reduction of functional AChE. The recording of $(MEPPs)_o$ was routinely conducted at 37°C at which the rate of decarbamoylation of PYR is rapid and occurs with a half-life of around 30 mins (see Chapter 5). When $(MEPPs)_o$ were recorded at two different times i.e. soon after extraction of tissues from mice, and after a delay of 1 hour, there was not found to be any significant difference between the $T_{50\%}$ values (Mann-Whitney, $P>0.1$) at the different time points. These results contradicted the expected results had functional AChE been inhibited when some prolongation of $(MEPPs)_o$ would have been expected at the earlier time point. Because PYR-inhibited AChE is known to rapidly decarbamoylate no inhibition would be expected at the later time point as almost complete decarbamoylation would have been expected by this time. This was not found to occur. The extent of $(MEPPs)_o$ prolongation at both times of assessment was found to be the same. This suggested that the prolongation of the time course of $(MEPPs)_o$ was due to a reduction in synaptic AChE during 14 days of PYR treatment as predicted by MDFE values and was not due to inhibition.

J (NF) activities obtained by the subtraction of MDFE from J (NE) which represented the component of J (NE) activity which was not involved in transmission termination,was not affected during PYR treatment. In the criteria

used to calculate EPS (NE) activity it was assumed that AChE activity found in parts of muscle fibres which were not specialised as endplates was uniformly distributed along the length of muscle fibres and the subtraction of NJ activity from J activity would give an measure of the AChE activity associated with the endplate alone. To verify this criterion a comparison was made between the J (NF) activity which represented enzyme in the J region not associated with transmission termination and NJ (NE) activity which represented the non-functional high molecular weight form of AChE found in the NJ regions. Statistically there was not found to be any significant difference between J (NF) and NJ (NE) at any of the time points during the treatment which suggested that J (NE) activity was a combination of endplate and non-endplate A12 and validated the criteria used to calculate EPS (NE).

The responses of MDFE synaptic AChE and EPS (NE) to PYR treatment suggested that the effects of PYR on the enzyme occur as early as the first day of treatment. Since the synaptic form has a slow turnover (Lazar et al., 1984; Newman et al., 1984) it is possible that this initial rapid reduction may be due to accelerated degradation. The rapid loss of synaptic AChE also occurs after denervation (Newman et al., 1984) and Younkin and Younkin (1988) proposed that the synaptic enzyme was not only regulated by the rate of synthesis but also by the rate of degradation. The loss of A12 may therefore be due to increased initial degradation possibly by factors which are released in the early stages after anti-ChEs such as Ca^{2+}-activated neutral proteases and the reduction in endplate AChE observed during the remainder of the treatment may be due to down-regulation induced by an unknown mechanism.

6.2.1.4 Endplate dimensions.

Table 6.3 shows the width (W), length (L) and width/length (W/L) ratio of endplates on days 1, 2, 4, 7 and 14 during continual administration of PYR at the rate of 11.4 nmol hr^{-1}. At each time point, the values given are means of averages of 30 endplates per hemidiaphragm (inter-hemidiaphragm variation was taken into account in the statistical evaluation of endplate data using a mixed-design MANOVA model). Figure 6.4a shows the changes in W and L and Figure 6.4b shows the changes in the W/L ratio. Figure 6.5 shows a set of histograms of the percentage of each population at each of the time points which have W/L ratios in the given ranges.

After 1 day of continual dosing with PYR the mean W/L ratio of endplates significantly increased by around 50%. This extent of deformation was maintained

Time	Width (μm) †	Length (μm) †	W/L ratio †	No.of HD No. of EP
Untreated	19.3±0.7 +	34.8±2.9 +	0.56±0.04 +	8 240
1 day	21.9±0.9*	27.7±3.0*	0.82±0.10*	5 150
2 days	21.8±1.3*	30.1±5.2*	0.75±0.11*	4 120
4 days	21.5±0.8 * +	27.1±1.8*	0.82±0.05*	5 150
7 days	23.2±1.4* +	28.4±2.6*	0.83±0.06*	4 120
14 days	21.4±0.3*	27.4±4.5*	0.85±0.07*	3 90

Table 6.3: Endplate dimensions after 11.4 nmol hr^{-1} PYR (1-14 days). The table shows the variation in endplate width, length and width/length (W/L) ratio. HD gives the no. of hemidiaphragms and EP gives the total no. of endplates. Values are means±s.d. † denotes sets with different groups (ANOVA, $P<0.05$), * denotes groups which differ from the untreated group (MANOVA, $P<0.05$) and + denotes different adjacent groups (MANOVA, $P<0.05$).

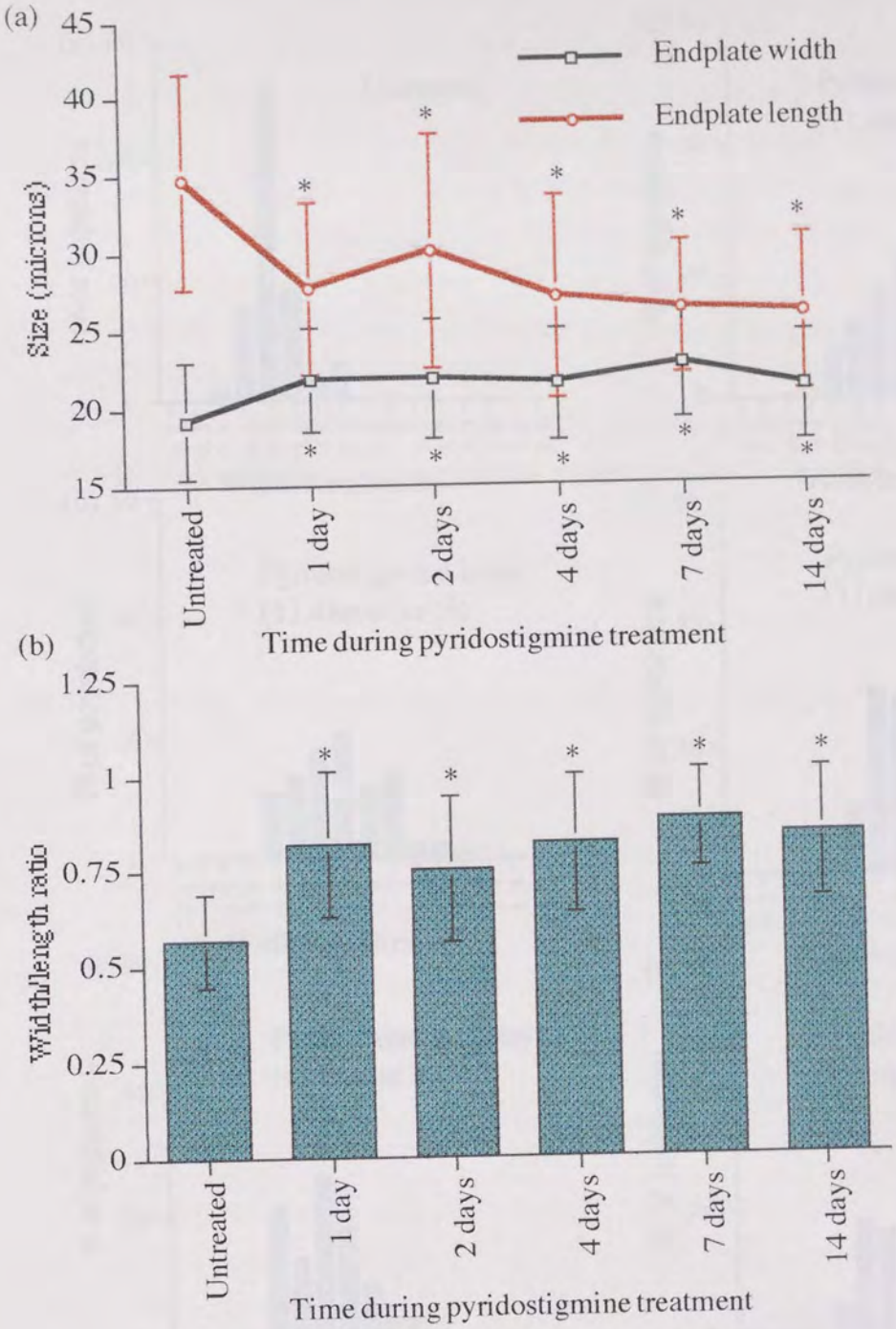

Figure 6.4: Width, length and width/length ratio of endplates after 11.4 nmol hr^{-1} PYR (1-14 days). Variation in endplate population (a)widths and lengths and (b) width/length ratios. * denotes groups which differ from the untreated group: $P<0.05$ (Kruskal-Wallis mutli-comparison test).

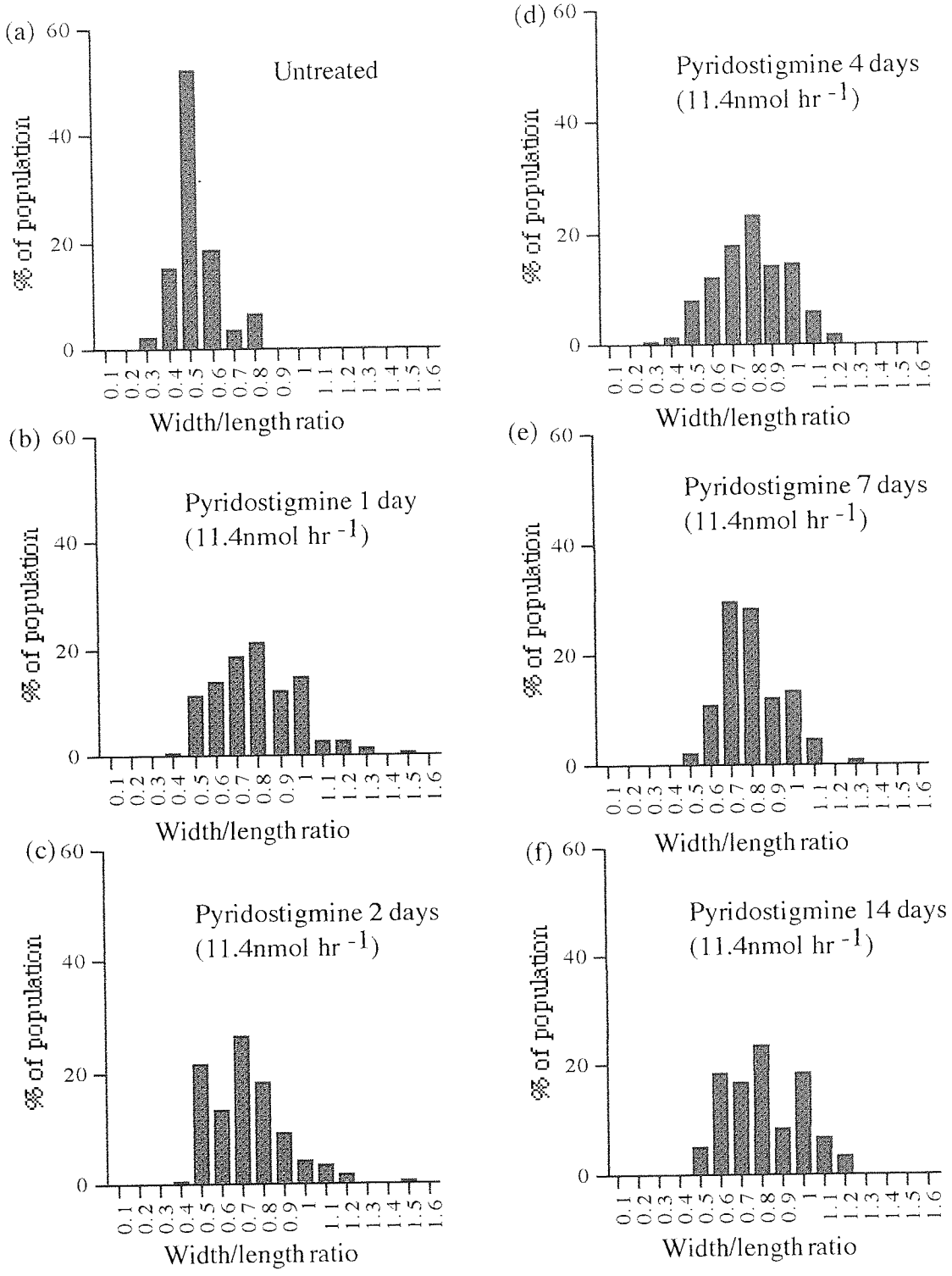

Figure 6.5: Histograms of endplates after 11.4 nmol hr^{-1} PYR (1-14 days). Percentage of endplates per population at given width/length ratios for (a) untreated, (b) 1 day, (c) 2 days, (d) 4 days, (e) 7 days and (f) 14 days.

for the entire 14 day dosing period. No progressive effects were observed as there were no differences between the ratios at each of the time points during the treatment. At each of the time points, endplate W were increased and L reduced, suggesting that endplates had become rounder due to hypercontrations. The histograms show that there was a shift in the endplate populations at each of the time points such that a higher percentage had larger ratios and a smaller percentage had ratios around the untreated mean.

Continual PYR infusion was found to rapidly induce abnormal calcium influx into endplates and alter muscle fibre morphology which was evident by the rapid deformation of endplates which occurred within 1 day of treatment. The effect persisted for the duration of the treatment and was similar to that observed after a 100 nmol kg^{-1} dose of ECO; when the populations at each time point were tested against the population treated with ECO, no significant differences were found between them (MANOVA, $P>0.05$).

6.2.2 Recovery of mouse skeletal muscle after 7 days of PYR.

6.2.2.1 Whole blood ChE.

Table 6.4 and Figure 6.6 show the recovery of whole blood ChE during a period of 14 days after mice had continually been infused with PYR at the rate of 11.4 nmol hr^{-1} for a period of 7 days. Two days after osmotic pump removal, whole blood ChE was still reduced by around 40%. Seven days later, the activity was not different from the untreated level. The value at this time point was different from the previous time point suggesting that a change in ChE activity had occurred. Between 7 and 14 days after removal of the pump a reduction occurred in the ChE activity such that it was 37% lower than the untreated level.

In Section 6.2.1.1, blood ChE was shown to be inhibited during 7 days of continual PYR treatment in the order of 30-50%. The response of blood ChE to the removal of the inhibitor from the system when the treatment was terminated was unexpected. It was unlikely that PYR persisted in the blood once the treatment had been terminated because it would be rapidly metabolised. It was unlikely also that carbamoylated ChE would still exist 2 days or 14 days after the treatment was terminated because these would rapidly decarbamoylate in the system. The reductions observed at these time points could not, therefore, be due to inhibition but may be due to down-regulation of blood ChE. The reason for the transient recovery in activity 7 days after treatment termination was unclear.

Time during treatment	N number	Whole blood ChE (μmol $min^{-1}ml^{-1}$) †	% I (Whole blood ChE)
Untreated	15	3.03 ±0.97 +	-
7 days	13	1.69* ±0.36	44.2
9 days (2 day recovery)	16	1.75* ±0.48 +	42.2
14 days (7 day recovery)	11	2.27 ±0.35 +	25.1
21 days (14 day recovery)	4	1.92 * ±0.19	36.6

Table 6.4: Whole blood ChE 2-14 days after termination of continual PYR infusion for 7 days at 11.4 nmol hr^{-1}. Values shown are means±s.d. † denotes the set has different groups (K-S ANOVA, $P<0.05$), * denotes groups which differ from the untreated group (K-S multi comparison test, $P<0.05$) and + denotes different adjacent groups (K-S multi-comparison test, $P<0.05$).

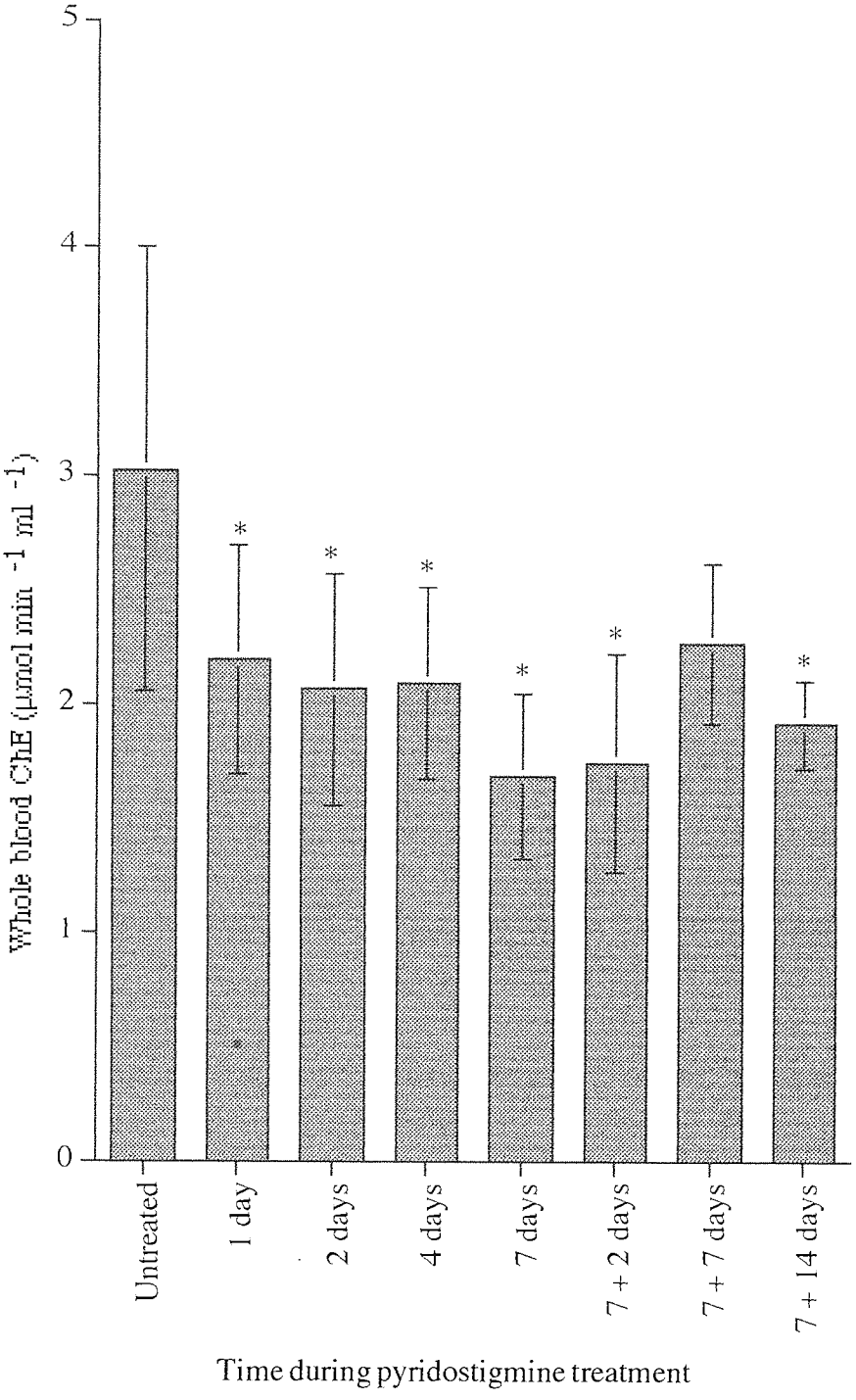

<u>Figure 6.6:</u> Whole blood ChE 2-14 days after termination of continual PYR infusion for 7 days at 11.4 nmol hr^{-1}. * denotes groups which differ from the untreated group: P<0.05 (Kruskal-Wallis multi-comparison test).

The observations made of the recovery of blood ChE following 7 days of continual PYR administration may dispute the suggestion made in Section 6.2.1.1 that the reductions seen during the actual dosing period were due to inhibition of ChE. As discussed in the section, the assay of blood was rapid and spontaneous decarbamoylation was not thought to effect the overall results. However, it is possible that some down-regulation of blood ChE may also occur (this was observed for diaphragm AChE) during the dosing period. It was unclear, therefore whether the reductions which occurred during the dosing period where due to inhibition, down-regulation or a combination of both.

6.2.2.2 Molecular forms of AChE.

Table 6.5 shows the recovery of J, NJ and EPS: G, A and NE forms of AChE during 14 days after the removal of osmotic pump which had continually infused mice with PYR for 7 days at the rate of 11.4 nmol hr^{-1}. Also shown are the MDFE activities (predicted synaptic AChE) and the J (NF) activity (non-functional component of J (NE) activity).

Figure 6.7a shows the responses of J region AChE. Two days after the removal of the 7 day pump, J (G) was still reduced by 21% but 5 days later it had exceeded the untreated level by 14%. Seven days later J (G) was normal. Two days after the removal of the pump, the activity of J (A) was lower than the untreated level by 37%. Five days later, it exceeded the untreated activity by 52%. Seven days later it exceeded the untreated activity by 25%. J (NE) however, had made a complete recovery 2 days after pump removal. Five days later, it exceeded the normal level by 71.3%. This was maintained for a further 7 days.

Figure 6.7b shows the responses of NJ region AChE. NJ (G) was normal 2 days after pump removal. Five days later it exceeded the untreated level by 57% which was maintained for a further 7 days. NJ (A) which was unaffected on the 7th day of treatment, was reduced 2 days after pump removal by 65%. Between the 2nd and 7th days after removal NJ (A) increased above the normal level by 83%. Seven days later, NJ (A) still exceeded the normal level by 58%. NJ (NE) was normal 2 days after pump removal. Five days later it exceeded the normal level by 314% and 7 days later NJ (NE) returned to normal.

Figure 6.8a shows the response of EPS AChE. EPS (G) was still reduced by 56% two days after pump removal. Five days later it had completely recovered. EPS (A) which was reduced by 71% after 7 days of PYR completely recovered 2 days after pump removal. EPS (NE) which was reduced by 40% after 7 days of PYR, completely recovered 2 days after pump removal.

Enzyme	Untreated	7 days	9 days (2 day recovery)	14 days (7 day recovery)	21 days (14 day recovery)
N number	13	9	10	6	4
J (G) †	3.48+	2.48*	2.73*+	3.93	3.91
	±0.80	±0.48	±0.64	±0.52	±0.71
J (A) †	1.29+	0.79*	0.83*+	2.01*	1.65*
	±0.31	±0.18	±0.30	±0.35	±0.14
J (NE) †	0.79+	0.59*	0.73+	1.37*	1.29*
	±0.20	±0.21	±0.36	±0.42	±0.25
NJ (G) †	1.90	1.81	1.91+	3.08*	3.16*
	±0.49	±0.32	±0.43	±0.60	±0.13
NJ (A) †	0.73	0.60	0.27+	1.41*	1.22*
	±0.30	±0.32	±0.25	±0.20	±0.14
NJ (NE) †	0.29	0.29	0.34+	1.20*+	0.39
	±0.16	±0.25	±0.36	±0.18	±0.30
EPS (G) †	1.63+	0.68*	0.71*	1.15	0.75
	±0.62	±0.48	±0.63	±0.92	±0.64
EPS (A) †	0.62+	0.19*	0.55	0.60	0.43
	±0.25	±0.28	±0.37	±0.37	±0.20
EPS (NE) †	0.50+	0.30*	0.39	0.16+	0.91
	±0.18	±0.17	±0.44	±0.40	±0.46
MDFE †	0.47+	0.22*+	0.45	0.45	0.44
	±0.04	±0.11	±0.03	±0.03	±0.00
	(NS)	(NS)	(NS)	(NS)	(NS)
J (NF) †	0.33	0.25	0.41+	0.92*	0.91*
	±0.20	±0.28	±0.32	±0.42	±0.28
	(NS)	(NS)	(NS)	(NS)	(NS)

Table 6.5: Diaphragm AChE 2-14 days after termination of continual PYR infusion for 7 days at 11.4 nmol hr^{-1}. The table shows J, NJ and EPS: G, A and NE AChE activities in nmol min^{-1} mg^{-1}. Also shown are the $(MEPP)_O$-derived functional enzyme (MDFE) and junctional non-functional AChE (J(NF)). Values shown are means±s.d. † denotes sets with different groups (K-S ANOVA, $P<0.05$), * denotes groups which differ from the untreated group and + denotes different adjacent groups (K-S multi-comparison test, $P<0.05$).

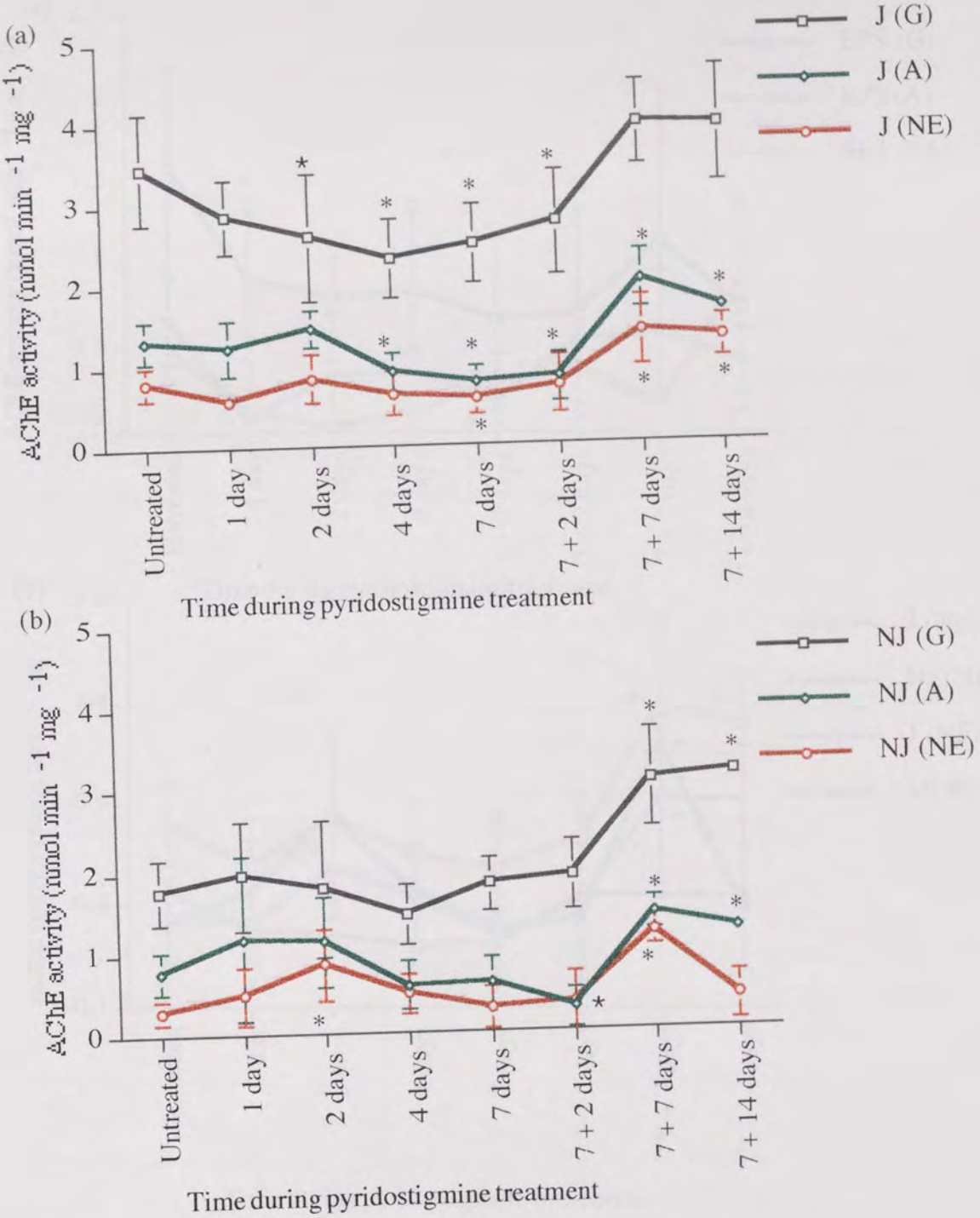

<u>Figure 6.7:</u> Junctional and non-junctional AChE 2-14 days after termination of continual PYR infusion for 7 days at 11.4 nmol hr^{-1}. Globular (G), asymmetric (A) and non-extractable (NE) AChE activity in (a) junctional (J) and (b) non-junctional (NJ) regions of mouse diaphragm. * denotes groups which differ from the untreated group: $P<0.05$ (Kruskal-Wallis multi-comparison test).

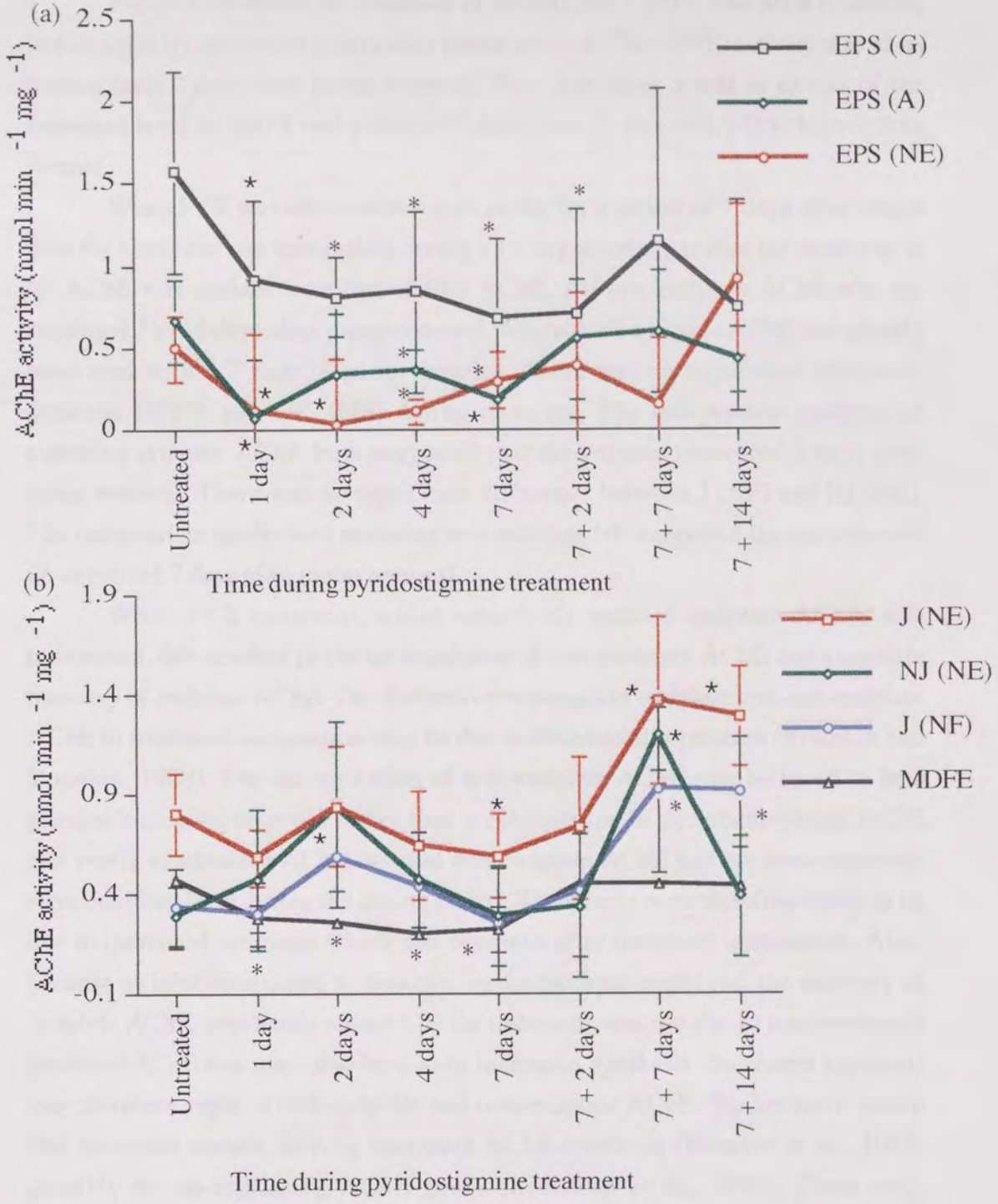

Figure 6.8: Endplate-specific AChE 2-14 days after termination of continual PYR infusion for 7 days at 11.4 nmol hr^{-1}. (a) EPS: globular (G), asymmetric (A) and non-extractable (NE) AChE, (b) junctional non-extractable (J (NE)), non-junctional non-functional (NJ (NE)), junctional non-functional (J NF)) and $(MEPP)_O$-derived functional AChE (MDFE). * denotes groups which differ from the untreated group: $P<0.05$ (Kruskal-Wallis multi-comparison test).

Figure 6.8b shows the response of MDFE and J (NF). The MDFE activity had completely recovered 2 days after pump removal. The J (NF) activity was at its normal level 2 days after pump removal. Five days later it was in excess of the untreated level by 160% and a further 7 days later it was still 143% higher than normal.

When PYR was administered continually for a period of 7 days after which time the treatment was terminated, during a 14 day recovery period the response of NJ AChE was distinct from that of EPS AChE. All non-endplate AChE was up-regulated 7 to 14 days after pump removal, whereas all endplate AChE completely recovered within 7 days of pump removal. There was no significant difference between MDFE and EPS (NE) during recovery. The independent methods of assessing synaptic AChE both suggested that the enzyme recovered 2 days after pump removal. There was no significant difference between J (NF) and NJ (NE). The independent methods of assessing non-endplate NE suggested the enzyme was up-regulated 7 days after pump removal.

When PYR treatment, which selectively reduced endplate AChE, was terminated, this resulted in the up-regulation of non-endplate AChE and complete recovery of endplate AChE. The distinctive responses of endplate and non-endplate AChE to treatment termination may be due to differential regulation (Younkin and Younkin, 1988). The up-regulation of non-endplate AChE was believed to be a genuine biological response rather than a combination of decarbamoylated AChE and newly synthesised AChE because non-endplate AChE had not been measured at an inhibited level during the dosing period. The effects were therefore likely to be due to increased synthesis which had occurred after treatment termination. Also, because no inhibition could be detected by the methods employed, the recovery of endplate AChE, previously reduced by the treatment, was not due to reactivation of inhibited AChE and may also be due to increased synthesis. Increased synthesis may therefore apply to both endplate and non-endplate AChE. Studies have shown that increased muscle activity increases AChE synthesis (Barnard et al., 1984) possibly by up-regulating AChE genes (Sveistrup et al., 1995). There was, however, no direct evidence to suggest that muscle activity had increased after treatment termination as $(MEPPs)_0$ were normal (A. Crofts, unpublished) although the effects on AChE activity may be due to a component of muscle activity which was not investigated in this study.

6.2.2.3 Endplate dimensions.

Table 6.6 shows the recovery of endplate widths (W), lengths (L) and width/length (W/L) ratios during 14 days after removal of pumps which had continually administered PYR for 7 days at the rate of 11.4 nmol hr^{-1}. Figure 6.9a shows the response of W and L and Figure 6.9b shows the variation in the W/L ratios. Figure 6.10 shows histograms of the percentage of each population with ratios within the shown ranges at the various recovery time points.

When the W/L ratios were assessed 2 days, 7 days and 14 days into the recovery period, they were still larger than the untreated ratio by 27-37%. There was not found to be any differences between the ratio measured on the 7th day of treatment and any of the time points during the recovery period. Hence, despite the observed trend that there was some improvement in the ratio during the recovery period, statistical analysis (MANOVA) indicated that the groups were not different and therefore indicated that no substantial recovery was observed in this study. It is possible that the endplates do recover at a slow rate during the recovery period, there was some improvement in the W at the 14 day recovery time point, although this could not be substantiated by this study and would require further investigation.

Hence, when PYR was administered continually for 7 days and the treatment was terminated for a period of 14 days, at the end of the recovery period the W/L ratios were still higher than in untreated tissues suggesting that during the 14 day recovery period, hypercontrations in muscle fibres were still occurring in the absence of PYR and endplates were still deformed although some recovery may occur at a slow rate. Since PYR treatment had been terminated, it was unlikely that any drug persisted in the system and synaptic AChE recovered rapidly suggesting that the action of ACh on its post-synaptic receptors may no longer be prolonged and the hypercontractions may not be due enzyme inhibition. The extent of endplate deformation induced by continual PYR infusion was equivalent to that after a single necrotising dose of 500 nmol kg^{-1} ECO. Both treatments increased the W/L ratio by around 50%. Endplate shape after ECO recovered rapidly: 7 days after the dose, W/L ratios were normal, whereas endplate shape after PYR recovered slowly: 14 days after the last day of treatment the W/L ratio was still increased by 27%. Hence, continual long-term, low dosing with PYR has a longer lasting effect on endplate morphology than a single necrotising dose of OP suggesting that the mechanism by which muscle fibres recover after anti-ChEs does not operate as effectively after long-term exposure and the associated myopathy is more persistent. The complete

Time	Width (μm) †	Length (μm) †	W/L ratio †	No. of HD No. of EP
Untreated	19.3±0.7 +	34.8±2.9 +	0.56±0.04 +	8 240
7 days	23.2±1.4* +	28.4±2.6* +	0.83±0.06*	4 120
9 days (2 day recovery)	27.5±2.1* +	36.9±4.2	0.76±0.05*	5 150
14 days (7 day recovery)	24.1±0.3* +	34.0±1.3	0.72±0.03*	3 90
21 days (14 day recovery)	21.5±4.0*	31.3±5.8*	0.71±0.18*	3 90

Table 6.6: Endplate dimensions 2-14 days after termination of continual PYR infusion for 7 days at 11.4 nmol hr^{-1}. The table shows endplate width, length and width/length (W/L) ratio. HD gives the no. of hemidiaphragms and EP gives the total no. of endplates. Values are means±s.d. † denotes sets with different groups (ANOVA, $P<0.05$), * denotes groups which differ from the untreated group (MANOVA, $P<0.05$) and + denotes different adjacent groups (MANOVA, $P<0.05$).

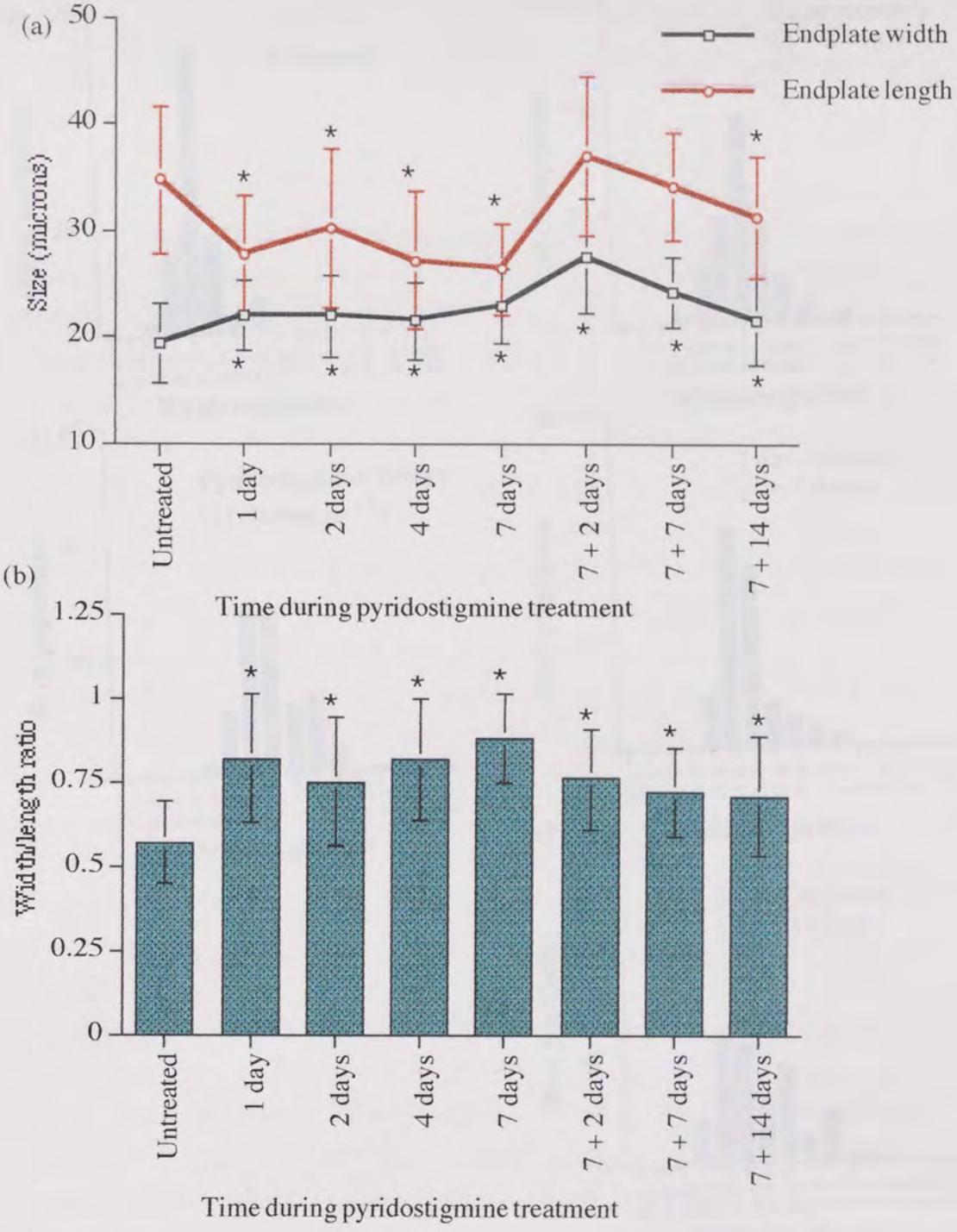

Figure 6.9: Width, length and width/length ratio of endplates 2-14 days after termination of continual PYR infusion for 7 days at 11.4 nmol hr^{-1}. Variation in endplate population (a) widths and lengths and (b) width/length ratio. * denotes groups which differ from the untreated group: $P<0.05$ (MANOVA).

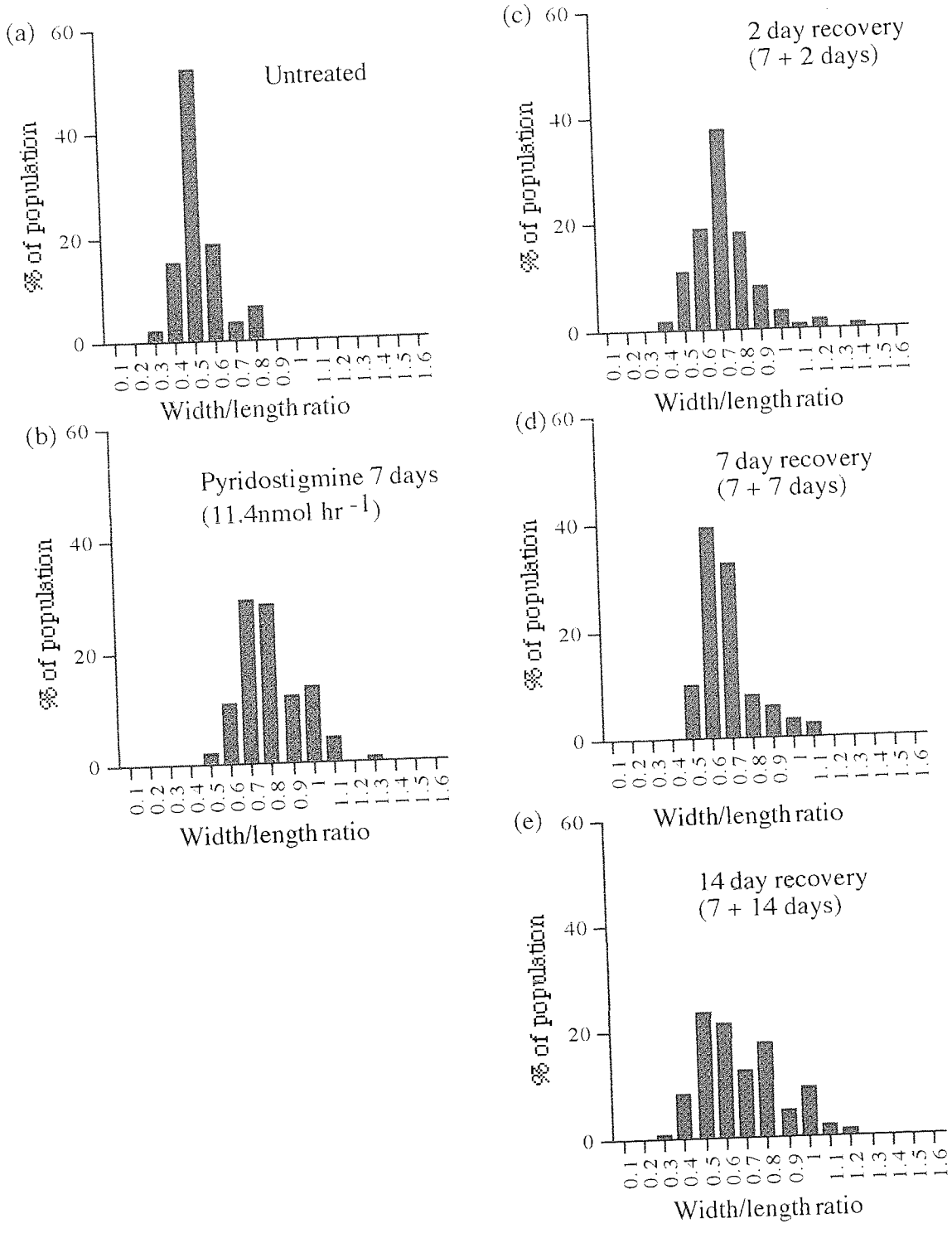

Figure 6.10: Histograms of endplates 2-14 days after termination of continual PYR infusion for 7 days at 11.4 nmol hr^{-1}. Percentage of endplates per population at given width/length ratios for (a) untreated, (b) 7 days of PYR, (c) 2 day recovery, (d) 7 day recovery and (e) 14 day recovery.

recovery of muscle fibres after 7 days of PYR takes longer than the time allowed for this study.

6.2.3 Pre-treatment with PYR as protection against OP toxicity.

6.2.3.1 Molecular forms of AChE.

PYR was administered continually for a period of 4 days, the treatment was discontinued by removing pumps and immediately giving a single subcutaneous injection of ECO was administered at 500 nmol kg^{-1}. PYR was administered for a pre-treatment period during which there were no observed increases in the latency of action potentials i.e. increased jitter (A. Crofts, unpublished; Kelly et al., 1990). This was to ensure that the pre-treatment was administered at a low and generally sign-free dose. Five days after the ECO injection, the various AChE fractions were measured and a comparison was made with AChE levels when only an ECO injection was given in the absence of any pre-treatment with PYR (see Table 6.7 and Figure 6.11). The aim of this experiment was to see if pre-treatment with PYR protected against the effects of ECO 5 days after it was administered.

Five days after ECO alone, J (G) activity was normal but after PYR pre-treatment, it was reduced by 35%. J (A) activity was normal 5 days after ECO alone and after PYR pre-treatment. J (NE) activity was reduced by 36% 5 days after ECO alone and after PYR pre-treatment. No NJ forms were affected 5 days after ECO alone or after PYR treatment. EPS (G) and EPS (A) activities which were normal 5 day after ECO alone, were reduced by 80% and 60% respectively after PYR pre-treatment. EPS (NE) which represented synaptic AChE was reduced by 48% after ECO alone and 70% after PYR pre-treatment.

MDFE activity, which gave an indication of functional synaptic AChE by an alternative method to assay, was reduced by 40% five days after ECO alone. Pre-treatment with PYR did not prevent this and the functional enzyme which was still reduced by 34%. There was not found to be any significant difference between the activities of MDFE and EPS (NE) after ECO treatment alone or after ECO and PYR pre-treatment. J (NF) activity which represented the non-functional component of the J (NE) fraction was not different from the untreated level 5 days after ECO alone or after PYR pre-treatment. There was not found to be any significant difference between the J (NF) and NJ (NE) activities which suggested that neither ECO alone nor ECO and PYR treatment affected the activity non-endplate A12.

Pre-treatment with PYR before ECO intoxication, did not effect the response of non-endplate AChE 5 days after ECO. However, whereas only

Enzyme	Untreated	ECO (500nmol kg^{-1}) 5 days	Pyridostigmine (4 days) + ECO (500nmol kg^{-1}) 5 days
N	13	8	4
J (G) †	3.48	3.30+	2.25*
	±0.80	±0.61	±0.25
J (A)	1.29	1.05	1.20
	±0.31	±0.37	±0.05
J (NE) †	0.79+	0.51*	0.54*
	±0.20	±0.20	±0.11
NJ (G)	1.90	1.95	1.95
	±0.49	±0.26	±0.16
NJ (A)	0.73	0.65	0.99
	±0.30	±0.21	±0.09
NJ (NE)	0.29	0.25	0.39
	±0.16	±0.12	±0.07
EPS (G) †	1.63	1.36+	0.31*
	±0.62	±0.70	±0.16
EPS (A) †	0.62	0.40+	0.21*
	±0.25	±0.26	±0.11
EPS (NE) †	0.50+	0.26*	0.15*
	±0.18	±0.14	±0.07
MDFE †	0.47+	0.28*	0.31*
	±0.04	±0.08	±0.02
	(NS)	(NS)	(NS)
J (NF)	0.33	0.25	0.29
	±0.20	±0.26	±0.05\
	(NS)	(NS)	(NS)

Table 6.7: AChE in untreated diaphragms, 5 days after 500 nmol kg^{-1} ECO and 5 days after 500 nmol kg^{-1} ECO with 4 days of pre-treatment with PYR 11.4 nmol hr^{-1}. J, NJ and EPS: G, A and NE AChE and MDFE and J (NF) activities in nmol min^{-1} mg^{-1}. All values shown are means ± s.d. † denotes sets with different groups (K-S ANOVA, $P<0.05$), * denotes groups which differ from the untreated group (K-S multi-comparison test, $P<0.05$) and + denotes different adjacent groups (K-S multi-comparison test, $P<0.05$).

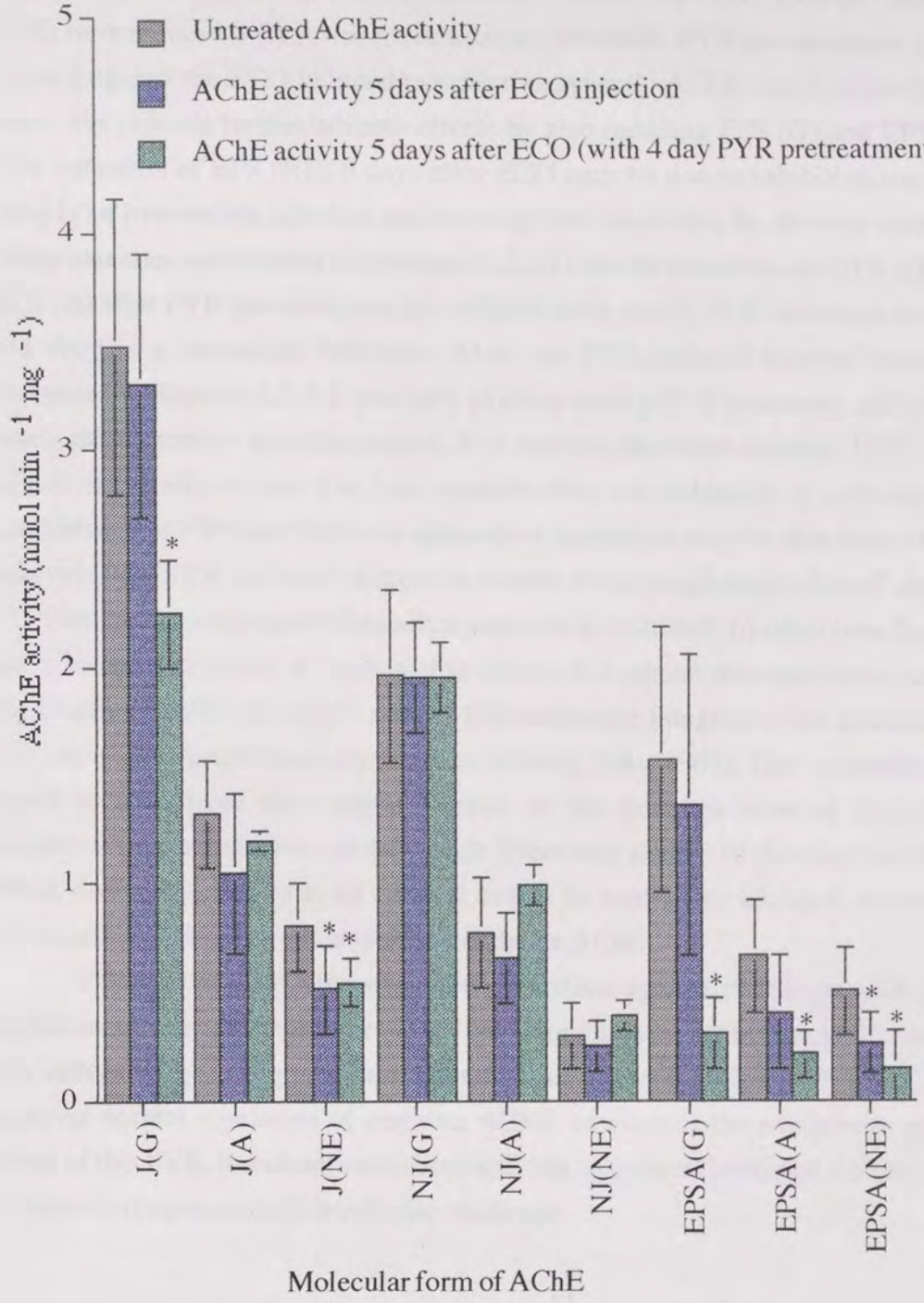

Figure 6.11: AChE in untreated diaphragms, 5 days after 500 nmol kg^{-1} ECO and 5 days after 500 nmol kg^{-1} ECO with 4 days of pre-treatment with PYR 11.4 nmol hr^{-1} . * denotes groups which differ from the untreated group: $P<0.05$ (Kruskal-Wallis multi-comparison test).

synaptic AChE was reduced 5 days after ECO alone, EPS (G), EPS (A) and EPS (NE) were reduced if PYR was given as a pre-treatment. PYR pre-treatment did not protect against the ECO-induced reduction in synaptic AChE seen 5 days after the dose, but induced further adverse effects by also reducing EPS (G) and EPS (A). The reduction of EPS (NE) 5 days after ECO may be due to inhibition since the drug is an irreversible inhibitor and recovery can occur only by *de novo* synthesis or spontaneous reactivation (see section 4.2.2.2) but the reductions in EPS (G) and EPS (A) after PYR pre-treatment are unlikely to be due to PYR inhibition because the drug is a reversible inhibitor. Also, the PYR-induced enzyme reduction discussed in Section 6.2.1.2 was only evident during PYR treatment and ceased when the treatment was terminated. It is unclear therefore whether PYR alone causes these effects and it is also possible that the reduction is induced by a combination of PYR and ECO. An alternative hypothesis may be that these effects originate from PYR-induced changes in muscle fibre morphology. After 7 days of PYR treatment, endplate deformation persisted for at least 14 days (see Section 6.2.2.3) and the extent of deformation during this period was equivalent to that observed after a 300 nmol kg^{-1} dose of ECO when the integrity of the sarcolemma was lost and the membrane was found to be leaky (Das, 1989). This myopathy was found to stem from the endplate hence, at the time the dose of ECO was administered, the membrane of the muscle fibres may already be damaged and ECO which does not normally enter the cell due to its quaternary nitrogen, can easily access and inhibit intra-cellular pools of endplate AChE.

PYR did not offer the expected protection against challenge with ECO despite protecting target sites for the OP compound in a reversible nature because it may induce long-lasting muscle myopathy and in combination with ECO, may upset the normal regulation of endplate AChE. In view of the complexity of the action of this PYR, it was not considered suitable to protect functional AChE in the synaptic cleft against a high level toxic challenge.

6.2.3.2 Endplate dimensions.

Table 6.8 shows the dimensions of endplates 5 days after the administration of ECO given as an acute dose at 500 nmol kg^{-1} and 5 days after ECO when PYR was given as a pre-treatment for 4 days. Figure 6.12(a) show endplate W and L and Figure 6.12(b) shows endplate W/L ratios. Figure 6.13 shows the percentage of each population of endplates assessed with W/L ratios within the given ranges.

When the dimensions of endplates were assessed after 5 days, W were still increased by 15%, L were decreased by 15% and the W/L ratio was higher than normal by 35%. If PYR was given as a pre-treatment for 4 days, then the W were still longer by 12%, the L were shorter by 13% and the W/L ratio was higher than normal by 28%. There were no differences between ECO treated and PYR pre-treated ECO treated W, L and W/L ratios after 5 days suggesting that PYR did not greatly improve ECO-induced myopathy.

Pre-treatment with PYR did not successfully protect the diaphragm from the anti-ChE induced myopathy caused by ECO. Hypercontrations in muscle fibres due to the influx of Ca^{2+} ions still occurred as endplates were still observed to be rounded. Since PYR administered alone induced rapid myopathy which persisted long after PYR treatment was terminated, it was not expected that PYR would prevent the distortion of endplates induced by ECO. Hence, PYR pre-treatment neither protected against nor enhanced ECO-induced myopathy.

6.3. Summary.

During 14 days of continual PYR treatment, whole blood ChE was constantly and not progressively inhibited between 30 and 50% which was equivalent to inhibition after 25 nmol kg^{-1} ECO. Hence, blood ChE indicated that during the treatment PYR was continually administered at a low dose. PYR did not generally affect non-endplate AChE, other than transiently up-regulating its activity but endplate G, A and NE AChE was reduced between 2 and 7 days by around 50-60%. The responses were probably not due to inhibition due to rapid decarbamoylation rates and were unlikely to be due to selective inhibition because all forms of AChE are equally susceptible. The response of endplate AChE was distinct from non-endplate AChE suggesting that the enzymes are biologically distinct and regulated by different mechanisms. The lack of response of non-endplate AChE which is regulated by muscle activity but the reduction in endplate AChE which is regulated by both muscle activity and neurotrophic factors suggests that the effects on endplate AChE may be due to neurotrophic regulators.

Time	Width (μm) †	Length (μm) †	W/L Ratio †	No. of HD No. of EP
Untreated	19.3±0.7 +	34.8±2.9 +	0.56±0.04 +	8 240
5 days ECO (500nmol kg^{-1})	22.2±1.1* +	29.5±2.3*	0.77±0.07*	5 150
4 days PYRIDO + 5 days ECO (500nmol kg^{-1})	21.7±2.8	30.2±0.7*	0.74±0.10*	4 120

Table 6.8: Endplate dimensions 5 days after 500 nmol kg^{-1} ECO and 5 days after 500 nmol kg^{-1} ECO with 4 days of pre-treatment with PYR 11.4 nmol hr^{-1}. The table shows endplate width, length and width/length (W/L) ratio. HD gives the no. of hemidiaphragms and EP gives the total no. of endplates. Values are means±s.d. † denotes sets with different groups (ANOVA, $P<0.05$), * denotes groups which differ from the untreated group (MANOVA, $P<0.05$) ans + denotes different adjacent groups (MANOVA, $P<0.05$).

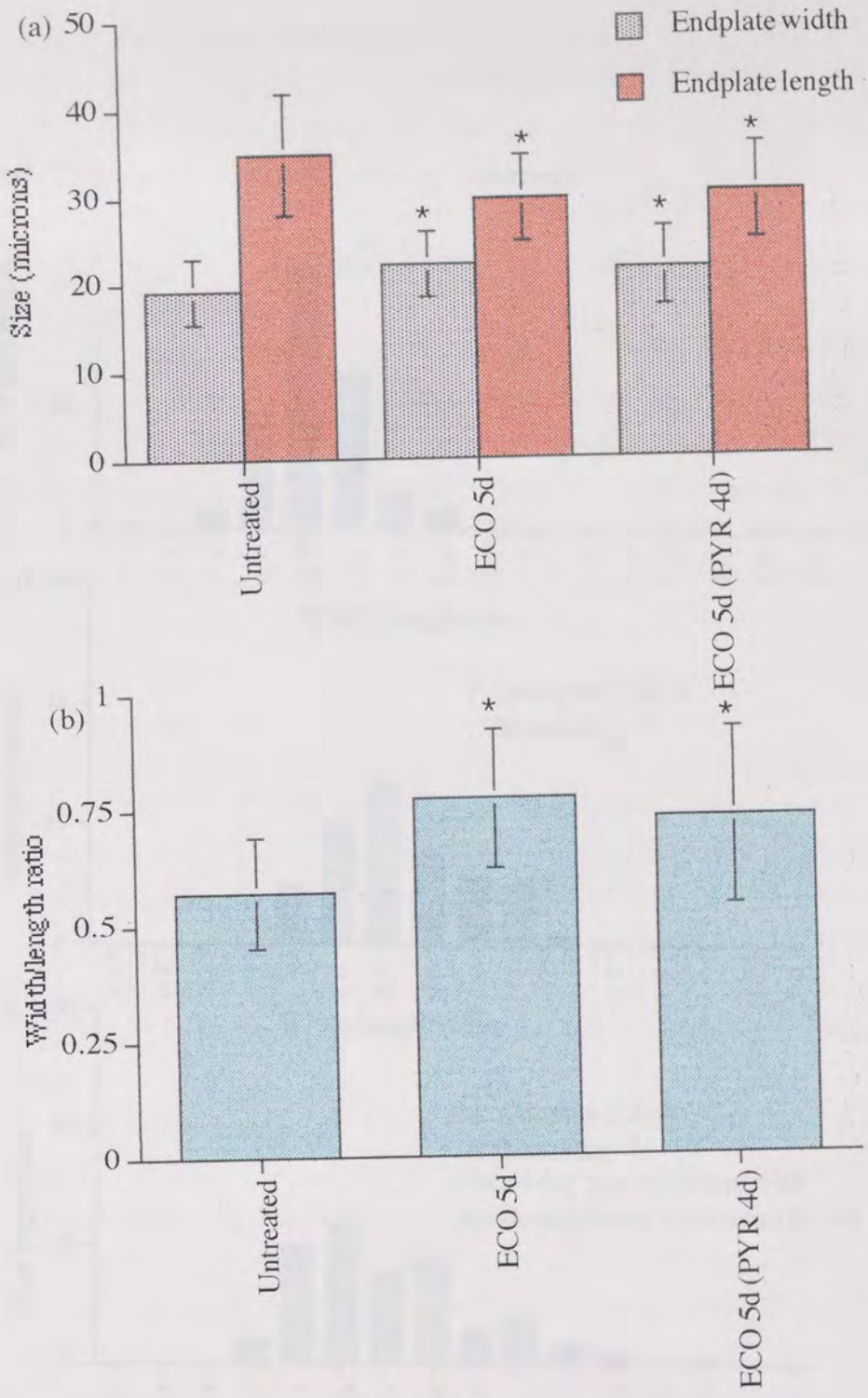

Figure 6.12: Width, length and width/length ratio of untreated endplates, 5 days after 500 nmol kg^{-1} ECO and 5 days after 500 nmol kg^{-1} ECO with 4 days of pre-treatment with PYR 11.4 nmol hr^{-1}. Shown are (a) widths and lengths and (b) width/length ratios. * denotes groups which differ from the untreated group: $P<0.05$ (MANOVA).

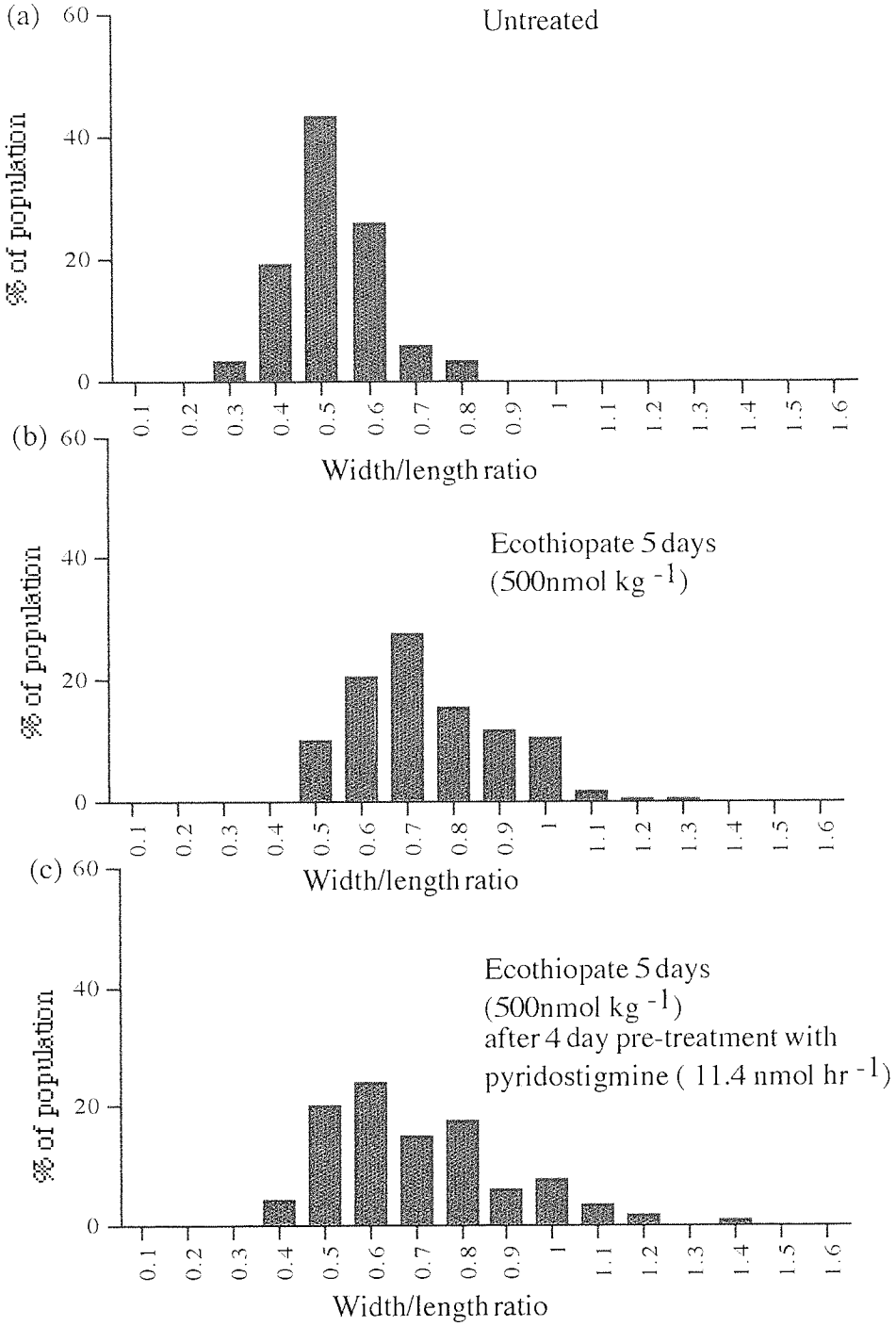

Figure 6.13: Histograms of untreated endplates, 5 days after 500 nmol kg^{-1} ECO and 5 days after 500 nmol kg^{-1} ECO with 4 days of pre-treatment with PYR 11.4 nmol hr^{-1}. Percentage of endplates per population at given width/length ratios for (a) untreated, (b) 5 days after ECO 500 nmol kg^{-1} and (c) 5 days after ECO with 4 days of PYR pre-treatment.

Alternatively, different components of muscle activity may be responsible for the selective responses and the reduction in endplate AChE may arise from PYR-induced structural and physiological changes at the neuromuscular junction. The transient up-regulation of non-endplate AChE may due to PYR-induced effects which have spread to non-endplate parts of muscle fibres. The response of the enzyme suggests that a component of muscle activity acting in the non-endplate region may have transiently increased.

Studies of $(MEPP)_o$ prolongation supported the theory that the reduction in AChE activity was not due to inhibition but due to genuine reductions. MDFE activities were found to better represent the response of synaptic AChE than EPS (NE) and suggested that PYR-induced effects may be more persistent. The initial rapid loss of synaptic AChE may not be due to down-regulation because this enzyme has a slower turnover rate than its precursors, but may be due to increased degradation mediated by proteases released soon after anti-ChE treatment. Since both the synaptic AChE and its precursor forms were also reduced during the remainder of the treatment, this suggested that endplate AChE genes may be down-regulated. The mechanism by which this occurs is unknown but may involve muscle activity, ACh itself, POMC peptides, glucocorticoids and a host of other factors which have been associated with AChE regulation. $(MEPPs)_o$-derived data validated the criteria for calculating EPS (NE) activity and indicated that J (NE) activity consisted of endplate and non-endplate components. Endplates were deformed within 1 day of PYR treatment and persisted for the duration of the treatment. The extent of deformation corresponded to that after 100 nmol kg^{-1} ECO.

After 7 days of PYR, blood ChE was still reduced 2 days after treatment was ceased, normal 5 days later and reduced a further 7 days later suggesting that it may be down-regulated. During the 14 day recovery period, all non-endplate AChE was visibly up-regulated whereas EPS (G) completely recovered within 7 days and EPS (A), EPS (NE) and MDFE recovered within 2 days. Non-endplate and endplate AChE displayed selective responses to treatment termination which may be due to differential regulation and PYR-induced endplate AChE reduction was only evident during treatment and not evident when the treatment was terminated. The up-regulation of non-endplate AChE was thought to be a genuine response and the recovery of endplate AChE was not thought to occur by reactivation of previously inhibited AChE. Both non-endplate and endplate AChE displayed increased synthesis after treatment termination which may be mediated by a component of muscle activity. Endplate dimensions did not substantially recover during a 14 day period after the treatment but some slight recover may occur and complete recovery

is likely to take longer than the time allowed in the study. Hypercontractions persisted even when cholinergic transmission was apparently normal. The myopathy induced by long-term, low doses of PYR was found to be more persistent than that after a single necrotising dose of ECO which was recovered within 7 days. Hence, long term myopathy was a consequence of long-term PYR exposure which was in contrast to the short-term myopathy induced by incidental exposure to a large dose of OP.

Pre-treatment with PYR for 4 days before a exposure to a large dose of ECO did not affect the response of non-endplate AChE 5 days after ECO. However, the pre-treatment heightened the response of endplate AChE to ECO. After ECO alone, only EPS (NE) was reduced. After PYR and ECO all EPS AChE was reduced. PYR did not therefore protect against but enhanced the effect of the OP. It was unclear whether the AChE reductions where due to PYR-induced or (PYR+ECO)-induced down-regulation or due to inhibitory effects of ECO facilitated by alterations to the sarcolemma induced by PYR. PYR therefore was not useful as a pre-treatment because it induced a long-lasting myopathy and had a complex action on endplate AChE. PYR pre-treatment neither protected nor enhanced ECO-induced myopathy.

CHAPTER 7

LONG-TERM EFFECTS OF LOW DOSES OF PHYSOSTIGMINE ON MOUSE SKELETAL MUSCLE

7.1 Introduction.

In this section, a similar set of experiments were carried out to those using PYR, using the natural alkaloid CB compound physostigmine (PHY). PHY is routinely used to treat a variety of conditions including: the reduction of intraocular pressure in glaucoma, to treat muscle weakness in myasthenia gravis, to counteract atropine coma and scopolamine delirium and as an antidote against hallucinogenic agents. Unlike PYR which is a quaternary compound, PHY is a tertiary compound which can penetrate the blood-brain and exert effects on the central nervous system. The exact experimental protocol was followed as for PYR and the effects of the drugs compared. PHY was administered by an osmotic pump and an assessment was made of blood ChE, diaphragm AChE, synaptic AChE, endplate deformation and electrophysiological responses (conducted by A. Crofts) with the following objectives in mind:

(a) To assess the effects on days 1, 2, 4, 7 and 14 after the implantation of an osmotic pump which continually administered PHY at the rate of 14 nmole hr^{-1} during a 2 week period.
(b) To investigate whether there was any recovery 2, 6 and 14 days after a pump which has administered PHY for 7 days was removed and treatment terminated.
(c) To investigate whether PHY administered at 14 nmol hr^{-1} for 2 days by the osmotic pump successfully protected against the inhibitory effects of a 500 nmol kg^{-1} dose of ECO administered at the end of the pre-treatment period and assessed 5 days later.

7.2 Results and discussion.

7.2.1 Long-term effects of PHY administered for 14 days on mouse skeletal muscle.

7.2.1.1 Whole blood ChE.

Table 7.1 and Figure 7.1 show whole blood ChE during 2 weeks of PHY treatment given at the rate of 14 nmol hr^{-1}. During the first 7 days of treatment, blood ChE was constantly and not progressively inhibited between 60-70%. The extent of inhibition was similar to that after a 50 nmol kg^{-1} dose of ECO, but greater than that after PYR infusion at 11.4 nmol hr^{-1}. On the 14th day there was a

Time during treatment	N	Blood ChE activity † (μmol min^{-1}ml^{-1})	% Inhibition
Untreated	10	3.03 ±0.97 +	-
1 day	6	0.94* ±0.37	69.0
2 days	6	1.16* ±0.53	61.7
4 days	6	0.88* ±0.13 +	71.0
7 days	9	1.07* ±0.14	64.7
14 days	4	2.20 ±0.89	27.4

Table 7.1: Whole blood ChE after 14 nmol kg^{-1} PHY (1-14 days). Values shown are means±s.d. Activity values are in μmol min^{-1}ml^{-1}. † denotes the set has different groups (K-S ANOVA, $P<0.05$), * denotes groups which differ from the untreated group (K-S multi-comparison test, $P<0.05$) and + denotes different adjacent groups (K-S multi-comparison test, $P<0.05$).

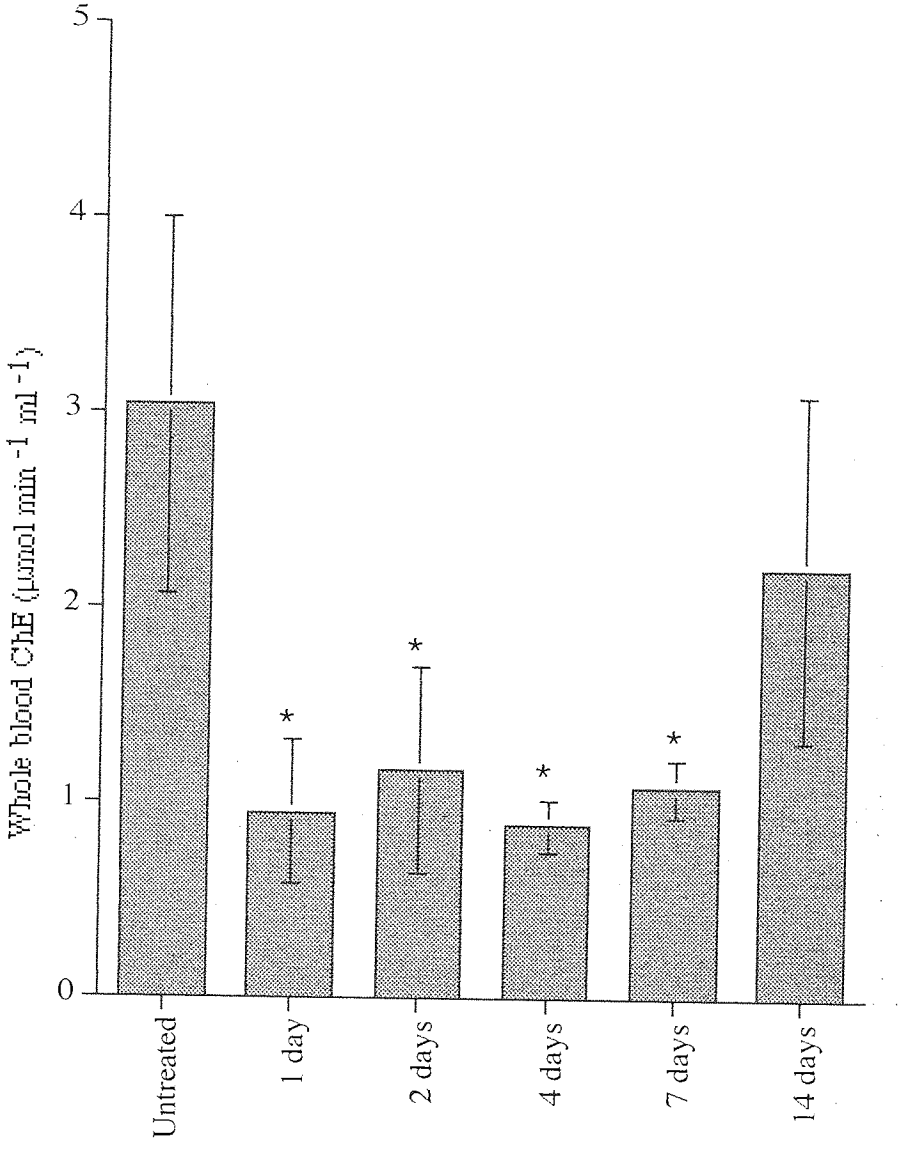

Figure 7.1: Whole blood ChE after 14 nmol hr^{-1} PHY (1-14 days). * denotes groups which differ from the untreated group: $P<0.05$ (Kruskal-Wallis multi-comparison test).

increase in ChE activity such that it was only 30% inhibited. This effect was also observed after 21 days of repetitive dosing with PYR but not after continual infusion with PYR. Similar effects were observed when PHY was administered by osmotic pump at a level which caused around 30% inhibition of blood erythrocyte AChE in guinea pigs as reported by J. Wetherell (1994) who observed that after 13 days of continual drug administration, there was a reduction in the level of inhibition.

Because samples were rapidly removed from mice and assayed quickly, it was assumed that very little if any spontaneous decarbamoylation occurred and the reductions in ChE activity were due to inhibition. Since the method employed to study blood ChE responses to anti-ChE treatment in these experiments is a rapid one, designed only to give an indication of the level of inhibition at various time points during drug treatment, it does not distinguish between the effects on plasma ChE, which is predominantly BChE, and on erythrocyte AChE. It was therefore not possible in this study to determine whether the reduction in inhibition observed after 14 days of PHY was due to up-regulation of plasma ChE or erythrocyte AChE. However, J. Wetherall (1994) reported that the reduction in the inhibition of guinea pig AChE after 13 days of PHY was exclusively observed in erythrocyte AChE and was not observed in plasma ChE. This would suggest that continual administration of PHY results in the up-regulation of erythrocyte AChE.

7.2.1.2 Molecular forms of AChE.

Table 7.2 shows the activities of diaphragm AChE in J and NJ regions (also see Figure 7.2) and EPS AChE activity (also see Figure 7.3a) at various time intervals during 14 days of continual infusion of mice with 14 nmol hr^{-1} PHY. Also shown are MDFE and J (NF) activities (also see Figure 7.3b). The untreated values include the activities obtained from mice which were implanted with pumps containing 0.9% saline only (see Section 6.2.1.2 ans Appendix A.6).

J (G) was reduced by around 40% during the first 7 days of treatment, but normal on the 14th day. J (G) and J (A) molecular forms of AChE were measured at their normal levels throughout the treatment. NJ (G) was reduced by around 20% on the 4th day of treatment and returned to normal. NJ (A) was measured at the untreated level throughout the treatment and no changes were measured in the activity of NJ (NE). EPS (G) was found to be reduced by around 60% for the first 7 days of treatment and normal on the 14th day. EPS (A) was reduced by around 50% after 1 and 4 days of treatment and EPS (NE) was only reduced on the 4th day

Region	Un-treated	1 day	2 days	4 days	7 days	14 days
N	13	4	4	4	6	7
J (G) †	3.48+	2.17*	2.24*	2.03*	2.31*+	3.60
	±0.80	±0.12	±0.22	±0.34	±0.52	±0.88
J (A)	1.29	1.18	1.08	0.94	1.06	1.55
	±0.31	±0.09	±0.30	±0.10	±0.38	±0.46
J (NE)	0.79	0.75	0.70	0.48	0.64	1.07
	±0.20	±0.13	±0.25	±0.18	±0.33	±0.51
NJ (G) †	1.90	1.54	1.81	1.32 *	1.88	2.38
	±0.49	±0.22	±0.35	±0.31	±0.29	±0.57
NJ (A)	0.73	0.84	0.85	0.80	0.79	1.16
	±0.30	±0.03	±0.03	±0.16	±0.15	±0.38
NJ (NE)	0.29	0.35	0.38	0.27	0.26	0.42
	±0.16	±0.04	±0.22	±0.08	±0.07	±0.38
EPS (G) †	1.63+	0.63*	0.44*	0.71*	0.43*	1.22
	±0.62	±0.19	±0.16	±0.29	±0.42	±0.44
EPS (A) †	0.62 +	0.34*	0.40	0.26*	0.27	0.39
	±0.25	±0.09	±0.18	±0.08	±0.30	±0.40
EPS (NE) †	0.50	0.40	0.32	0.21*	0.38	0.60
	±0.18	±0.14	±0.11	±0.19	±0.31	±0.60
MDFE †	0.47+	0.26*	0.20*	0.16*	0.10*	0.12*
	±0.04	±0.04	±0.05	±0.02	±0.01	±0.08
	(NS)	(NS)	(NS)	(NS)	(NS)	(NS)
J (NF) †	0.33	0.44	0.48	0.32	0.72	0.94*
	±0.20	±0.14	±0.33	±0.21	±0.37	±0.46
	(NS)	(NS)	(NS)	(NS)	(NS)	(NS)

Table 7.2: Diaphragm AChE after 14 nmol hr^{-1} PHY (1-14 days). G, A and NE AChE activities in nmol min^{-1} mg^{-1} in J, NJ and EPS regions. Also shown are the $(MEPP)_o$ derived functional enzyme activities (MDFE) and non-functional enzyme activity in the junctional region (J (NF)). † denotes sets with different groups (K-S ANOVA, $P<0.05$), * denotes groups which differ from the untreated group and + denotes different adjacent groups (K-S multi-comparison test, $P<0.05$) and (NS) denotes no significance between MDFE and EPS (NE) or between J (NF) and NJ (NE).

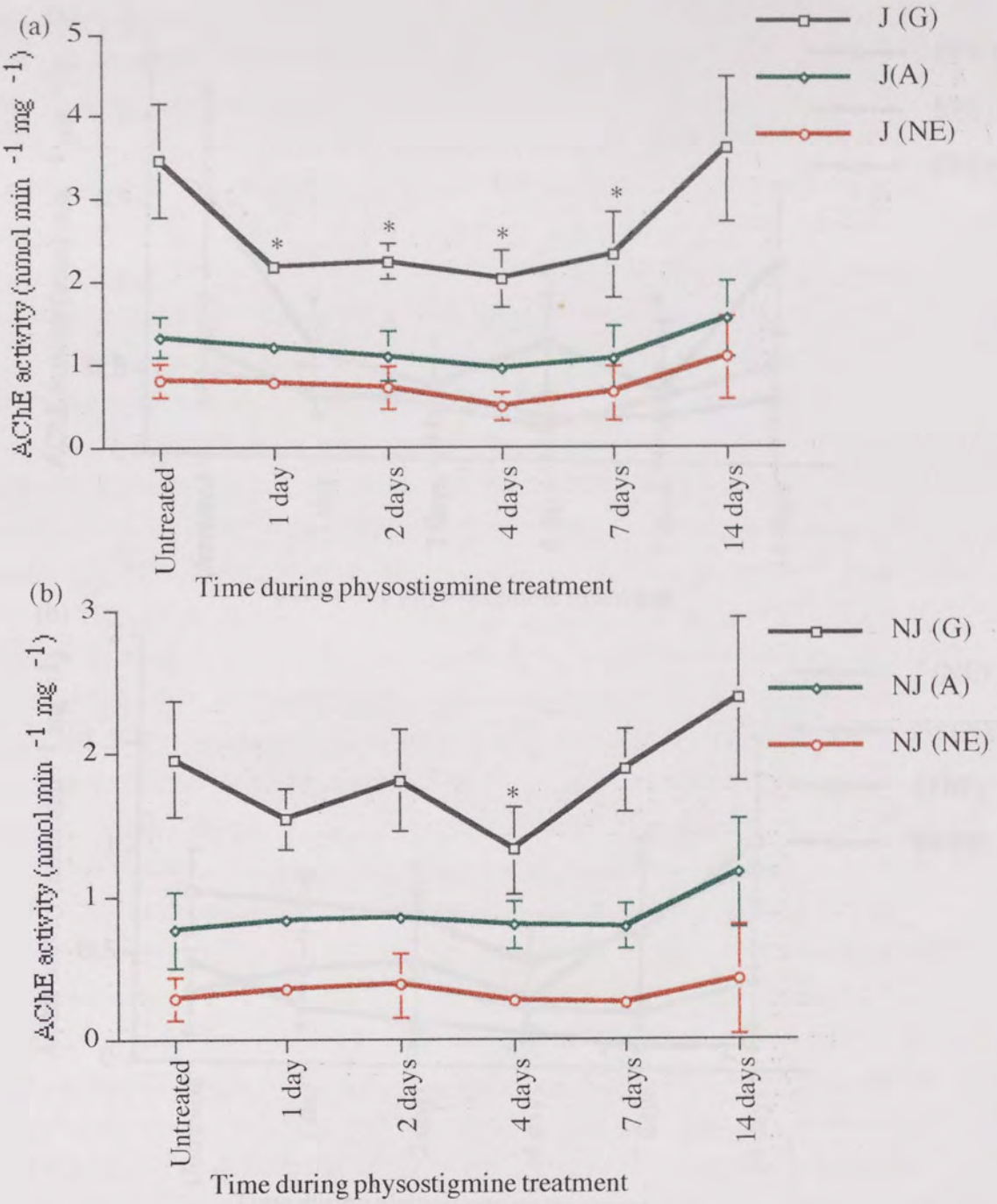

Figure 7.2: Junctional and non-junctional AChE after 14 nmol hr^{-1} PHY (1-14 days). Globular (G), asymmetric (A) and non-extractable (NE) AChE activity in (a) junctional (J) and (b) non-junctional (NJ) regions of mouse diaphragm. * denotes groups which differ from the untreated group: $P<0.05$ (Kruskal-Wallis multi-comparison test).

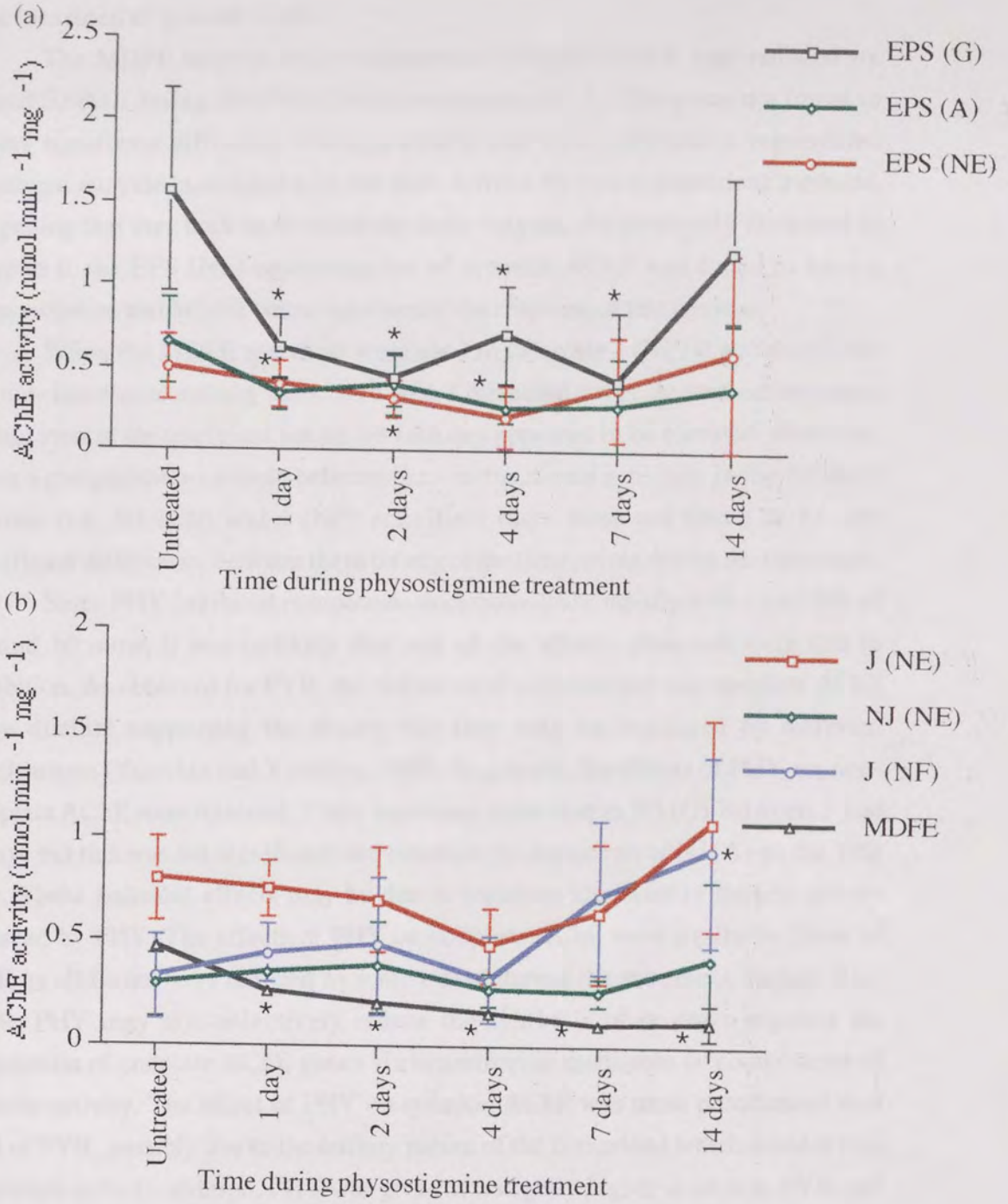

Figure 7.3: Endplate-specific AChE after 14 nmol hr^{-1} PHY (1-14 days). (a) Endplate-specific (EPS) globular (G), asymmetric (A) and non-extractable (NE) AChE determined by assay and (b) junctional non-extractable (J (NE)), non-junctional non-functional (NJ (NE)), junctional non-functional (J NF)) and $(MEPP)_o$-derived functional AChE (MDFE) associated with the synapse. * denotes groups which differ from the untreated group: $P<0.05$ (Kruskal-Wallis multi-comparison test).

of treatment by around 50%. At all the other time points EPS (A) and EPS (NE) were measured at normal levels.

The MDFE activity which represented synaptic AChE was reduced by around 50-80% during the entire 14 day treatment period. There was not found to be any significant difference between MDFE and EPS (NE) which represented functional enzyme associated with the cleft derived by two independent methods, suggesting that they both represented the same enzyme. As previously discussed in Chapter 6, the EPS (NE) representation of synaptic AChE was found to have a large variation and MDFE better represented the response of this enzyme.

When the MDFE activities were used to calculate J (NF) it was found that the non-functional activity associated with J dissected strips showed no responses during most of the treatment but on the 14th day appeared to be elevated. However, when a comparison was made between the non-functional activities in the NJ and J regions (i.e. NJ (NE) and J (NF) activities) there were not found to be any significant differences between them on any of the time points during the treatment.

Since PHY-inhibited compounds decarbamoylate rapidly with a half-life of around 10 mins, it was unlikely that any of the effects observed were due to inhibition. As observed for PYR, the responses of endplate and non-endplate AChE were distinct supporting the theory that they may be regulated by different mechanisms (Younkin and Younkin, 1988). In general, the effects of PHY on non-endplate AChE were minimal. There was some reduction in NJ (G) between 1 and 4 days but this was not significant and transient up-regulation of NJ (A) on the 14th day. These transient effects may be due to transient increases in muscle activity induced by PHY. The effects of PHY on endplate AChE were similar to those of PYR as all forms were reduced to some extent during the treatment. Hence, like, PYR, PHY may also selectively reduce the synthesis of or down-regulate the expression of endplate AChE genes via neurotrophic mediators or components of muscle activity. The effect of PHY on synaptic AChE was more pronounced than that of PYR, possibly due to the tertiary nature of the compound which enables it to penetrate cells. In addition, PHY was given at a slightly higher dose than PYR and inhibited blood ChE to a greater extent than PYR. The greater potency of PHY was therefore not unexpected. After PHY, there was also a rapid initial loss of synaptic AChE which implied that the enzyme may initially be degraded rather than down-regulated.

7.2.1.3 Endplate dimensions.

Table 7.3 and Figure 7.4 show the variation in the width (W), length (L) and width/length (W/L) ratio of endplates on various days during two weeks of continual infusion with PHY. Histograms corresponding to endplate W/L ratio distributions are shown in Figure 7.5.

One day into the treatment, the W/L ratio had increased by 61%. This was complemented by a corresponding increase in the W and a decrease in the L suggesting that the endplates had become more rounded due to hypercontrations in underlying muscle fibres. Between the 1st and 2nd day of treatment there was a slight improvement in the ratio although statistically these ratios did not differ from each other. This level of deformation persisted throughout the duration of the treatment. The histograms show that during the treatment there was a shift in the populations such that there was a larger percentage of endplates with a larger ratio and a smaller percentage with ratios around the untreated mean.

The extent of endplate deformation after PHY was similar to that after a 300 nmol kg^{-1} dose of ECO (statistically there were no differences between the PHY treated and ECO treated population; MANOVA, $P>0.05$) and slightly more severe than similar treatment with PYR although this was expected due to slight differences in the doses of each drug. The onset of PHY-induced myopathy was rapid and persisted for the duration of the treatment suggesting that abnormal cellular calcium levels and muscle fibre morphology were a characteristic feature of PHY administration.

7.2.2 Recovery of mouse skeletal muscle after 7 days of PHY.

7.2.2.1 Whole blood ChE.

Table 7.4 and Figure 7.6 show whole blood ChE during a 14 day recovery period after continual infusion of mice with PHY at 14 nmol hr^{-1} for 7 days. During the entire 14 day recovery period blood ChE was reduced by around 50% and there were no differences between the activities at any of the time points suggesting that no recovery in the activity had occurred. Since it was unlikely that PHY persisted in the cell when the treatment was terminated it was unlikely that the effects were due to inhibition and may be due to down-regulation.

Time	Width † (μm)	Length † (μm)	Width /length † ratio	No. of HD No. of EP
Untreated	19.3±0.7 +	34.8±2.9 +	0.56±0.04 +	8 240
1 day	21.7±0.4*	23.9±1.3*	0.92±0.04*	4 120
2 days	20.4±1.0 +	25.9±0.9*	0.81±0.01*	4 120
4 days	21.9±0.7*	26.7±2.5*	0.85±0.07*	4 120
7 days	22.3±1.1*	28.4±1.3* +	0.81±0.05*	4 120
14 days	21.5±1.9*	24.9±1.8*	0.88±0.07*	3 90

Table 7.3: Endplate dimensions after 14 nmol hr^{-1} PHY (1-14 days). The table shows endplate width, length and width/length ratios. HD gives the no. of hemidiaphragms and EP gives the total no. of endplates. Values are means±s.d. of averages of 30 EP per HD. † denotes sets with different groups (ANOVA, $P<0.05$), * denotes groups which differ from the untreated group (MANOVA, $P<0.05$) and + denotes different adjacent groups (MANOVA, $P<0.05$).

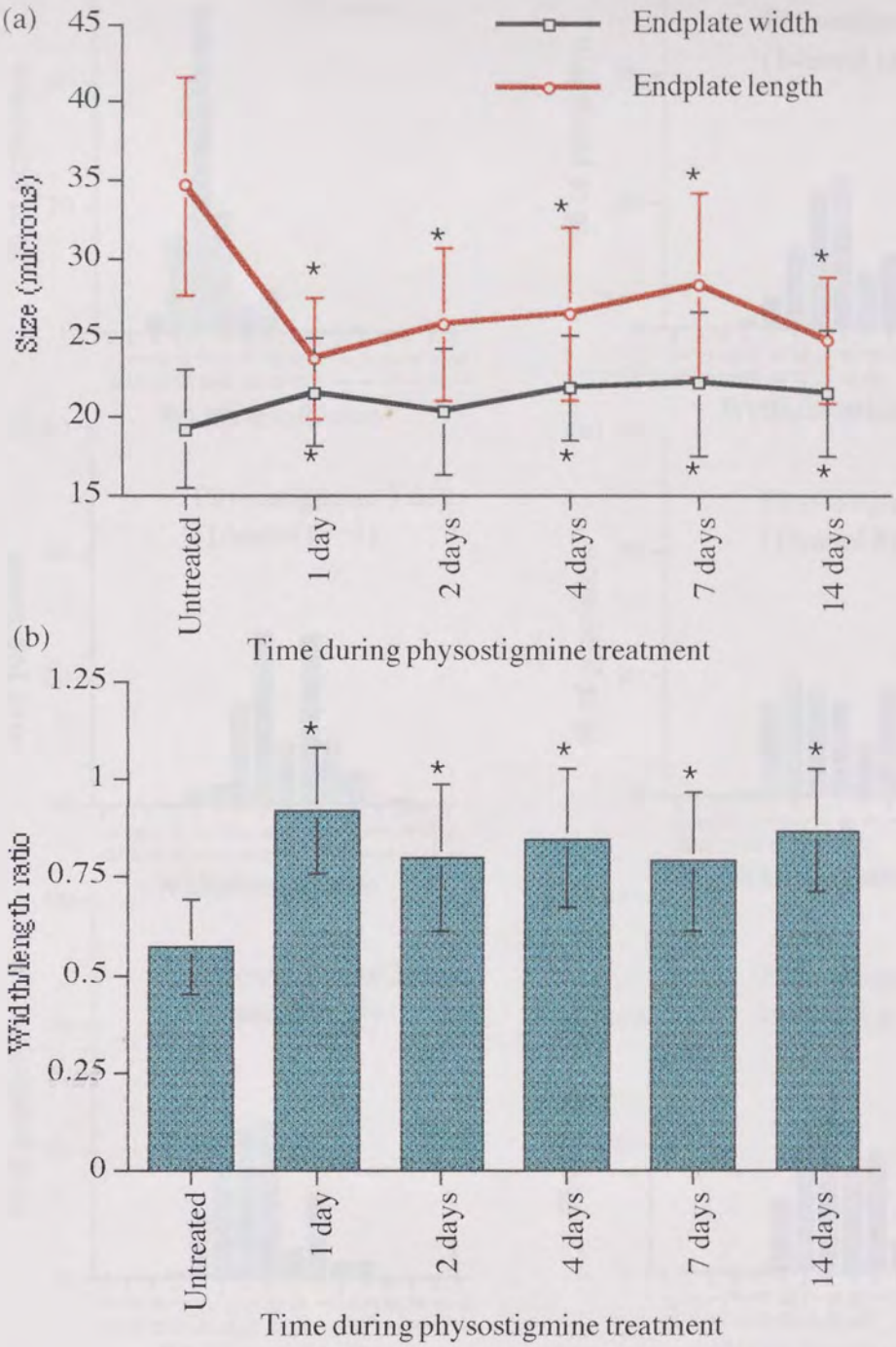

Figure 7.4: Width, length and width/length ratio of endplates after 14 nmol hr^{-1} PHY (1-14 days). Variation in endplate population (a) widths and lengths and (b) width/length ratios. * denotes groups which differ from the untreated group $P<0.05$ (MANOVA).

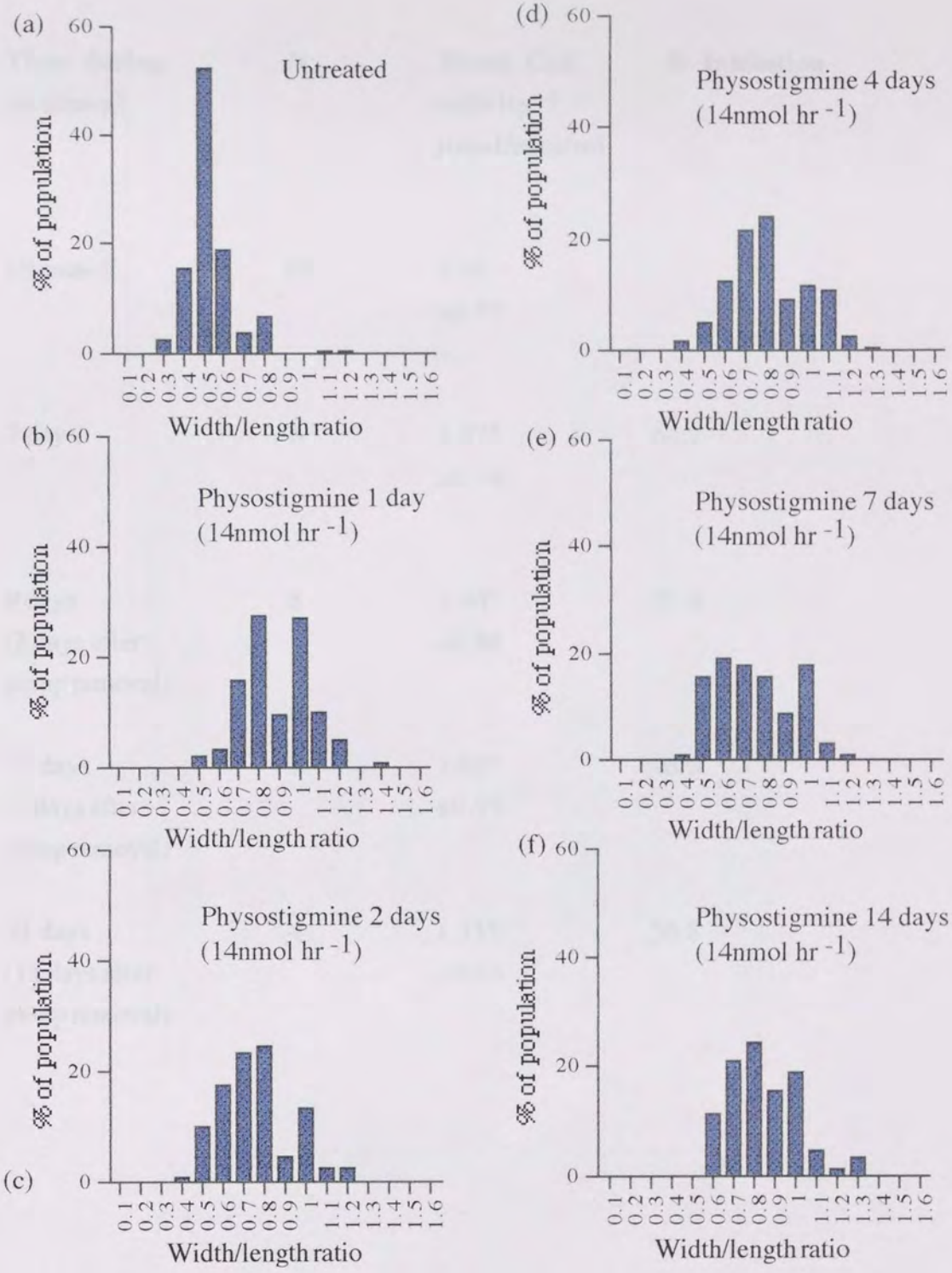

<u>Figure 7.5:</u> Histograms of endplates after 14 nmol hr^{-1} PHY (1-14 days). Percentage of endplates per population at given width/length ratios for (a) untreated, (b) 1 day, (c) 2 days, (d) 4 days, (e) 7 days and (f) 14 days.

Time during treatment	N	Blood ChE activity † μmol/min/ml	% Inhibition
Untreated	10	3.03 ±0.97 +	-
7 days	6	1.07* ±0.14	64.7
9 days (2 days after pump removal)	8	1.44* ±0.86	52.5
14 days (7 days after pump removal)	7	1.62* ±0.73	46.5
21 days (14 days after pump removal)	4	1.31* ±0.05	56.8

Table 7.4: Whole blood ChE activity 2-14 days after termination of continual PHY infusion for 7 days at 14 nmol hr^{-1}. † denotes that the set has different group (K-S ANOVA, $P<0.05$), * denotes groups which differ from the untreated group (K-S multi-comparison test, $P<0.05$) and + denotes different adjacent groups (K-S multi-comparison test, $P<0.05$).

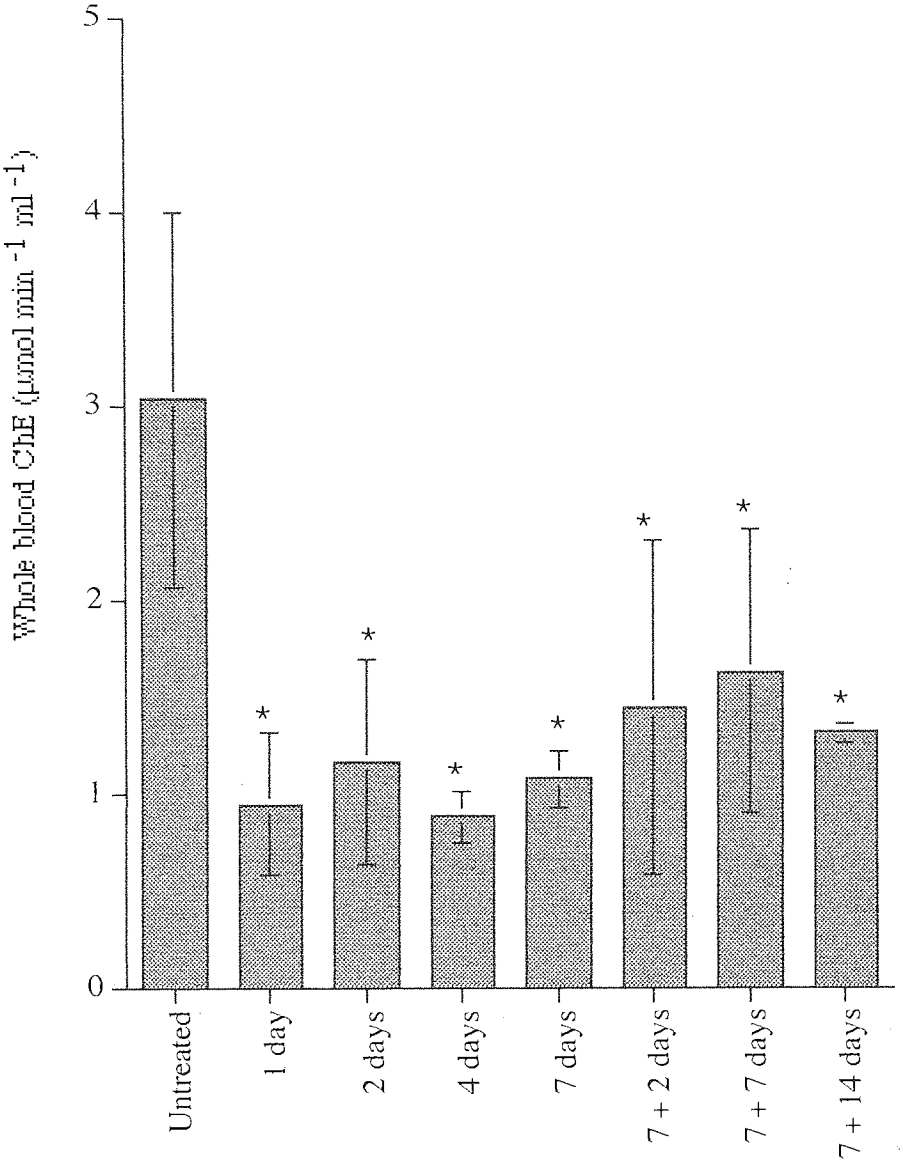

Figure 7.6: Whole blood ChE 2-14 days after termination of continual PHY infusion for 7 days at 14 nmol hr^{-1}. * denotes groups which differ from the untreated group: $P<0.05$ (Kruskal-Wallis multi-comparison test).

7.2.2.2 Molecular forms of AChE.

Table 7.5 shows the responses of J, NJ and EPS: G, A and NE AChE (also see Figures 7.7 and 7.8a) during a 14 day recovery period after 7 days of continual PHY infusion at 14 nmol hr^{-1}. Also shown are MDFE and J (NF) activities (see Figure 7.8b).

J (G) was still reduced by about 15% seven days after pump removal but normal 7 days later. J (A) exceeded the normal level by 40% after 2 days of recovery, returned to normal on the 7th day and exceeded the normal level by around 40% on the 14th day. J (NE) was reduced by 50% after 2 days of recovery but exceeded the normal level by 80% on the 14th day. NJ (G) was normal on the 7th day of treatment and after 2 days of recovery but exceeded the normal level by 30% and 70% after 7 and 14 days of recovery respectively. NJ (A) exceeded the normal level by 50% after 2 days of recovery, was normal after 7 days and exceeded normal by 70% after 14 days. NJ (NE) was normal after 7 days of treatment and after 2 days of recovery, but exceeded the normal level by 160% after 14 days of recovery. EPS (G) was reduced by 50% and 70% after 2 and 7 days of recovery respectively but had recovered by the 14th day. EPS (A) was normal on the 7th day of dosing and remained unchanged during the recovery period. EPS (NE) was reduced by 70% after 2 days of recovery, but completely recovered after 7 days of recovery.

MDFE activity which was 80% lower then normal on the 7th day of drug treatment was still reduced by 50% after 2 days of recovery but completely recovered by the 7th day. When the MDFE was compared with the EPS (NE) activity there was not found to be any significant difference between the activities on any of the time points and because EPS (NE) was largely variable, MDFE better represented the response of synaptic AChE. J (NF), representing changes in non-functional enzymes in the J region was normal during days 2 and 7 of the recovery period but on the 14th day exceeded the normal level by 245%. When the NJ (NE) and J (NF) activities were compared both were found to follow similar trends. Both were normal one week after the pumps were removed and two weeks after the pumps were removed, both exceeded their normal levels by a considerable amount. There was not found to be any significant differences between NJ (NE) and J (NF) on any of the recovery time points except 14 days after the pumps were removed. At this time point, the non-functional form of A12 located in close vicinity to the endplates was found to increase by a significantly greater extent than the non-

Region	Untreated	7 days	9 days (2 days after pump removal)	14 days (7 days after pump removal)	21 days (14 days after pump removal)
N	13	6	6	5	4
J (G) †	3.48	2.31*	2.78	2.95+	4.25
	±0.80	±0.52	±1.17	±0.34	±1.07
J (A) †	1.29	1.06+	1.82*+	1.02+	1.71*
	±0.31	±0.38	±0.37	±0.33	±0.42
J (NE) †	0.79	0.64 +	0.40 *	0.47*+	1.44*
	±0.20	±0.33	±0.29	±0.40	±0.38
NJ (G) †	1.90	1.88	2.06+	2.59*+	3.41*
	±0.49	±0.29	±0.32	±0.24	±0.37
NJ (A) †	0.73	0.79	1.20*	0.66+	1.33*
	±0.30	±0.15	±0.27	±0.37	±0.11
NJ (NE)†	0.29	0.26	0.26	0.21+	0.75*
	±0.16	±0.07	±0.19	±0.25	±0.08
EPS (G)†	1.63	0.43*	0.79	0.36*	0.72
	±0.62	±0.42	±1.38	±0.42	±0.76
EPS (A)	0.62	0.27	0.63	0.36	0.38
	±0.25	±0.30	±0.51	±0.23	±0.34
EPS (NE)	0.50	0.38	0.14 *	0.26+	0.69
†	±0.18	±0.31	±0.24	±0.15	±0.38
MDFE †	0.47	0.10*+	0.23*+	0.45	0.45
	±0.04	±0.01	±0.01	±0.02	±0.01
	(NS)	(NS)	(NS)	(NS)	(NS)
J (NF) †	0.33	0.72	0.31	0.27+	1.14*
	±0.20	±0.37	±0.40	±0.34	±0.31
	(NS)	(NS)	(NS)	(NS)	(NS)

Table 7.5: Diaphragm AChE 2-14 days after termination of continual PHY infusion for 7 days at 14 nmol hr^{-1}. Activity of J, NJ and EPS: G, A and NE AChE in nmol min^{-1} mg^{-1}. Also shown are MDFE and J (NF).Values shown are means±s.d. † denotes sets with different groups (K-S ANOVA, $P<0.05$), * denotes groups which differ from the untreated group and + denotes different adjacent groups (K-S multi-comparison test, $P<0.05$).

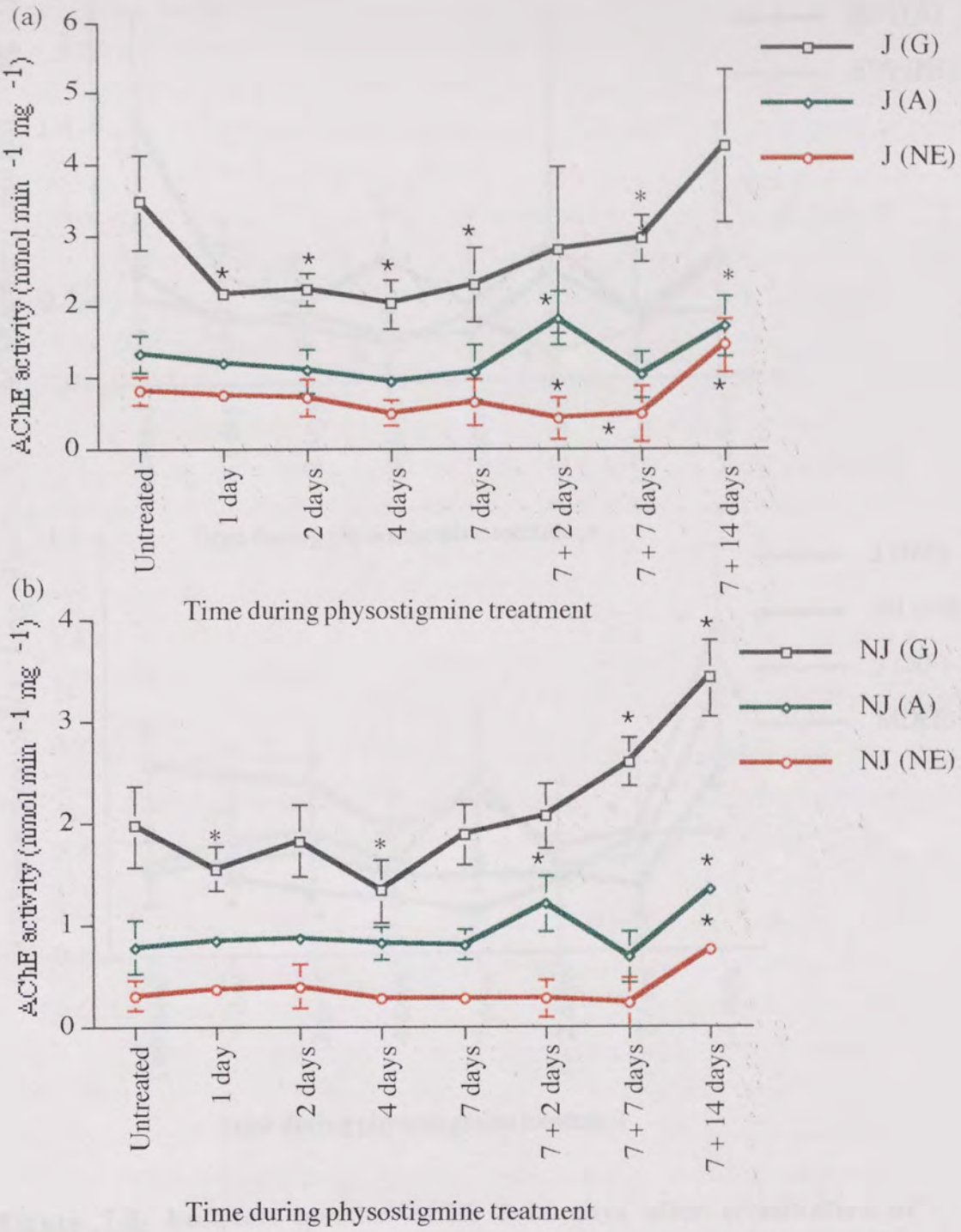

Figure 7.7: Junctional and non-junctional AChE 2-14 days after termination of continual PHY infusion for 7 days at 14 nmol hr^{-1}. Globular (G), asymmetric (A) and non-extractable (NE) AChE activity in (a) junctional (J) and (b) non-junctional (NJ) regions. * denotes groups which differ from the untreated group: $P<0.05$ (Kruskal-Wallis multi-comparison test).

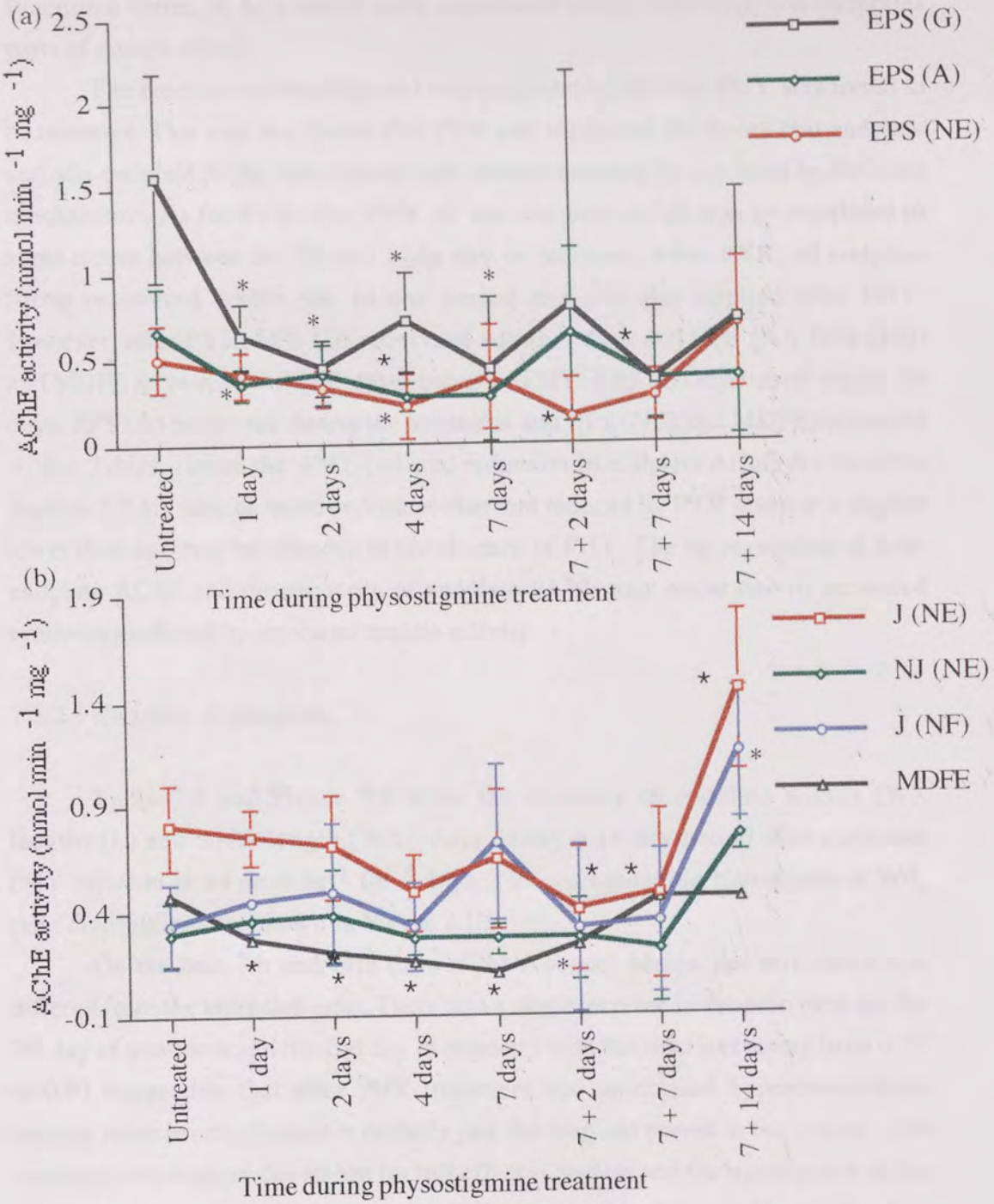

Figure 7.8: Endplate-specific AChE 2-14 days after termination of continual PHY infusion for 7 days at 14 nmol hr^{-1}. (a) Endplate-specific (EPS) globular (G), asymmetric (A) and non-extractable (NE) AChE determined by assay and (b) junctional non-extractable (J (NE)), non-junctional non-functional (NJ (NE)), junctional non-functional (J NF)) and $(MEPP)_O$-derived functional AChE (MDFE) associated with the synapse. * denotes groups which differ from the untreated group: $P<0.05$ (Kruskal-Wallis multi-comparison test).

functional forms of A12 which were associated exclusively with non-endplates parts of muscle fibres.

The recovery of endplate and non-endplate AChE after PHY was found to be selective. This was also found after PYR and supported the theory that endplate and non-endplate AChE were biologically distinct and may be regulated by different mechanisms. As for PYR, after PHY all non-endplate AChE was up-regulated to some extent between the 7th and 14ths day of recovery. After PYR, all endplate forms recovered within the 14 day period and this also applied after PHY. However, after PYR, EPS (G) recovered within 7 days and EPS (A), EPS (NE) and MDFE recovered within 2 days, but after PHY, EPS (G) recovered within 14 days, EPS (A) recovered during the treatment and EPS (NE) and MDFE recovered within 7 days. Hence the PHY-induced reduction in endplate AChE discussed in Section 7.2.1.2 may be more persistent than that induced by PYR given at a slightly lower dose and may be effective in the absence of PHY. The up-regulation of non-endplate AChE and the recovery of endplate AChE may occur due to increased synthesis mediated by increased muscle activity.

7.2.2.3 Endplate dimensions.

Table 7.6 and Figure 7.9 show the recovery of endplate widths (W), lengths (L) and width/length (W/L) ratio during a 14 day period after continual PHY infusion at 14 nmol hr^{-1} for 7 days. The corresponding histograms of W/L ratio distributions are shown in Figure 7.10.

On the 2nd, 7th and 14th days of the recovery period, the W/L ratios still differed from the untreated ratio. There was a slight increase in the ratio between the 7th day of treatment and the 2nd day of recovery with the ratio increasing from 0.79 to 0.91 suggesting that after PHY treatment had terminated, hypercontractions became more severe. Since it is unlikely that the drug can persist in the system after treatment termination, the reason for this effect is unclear and the significance of the effect may be questionable as the population size at this time point is smaller than others tested. There was a definate improvement in the ratios during the recovery period and on the 14th day the ratio was only 45% in excess of the normal ratio suggesting that some recovery had occurred.

During the 14 day recovery period after 7 days of PHY, endplates were still deformed, although some recovery had occurred. Complete recovery of muscle fibre morphology took longer than time allowed for this study. On termination of the treatment, PHY-induced myopathy was transiently enhanced and at the end of the recovery period the extent of deformation was equivalent to that after 100 nmol

Time	Width † (μm)	Length † (μm)	Width /length † ratio	No. of HD No. of EP
Untreated	19.3±0.7 +	43.8±2.9 +	0.56±0.04 +	8 240
7 days	22.3±1.1*	28.4±1.3*	0.81±0.05* +	4 120
9 days (2 days after pump removal)	22.2±0.6*	24.8±0.1*	0.91±0.01* +	2 60
14 days (7 days after pump removal)	21.6±0.8*	28.1±2.7* +	0.80±0.09* +	4 120
21 days (14 days after pump removal)	22.3±1.5*	33.2±4.6	0.70±0.08*	4 120

Table 7.6: Endplate dimensions 2-14 days after termination of continual PHY infusion for 7 days at 14 nmol hr^{-1}. The table shows endplate width, length and width/length ratio. HD gives the no. of hemidiaphragms and EP gives the total no. of endplates. Values are means±s.d of averages of 30 EP per HD (9 day value±min/max). † denotes sets with different groups (ANOVA, $P<0.05$), * denotes groups which differ from the untreated group (MANOVA, $P<0.05$) and + denotes different adjacent groups (MANOVA, $P<0.05$).

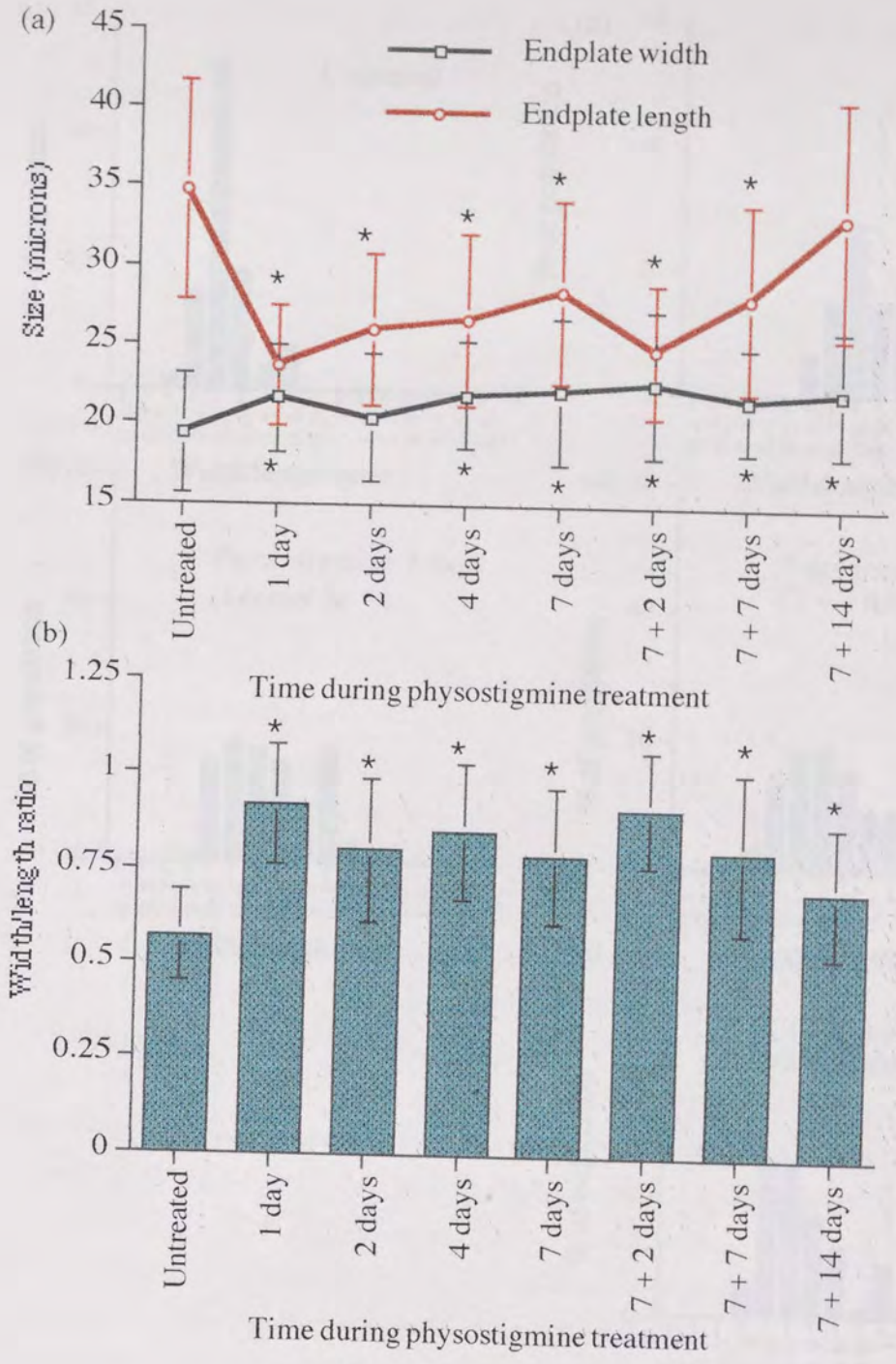

Figure 7.9: Width, length and width/length ratio of endplates 2-14 days after termination of continual PHY infusion for 7 days at 14 nmol hr^{-1}. Variation in endplate population (a) widths and lengths and (b) width/length ratios. * denotes groups which differ from the untreated group: $P<0.05$ (MANOVA).

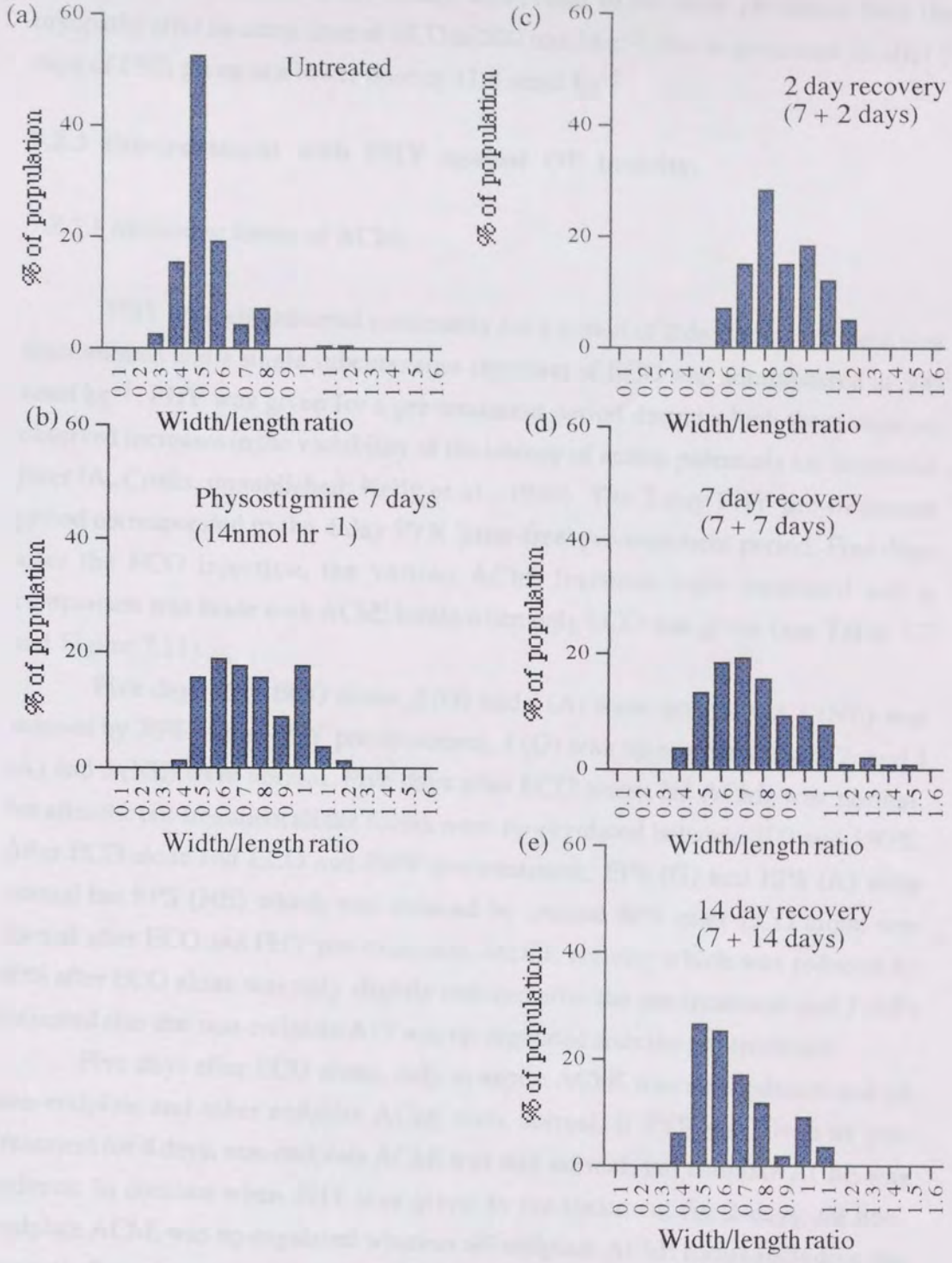

Figure 7.10: Histograms of endplates 2-14 days after termination of continual PHY infusion for 7 days at 14 nmol hr^{-1}. Percentage of endplates per population at given width/length ratios for (a) untreated, (b) 7 days of PHY, (c) 2 day recovery, (d) 7 day recovery and (e) 14 day recovery.

kg^{-1} ECO. PHY-induced myopathy was found to be more persistent than the myopathy after an acute dose of ECO of 500 nmol kg^{-1}, but as persistent as after 7 days of PYR given at a lower dose of 11.4 nmol kg^{-1}.

7.2.3 Pre-treatment with PHY against OP toxicity.

7.2.3.1 Molecular forms of AChE.

PHY was administered continually for a period of 2 days, the treatment was discontinued and a single subcutaneous injection of ECO was administered at 500 nmol kg^{-1}. PHY was given for a pre-treatment period during which there were no observed increases in the variability of the latency of action potentials i.e. increased jitter (A. Crofts, unpublished; Kelly et al., 1990). The 2 day PHY pre-treatment period corresponded to the 4 day PYR 'jitter-free' pre-treatment period. Five days after the ECO injection, the various AChE fractions were measured and a comparison was made with AChE levels when only ECO was given (see Table 7.7 and Figure 7.11).

Five days after ECO alone, J (G) and J (A) were normal but J (NE) was reduced by 36%. After PHY pre-treatment, J (G) was up-regulated by 36% and J (A) and J (NE) were normal. Five days after ECO alone, NJ AChE was normal, but after the pre-treatment all the forms were up-regulated between 100 and 150%. After ECO alone and ECO and PHY pre-treatment, EPS (G) and EPS (A) were normal but EPS (NE) which was reduced by around 50% after ECO alone was normal after ECO and PHY pre-treatment. MDFE activity which was reduced by 80% after ECO alone was only slightly reduced after the pre-treatment and J (NF) indicated also that non-endplate A12 was up-regulated after the pre-treatment.

Five days after ECO alone, only synaptic AChE was still reduced and all non-endplate and other endplate AChE were normal. If PYR was given as pre-treatment for 4 days, non-endplate AChE was still normal, but endplate AChE was reduced. In contrast when PHY was given as pre-treatment for 2 days, all non-endplate AChE was up-regulated whereas all endplate AChE forms including the synaptic form were normal. PYR and PHY pre-treatments affect the recovery of diaphragm AChE after ECO differently. PYR was not found to protect synaptic AChE against the ECO-induced reduction whereas PHY completely protected the synaptic enzyme from the ECO-induced effect 5 days after the dose.

The protection effects of PHY against OP toxicity have been demonstrated in other studies. When PHY was administered at a dose which inhibited blood ChE around 60-70% prior to challenge with OP compounds it successfully protected

Enzyme	Untreated	ECO 500 nmol kg^{-1} (5 days)	PHY (2 days) + ECO 500 nmol kg^{-1} (5 days)
N	13	8	4
J (G) †	3.48	3.30+	4.70*
	±0.80	±0.61	±1.08
J (A) †	1.29	1.05+	1.73
	±0.31	±0.37	±0.41
J (NE) †	0.79	0.51*+	1.18
	±0.20	±0.20	±0.43
NJ (G) †	1.90	1.95+	3.95*
	±0.49	±0.26	±0.31
NJ (A) †	0.73	0.65+	1.33*
	±0.30	±0.21	±0.13
NJ (NE) †	0.29	0.25+	0.63 *
	±0.16	±0.12	±0.10
EPS (G)	1.63	1.36	0.75
	±0.62	±0.70	±1.08
EPS (A)	0.62	0.40	0.41
	±0.25	±0.26	±0.50
EPS (NE) †	0.50+	0.26*	0.55
	±0.18	±0.14	±0.48
MDFE †	0.47+	0.08*+	0.39*
	±0.04	±0.03	±0.01
	(NS)	(NS)	(NS)
J (NF) †	0.33	0.08+	1.02*
	±0.20	±0.13	±0.18
	(NS)	(NS)	(NS)

Table 7.7. AChE in untreated diaphragm, 5 days after 500 nmol kg^{-1} ECO and 5 days after 500 nmol kg^{-1} ECO with 2 days of pre-treatment with PHY 14 nmol hr^{-1}. The table shows J, NJ and EPS: G, A and NE AChE in nmol min^{-1} mg^{-1} and MDFE and J (NF). Values are means± s.d. † denotes sets with different groups (K-S ANOVA, $P<0.05$), * denotes groups which differ from the untreated group and + denotes different adjacent groups (K-S muti-comparison test). NS denotes no difference between MDFE and EPS (NE) or J (NF) and NJ (NE).

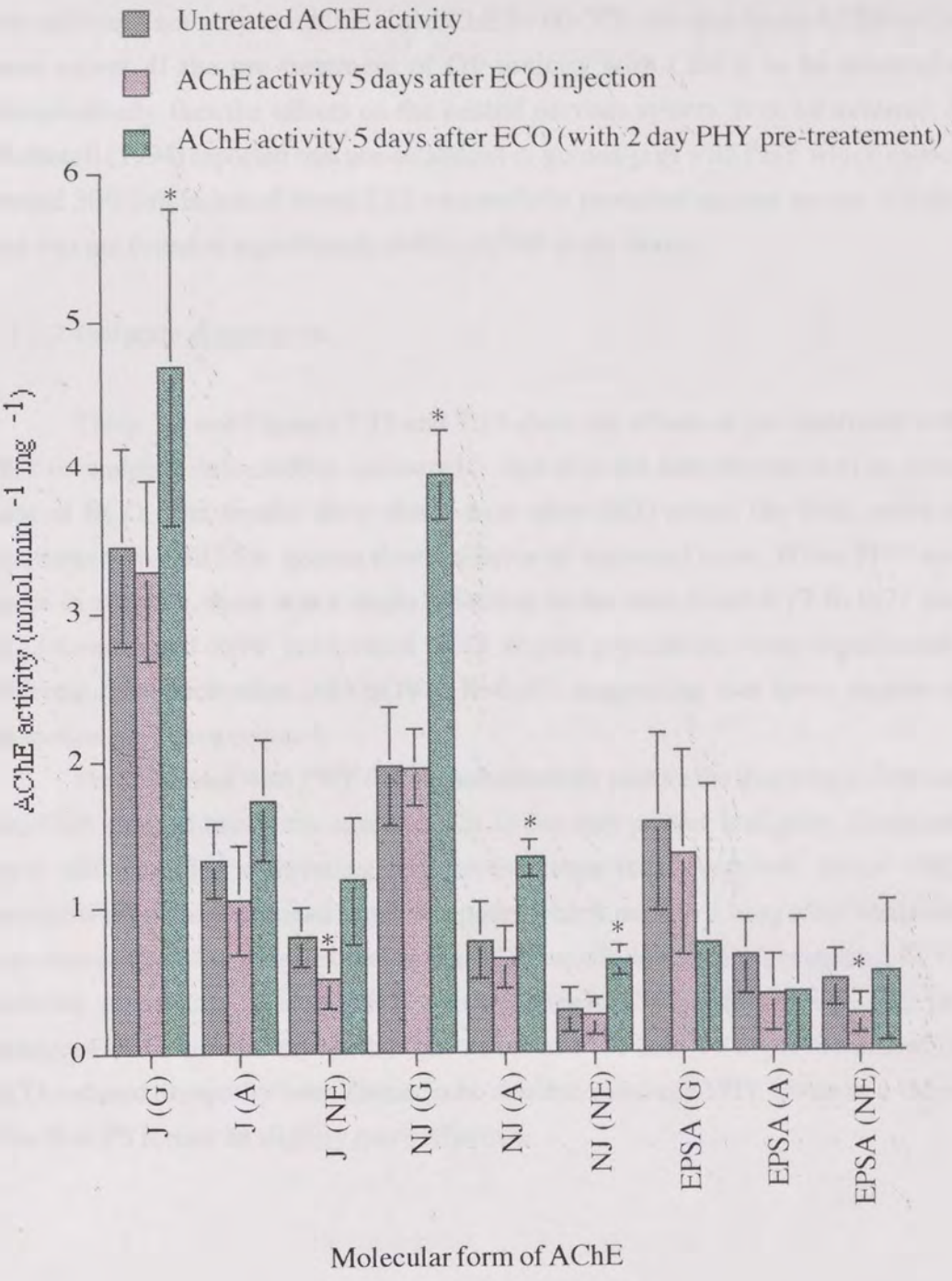

Figure 7.11: AChE in untreated diaphragms, 5 days after 500 nmol kg^{-1} ECO and 5 days after 500 nmol kg^{-1} ECO with 2 days of pre-treatment with PHY 14 nmol hr^{-1}. * denotes groups which differ from the untreated group: $P<0.05$ (Kruskal-Wallis multi-comparison test).

against the toxicity in the guinea-pig (Leadbeater et al., 1995; Lennox et al., 1992) and in the rhesus monkey (von Bredow et al., 1991). However, in this study and those mentioned previously, the concentration of PHY used in the pre-treatment was sufficient not only to inhibit blood ChE by 60-70% but also brain AChE to the same extent. If the pre-treatment of OP toxicity with CBs is to be successful therapeutically, then the effects on the central nervous system must be minimal. J. Wetherell (1994) reported that pre-treatment of guinea-pigs with PHY which caused around 30% inhibition of blood ChE successfully protected against soman toxicity and was not found to significantly inhibit AChE in the brain.

7.2.3.2 Endplate dimensions.

Table 7.8 and Figures 7.12 and 7.13 show the effects of pre-treatment with PHY on endplate deformation measured 5 days after the administration of an acute dose of ECO. The results show that 5 days after ECO alone, the W/L ratios of endplates were still 35% greater than the ratios of untreated mice. When PHY was given in advance, there was a slight reduction in the ratio from 0.77 to 0.71 and ECO-treated and PHY pre-treated ECO-treated populations were significantly different from each other (MANOVA, $P>0.05$) suggesting that some degree of protection may have occured.

Pre-treatment with PHY did not substantially protect the diaphragm from the anti-ChE induced myopathy caused by ECO but may protect it slightly. Endplates were still rounded suggesting hypercontrations still occurred. Since PHY administration alone induced rapid myopathy which persisted long after treatment was terminated, it was not expected that PHY would totally protect against ECO-induced myopathy. Hence, PHY neither sucessfully protected against, nor enhanced ECO-induced myopathy. The effect of PHY and PYR pre-treatment on ECO-induced myopathy were found to be similar, although PHY given at a larger dose than PYR may be slightly more effective.

Treatment	Width † (μm)	Length † (μm)	Width/length ratio †	No. of HD No. of EP
Untreated	19.3±0.7 +	34.8±2.9 +	0.56±0.04 +	8 240
ECO 5 days 500nmol kg^{-1}	22.2±1.1*	29.5±2.3* +	0.77±0.07* +	5 150
PHYS 2 days + ECO 5 days 500nmol kg^{-1}	22.2±0.8*	32.6±2.7	0.71±0.06*	4 120

Table 7.8: Endplate dimensions, 5 days after 500 nmol kg^{-1} ECO and 5 days after 500 nmol kg^{-1} ECO with 2 days of pre-treatment with PHY 14 nmol hr^{-1}. The table shows endplate width, length and width / length ratios. HD gives the no. of hemidiaphragms and EP gives the total no. of endplates. Values are means±s.d. of averages of 30 EP per HD. † denotes sets with different groups (ANOVA, $P<0.05$), * denotes groups which differ from the untreated group (MANOVA, $P<0.05$) and + denotes different adjacent groups (MANOVA, $P<0.05$).

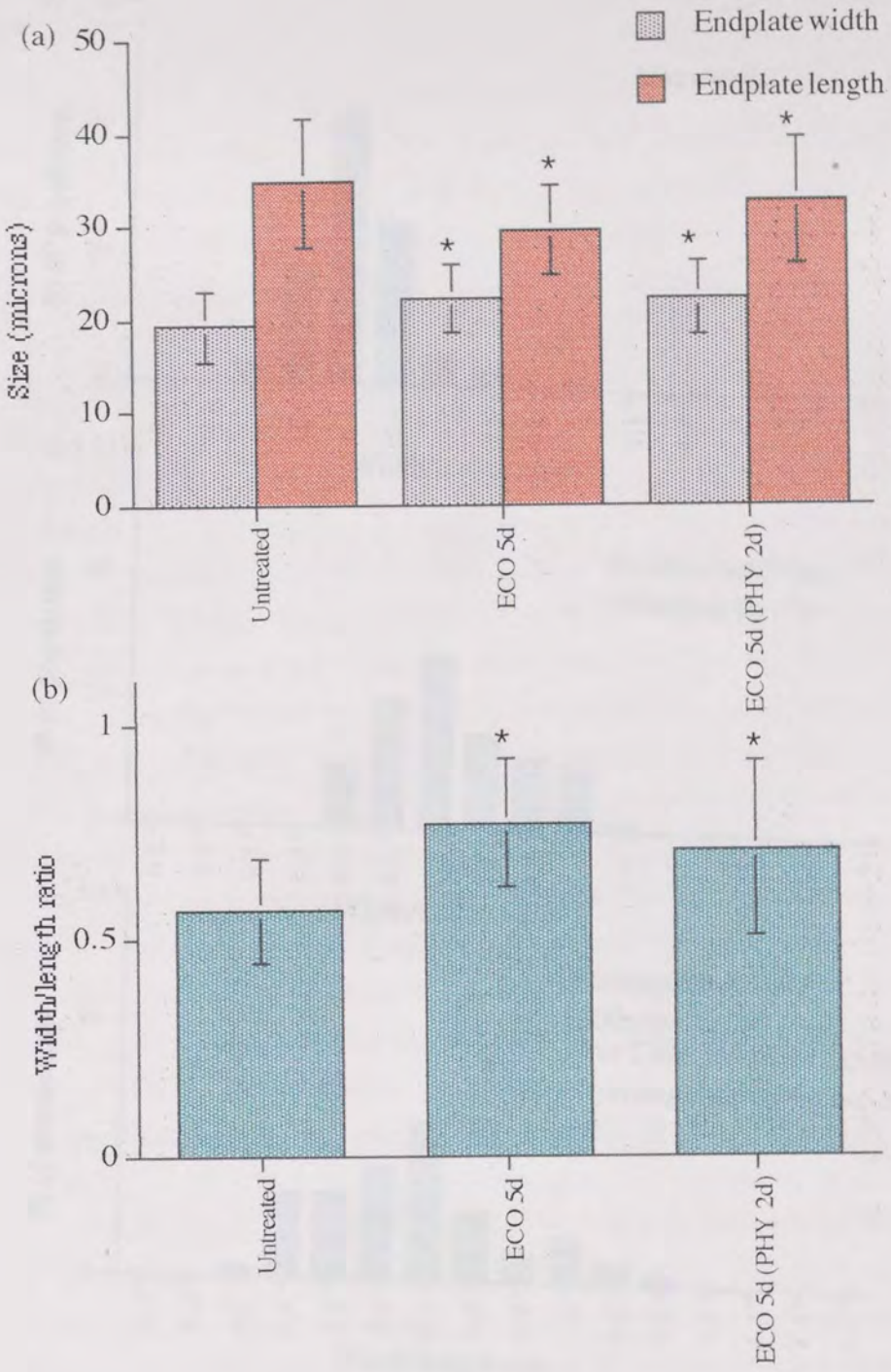

Figure 7.12: Width, length and width/length ratio of untreated endplates, 5 days after 500 nmol kg^{-1} ECO and 5 days after 500 nmol kg^{-1} ECO with 2 days of pre-treatment with PHY 14 nmol hr^{-1}. Shown are (a)widths and lengths and (b) width/length ratios. * denotes groups which differ from the untreated group: $P<0.05$ (MANOVA).

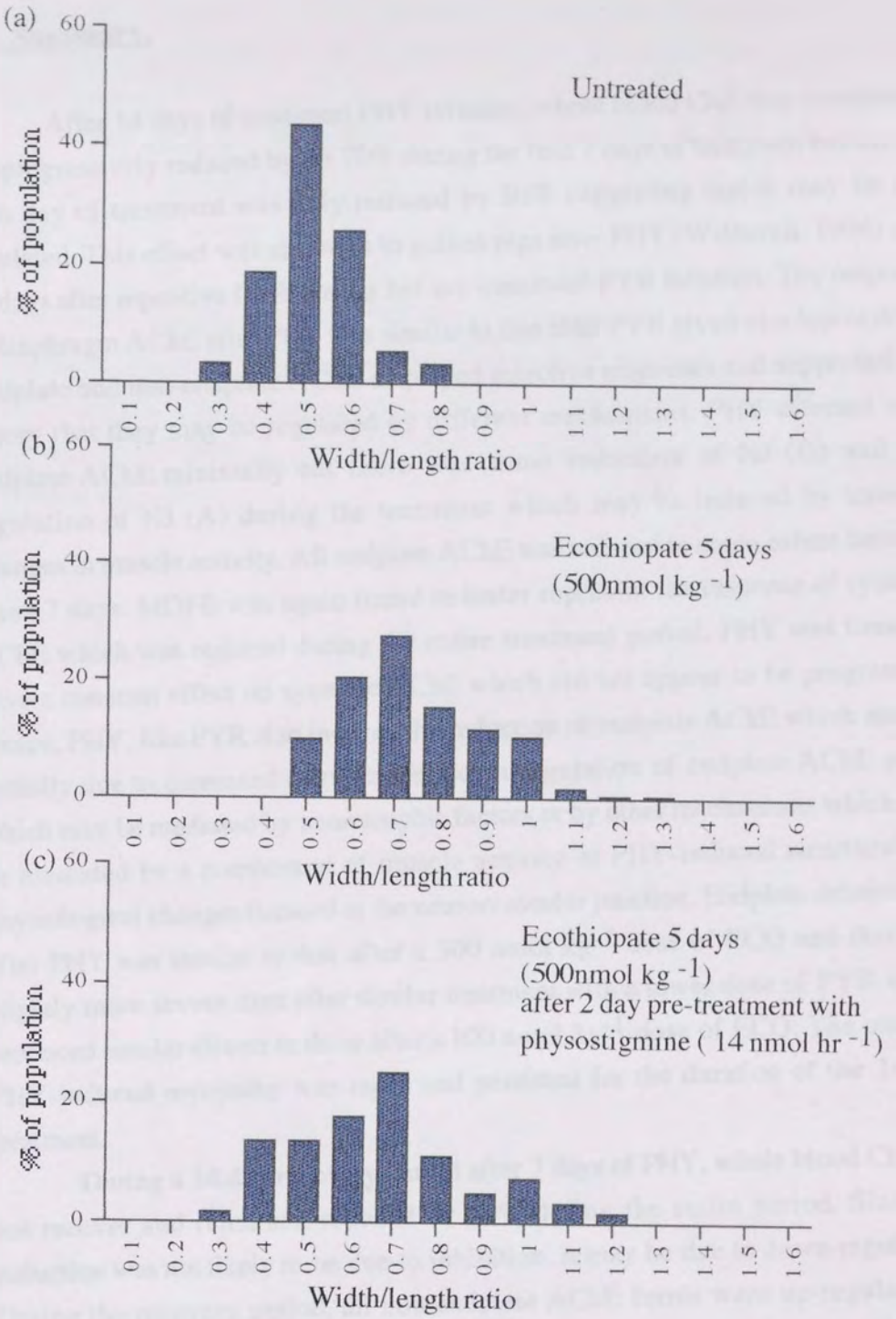

Figure 7.13: Histograms of untreated endplates, 5 days after 500 nmol kg^{-1} ECO and 5 days after 500 nmol kg^{-1} ECO with 2 days of pre-treatment with PHY 14 nmol hr^{-1}. Percentage of endplates per population at given width/length ratios for (a) untreated, (b) 5 days after ECO 500 nmol kg^{-1} and (c) 5 days after ECO with 2 days of PHY pre-treatment.

7.3 Summary.

After 14 days of continual PHY infusion, whole blood ChE was constantly, not progressively reduced by 60-70% during the first 7 days of treatment but on the 14th day of treatment was only reduced by 30% suggesting that it may be up-regulated. This effect was also seen in guinea pigs after PHY (Wetherall, 1994) and 21 days after repetitive PYR dosing but not continual PYR infusion. The response of diaphragm AChE after PHY was similar to that after PYR given at a lower dose. Endplate and non-endplate AChE displayed selective responses and supported the theory that they may be regulated by different mechanisms. PHY affected non-endplate AChE minimally but there was some reduction of NJ (G) and up-regulation of NJ (A) during the treatment which may be induced by transient changes in muscle activity. All endplate AChE was reduced to some extent between 1 and 7 days. MDFE was again found to better represent the response of synaptic AChE which was reduced during the entire treatment period. PHY was found to have a constant effect on synaptic AChE which did not appear to be progressive. Hence, PHY, like PYR also induces the reduction of endplate AChE which may be initially due to increased degradation, down-regulation of endplate AChE genes which may be mediated by neurotrophic factors or by other mechanisms which may be mediated by a component of muscle activity or PHY-induced structural and physiological changes focused at the neuromuscular junction. Endplate deformation after PHY was similar to that after a 300 nmol kg^{-1} dose of ECO and therefore slightly more severe than after similar treatment with a lower dose of PYR which produced similar effects to those after a 100 nmol kg^{-1} dose of ECO. The onset of PHY-induced myopathy was rapid and persisted for the duration of the 14 day treatment.

During a 14 day recovery period after 7 days of PHY, whole blood ChE did not recover and remained reduced by 50% during the entire period. Since the reduction was not likely to be due to inhibition, it may be due to down-regulation. During the recovery period, all non-endplate AChE forms were up-regulated to some extent whereas all the endplate AChE completely recovered within this time. The selective responses of endplate and non-endplate AChE to drug termination was similar to those observed during PYR recovery. However after PHY, endplate AChE took longer to recover suggesting that PHY-induced reduction in endplate AChE may be more persistant even when the drug has been cleared from the system. The up-regulation of non-endplate AChE and recovery of endplate AChE may occur due to increased components of muscle activity or other mechanisms. Endplates did not recover during the recovery period and PHY-induced myopathy

was found to persist longer than that after a necrotising dose of ECO. The rate of recovery of PHY-induced myopathy was slow but there was generally some improvement.

The effect of 2 days of PHY pre-treatment on diaphragm AChE 5 days after an ECO dose differed greatly from the effects after 4 days of lower dose PYR pre-treatment. PHY up-regulated all non-endplate AChE; PYR did not affect them and PHY protected synaptic AChE without affecting other endplate AChE; PYR reduced all endplate AChE. PHY was therefore found to be useful as a pre-treatment against OP toxicity provided it could be given at a dose that did not inhibit brain AChE. PHY pre-treatment neither substantially protected against nor enhanced ECO-induced myopathy. The effect was similar to that observed for PYR given at a lower dose.

CHAPTER 8

GENERAL DISCUSSION AND CONCLUSIONS

8.1. The extraction of mouse diaphragm AChE and the representation of synaptic AChE.

In studying the effects of anti-ChE on mouse skeletal muscle it is important not only to accurately extract AChE but also to accurately represent functionally important AChE associated with the synaptic cleft. The simple method of assaying muscle homogenates, used frequently in previous studies to routinely assess the effects of anti-ChEs, gives a measure of ChE which is a combination of intra- and extra-cellular AChE as well as BChE and does not distinguish between functional and non-functional enzyme. In previous studies of the responses of ChE obtained by this method and the responses of endplate potentials after OP intoxication many discrepancies were found (Bamforth, 1989).

The A12 molecular form of AChE, by the terminology of Massoulie (Massoulie, 1980; Massoulie and Bon, 1982) is involved in the termination of cholinergic transmission at the neuromuscular junction (Hall, 1973). Since the synaptic molecule is part of a family of six different molecular forms of AChE, a suitable method was needed to study the enzyme in isolation which was also suitable for investigating the actions of reversible and irreversible inhibitors. The adapted sequential extraction technique of Younkin et al., (1982) was found in this study to be a rapid and reproducible method for selectively extracting mouse diaphragm AChE and rendered three fractions: G (S1+S2), A (S3+S4) and NE (H5) for junctional and non-junctional muscle strips dissected from diaphragms which corresponded to globular, readily-extractable asymmetric and non-extractable asymmetric AChE fractions respectively. In the absence of a suitable, rapid method for determining endplate AChE directly, it was calculated by subtracting NJ activity from J activity. The sequential extraction method enabled the rapid investigation of responses of endplate and non-endplate low and high molecular weight forms of AChE after a range of treatments.

Velocity sedimentation studies and selective inhibition using ECO on the various forms of AChE, identified the EPS (NE) activity as representing the synaptic A12 functionally active enzyme which agreed with previous work (Younkin et al., 1982). When AChE extracted by the sequential method was used to investigate the relationship between AChE and endplate potentials studied by Bamforth et al., (1989) after OP treatment, it confirmed that the method used by Bamforth did not represent functionally important AChE but only the responses of low molecular weight precursors. Of the sequential extraction fraction activities, EPS (NE) correlated highly with the prolongation of extra-cellular miniature endplate potentials characterised by Fatt and Katz (1950, 1952) 3 hours after a

range of ECO doses and confirmed that this enzyme activity represented synaptic AChE. A relationship was established under known inhibitory conditions between functional AChE activity determined by assay and the consequences of its action determined electrophysiologically and was represented in the form of a reproducible exponential equation. Because, EPS (NE) was determined by a calculation which depended on the activity of other diaphragm enzymes, in ECO recovery and long-term PYR and PHY studies, its activity was largely variable and assumed to give only an indication of the response of synaptic AChE after these treatments, rather than an accurate representation of its biological response. Substitution of $(MEPP)_o$ data into the exponential equation enabled the determination of synaptic AChE activity by an alternative method which was considered to give a better representation of its response in these experiments.

8.2. The distribution of mouse diaphragm AChE.

Many studies have demonstrated that the different molecular forms of AChE have different but overlapping cellular locations (Rotundo and Famborough, 1980a,b; Brockman et al., 1982; Younkin et al., 1982). In the mouse diaphragm neither the globular, nor the readily-extractable asymmetric AChE molecular forms were exclusively associated with endplates or non-endplate regions but were found in both. The high molecular weight A12 collagen-tailed form was largely associated with endplates but a small amount was located in peripheral parts of muscle fibres. This distribution was generally similar to that in the rat diaphragm determined by Younkin et al., (1982) who also discovered by bungarotoxin binding studies that the A12 found in the non-endplate region was not due to stray endplates and therefore genuinely expressed in this region.

A profile of the distribution of internal and external AChE in mouse diaphragm was obtained by selectively inhibiting external AChE with ECO. The use of ECO as a selective inhibitor was demonstrated by Younkin et al., (1982), but the distribution obtained was not found to be precise because ECO had a slow cell-penetrating property and was regarded as an indication of AChE location. In the mouse diaphragm, both endplate and non-endplate regions were found to contain intra- and extra-cellular pools of globular and asymmetric AChE in varying proportions. In the endplate region the A12 form was predominately external which supported its role in the termination of cholinergic transmission, and some A12, of unknown function was also expressed externally in the non-endplate region. The internal and external distributions were similar to those observed in the rat diaphragm (Younkin et al., 1982) and were in agreement with the studies of

Rotundo and Famborough, 1980a,b, Brockman et al., 1982, Donoso and Fernandez, 1985. The location of molecular forms proposed by this study was also in agreement with current knowledge of the synthesis, assembly and processing of AChE. Intra-cellular G AChE corresponds to G1 precursors translated in the RER from AChE mRNA transcribed from AChE genes in endplate and non-endplate nuclei (Rotundo, 1984; Li et al., 1991), G2 and G4 molecules assembled from G1 catalytic subunits by disulphide bonding, molecules at various stages of processing in the Golgi (Bon et al., 1976), molecules in vesicles at various stages of transit through the cell (Porter-Jordan et al., 1986) and in lysosomes associated with degradation (Wake, 1976; Sawyer et al., 1976). In addition, some G AChE is associated with the sarcoplasmic reticulum (Tennyson et al., 1973) and a sizeable proportion of the enzyme is located internally as an inactive pool (Kerem et al., 1993; Lazar et al., 1984). Extra-cellular G AChE is known to be either secreted (Wilson et al., 1973) or exist as integral membrane proteins (Rotundo, 1984a; Inestrosa and Perelman, 1989). Internal A AChE is enzyme at various stages of processing (Rotundo 1984a; Inestrosa, 1984) whereas external A and NE AChE may be either secreted or associated with the extra-cellular matrix.

8.3. CB-induced myopathy.

The measurement of endplate deformation was found to be a rapid and sensitive marker for anti-ChE myopathy (Ancilewski et al., 1994) and provided a quantification of hypercontrations caused by the prolonged action of ACh (Das, 1989; Burd and Ferry, 1987). Anti-ChE induced myopathy is initiated by abnormal cellular Ca^{2+} ion levels (Howl and Publicover, 1987; Rudge and Duncan, 1984; Duncan et al., 1979; Duncan, 1987; Leonard and Salpeter, 1979, Bright et al., 1991, Burd et al., 1989) and is characterised by ultrastructural damage at the neuromuscular junction (Ariens et al., 1969; Fenichel et al., 1972; Fenichel et al., 1974; Laskowski et al., 1975; Kawabuchi et al., 1976; Hudson et al., 1978; Salpeter et al., 1979). Anti-ChE induced hypercontractions initially occur at the synapse but in severe cases, may rapidly progress and affect non-endplate parts of muscle fibres leading to myopathy which affects the whole of the fibre possibly due to inhomogenous contractile states (Ferry and Cullen, 1991). The severity of myopathy and the extent of associated ultrastructural and morphological changes was established after ECO intoxication to be dose-dependent; below 300 nmol kg^{-1} ECO muscle fibre myopathy was defined as mild consisting of slight abnormalities and changes in endplate shape whereas above this dose, the myopathy was characterised by gross cellular changes, loss of sarcolemmal integrity and creatine

kinase release and necrosis (Das, 1989; Townsend, 1988). The development of severe myopathy after OP is associated with a critical level of AChE inhibition in the range 85-90% (Das, 1989; Wecker et al., 1978a,b; Gupta et al., 1985, 1987a,b).

This study demonstrated that the onset and progress of anti-ChE-induced myopathy and fibre hypercontraction frequently demonstrated after OP intoxication also applied to low dose treatment with PYR and PHY. This was previously demonstrated after neostigmine treatment at therapeutic doses which was found to adversely affect neuromuscular ultrastructure and physiology (Tiedt et al., 1978) and induce a myopathy which was initiated by the anti-ChE action of the drug and the prolonged action of unhydrolysed ACh on the post-synaptic membrane (Hudson et al., 1978).

Repetitive low doses of 383 nmol kg^{-1} PYR and continual low dose infusion with 14 nmol hr^{-1} PHY and 11.4 nmol hr^{-1} PYR commonly induced a myopathy which corresponded to that after between 100 and 300 nmol kg^{-1} of ECO and was therefore on the threshold between mild and severe myopathy although no necrosis was seen. In all cases the onset of the CB-induced myopathy, irrespective of treatment was rapid, occurring within a day of treatment, was maintained at a consistent level for the duration of treatment and after 7 days of continual infusion, persisted for more that 14 days after the treatment was terminated. After a 'necrotising' dose of 500 nmol kg^{-1} ECO, the myopathy was completely reversed within 7 days, however, after continual, low dose CB treatment, the rate of recovery was very much slower. The delay in recovery after CB-induced myopathy may be due to subtle effects of these compounds on components of the extra-cellular matrix which direct the regeneration of the neuromuscular junction after damage (McMahan et al., 1980) although this is unlikely as no actual necrosis was observed. Alternatively, hypercontractions may persist after treatment termination due to other CB-induced physiological changes. Current knowledge of the long-term, low dose effects of CBs is limited and largely unclear. This study has demonstrated that long-term low doses of CBs induce a mild myopathy which is persistent and since CBs have important therapeutic roles and have been demonstrated to protect against OP toxicity, this associated myopathy may cause additional problems (Tiedt et al., 1978; Hudson et al., 1978).

8.4. Effects of long-term CB treatment on AChE.

There is currently very limited knowledge available on the long-term, low dose effects of CBs on skeletal muscle molecular forms of AChE or the

mechanisms by which these effects become manifest. In this study, it was evident that CB treatment influences the metabolism and regulation of AChE not only during drug administration but also in the period after the drug treatment ended. The responses of AChE molecular forms have generally been studied after OP intoxication and the mechanisms by which enzyme activity recovers after anti-ChE treatment is poorly understood as data provided by the literature is confusing.

Preliminary investigations indicated that the methods employed in the study did not give a measure of the inhibitory effects of CBs, or indicate to what extent inhibition had occurred *in vivo*. The data, therefore presented a profile of the metabolic responses of AChE molecular forms to the treatments. A common feature of AChE response to CBs was the selective responses of endplate and non-endplate AChE during treatment and recovery suggesting that they may exist in biologically distinct compartments which are subject to differential regulation. Several studies have demonstrated that endplate and non-endplate regions of muscle fibres represent highly differentiated domains with respect to structure and molecular accumulation (Froehner, 1991; Cartaud and Chanqeux, 1993; Hall and Sanes, 1993). The organisation of non-endplate muscle fibre parts is regulated by muscle activity whereas the integrity of neuromuscular junction is maintained by both muscle activity and nerve-derived trophic factors (Jasmin et al., 1995). The activity of endplate and non-endplate AChE is also subject to this differential regulation; non-endplate AChE is regulated by muscle activity whereas endplate activity is regulated by both muscle activity and neurotrophic factors (Younkin and Younkin, 1988). However, the mechanism by which this regulation is implemented or the precise level at which it acts in the metabolism of AChE is unknown and Ca^{2+} ion loading into the endplate may additionally contribute to the complexity of the events. After OP-intoxication, non-endplate and endplate AChE also displayed selective responses and were found to recover at different rates (Van Dongen et al., 1988; Grubic et al., 1981; Fernandez and Stiles, 1984) supporting the theory that the enzyme may be differentially regulated.

PYR and PHY both reduced the activity of all endplate AChE during 14 days of continual infusion but a corresponding effect was not observed in non-endplate AChE which tended to be only transiently increased or decreased. During 14 days of recovery after 7 days of PYR or PHY treatment at their respective doses, all affected endplate AChE completely recovered within the 14 day period, whereas non-endplate AChE was up-regulated, in some cases by a considerable amount. Studies of endplate potentials indicated that synaptic AChE during both treatments was reduced rapidly and remained so until the treatment was terminated. The effects induced by PHY were in general more pronounced than those induced by PYR

which was expected due to the differences in the doses given although the myopathies induced by each compound were largely the same. The prolongation of $(MEPPs)_o$ at each of the time points after each drug treatment was not found to be significantly different when a comparison was made, but the onset of jitter occured earlier after PHY treatment (A. Crofts, unpublished) suggesting that the differences in effects were probably not largely due to the slight difference in doses used of each drug, but may be due to drug potency. This was best demonstrated by the response of blood ChE: PHY caused around 60-70% inhibition whereas PYR caused only 30-50% inhibition. The distinction may arise from the structures of the compounds: PYR is a quaternary compound which does not readily access the cell, whereas PHY is tertiary and can traverse cell membranes.

Since the preliminary CB studies indicated that due to the rapid decarbamoylation rates of PYR and PHY-inhibited AChE, which could not be prevented during assay preparation, it was unlikely that the reductions in endplate AChE were due to inhibition and were probably due to genuine reductions. Studies of $(MEPPs)_o$ also indicated that the prolonged decay phase observed during the treatments was not due to inhibition but enzyme depletion (A. Crofts, unpublished). In addition, it is unlikely that the effects on AChE induced by the CBs resulted indirectly from pre- or post-synaptic membrane or receptor effects of these drugs because the concentrations used were low (Alderdice, 1982) and no pre-synaptic effects were observed during the treatments (A. Crofts, unpublished). It was evident therefore that the changes in AChE metabolism were additional to any inhibition which had occurred during the treatments and were probably indirectly due to the anti-ChE action of these CBs and physiological changes induced by them. The synaptic AChE form appeared to be affected before there was evidence of any significant reduction in the precursory forms. The rapid disappearance of endplate AChE also occurs after denervation (Newman et al., 1984). Because the reduction in synaptic AChE after CBs and denervation occurs so rapidly and the enzyme is known to have a slow turnover, (Lazar et al, 1984; Newman et al., 1984), it is unlikely that the initial reduction is due to the down-regulation of endplate AChE genes and may be due to accelerated degradation. Younkin and Younkin (1988) proposed that endplate AChE may be regulated not only by the rate of synthesis but also by the rate of degradation and both rates may depend on muscle activity, trophic factors or both. After denervation rapid AChE decline may be due to proteolysis induced by nerve degeneration whereas, after CBs, synaptic AChE degradation may be due to proteolysis by factors which are released and mediate early events in anti-ChE induced myopathy such as Ca^{2+}-activated neutral proteases (Kar and Pearson, 1976). It is possible that the reductions in synaptic

AChE and precursory forms observed during the remainder of the treatment may be due to down-regulation of endplate AChE genes because all the molecular forms are affected. Since, the non-endplate enzymes are not largely effected by PYR or PHY, the endplate reductions may be due to CB-induced effects on trophic factors which only regulate endplate AChE.

The mechanisms by which neurotrophic factors regulate AChE expression and activity after CB treatment is unknown. A wide variety of factors have been implicated in the regulation of AChE expression. These include POMC peptides which are released into circulation following stress and myopathy (Rosier et al., 1977). These peptides and their derivatives directly regulate AChE expression in the superior cervical ganglion of cat (Koelle, 1988) and cultured embryonic cells (Haynes and Smith, 1984, 1985). Plasma-circulating glucocorticoids, which are known transcriptional controllers (Muller and Renkavitz, 1991) have also been shown to regulate AChE synthesis (Brank and Grubic, 1993) and may do so according to environmental demands. In addition, a host of other substances including: diffusible substances produced by the spinal cord, brain extracts, soluble extracts of peripheral nerves, sciatic nerve extracts, transferrin in the serum and neural peptides (reviewed by Oh et al., 1988) may be involved. ACh can also be categorised as a neurotrophic factor (Drachman et al., 1982) and have a potential influence on muscle AChE. It is possible that pre-synaptic responses to prolonged post-synaptic receptor agonism induced by anti-ChEs may affect the muscle AChE activity and there is believed to be a relationship between neurally regulated ACh release and AChE synthesis (Karalliedde and Henry, 1993). Studies have shown that the prolonged action of ACh on its receptor leads to receptor desensitisation and despite the initial high levels of ACh in the cleft, the synthesis and release of ACh from the nerve terminal decreases (Karalliedde and Henry, 1993). ACh down-regulation may arise from negative feedback control of its synthesis (Bowman et al., 1984) after anti-ChE-induced prolonged action or because the nerve is deprived of choline which it required for ACh re-synthesis (Karalliedde and Henry, 1993). It is possible that the down-regulation of ACh may also induce the down-regulation of ACh receptors and since the receptors and AChE are synthesised in the muscle and co-transported to the sarcolemma (Rotundo and Fambrough, 1980b), the reduction in endplate AChE may be a side-effect of reduced receptor production or targeting. In addition, if anti-ChE indirectly affect ACh or ACh receptor metabolism, then it is possible that associated factors which also function in AChE metabolism may be responsible for the observed changes. For instance, agrin, which functions in the selective accumulation of ACh receptors at their membrane target sites, also has a role in directing the extra-cellular location of AChE (Leith and Fallon, 1993;

Wallace, 1989). Whether the selective endplate AChE reductions are due to neurotrophic factors or are a by-product of CB-induced changes in the metabolism of other synaptic components cannot however be clarified by this study and requires further investigation.

Muscle activity cannot, however, be completely ruled out as a possible mediator between CB action and changes in AChE metabolism. Many studies have demonstrated that muscle activity, which collectively describes the occurrence and frequency of muscle contractions and all the associated electrical and ionic events, is important in regulating the expression and activity of muscle proteins and enzymes. The pattern of impulses passing from the nerve to the muscle has been demonstrated to regulate the transcription of myosin proteins (Weeds et al., 1974; Buckingham et al., 1984) and nerve-dependent muscle activity has also been linked to the regulation of both endplate and non-endplate AChE by controlling its synthesis although trophic factors additionally regulate endplate AChE (Younkin and Younkin, 1988). In addition, innervation has also been shown to control the amounts of AChE oligomers synthesised (Lomo et al., 1983). Muscle activity however defines a broad range of cellular processes and it is not known which component or collection of components is directly responsible for maintaining the synthesis, diversity and activity of AChE. Several studies have shown that both the amount and pattern of transmission across the neuromuscular junction can directly effect AChE activity (Reiger et al., 1980a; Rubin, 1985; Guth and Zalewski, 1963; Lubinska, 1966; Hall, 1973; Collins and Younkin, 1982; Bacou et al, 1978; Silman et al, 1979; Fernandez et al, 1980) but the mechanism by which muscle activity regulates AChE has not yet been eludicated. In addition, the effects of anti-ChE on the normal regulation of diaphragm AChE by muscle activity is unclear. Increased muscle hyperactivity has been associated with anti-ChE action due to the prolonged action of ACh on its receptors but the responses observed in this study of AChE activity after anti-ChE which occur in parallel to the inhibition caused by the CB agents are not consistent with the documented responses to increased muscle activity. Studies have shown that increased muscle activity increases AChE synthesis (Barnard et al, 1984) possibly by up-regulating AChE genes (Sveistrup et al., 1995) which contrasted with the observed reduction in all endplate AChE activity following anti-ChEs in this study. It would appear therefore that whilst the CBs had little effect on the synthesis or activity of non-endplate AChE, other than possibly inhibiting it *in vivo* during the treatment, on the contrary endplate AChE was increasing degraded, down-regulated or its synthesis depressed in addition to being inhibited *in vivo*. This is in conflict with the expected response of endplate AChE when ACh in the cleft is in excess which should be up-regulated to destroy

the excess ACh and the loss of synaptic AChE may contribute to the affects posed by the CBs, rather than counteract them. However, the significance of the transient changes during treatment in non-endplate AChE cannot be over-looked and may arise from changes in components of muscle activity which may have arisen in the non-endplate parts of muscle fibres. During severe myopathy which leads to necrosis, contractions clumps have been located in fibres around the endplate regions (Ferry and Cullen, 1991; Das, 1989). It is unlikely, however, that the low doses of CBs used would cause any dramatic morphological changes in non-endplate fibres; diaphragms were checked using the Procion Yellow stain for damaged membranes (Flanagan et al., 1974) after CB treatment and all fibres tested were found to be intact. The transient changes in non-endplate AChE may therefore be due to subtle alterations in components of muscle activity which could not be detected by the methods used. Also, since it not known which component or collection of inter-acting components of muscle activity are responsible for regulating AChE activity, it is possible that whilst overall, the CBs apparently increased muscle activity, some components of muscle activity which regulate AChE activity may be affected such that a conflicting signal is sent to down-regulate the expression of the enzyme at the endplate. It is possible that receptor desensitisation which occurs when the ACh receptor is continuously exposed to ACh for more that several milliseconds (Katz and Thesleff, 1957; Magleby and Pallotta, 1981) may act as such a signal. In addition, there was some evidence of spontaneous twitching occuring late in the drug infusion periods (A. Crofts, unpublished) suggesting that the endplate region may become more excitable but it is unknown what relevence, if any, these changes have to the effects observed in enzyme levels. Alternatively, since many of the cellular responses induced by anti-ChE are localised at the endplate where the onset of myopathy occurs, it is possible that the disruption of neuromuscular structure and integrity may also disrupt the intra-cellular organisation of organelles important in the metabolism of AChE (the small drug doses used may dilate the sarcoplasmic reticulum and affect nuclei) resulting in the inability of the region to successfully express, process or target the enzyme. It was concluded therefore, that during continuous CB treatment, the metabolism of both endplate and non-endplate AChE may be affected by unknown mechanisms which may be mediated by normal or abnormal muscle activity, neurotrophic factors or CB-induced structural and physiological changes at the neuromuscular junction or peripheral parts of muscle fibres.

When PYR and PHY treatment given continually at a low dose for 7 days was terminated, endplate AChE levels gradually returned to normal, but non-endplate AChE activities, previously unaffected were in excess of normal levels.

These increases were not thought to reflect a combination of decarbamoylated and newly synthesised AChE which only manifested on treatment termination because these enzyme were measured at normal levels during dosing and not at inhibited levels. Up-regulation of mouse diaphragm AChE was also observed during recovery after long-term repetitive PYR dosing (Lintern et al., 1996). Non-endplate AChE is primarily regulated by muscle activity (Newman et al., 1984; Younkin and Younkin, 1988) and evidence of the up-regulation of this enzyme suggests that the non-endplate region has received a signal that muscle activity has increased. There was no evidence of up-regulation in the endplate region but because no inhibition was assessed in this study, the recovery of endplate AChE, previously reduced throughout the treatment was not due to reactivation of inhibited enzyme and must therefore be due to increased synthesis. It is possible therefore that synthesis of AChE in both regions was increased, but this effect in the endplate region was observed as a recovery rather than as up-regulation because it was previously reduced.

The signal which initiates this increase in synthesis is unclear, but may be due to the increased influence of a regulatory component of muscle activity. There was no evidence to suggest that cholinergic transmission after treatment termination had increased as $(MEPPs)_o$ were recorded as normal (A. Crofts, unpublished). However, observations of muscle fibre morphology showed that hypercontractions persisted long after the CB drugs had been cleared from the circulation. Hypercontractions after anti-ChEs are associated with increases in cellular Ca^{2+} ion concentrations. Studies of developing synapses have shown that transient increases in intra-cellular Ca^{2+} enhance the expression of AChE by stabilising AChE mRNA transcripts (Luo et al., 1994). There may therefore be an important link between hypercontractions and cellular Ca^{2+} levels and the increased synthesis of AChE after CB treatment. The relationship between muscle activity and AChE synthesis and activity after CBs could not be elucidated from this study and requires further investigation. From the electrophysiological studies which were conducted in parallel to the assessment of AChE activity during CB treatment, there was no evidence to suggest that during the dosing or recovery period, muscle activity in general had been dramatically affected (A. Crofts, unpublished) and does not provide an adequate explanation for the up- and down-regulation of diaphragm AChE. However, after low doses of both PYR and PHY, an increase was observed in the latency of action potentials (i.e. increased jitter characterised by Kelly et al, 1990) which began during the treatments and persisted until after the treatments were terminated (A. Crofts, unpublished). Since the cause and origin of jitter is unclear but manifested as a subtle change after anti-ChE treatment, a connection

between effects on AChE regulation and this phenomenon cannot be strictly ruled out.

The mechanism by which AChE activity recovers after anti-ChE is unclear and complex. However, several analogies could be made between the recovery of AChE after OP treatment and the responses observed in this study after CBs. Several studies have suggested that after reversible inhibition, AChE activity recovers by a bi-phasic mechanism (Goudou and Reiger, 1983; Koelle et al., 1982) which comprises of a rapid initial phase of precursor synthesis followed by a slow period when asymmetric forms are restored. An early event after OP-induced AChE inactivation is the increased synthesis of G1 (Reiger et al., 1976; Grubic et al., 1981; Goudou and Rieger, 1981). Since after CB treatment termination, the synthesis of AChE also increased, it is possible that the regulatory signal which triggers this event is the same after both OP and CB compounds. In addition, after OPs, a delay was observed in the appearance of asymmetric forms which may be due to an inability of these newly synthesised forms to attach to their locations (Grubic et al., 1981), problems with targeting and exocytosis which may be related to abnormal Ca^{2+} levels or effects of neurotrophic factors such as agrin which function in accumulating AChE at the basal lamina (Leith and Fallon, 1993; Wallace, 1989). Hence, OPs like CBs also appear to affect the metabolism of AChE and these effects may manifest through a common mediator. After the OP soman, AChE synthesis was found to be induced not only in the RER but also in the sarcoplasmic reticulum and specialised tubule structures under the endplate region. A similar pattern of AChE synthesis was observed in the post natal development of rats and suggested that there were analogies between the regulation of developing systems and systems affected by anti-ChEs. Since the POMC peptides have an important role in regulating AChE in post natal vertebrates (Haynes et al., 1984) these may also have an important role in AChE regulation after OPs and CBs. Goudou and Reiger (1983) demonstrated that after OPs, the A12 functional form was synthesised in the non-endplate region which suggests that after endplate AChE depletion or suppression, the enzyme may be made in regions not effected by the metabolic restraints and mobilised to regions where it is needed. This may account for the up-regulation of non-endplate AChE after CB treatment and suggests that the function of non-endplate AChE, which is largely unclear, may be to replenish endplate AChE in the event of cellular stress.

In recent literature, is has been documented that after chronic as well as acute anti-ChE treatment, target systems may develop a 'tolerance' to these drugs (Van Dongen and Wolthuis, 1989). It is possible that during the treatment, the metabolism of AChE adapts or 'learns' to operate under a different set of signals

dictated by the drug treatment but when the signals are removed, the synthesis of AChE increases because the physiological restrictions imposed by the treatment have been removed. The development of tolerance to continual drug administration may occur at various levels; pre-synaptically, synaptically and post-synaptically (Van Dongen and Wolthuis, 1989) and it is possible that once these cellular changes or adaptations have been instigated, they are maintained for a period of time after the drug treatment has been terminated and may be responsible for the 'abnormal' levels of mouse diaphragm AChE seen after CB treatment.

The responses of endplate and non-endplate AChE to continuous low doses of PYR and PHY suggest that as well as inhibiting these enzymes, the CBs may also effect their regulation and metabolism. The level at which these metabolic effects manifest is unclear and extremely complex and beyond the scope of this study. It is evident from the study, that CB compounds can instigate a host of unexplained responses other than reversibly inhibiting AChE or at higher doses, having direct actions on the pre- and post- synaptic membranes. It is not known to what extent these responses can adversely effect skeletal muscle function after long-term treatment and the issues raised in the study open a host of research possibilities.

8.5. CB protection against OP-induced AChE inhibition and myopathy.

The protection against OP-intoxication by CB pre-treatment has previously been demonstrated using PYR (Berry and Davis, 1970; Gordon et al., 1978; Ellin and Kaminskis, 1989; French at al., 1979; Dirnhuber at al., 1979) and PHY (Leadbeater et al., 1985; Lennox et al., 1992; von Bredlow et al., 1991) and depends primarily on the reversible inhibitory properties of these compounds (Berry and Davies, 1970). Chronic CB treatment also reduces the number of post-synaptic ACh receptors and the amount of ACh released after nerve stimulation (Change et al., 1973) which may also be of therapeutic significance after OP treatment. However, none of these previous studies have investigated the effects of long-term low dosing with CBs on the various molecular forms of AChE or the isolated response of synaptic AChE.

In this study, it was found that 4 days of low dose PYR pre-treatment did not protect synaptic AChE against a large dose of ECO and reduced the activity of other endplate molecular forms. The lack of protection offered by PYR conflicted with data proposed by French et al., (1979), but was confirmed by responses recorded electrophysiologically from experiments run in parallel (A. Crofts,

personal communication). PHY, in contrast, protected the synaptically important enzyme but also induced abnormally high levels of AChE in non-endplate parts of muscle. The protective property of PHY agreed with data provided in the literature and data recorded electrophysiologically (A. Crofts, unpublished). The differences in the levels of protection offered by these compounds to diaphragm AChE is unclear but it is evident that a combination of low dose CB pre-treatment and large dose OP induces alterations in skeletal muscle metabolism.

Both PYR and PHY induce a moderate and persistent myopathy which may manifest during any therapeutic or prophylactic use and the use of PHY as a pre-treatment slightly improvement but generally pre-treatment with both drugs did not enhance the myopathy 5 days after a large dose of ECO. However, the study did not investigate whether the myopathy associated with ECO alone would be made more persistent if either CB was given in advance and did not eliminate any possible long-term side affects associated with such pre-treatment.

APPENDIX

A.1. Composition of solutions used in ChE assays.

A.1.1. Colour reagent: 5-5 dithiobis (2 nitro-benzoic) acid (DTNB).

A stock solution of concentration 0.01M was prepared which kept for approx. 1 week at 4°C. Table A.1.1 shows the composition of the stock solution. The assay solution of DTNB was prepared by diluting the stock solution 1:40 with distilled water. Table A.1.2 shows the composition of the phosphate buffer used in the preparation of DTNB stock.

	Amount
DTNB	39.6 mg
$NaHCO_3$	15.0 mg
0.1M phosphate buffer pH7.0	10.0 ml

Table A.1: Composition of 0.01M DTNB stock solution.

	Amount
0.2M $Na_2PO_4.12H_2O$	30.5 ml
0.2M $NaH_2PO_4.2H_2O$	19.5 ml
Distilled water	50.0 ml

Table A.2: Composition of 0.1M phosphate buffer pH7.0.

A.1.2. Substrate: Acetylthiocholine iodide

Acetylthiocholine iodide substrate was prepared to give a final cuvette concentration of 0.5mM. The substrate was prepared as required as it was too unstable to be stored. The composition of the stock solution is shown below.

	Amount
Acetylthiocholine iodide	21.7 mg
Distilled water	50.0 ml

Table A.3: Composition of acetylcholine iodide solution.

A.1.3. Phosphate buffer, pH8.0.

Phosphate buffer, pH8.0 was used routinely in the extraction of blood ChE and the composition is shown below.

	Amount
0.2M Na_2HPO_4	47.4 ml
0.2M NaH_2PO_4	2.6 ml
Distilled water	50.0 ml

Table A.4: Composition of 0.1M phosphate buffer pH8.0

A.1.4. Low ionic strength buffer.

Low ionic strength pH7.0 phosphate buffer (LIB) was used routinely in the extraction of low molecular weight molecular forms of AChE from the mouse diaphragm. The composition of the buffer is shown below.

	Amount
Phosphate buffer, pH7.0	10 mM
Triton X100	1.0%

Table A.5: Composition of low ionic strength phosphate buffer.

A.1.5. High ionic strength buffer.

High ionic strength buffer (HIB) was used routinely to extract high molecular weight forms of AChE from the mouse diaphragm. It was prepared by adding 1.0M sodium chloride to LIB in Table A.5.

A.2. Enzyme kinetics.

The kinetics of purified electric eel AChE ($AChE_{(eel)}$) obtained from Sigma and ChE from junctional and non-junctional homogenates obtained by the conventional extraction technique was investigated to determine to optimum concentration of substrate to be used in routine assays. Figure A.1(a) shows the Lineweaver-Burke double reciprocal plots of the inverse of substrate (acetylthiocholine iodide) concentration (mM) versus the inverse of $AChE_{(eel)}$

activity expressed as the rate of change of absorbance at 412nm at enzyme concentrations of 0.002 and 0.02 units ml^{-1}. Figure A.1 (b) shows the Lineweaver-Burke plots of the inverse of substrate concentration versus the inverse of junctional and non-junctional activity expressed as the rate of change of absorbance at 412nm. From the plots the x-axis intercept rendered -1/Km and the y-axis intercept rendered 1/Vmax. The slope of the lines gave Km/Vmax.

Km and Vmax values for the enzymes are shown below.

Enzyme	**Km (mM)**	**Vmax (rate of change of absorbance min^{-1}**
$AChE_{(eel)}$ 0.002 units ml^{-1}	0.24	0.018
$AChE_{(eel)}$ 0.02 units ml^{-1}	0.10	0.036
Junctional ChE	0.19	0.017
Non-junctional ChE	0.23	0.013

Table A.6: Km and Vmax values for $AChE_{(eel)}$ and diaphragm ChE.

A.3. Verification of biological effects.

To test whether the effects observed during continual infusion experiments in Chapters 6 and 7 were truly biological it was important to eliminate all possible experimental factors. Since fluctuations were observed in the levels of AChE an experiment was set up to check to pumping rate of the Alzet pumps to establish whether the drugs were being administered at a constant daily dosage. Hence, the release of a coloured compound with a distinctive absorbance peak, Coomasie Brilliant Blue was monitored using spectrophotometric analysis (see Chapter 2, Section 2.2.3.5)

Table A.1 shows the daily emission of Coomasie Blue in μg during a period of 10 days. The pump was filled with a known concentration and based on the pump specifications the expected compound emission was calculated to be 198μg in 24 hours. It was observed that a steady pumping rate was not achieved until the second day of pumping and after the recommended pumping life there was still some emission on days 8-10. However, during the intermediary period of 2-7

days, the compound was being emitted at a relatively consistent rate which was not coincidental with enzyme activity fluctuations hence, the effects observed during the administration of drugs were likely to be biological and not due to erratic pumping.

In addition to testing the constancy of drug delivery, a further precaution was taken against the influence of pump action on the data by exploring the authenticity of the progressive effects observed during the drug dosing regimes. Since, the general trend of the progression appeared to be a reduction in enzyme activity reaching a minimum at 7 days, an experiment was performed to check that this effect was not attributable only to the Alzet Model 2001 ($1.0\mu l\ hr^{-1}$) 7 day pump. Enzyme levels were measured in mice which received to same daily dose of pyridostigmine but were implanted with the Alzet Model 2002 ($0.5\mu l\ hr^{-1}$) 14 day pump. There was found to be no significant difference (Mann-Whitney non-parametric test) between enzyme activity after 7 days of drug delivery by either model and the same biological effects were observed in each case.

From the pump test experiments, it was evident that there was still some emission from the pump after 7 days, i.e. on days 8 and 9. Hence, in recovery experiment, the pumps had to be surgically removed form the mice to ensure that an accurate assessment of recovery was being made.

Time during Alzet Pumping Life	**μg of Coomasie Blue**
0-4 hrs (Priming Period)	1.9
1 day	85.6
2 days	112.1
3 days	124.3
4 days	118.7
5 days	126.2
6 days	123.2
7 days	105.2
8 days	87.7
9 days	79.1
10 days	27.2

Table A.7: Daily emission of Coomassie Blue in μg from osmotic pump over a ten day period.

A.4 Electrophysiological data.

Table A.8 shows the means of the time to half amplitude of extracellularly recorded miniature endplate potentials ($T_{50\%}$ of $(MEPPs)_o$) for pyridostigmine (PYR) and physostigmine (PHY) Alzet osmotic pump infusion experiments. The data was recorded and processed by A. Crofts and was carried out in conjunction with the analysis of the effects of PYR and PHY on mouse skeletal muscle AChE activities. The $T_{50\%}$ values were used to predict functional AChE activities in Chapters 6 and 7 using the relationship established in Chapter 4.

Time during drug infusion	**$T_{50\%}$ (ms) for PYR dosing**	**$T_{50\%}$ (ms) for PHY dosing**
Untreated	0.46 ±0.05	0.46 ±0.05
1 day	0.62 ±0.11	0.63 ±0.11
2 days	0.72 ±0.11	0.67 ±0.06
4 days	0.82 ±0.07	0.70 ±0.08
7 days	0.97 ±0.18	0.72 ±0.09
14 days	1.08 ±0.14	0.91 ±0.12
7 day + 2 day recovery	0.66 ±0.05	0.66 ±0.17
7 day + 7 day recovery	0.46 ±0.04	0.46 ±0.11
7 day + 14 day recovery	0.45 ±0.05	0.46 ±0.05

Table A.8: $T_{50\%}$ values of $(MEPPs)_o$ at various time points during PYR and PHY infusion and recovery experiment. Values shown are means ± s.d.

A.5 Inter-slide variation of endplates (ANOVA test).

The normal procedure for sampling endplates from hemidiaphragms after different treatments involved measuring 30 endplates from each slide at a given dose. The ANOVA one-way test was applied to groups of 30 endplates from a range of hemidiaphragms after the same treatment to investigate the occurence of inter-slide variation. The F-test (i.e ratio of between slide varience to within endplate group (n=30) varience results are shown in Table A.9.

Dose	Width F-test	Width p value	Length F-test	Length p value	W/L F-test	W/L p value	No. of slides
Un-treated	1.5	<0.25	**7.4**	<0.0001	4.8	<0.005	8
ECO 25	**8.0**	<0.0001	**13.4**	<0.0001	2.7	<0.05	4
ECO 50	0.3	>0.25	1.6	<0.25	1.2	>0.25	3
ECO 100	5.8	<0.005	**16.8**	<0.0001	4.1	<0.01	4
ECO 300	3.5	<0.1	0.6	>0.25	0.9	>0.25	2
ECO 500	3.4	<0.01	**14.7**	<0.0001	**8.0**	<0.0001	6
ECO 6HR	1.3	<0.25	1.6	<0.25	0.1	>0.25	2
ECO 1D	9.1	<0.005	1.3	>0.25	8.0	<0.005	3
ECO 5D	2.9	<0.05	**7.4**	<0.0001	**6.8**	<0.0001	5
ECO 7D	0.4	>0.25	0.5	>0.25	3.0	<0.1	2
PYR 1D	2.4	<0.1	**11.6**	<0.0001	**9.5**	<0.0001	5
PYR 2D	3.5	<0.025	**22.0**	<0.0001	**14.1**	<0.0001	4
PYR 4D	1.7	<0.25	2.3	<0.1	2.8	<0.05	5
PYR 7D	5.1	<0.005	**10.1**	<0.0001	6.9	<0.005	4
PYR 14D	0.1	>0.25	4.5	<0.025	5.9	<0.005	3
PYR 2DR	5.2	<0.005	**12.6**	<0.0001	3.6	<0.01	5
PYR 7DR	0.2	>0.25	24.0	<0.25	1.8	<0.25	3
PYR 14DR	**5.1**	<0.0001	**10.1**	<0.0001	**10.5**	<0.0001	7
PYR/ECO	**15.2**	<0.0001	0.5	>0.25	**18.7**	<0.0001	4
RD 3HR	2.9	<0.05	0.6	>0.25	1.1	>0.25	4
RD 1D	0.4	>0.25	1.0	>0.25	0.5	>0.25	4
RD 2D	5.1	<0.005	4.2	<0.01	**11.1**	<0.0001	4
RD 3D	2.8	<0.05	0.6	>0.25	0.6	>0.25	4
RD 4D	0.5	>0.25	5.4	<0.005	2.7	<0.05	4
RD 7D	6.7	<0.005	**8.0**	<0.0001	**22.0**	<0.0001	4
RD 14D	2.1	<0.1	4.7	<0.005	7.8	<0.005	4
RD 21D	4.7	<0.005	6.2	<0.005	**16.4**	<0.0001	4
PHY 1D	0.5	>0.25	3.3	<0.025	1.6	<0.25	4
PHY 2D	1.8	<0.25	1.0	>0.25	0.1	>0.25	4
PHY 4D	1.1	>0.25	6.9	<0.005	4.9	<0.005	4
PHY 7D	3.2	<0.05	7.5	<0.005	3.2	<0.05	4
PHY 14D	7.8	<0.005	6.5	<0.005	5.3	<0.01	3
PHY 2DR	1.0	>0.25	0.0	>0.25	0.3	>0.25	2
PHY 7DR	1.6	<0.25	7.0	<0.005	6.6	<0.005	4
PHY 14DR	4.5	<0.01	**15.2**	<0.0001	7.9	<0.005	4
PHY/ECO	1.4	<0.25	5.7	<0.005	3.1	<0.05	4

Table A.9: F-test and p values obtained by ANOVA analysis of inter-slide variation. Endplate groups from slides which display a highly significant inter-slide variation are highlighted in bold.

A.6 Molecular form activities after implantation of osmotic pump filled with 0.9% saline.

To investigate whether the implantation of osmotic pumps affected the activity of AChE molecular forms, mice were implanted with pumps containing only 0.9% saline. Table A.10 shows the AChE activities from untreated mice and mice which had been implanted with saline-filed pumps. Statistically there was not found to be any significant difference between untreated activities and those after pump implantation (Mann-Whitney, P>0.1 in all cases) hence in PYR and PHY experiments the data was pooled together.

AChE	**Untreated**	**0.9% Saline-filled pumps**
N	10	3
J (G)	3.46±0.48	3.56±1.23
J (A)	1.32±0.25	1.21±0.49
J (NE)	0.80±0.20	0.78±0.18
NJ (G)	1.96±0.40	1.71±0.75
NJ (A)	0.77±0.26	0.68±0.40
NJ (NE)	0.29±0.15	0.28±0.22
EPS (G)	1.57±0.61	1.86±0.57
EPS (A)	0.66±0.26	0.83±0.56
EPS (NE)	0.50±0.26	0.50±0.06

Table A.10: Molecular forms activities from untreated mice and 24 hours after implantation of 0.9% saline-filled pumps.

REFERENCES

Affolter, H. and Carfoli, E. (1980). The Ca^{2+}-Na^{+} antiporter of heart mitochondria operates electroneutrally. Biochem. Biophys. Res. Commun. **95**, 193-196.

Alderdice, M.T. (1982). Further comparison of the effects of physostigmine and neostigmine on frog neuromuscular transmission. Clin. Exp. Pharm. Physiol. **9**, 35-43.

Amos, M.L., Smith, M.E. and Ferry, C.B. (1995). Effect of anticholinesterase treatment on the expression of pro-opiomelanocortin in motoneurones. Brain Research Association Abstracts. **12**, 76.

Ancilewski, A., Crofts, A., Ferry, C.B. and Smith, M.E. (1996). Endplate deformation: a sensitive indicator of anticholinesterase intoxication. Human and Experimental Toxicology, in Press .

Anderson, M.G. and Fambrough, D.M. (1983). Aggregates of acetylcholine receptors are associated with plaques of a basal lamina heparan sulfate proteoglycan on the surface of skeletal muscle fibres. J. Cell. Biol. **97**, 1396-1411.

Anglister, L. and McMahan, U.J. (1985). Basal lamina directs acetylcholinesterase accumulation at synaptic sites in regenerating muscle. J. Cell. Biol. **101**, 735-743.

Appleyard, M.E. (1992). Secreted acetylcholinesterase: non-classical aspects of a classical enzyme. Trends Neuroscience. **15**, 485-490.

Anglister, L. and Silman, I. (1978). Molecular structure of elongated forms of electric eel acetylcholinesterase. J. Mol. Biol. **125**, 293-311.

Ariens, A. T., Meeter, E., Wolthius, O. L. and Van Bethem, R. M. J. (1969). Reversible necrosis at the endplate region in striated muscles of the rat poisoned with cholinesterase inhibitors. Experientia. **23**, 57-59.

Bacou, F., Vigneron, P. and Massoulie, J. (1982). Acetylcholinesterase forms in the fast and slow rabbit muscle. Nature. **296**, 661-663.

Bamforth, J. P. (1989). The effects of persistant anticholinesterase action at the neuromuscular junction. PhD thesis, Aston University.

Banker, B. Q., Kelly, S. S. and Robbins, N. (1982). Neuromuscular transmission and correlative morphology in young and old mice. J. Physiol. **339**, 353-375.

Barker, M.D. and Brin, M (1975). Mechansims of lipid peroxidation in erythrocytes of Vitamin E-defficient rats and in phospholipid model systems. Arch. Biochem. Biophys. **116**, 32-40

Barnard, E.A., Barnard, P.J., Jarvis, J., Jedrzejczyk, J., Lai, J., Pizzey, J. A. and Randall, W.R. (1984). Multiple molecular forms of acetylcholinesterase and their relationship to muscle function. In: "Cholinesterases." Walter de Gruyter and Co., Berlin-New York.

Barnard, E. A., Rimazewska, T. and Wieckowski, J. (1971). Cholinesterases at individual neuromuscular junctions. In: Triggle, D. J., Moran, J. F. and Barnard, E. A. (ed.) Cholinergic Ligand Interactions. New York, Academic Press, 175-200.

Barnard, E.A., Wieckowski, J. and Chiu, T. H. (1971). Cholinergic receptor molecules and cholinesterase molecules at skeletal muscle junctions. Nature. **234**, 207-209.

Bayne, E.K., Anderson, M.J. and Fambrough, D.M. (1984). Extracellular matrix organisation in developing muscle: correlation with acetylcholine receptors. J. Cell. Biol. **99**, 1486-1501.

Bazelyansky, M., Robey, E. and Kirsch, J. F. (1986). Biochemistry **25**, 125-130.

Berry, W. K. (1951). The turnover number of cholinesterase. Biochem. Journal. 49, 615-620.

Berry, W.K. and Davies, D.R. (1970). The use of carbamates and atropine in the protection of animals against poisoning by 1,2,2-trimethylpropyl methylphosphonofluoridate. Biochem. Pharamacol. **19**, 927-934.

Betz, W. and Sakmann, B. (1973). Effects of proteolytic enzymes on function and structure of frog neuromuscular junctions. J. Physiol. (Lond.). **230**, 673-688.

Blaber, L.C. and Christ, D.D. (1967). The action of facilitatory drugs on the isolated tenuissimus muscle of the cat. Int. J. Neuropharmacol. **6**, 473-484.

Bon, S., Huet, M., Lemonnier, M., Reiger, F. and Massoulie, J. (1976). Molecular forms of electrophorous acetylcholinesterase: Molecular weight and composition. Eur. J. Biochem. **68**, 523-530.

Bon, S. and Massoulie, J (1978). Collagenase activity and aggregation properties of electrophorous acetylcholinesterase. Eur. J. Biochem. **89**, 89-94.

Bon, S. and Massoulie, J. (1980). Collegen-tailed and hydrophobic components of acetylcholinesterase in *Torpedo marmorata* electric organ. Proc. Natl. Acad. Sci. USA. 77, 4464-4468.

Bon, S., Vigny, M. and Massoulie, J. (1979). Asymmetric and globular forms of acetylcholinesterase in mammals and birds. Proc. Natl. Acad. Sci. USA. **76**, 2546-2550.

Bouma, S.R., Drislane, F.W. and Huestis, W.H (1977). Selective extraction of membrane-bound proteins by phospholipid vesicles. J. Biol. Chem. **252**, 6759-6763.

Bowden, R. E. M. and Duchen, L. W. (1976). The anatomy and pathology of the meuromuscular junction. In: Zaimis, W. (ed.) Neuromuscular Junction. Handbook of Experimental Pharmacology. Vol. 42. Berlin, Springer-Verlag. 23-97.

Boyd, I.A. and Martin, A.R. (1956). Spontaneous subthreshold activity at mammalian neuromuscular junctions. J. Physiol. **132**, 61-73.

Bradley, W.G. and Fulthorpe, J.J. (1978). Studies of sarcolemmal integrity in myopathc muscle. Neurology. **28**, 670-677.

Brank, M. and Grubic, Z. (1993). The influence of chronic treatment with dexamethasone on the acetylcholinesterase activity in rat skeletal muscle. Chem. Biol. Interac. **87**, 249-252.

Braughler, J.M., Duncan, L.A. and Goodman, T. (1985). Calcium enhances *in vitro* free radical-induced damage to brain synaptosomes, mitochondria and cultured spinal cord neurons. J. Neurochem. **45**, 1288-1293.

Bright, J.E., Inns, R.H., Tuckwell, N.J. Griffiths, G.D. and Marrs, T.C. (1991). A histochemical study of changes observed in the mouse diaphragm after organophosphate poisoning. Human and Exp. Toxicol. **10**, 9-14.

Brimijoin, S. (1983). Molecular forms of acetylcholinesterase in brain, nerve, and muscle: Nature, localization, and dynamics. Prog. Neurobiol. **21**, 291-322.

Brimijoin, S., Skau, K. and Weirman, M.J. (1978). On the origin and fate of external acetylcholinesterase in peripheral nerves. J. Physiol. **285**, 143-158.

Brimijoin, S. and Weirman, M.J. (1978). Rapid orthograde and retrograde axonal transport of acetylcholinesterase as characterised by the step-flow technique. J. Physiol. (Lond). **285**, 129-142.

Brockman, S.K., Przybylski, R.J. and Younkin, S.G. (1982). Cellular localization of the molecular forms of acetylcholinesterase in cultured embryonic rat myotubes. J. Neurosci. **2**, 1775-1785.

Brockman, S.K., Usiak, M.F. and Younkin, S.G. (1986). Assembly of monomeric acetylcholinesterase into tetrameric and asymmetric forms. J. Biol. Chem. **261**, 1201-1207.

Brzin, M., Sketelj, J., Tennyson, V.M., Kiauta, T. and Budininkas-Schoenebeck, M. (1981). Activity, molecular forms and cytochemistry of cholinesterases in developing rat diaphragm. Muscle and Nerve, **6**, 505-513.

Buckingham, M.E., Alonso, S., Barton, P., Buquaisky, G., Cohen, A., Daubas, P., Garner, I., Minty, A., Robert, B. and Weydert, A. (1984). Actin and myosin genes, and their expression during myogenesis in the mouse. In Davidson, E.H, Firtel, R.A. (eds): "Molecular Biology of Development." Alan R. Liss, Inc. 275-292.

Burd, P.F. and Ferry, C.B. (1987). A prolonged contraction at the endplate region of the diaphragm of rats and mice after anticholinesterases *in vitro.* J. Physiol. **391**, 429-440.

Burd, P.F., Ferry, C.B. and Smith, J.W. (1989). Accumulation of extracellular calcium at the endplate of mouse diaphragm after ecothiopate *in vitro.* Br. J. Pharmacol. **98**, 243-251.

Cabezas-Herrera, J., Campoy, F.J. and Vidal, C.J. (1993). Molecular forms of acetylcholinesterase in microsmal membranes of normal and dystrophic muscle. Biochem. Soc. Trans. **21**, 108S.

Carafoli, E. and Zurini, M. (1982). The Ca^{2+} pumping ATPase of plasma membranes. Biochem. Biophys. Acta. **683**, 279-301.

Carson, S., Bon, S., Vigny, M., Massoulie, J. and Fardeau, M. (1979). Distribution of acetylcholinesterase molecular forms in neural and non-neural sections of human muscle. FEBS Lett. **97**, 348-352.

Cartaud, J. and Changeux, J-P. (1993). Post-transcriptional compartentalization of acetylcholine receptor biosynthesis in the subneural domain of muscle and electrocyte junctions. Euro. J. of Neurosci. **5**, 191-202.

Chandler, W. K., Rakowski, R. F. and Schneider, M. F. (1976). A non-linear voltage dependent charge movement in frog skeletal muscle. J. Physiol. (Lond.). **254**, 254-283.

Chang, C.C., Chen, T.F. and Chuang, S. (1973). Influence of chronic neostigmine treatment on the number of acetylcholine receptors and the release of acetylcholine from the rat diaphragm. J. Physiol. **230**, 613-618.

Cohen, J. B., Oosterbaan, R. A. and Warring, P. J. (1955). The turnover number of ali-esterase, pseudo- and true-cholinesterase and the combination of these enzymes with diisopropylfluorophosphate. Biochemica et Biophysica Acta. **18**, 228-235.

Collins, P.L. and Younkin, S.G. (1982). Effect of denervation on the molecular forms of acetychlinesterase in rat diaphragm. J. Biol. Chem. **257**, 13638-13644.

Csillik, B. and Knyihar, E. (1968). On the effect of motor nerve degeneration on the fine structure localisation of esterases in the mammalian motor endplate. Journal of Cell Science. **3**, 529-538.

Dale, H. H. (1914). The action of certain esters and ethers of choline and their relation to muscarine. J. of Pharma. and Exp. Thera. **6**, 147-190.

Das, S. (1989). Mechanisms of anticholinesterase induced myopathy and its prevention. PhD Thesis. Univeristy of Aston in Birmingham.

Davey, B., Younkin, L.H. and Younkin, S.G. (1979). Neural control of skeletal muscle cholinesterase: a study using organ cultured. J. Physiol. **288**, 501.

Davis, R. and Koelle, G.B. (1978). Electron microscope localisation of acetylcholinesterase in the superior cervical ganglion of the cat: I. Normal ganglion. J. Cell. Biol. **78**, 785-809.

Dayton, W.R., Revile, W.J. Goll, D.E. and Stromer, M.H. (1976). A Ca^{2+}-activated protease possibly involved in myofibrillar protein turnover, partial characterisation of the purified enzyme. Biochem. **15**, 2159-2167

De Clemont (1854). Chimie organique note sur la preparation de quelques ethers. C. R. Acad. Sci. (Paris). **39**, 338-341.

Deprez, P.N. and Inestrosa, N.C. (1995). Two heparin-binding domains are present on the collagenic tail of asymmetric acetylcholinesterase. J. Biol Chem. **270**, 11043-11046.

Devreotes, P.N. and Fambrough, D.M. (1976). Turnover of acetylcholine receptors in skeletal muscle. Cold Spring Harbor Symp. Quant. Biol. **40**, 237-251.

DiGiamberardine, L. and Couraud, J.Y. (1978). Rapid accumulation of high molecular weight acetylcholinesterase in transected sciatic nerve. Nature. **271**, 170-172.

Dirnhuber, P., French, M. C., Green, D. M., Leadbeater, L. and Stratton, J. A. (1979). The protection of primates against soman poisoning by pretreatment with pyridostigmine. J. Pharm. Pharmacol. **31**, 295-299.

Dirnhuber, P. and Green, D. M. (1978). Effectiveness of pyridostigmine in reversing neuromuscular blockade produced by soman. J. Pharm. Pharmac. **30**, 419-425.

Doctor, B. P., Raveh, L., Wolfe, A. D., Maxwell, D. M., and Ashani, Y. (1991). Enzymes as pretreatment drugs for organophosphate toxicity. Neurosci. Behav. Rev. **15**, 123-128.

Donoso, J.A. and Fernandez, H.L (1985). Cellular localization of cytochemically stained acetylcholinesterase activity in adult rat skeletal muscle. J. Neurocytology. **14**, 795-808.

Drachman, D.B. (1972). Neurotrophic regulation of muscle cholinesterase: effects of botulinum toxin and denervation. J. Physiol. **226**, 619-627.

Drachman, D. B. (1976). Trophic interactions between nerves and muscles: the role of cholinergic transmission (including usage) and other factors. In: Goldberg, A. M. and Hanin, I. (ed.) Biology of Cholinergic Function. New York, Raven Press. 162-201.

Drachman, D.B., Stanley, E.F., Pestronk, A., Griffin, J.W. and Price, D.L. (1982). Neurotrophic regulation of two properties of skeletal muscle by impulse-dependent and spontaneous acetylcholine transmission. J. Neurosci. **2**, 232-243.

Dudai, Y., Herzberg, M. and Silman, I. (1973). Molecular structures of acetylcholinesterase from electric organ tissue of the electric eel. Proc. Natl. Acad. Sci. USA. **70**, 2473-2476.

Duncan, C. J. (1987). Role of calcium in triggering rapid ultra-structural damage in muscle. A study with chemically skinned fibres. J. Cell Science. **87**, 581-594.

Duncan, C. J. and Griffith, J. (1992). Screening of agricultural workers for exposure to anticholinesterases. In : "Clinical & Experimental Otoxicity of Organophosphates and Carbamates." Ballantyne, B. and Marrs, T.C. (eds). Butterworth-Heinemann. 412-429.

Duncan, C. J. and Smith, J. L. (1980). Action of caffeine in initiating myofilament degredation and subdivision of mitochondria in mammalian skeletal muscle. Comp. Biochem. Physiol. **65c**, 143-145.

Duncan, C. J., Smith, J. L. and Greenway, H. C. (1979). Failure to protect frog skeletal muscle from ionophore-induced damage by the use of the protease inhibitor leupeptin. Comp. Biochem. Physiol. **63c**, 205-207.

Dutta-Choudhury, T.A. and Rosenberry, T.L. (1984). Human erythrocyte acetylcholinesterase is an amphipathic whose short membrane-binding domain is removed by papain digestion. J. Biol. Chem. **259**, 5653-5660.

Ecobichon, D. J., and Comeau, A. M. (1972). Pseudocholinesterase of mammalian plasma: Physiochemical properties and organophosphate inhibition in eleven species. Toxicol. Appl. Pharmacol. **24**, 92-100.

Ekstrom, T.J., Klump, W.M., Getman, D., Karin, M. and Taylor, P. (1993). Promotor elements and transcriptional regulation of the AchE gene. DNA & Cell Biol. **12**, 63-72.

Ellin, R.I. and Kaminskis, A. (1989). Carbamoylated enzyme reversal as a means of predicting pyridostigmine protection against soman. J. Pharm. Pharmacol. **41**, 633-635.

Ellman, G. L., Courtney, K. D., Andres, V. (1961). A new and rapid colorimetric determination of acetylcholinesterase activity. Biochem. Pharmacol. **7**, 88-95.

Endo, M. (1977). Calcium release from sarcoplasmic reticulum. Physiol. Rev. **57**, 71-108.

Evans, R. H. (1974). The entry of labelled calcium into the innervated regions of the mouse diaphragm. J. Physiol. **240**, 517-533.

Fabiato, A. (1982). Calcium release in skinned cardiac cells: variations with species, tissues and development. Fed. Proc. **41**, 2238-2244.

Fambrough, D.M. and Hartzell, H.C. (1972). Acetylcholine receptors: number and distribution at neuromuscular junctions of rat diaphragm. Science. **176**, 189-191.

Fambrough, D.M., Engel, A.G. and Rosenberry, T.L. (1982). Acetylcholinesterase of human erythrocytes and neuromuscular junctions: Homologies revealed by monoclonal antibodies. Proc. Natl. Acad. Sci. UAS. **79**, 1078-1082.

Fatt, P., Katz., B. (1950). Some observations on biological noise. Nature. **166**, 597-598.

Fatt., P., Katz, B. (1952). Sponteneous subthreshold activity at motor nerve endings. J. Physiol. **117**, 109-128.

Fenichel, G. M., Dettbarn, W. D. and Newman, T. M. (1974). An experimental myopathy secondary to excessive acetylcholine release. Neurology. **24**, 41-45.

Fenichel, G. M., Kibler, W. B., Olson, W. H. and Dettbarn, W. D. (1972). Chronic inhibition of cholinesterase as a cause of myopathy. Neurology. **22**, 1026-1033.

Fernandez, H.L. and Duel, M.J. (1980). Protease inhibitors reduce effects of denervation on muscle endplate acetylcholinesterase. J. Neurochem. **35**, 1166-1171.

Fernandez, H.L., Duel, M.J. and Festoff, B.W. (1979a). Cellular distribution of 16S acetylcholinesterase. J. Neurochem. **32**, 581-585.

Fernandez, H.L., Duel, M.J. and Festoff, B.W. (1979b). Neurotrophic control of 16S acetylcholinesterase at the vertebrate neuromuscular junction. J. Neurobiol. **10**, 441-454.

Fernandez, H.L. and Inestrosa, N.C. (1976). Role of axoplasmic transport in neurotrophic regulation of muscle endplate acetylcholinesterase. Nature. **262**, 55-56.

Fernandez, H.L., Patterson, M.R. and Duel, M.J. (1980). Neurotrophic control of 16S acetylcholinesterase from mammalian skeletal muscle in organ culture. J. Neurobiol. **11**, 557-570.

Fernandez, H. L., Stiles, J. R. (1984). Intra- versus extracellular recovery of 16S acetylcholinesterase following organophosphate inactivation in the rat. Neuroscience Lett. **49**, 117-122.

Ferry, C.B. and Cullen, M.J. (1991). Myopathic changes in indirectly stimulated mouse diaphragm after ecothiopate *in vitro*. Int. J. Exp. Path. **72**, 329-343.

Fertuck, H.C. and Salpeter, M.M. (1976). Quantitation of junctional and extrajunctional acetylcholine receptors by electron microscope autoradiography after 125I-bungarotoxin binding at mouse neuromuscular junctions. J. Cell. Biol. **69**, 144-158.

Flanagan, M.T., Hesketh, T.R. and Chung, S.H. (1974). Procion yellow N-4RS binding to neuronal membranes. J. Histochem. Cytochem. **22**, 952-961.

French, M. C., Wetherell, J. R. and White, D. T. (1979). The reversal by pyridostigmine of neuromuscular block produced by soman. J. Pharm. Pharmacol. **31**, 290-294.

Froehner, S.C. (1991). The submembrane machinery for nicotinic acetylcholine receptor clustering. J. Cell Biol. **114**, 1-7.

Futerman, A.H., Fiorini, R.M., Roth, E., Michaelson, D.M., Low, M.G. and Silman, I (1984). Solubilisation of membrane-bound acetylcholinesterase by phosphatidylinositol-specific phospholipase C: Enzymatic and physiochemical studies. In Brzin, M., Barnard, E., Sket, D. (eds): "Cholinesterases: Fundamental and Applied Aspects." Berlin: Walter deGruyter.

Gibney, G., Camp, S., Dionne, M., MacPhee-Quigley, K. and Taylor, P. (1990). Mutagenesis of essential functional residues in AChE activity. PNAS. **87**, 7546-75550.

Gisiger, V. and Vigny, M. (1977). A specific form of acetylcholinesterase is secreted by rat sympathetic ganglia. FEBS. Lett. **84**, 253-256.

Gerard, K.W. and Schneider, D.L. (1979). Evidence for degradation of myofibrilar proteins in lysosomes. J. Biol. Chem. **254**, 11798-11805.

Getman, D.K., Eubanks, J.H., Camp, S., Evans, G.A. and Taylor, L. (1992). The human gene encoding acetylcholinesterase is located on the long arm of chromosome 7. Amer. J. Hum. Gen. **51**, 170-177.

Gordon, J. J., Leadbeater, L. and Maidment, M. P. (1978). Protection of animals against organophosphate poisoning by pretreatment with a carbamate. Toxicol. App. Pharmaco. **43**, 207-216.

Goudou, D. and Reiger, F. (1983). Recovery of acetylcholinesterase and its multiple molecular forms in motor endplate-free and motor endplate-rich regions of mouse striated muscle after irreversible inactivation by an organophosphate compound (Methyl-phosphorothiolate derivative). Biol. Cell. **48**, 151-158.

Grassi, J., Vigny, M. and Masoulie, J. (1981). Molecular forms of acetylcholinesterase in bovine caudate nucleaus and superior cervical ganglion: Solubility properties and hydrophobic character. J. Neurochem. **38**, 457-469.

Greenfield, S.A. (1984). Aceylcholinesterase may have novel functions in the brain. Trends Neurosci. **7**, 364-368.

Greenfield, S.A. (1992). Acetylcholinesterase as a modulatory neuroprotein and and its influence on motor control. In: Shafferman, A., Velan, B. (eds). Multidisciplinary approaches to cholinesterase functions. Plenum Press, New York, pp 233-242.

Grubic, Z., Sketelj, J., Klinar, B., Brzin, M. (1981). Recovery of acetylcholinesterase in the diaphragm, brain and plasma of the rat after irreversible inhibition by soman: a study of cytochemical localization and molecular forms of the enzyme in the motor endplate. J. Neurochem. **37**, 909-916.

Gupta, R. C., Patterson, G. T. and Dettbarn, W. D. (1987a). Acute tabun toxicity: Biochemical and histochemical consequences in brain and skeletal muscles of rat. Toxicol. **46**, 329-341.

Gupta, R. C., Patterson, G. T. and Dettbarn, W. D. (1987b). Biochemical and histochemical alteration following acute soman intoxication in the rat. Toxicol. APP. Pharm. **81**, 393-402.

Gupta, R. C., Patterson, G. T. and Dettbarn, W. D. (1985). Mechansims involved in the development of tolerence to DFP toxicity. Fund. Appl. Toxicol. **5**, S17-S28.

Guth, L. (1968). 'Trophic' influences of nerve on muscle. Physiological Reviews. **48**, 645-687.

Guth, L. (1969). Effect of immobilisation on sole-plate and background cholinesterase of rat skeletal muscle. Exp. Neurol. **24**, 508-513.

Guth, L. and Zalewski, A.A. (1963). Disposition of cholinesterase following implantations of nerve into innervated and denervated muscle. Exp. Neurol. **7**, 316-326.

Haas, R., Brandt, P.T., Knight, J. and Rosenberry, T.L. (1986). Identification of amine components in a glycolipid membrane-binding domain at the C-terminus of human erythrocyte acetylcholinesterase. Biochemistry. **25**, 3098-3104.

Hall, Z. W. (1973). Multiple forms of acetylcholinestase and their distribution in the endplate and non-endplate regions of rat diaphragm muscle. J. Neurobiol. **4**, No. 4, 343-361.

Hall, Z. W. and Kelly, R. B. (1971). Enzymatic detachment of endplate acetylcholinesterase from muscle. Nature, New Biology. 237, 62.

Hall, Z.W. and Sanes, J.R. (1993). Synaptic structure and development: The neuromuscular junction. Cell. **72**, (suppl.), 99-121.

Hand, D. and Haynes, L.W. (1992). Anchorage of asymmteric acetylcholinesterase by isodipepetide crosslinking in muscle cell. Biochem. Soc. Trans. **20**, 158S.

Haynes, L. W. and Smith, M. E. (1982). Selective inhibition of 'motor endplate' specific acetylcholineserase by ß-endorphin and related peptides. Neuroscience **7**, No.4, 1007-1013.

Haynes, L.W. and Smith, M.E. (1984). The actions of propiomelanocortin peptides at the developing neuromuscular junction. TiPs. **5**, 165-168.

Haynes, L.W. and Smith, M.E. (1985). Induction of endplate-specific acetylcholinesterase by ß-endorphin C-terminal dipeptide in rat and chick muscle cells. Biochem. Soc. Trans. 609th Meeting. 13, 174

Haynes, L.W., Smith, M.E. and Smyth, D.G. (1984). evidence for the neurotrophic regulation of collagen-tailed acetylcholinesterase in immature skeletal muscle by ß-endorphin. J. Neurochem. **42**, 1542-1551.

Heider, H. and Brodbeck, U. (1992) Monomerisation of tetrameric bovine caudate nucleus acetylcholinesterase. Implications for hydrophobic assembly and membrane anchor attachment site. Biochem. J. **281**, 279-284.

Hobbiger, F. (1976). Pharmacology of acetylcholinesterase drugs. p487-581. In: Handbook of Experimental Pharmacology, 42, Neuromuscular Junction. Ed: Zaimas. E. Publisher: Springer-Verlag, Berlin Heidelburg, NY.

Howl, J. D. and Publicover, S. J. (1987). Induction of myopathy in mammalian skeletal muscle *in vitro* by Bay K 8644. Neurosci. Lett. Suppl. **26**, S32.

Hudson, C. S., Foster, R. E. and Kahng, M. W. (1985). Neuromuscular toxicity of pyridostigmine in the diaphragm, EDL and soleus of rat. Funda. App. Toxicol. **5**, 5260-5269.

Hudson C. S., Foster, R. E. and Kahng, M. W. (1986). Ultrastructural effects of pyridostigmine on the neuromuscular junction in rat diaphragm. Neurotoxicol. **7**, 167-186.

Hudson, C. S., Rash, J. E. Tiedt, T. N. and Albuquerque, E. X. (1978). Neostigmine induced alterations at the mammalian neuromuscular junction. II Ultrastructure. J. Pharmacol. Exp. Ther. **205**, 340-356.

Hutchinson, D.O., Walls, T.J., Nakano, S., Camp, S., Taylor, P., Harper, C.M., Groover, R.V., Peterson, H.A., Jamieson, D.G. and Engel, A.G. (1993). Congenital endplate acetylcholinesterase deficiency. Brain. **116**, 633-653.

Inestrosa, N.C. (1980). Secretion of acetylcholinesterase: Relation to acetylcholine receptor metabolism. Cell. **22**, 595-602.

Inestrosa, N.C. (1984). 16S acetylcholinesterase of the extracellular matrix is assembled within mouse muscle cells in culture. Biochem. J. **217**, 377-381.

Inestrosa, N.C. and Fernandez, H.L. (1976). Muscle enzymatic changes induced by blockage of axoplasmic transport. J. Neurophysiol. **39**, 1236-1245.

Inestrosa, N.C. and Fernandez, H.L. (1977). Is there a correspondence between half-lives of motor endplate acetylcholineserase and junctional acetylcholine receptors? Neurosci. Lett. **5**, 91-93.

Inestrosa, N. C. and Perelman, A. (1989). Distribution and anchoring of molecular forms of acetylcholinesterase. TiPs. **10**, 325-329.

Inestrosa, N., Roberts, W.L., Marshell, T.L. and Rosenberry, T.L. (1987). Acetylcholinesterase from bovine caudate nucleus is attached to membranes by a novel subunit distinct from those of acetylcholinesterase in other tissues. J. Biol. Chem. **262**, 4441-4444.

Inestrosa, N.C., Silberstein, L. and Hall, Z.W. (1982). Association of the synaptic form of acetylcholinesterase with extracellular matrix in cultured mouse muscle cells. Cell. **29**, 71-79.

Jasmin, B.J., Campbell, R.J. and Michel, R.N. (1995). Nerve-dependent regulation of succinate dehydrogenase in junctional and extracjunctional compoartments of rat muscle fibres. J. Physiol. **484.1**, 155-164.

Jimmerson, V.R., Shih, T-M., and Mailman, R. B. (1989). Variability in soman toxicity in the rat: Correlation with biochemical and behavioral measures. Toxicol. **57**, 241-254.

Johnson, C.D. and Russel, R.L. (1975). A rapid, simple radiometric assay for cholinesterase, suitable for multiple determinations. Anal. Biochem. **64**, 229-238.

Kar, N.C. and Pearson, C.M. (1976). A calcium-activated neutral protease in normal and dystrophic human muscle. Clinica. Chimica Acta. **73**, 293-297.

Karalliede, L. and Henry, J.A. (1993). Effects of organophosphates on skeletal muscle. Hum. and Exp. Toxicol. **12**, 289-296.

Karnovsky, M. J. and Roots, L. (1964). A 'direct colouring' thiocholine method for cholinesterases. J. Histochem. Cytochem. **12**, 219-221.

Kasprzak, H. and Salpeter, M.M. (1985). Recovery of acetylcholinesterase at intact neuromuscular junctions after *in vivo* inactivation with diisopropylfluorophosphate. J. Neurosci. **5**, 951-955.

Katz, B. and Thesleff, S. (1957). A study of 'desensitization' produced by acetylcholine at the motor endplate. J. Physiol. (London). 138, 63-80

Kawabuchi, M. (1982). Neostigmine myopathy is a calcium ion-mediated myopathy initially affecting the motor endplate. J. Neuropath. Exp. Neurol. **41**, 298-314.

Kawabuchi, M., Osame, M., Watanabe, S., Igata, A. and Kanaseki, T. (1976). Myopathic changes at the endplate region induced by neostigmine methyl-sulfate. Experientia. **32**, 623-625.

Keeler, J. R., Hurst, C. G., Dunn, M. A. (1991). Pyridostigmine used as a nerve agent pretreatment under wartime conditions. J. Amer. Med. Assos. **266**, 693-695.

Kelly, S. S. (1978). The effect of age on neuromuscular transmission. J. Physiol (Lond.) **274**, 51-62.

Kelly, S.S., Ferry, C.B. and Bamforth, J.P. (1990). The effects of anticholinesterases on the latencies of action potentials in mouse skeletal muscles. Br. J. Pharmacol. **99**, 721-726.

Kerem, A., Kronman, C., Bar-Nun, S., Shafferman, A. and Velan, B. (1993). Interrelations between assembly and secretion of recombinant human acetylcholinesterase. J. Biol. Chem. **268**, 180-184.

Koelle, G. (1963). Cytological distributions and physiological functions of cholinesterase. In: Koelle, G. B (ed.) Cholinesterases and Anticholinesterase Agents. Handbuch der experimentellen Pharmakologie, Vol. XV. Berlin, Springer. 187-298.

Koelle, G. (1988). Enhancement of acetylcholinesterase synthesis by glycyl-L-glutamine: an example of a small peptide that regulates differential transcription. TiPs. **9**, 318-321.

Koelle, G. B., Davis, R. and Gromadzki, C. G. (1967). Electron microscope localisation of cholinesterases activity by means of gold salts. Annals of the New york Acadamy of sciences. **144**, 613-625.

Koelle, G. B. and Friendenwald, J. S. (1949). A histochemical method for localising cholinesterase activity. Proceedings of the Society for Experimental Biology, (NY). **70**, 617-622

Koelle, G.B., Ruch, G.A. Richard, F.F. and Sauville, U.J. (1982). Regeneration of cholinesterases in stellate and normal and denervated superior cervical ganglia of cat following inactivation by sarin. J. Neurochem. **38**, 1695-1698.

Koelle, W.A., Smyrl, E.G., Ruch, G.A., Siddons, V.E. and Koelle, G.B. (1977). Effects of protection of butyrylcholinesterase on regeneration of ganglionic acetylcholinesterase. J. Neurochem. **28**, 307-311.

Koenig, J. and Vigney, M. (1978). neural induction of the 16S acetylcholinesterase in muscle cell cultures. Nature **271**, 75-77.

Knapp, H.R., Oelz, O., Roberts, L.J., Sweetman, B.J., Oates, J.S. amd Reed, P.W. (1977). Ionophores stimulate prostaglandin and thromboxame biosynthesis. Proc. Natl. Acad. Sci. USA. **74**, 4251-4255.

Krejci, E., Coussen, F., Duval, N., Chatel, J-M., Legay, C., Puype, M., Vandekerckhove, J., Cartaud, J., Bon, S. and Massoulies, J. (1991). Primary structure of a collagenic tail peptide of Torpedo acetylcholinesterase: co-expression with catalytic subunit induces the production of collagen-tailed forms in transfected cells. EMBO J. **10**, 1285-1294.

Laskowski, M. B. and Dettbarn W.D. (1977). The pharmacology of experimental myopathies. Annu. Rev. Pharmacol. Toxicol. **17**, 387-409.

Laskowski, M. B., Olson, W. H. and Dettbarn, W. D. (1975). Ultrastructural changes at the motor endplate produced by an irreversible cholinesterase inhibitor. Experimental Neurobiology. **47**, 290-306.

Laskowski, M. B., Olson, W. H. and Dettbarn, W. D (1977). Initial ultrastructural abnormalities at the motor endplate produced by a cholinesterase inhibitor. Experimental Neurobiology. **57**, 13-33.

Lawler, H. C. (1961). Turnover time of acetylcholinesterase. J. of Biol. Chem. **236**, 2296-2301.

Lazar, M., Salmeron, E., Vigny, M. and Massoulie, J. (1984). Heavy isotope labeling study of the metabolism of monomeric and tetrameric acetylcholinesterase forms in the murine neuronal-like T-28 hybrid cell line. J. Biol. Chem. **259**, 3703-3713.

Leadbeater, L., Inns, R. H. and Rylands, J. M. (1985). Treatment of poisoning by soman. Fund. Appli. Toxicol. **5**, S225-S231.

Lee, S.L., Camp, S.J. and Taylor, P. (1982a). Characterisation of a hydrophobic, dimeric form of acetylcholinesterase from Torpedo. J. Biol. Chem. **257**, 12302-12309.

Lee, S.L., Heinemann, S. and Taylor, P. (1982b). Structural characterisation of the asymmetric (17+13)S forms of acetylcholinesterase from *Torpedo*. I. Analysis of subunit composition. J. Biol. Chem. **257**, 12283-12291.

Lee, S.L. and Taylor, P (1982). Structural characterisation of the asymmetric (17+13)S species of acetylcholinesterase from *Torpedo*. II Component peptides obtained by selective proteolysis and disulfide bond reduction. J. Biol. Chem. **257**, 12292-12301.

Leith, E. and Fallon, J.R. (1993). Muscle agrin: neural regulation and localization at nerve-induced acetylcholine receptor clusters. J. Neurosci. **13**, 2509-2514.

Lennox, W. J. , Harris, L. W., Anderson, D. R., Solano, R. P., Murrow, M. L. and Wade, J. V. (1992). Successful pretreatment/therapy of soman, sarin and VX intoxication. Drug. Chem. Toxicol. **15**, 271-283.

Lentz, T.L., Addis, J.S. and Chester, J. (1981). Partial purification and characterization of a nerve trophic factor regulating muscle acetylcholinesterase activity. Expl. Neurol. **73**, 542-557.

Leonard, J. P. and Salpeter, M. M. (1979). Agonist-induced myopathy at the neuromuscular junction is mediated by calcium. J. Cell Biol. **82**, 811-819.

Li, J.B. (1980). Protein synthesis and degradation in skeletal muscle of normal and dystrophic hamsters. Am. J. Physiol. 239 (Endocrinol. Metab. 2). E401-E406.

Li, Y., Camp, S. and Taylor. (1993). Tissue specifc expression and alternative mRNA processing of the mammalian AChE gene. J. Biol. Chem. **268**, 5790-5797.

Li, Y., Camp, S., Rachinsky, T.L., Getman. and Taylor, P. (1991). Gene structure of mammalian acetylcholinesterase. J. Biol. Chem. **266**, 23083-23090.

Li, Z-Y. and Bon, C. (1983). Presence of a membrane-bound acetylcholinesterase form in a preparation of nerve endings from *Torpedo marmorata* electric organ. J. Neurochem. **40**, 338-349.

Linkhart, T.A. and Wilson, B.W. (1975). Appearance of acetylcholinesterase and creatine kinase in plasma of normal chickens after denervation. J. Neurol. Sci. **26**, 193-201.

Lintern, M.C., Smith, M.E. and Ferry, C.B. (1995). The effect of repeated treatment with pyridostigmine on the activity of acetylcholinesterase molecular forms in mouse skeletal muscle. British J. of Pharmacol. **116**, 81P.

Lockbridge, O., Eckerson, H.W. and La Du, B.N. (1979). Interchain disulfide bonds and subunit organisation in human serum cholinesterase. J. Biol. Chem. **254**, 8324-8330.

Lomo, T., Massoulie, J. and Vigny, M. (1985). Stimulation of denervated rat soleus muscle with fast and slow activity patterns induces different expression of acetylcholinesterase molecular forms. J. Neurosci. **5**, 1180-1187.

Lomo, T. and Slater, C.R. (1980a). Control of junctional acetylcholinesterase by neural and muscular influences in the rat. J. Physiol. (Lond). **303**, 191-202.

Lomo, T. and Slater, C.R. (1980b). Acetylcholine sensitivity of developing ectopic nerve-muscle junctional in adult rat soleus muscles. J. Physiol. **303**, 173-189.

Lubinska, L (1966). Influence of denervation on acetylcholinesterase in developing fast and slow muscles of the rat. In "Exploratory Concepts in Muscular Dystrophy and Related disorders," pp 168-175. A.T. Milhorat (ed.) Experta Medica Foundation Amsterdam.

Luo, Z., Fuentes, M. and Taylor, P. (1994). Regulation of acetylcholinesterase mRNA stability by calcium during differentiation from myoblasts to myotubes. J. Biol. Chem. **269**, 27216-27223.

Lwebuga-Mukasa, J.S, Lappi, S. and Taylor P. (1976). Molecular forms of acetylcholinesterase from *Torpedo californica*. Their relationship to synaptic membranes. Biochemistry. **15**, 1425-1434.

MacPhee-Quigley, K., Taylor, P. and Taylor, S. (1985). J. Biol. Chem. **260**, 12185-12189.

Magleby, K.L. and Pallotta, B.S. (1981). A study of desensitization of acetylcholine receptors using nerve-released transmitter in the frog. J. Physiol. (London). **316**, 225-250.

Main, A. R. (1976). Structure and inhibitors of cholinesterase. In: Goldberg, A. M. and Hanin, I. (ed.) Biology of Cholinergic Function. New York, Raven Press. 269-353.

Marney, A. and Nachmansohn, D. (1938). Cholinesterase in voluntary muscle. J. Physiol. **92**, 47-57.

Massoulie, J. (1980). The polymorphism of cholinesterase and its physiological significance. Trends in Biochem. Sci. **5**, 160-164.

Massoulie, J. and Bon, S. (1982). The molecular forms of cholinesterase and acetylcholinesterase in vertebrates. Annu. Rev. Neurosci. **5**, 57-106.

Massoulie, J., Bon, S., Anselmet, A., Chatel., J-M., Cousen, F., Duval, N., Krejci, E., Legay, C. and Vallette, F. (1992). in Multidisciplinary Approaches to cholinesterase Research (Valen, B., and Shafferman, A., eds) pp 17-24, Plenum Publishing Corp., New York.

Massoulie, J., Pezzementi. L., Bon, S., Kreijci, E. and Vallettes, F-M. (1993). Molecular and cell biology of cholinesterases. Prog. Neurobiol. **41**, 31-91.

Massoulie, J. and Reiger, F. (1969). L'acetylcholinesterase des organes electriques de Poisons (torpille et gymnote): complexes membranaires. Eur. J. Biochem. **11**, 441-445.

Massoulie, J., Reiger F. and Bon, S. (1973). Les differentes formes moleculaires de l'acetylcholinesterase. In: La Transmission Cholinergique de l'Excitation. Paris, INSERM. 143-144.

Mays, C. and Rosenberry, T.L. (1981). Characterisation of pepsin-resistent collegen-like tail subunit fragments of 18S and 14S acetylcholinesterase from *Electrophorus electricus*. Biochem. **20**, 2810-2817.

McIssac, R.S. and Koelle, G.B. (1959). Comparison of the effects of inhibition of external, internal, and total acetylcholinesterase upon ganglionic transmission. J. Pharmacol. Exp. Ther. **126**, 9-20.

McMahan, U. J., Edgington, D. R. and Kuffler, D. P. (1980). Factors that influence regeneration of the neuromuscular junction. J. Exp. Biol. **89**, 31-42.

McMahan, U.J., Sanes, J.R. and Marshall, L.M. (1987). Cholinesterase is associated with the basal lamina at the neuromuscular junction. Nature. **271**, 172-174.

Miledi, R., Parker, I. and Schalow, G. (1977). Ca^{2+} entry across the post-junctional membrane during transmitter action. J. Physiol (Lond.). **268**, 32-33.

Merlie, J.P. (1984). Biogenesis of the acetylcholine receptor, a multisubunit integral membrane protein. Cell. **36**, 573-575.

Merlie, J.P. and Lindstrom, J. (1983). Assembly *in vivo* of mouse muscle acetylcholine receptor: Identification of a subunit species that may be an assembly intermediate. Cell. **34**, 747-757.

Merlie, J.P. and Sebbane, R. (1981). Acetylcholine receptor subunits transit a precursor pool before acquiring alpha-bungarotoxin binding activity. J. Biol. Chem. **256**, 3605-3608.

Meshul, C. K., Boyne, A. F., Deshpande, S. S. and Albuquerque, E. X. (1985). Comparison of the ultrastructural myopathy induced by anticholinesterase agents at the end-plates of rat soleus and extensor muscules. Experimental Neurology. **89**, 96-114.

Muller, M. and Renkawitz, R. (1991). The glucocorticoid receptor. Biochem. Biophys. Acta. **1088**, 171-182.

Mutero, A., Camp, S. and Taylor, P. (1995). J. Biol. Chem. **270**, 1866-1872.

Newman, J.R., Virgin, J.B., Younkin, L.H. and Younkin, S.G. (1984). Turnover of acetylcholinesterase in innervated and denervated rat diaphragm. J. Physiol. **352**, 305-318.

Nicolet, N. and Reiger, F. (1981). Molecular forms of frog acetylcholinesterase: effects of denervations. C.R. Seances. Soc. Biol. **175**, 316-322.

Oberc, M.A. and Engel, M.D. (1977). Ultrastructural localisation of calcium in normal and abnormal skeletal muscle. Lab. Invest. **36**, 566-577.

Oh, T.H, Chyu, J.Y. and Max, S.R. (1977). Release of acetylcholinesterase by cultured spinal cord cells. J. Neurobiol. **8**, 469-476.

Oh, T.H., Markelonis, G.J. and Shim, S.H. (1988). Trophic influences of neurogenic substances on skeletal muscle differentiation and growth in vitro. In: "Nerve-muscle cell trophic communication." Fernandez and Douso (eds). 81-99.

Ordentlich, A., Barak, D., Kronman, C., Ariel, N., Segall, Y., Velan, B. and Shafferman, A. (1995). Contribution of aromatic moieties of tyrosine 133 and of the anionic subsite tryptophan 86 to catalytic efficiency and allosteric modulation of acetylcholinesterase. J. Bio. Chem. **270**, 2082-2091.

Ott, P. and Brodbeck, U. (1978). Multiple molecular forms of acetylcholinesterase from human erythrocyte membranes. Eur. J. Biochem. **88**, 119-125.

Ott, P., Jenny, B. and Brodbeck, U. (1975). Multiple forms of purified human erythrocyte acetylcholinesterase. Eur. J. Biochem. **57**, 469-480.

Ott, P., Lustig, A., Brodbeck, U. and Rosenbusch, J. P. (1982). Acetylcholinesterase from human erythrocyte membranes: dimers as functional units. FEBS Lett. **138**, 187-189.

Porter-Jordan, K., Benson, R.J.J., Buoniconti, P. and Fine, R.E. (1986). An acetylcholinesterase-mediated density shift technique demonstrates that coated vesicles from chick myotubles may contain both newly synthesised acetylcholineserase and acetylcholine receptors. J. Neurosci. **6**, 3112-3119.

Randall, W.R., Tsim, K.W.K., Lai, J. and Barnard, E.A. (1987). Monclonal antibodies to purified acetylcholinesterase from chicken brain: Disclosure of two allelic forms of the catalytic subunit. Eur. J. Biochem.**164**, 95-102.

Ranish, N. and Ochs, S. (1972). Fast axoplasmic transport of acetylcholineserase in mammalian nerve fibres. J. Neurochem. **19**, 2641-2649.

Raveh, L., Ashani, Y., Levey, D., De la Hoz, D., Wolfe, A. D., and Doctor, B.P. (1989). Acetylcholinesterase prophylaxis against organophoshate poisoning. Biochem. Pharmacol. **38**, 529-534.

Reiger, F., Faivre-Bauman, A., Benda, P. and Vigny, M. (1976). Molecular forms of acetylcholinesterase: their de novo synthesis in mouse neuroblastoma cell. J. Neurochem, **27**, 1059-1063.

Reiger, F., Koenig, J. and Vigny, M. (1980). Spontaneous contractile activity and the presence of the 16S form of acetylcholinesterase in rat muscle cells in culture. Reversible suppressive action of tetrodotoxin. Dev. Biol. **76**, 358-365.

Reiger, F. and Vigny, M. (1976). Solubilisation and physicochemical characterisation of rat brain acetylcholinesterase: Development and maturation of its molecular forms. J. Neurochem. **27**, 121-129.

Richier, P., Arpagaus, M. and Toutant, J-P. (1992). Glycolipid-anchored acetylcholinesterase from rabbit lymphocytes and erythrocytes differ in their sensitivity to phosphatidylinositol-specific phospholipase C. Biochimica et Biophysica Acta. **1112**, 83-88.

Roberts, W.L., Doctor, B.P., Foster, J.D., and Rosenberry, T.L. (1991). Bovine brain acetylcholinesterase primary sequence involved in intersubunit disulfide linkages. J. Biol. Chem. **266**, 7481-7487.

Rogers, A.W., Darzynkiewicz, A., Ostrowski, K., Salpeter, M.M. and Barnard, E.A. (1969). Quantitative studies on enzymes in structures in striated muscles by labelled inhibitor methods. I. The number of acetylcholinesterase molecules and of other DFP-reactive sites at motor endplates measured by autoradiography. J. Cell Biol. **41**, 655.

Rosenberry, T.L. (1975). Acetylcholinesterase. Adv. Enzymol. **43**, 103-218.

Rosenberry, T.L. (1985). Structural distinctions among acetylcholinesterase forms. Enzymes Biol. Membr. **3**, 403-429.

Rosenberry, T.L. and Richardson, J.M. (1977). Structure of 18S and 14S acetylcholinesterase. Identification of collagen-like subunits that are linked by disulfide bonds to catalytic subunits. Biochemistry. **16**, 3550-3558.

Rosenberry, T.L. and Scoggin, D.M. (1984). Structure of human erythrocyte acetylcholinesterase. Characterisation of intersubunit disulfide bonding and detergent interactions. J. Biol. Chem. **259**, 5463-5652.

Rosenberry, T.L., Scoggin, D.M., Dutta-Choudhury, T.A. and Hass, R. (1984). In "Cholinesterases: Fundamental and Applied Aspects." Berlin: Walter deGruyter.

Rosier, J., French, E.D., Rivier, C., Ling, N., Guillemin, R. and Bloom, F.E. (1977). Foot-shock induced stress increases ß-endorphin levels in blood but not brain. Nature. **270**, 618-620.

Rossi, S.G. and Rotundo, R.L. (1992). Cell surface acetylcholinesterase molecules on multinucleated myotubes are clustered over the nucleus of origin. J. Cell Biol. **119**, 1657-1667.

Rotundo, R.L. (1983). Acetylcholinesterase biosynthesis and transport in tissue culture. Methods in Enzymol. **96**, 353-367.

Rotundo, R. L. (1984a). Asymmetric acetylcholinesterase is assembled in the Golgi apparatus. Proc. Nat. Acad. Sci. USA. **81**, 479-483.

Rotundo, R.L. (1984b). Purification and properties of the membrane bound form of acetylcholinesterase from chicken brain: Evidence for two distinct polypeptide chains. J. Biol. Chem. **259**, 13186-13194.

Rotundo, R.L. (1984c). Synthesis, assembly, and processing of acetylcholinesterase in tissue cultured muscle. In Brzin, M, Barnard, E, Sket, D. (eds): "Cholinesterases: Fundamental and Applied Aspects." Berlin: Walter deGruyter.

Rotundo, R.L. and Fambrough, D.M. (1979). Molecular forms of chicken embryo acetylcholinesterase *in vitro* and *in vivo*: Isolation and characterisation. J. Biol. Chem. **254**, 4790-4799.

Rotundo, R.L. and Fambrough, D.M. (1980a). Synthesis, transport, and fate of acetylcholinesterase in cultured chick embryo muscle cultures. Cell. **22**, 583-594.

Rotundo, R. L. and Fambrough, D. M. (1980b). Secretion of acetylcholinesterase: Relation to acetylcholine receptor metabolism. Cell. **22**, 595-602.

Rubenstein, N., Mabuchi, K., Pope, F., Salmons, S., Gergely, S. and Sreter, F. (1978). The use of specific anti-myosins to demonstrate the transformation of individual fibers in chronically stimulated rabbit fast muscle. J. Cell. Biol. **79**, 252-261.

Rubin, L.L. (1985). Increases in muscle Ca^{2+} mediate changes in acetylcholinesterase and acetylcholine receptors caused by muscle contraction. Proc. Natl. Acad. Sci. USA. 82, 7121-7145

Rubin, L.L., Schuetze, S.M.,Weill, C.L. and Fischbach, G.D. (1980). Regulation of acetylcholinesterase appearance at neuromuscular junctions *in vitro*. Nature. **283**, 264-267.

Rudge, M. F. and Duncan, C. J. (1984). Cooparative studies on the calcium paradox in cardiac muscle: the effect of temperature on the different phases. Cop. Biochem. Physiol. **79a**, 393-398.

Salmons, S. and Sreter, F.A. (1976). Significance of impulse activity in the transformation of skeletal muscle type. Nature, **263**, 30-34.

Salpeter, M. M (1967). Electronmicroscope autoradiography as a quantitative tool in enzyme cytochemistry. I. the distribution of acetylcholinesterase at motor endplates of a verebrate twitch muscle. J. of Cell Biol. **32**, 379-389.

Salpeter, M. M. (1969). Electronmicroscope autoradiography as a quantitative tool in enzyme cytochemistry. II. The distribution of DFP-reactive sites at motor endplates of a verebrate twitch muscle. J. of Cell Biol. **42**, 122-134.

Salpeter, M., Kasprzak, H., Feng, H. and Fertuk, H. (1979). Endplates after esterase inactivation *in vivo* : correlation between esterase concentration, functional response and fine structure. J. Neurocytol. **8**, 95-115.

Salpeter, M.M., Rogers, A.W., Kasprzak, H. and McHenry, F.A. (1978). Acetylcholinesterase in the fast extraocular muscle of the mouse by light and electron microscope autoradiography. J. Cell. Biol. **78**, 274-285.

Sawyer, H.R., Golder, T.K., Nieberg, P.S. and Wilson, B.W. (1976). Ultrastructural localization of AChE in cultured cells. I: Embryo muscle. J. Histochem. Cytochem. **24**, 969-978.

Schaumann, W. and Job, C. (1958). Differential effects of quaternary cholinesterase inhibitor, phospholine and its tertiary analogue, compound 217-AO, on central control of respiration and on neuromuscular transmission. The antagonism by 217-AO of the respiratory arrest caused by morphine. J. Pharmacol. Exp. Ther. **123**, 114-120.

Schneider, M. F. (1986). Voltage-dependent mobilisation of intracellular calcium in skeletal muscle. In 'Calcium and the Cell'. (Ciba Foundation Symposium, 122) 23-38. John Wiley and Sons (U.K.)

Schrader, G. (1952). Die entuicklung never insectizide auf. Grundlage von organischem flour-und phosphorverbindungen. Monographie No.62,2,Aufl, Verlagchemie Weinheim 1.

Schumacher,M., Camp,S., Maulet,Y., Newton,M., MacPee-Quigly, K., Taylor,S.S., Friedmann,T. and Taylor,P.(1986) Primary structure of Torpedo californica AChE deduced from its cDNA sequence.Nature.**319**,407-409.

Schumacher, M.,Maulet, Y., Camp, S. and Taylor, P.(1988). Multiple messenger RNA species give rise to structural diversity in AChE. J. Biol. Chem. **263**, 18979-18987.

Seigel, S. and Castellan, N.J. (1988). Non-parametric statistics for behavioral sciences. 2nd Ed. McGraw-Hill Book Company.

Shafferman, A., Kronman, C., Flashner, Y., Leitner, M., Grosfeld, H., Ordentlich., Gozes, Y., Cohen, S., Ariel., Barak, D, Harel, M., Silman, I., Sussman, J.L. and Velan, B. (1992). Mutagenesis of human acetylcholinesterase. J. Biol. Chem. **267**, 17640-17648.

Sikorav, J.L., Grassi, J. and Bon, S. (1984). Synthesis in vitro of precursors of the catalytic subunits of acetylcholinesterase from Torpedo marmorata and Electrophorus electricus. Eur. J. Biochem. **145**, 519-524.

Silman, I., DiGamberardino, L., Lyles, J., Conrand, J.Y. and Barnard, E.A. (1979). Parallel regulation of acetylcholineserase and pseudocholinesterase in normal, denervated, and dystrophic chicken skeletal muscle. Nature. **280**, 160-162.

Sketelj, J. and Brzin, M. (1985). Asymmetric molecular forms of acetylcholinesterase in mammalian skeletal muscles. Journal of Neuroscience Reasearch. 14, 95-103.

Sketelj, J., McNamee, M.G. and Wilson, B.W. (1978). Effect of denervation on the molecular forms of acetylcholinesterase in normal and dystrophic chicken muscles. Exp. Neurol. **60**, 624-629.

Small, D.H. (1989). Acetylcholinesterase: zymogens of neuropeptide processing enzymes? Neuroscience. **2**, 241-249.

Soreq, H., Zevin-Sonkin, D. and Razon, N. (1984). Expression of cholinesterase gene (s) in human brain tissues: translational evidence for multiple mRNA species. EMBO J. **3**, 1371.

Sussman, J.L., Harel, M., Frolow, F., Oefner, C., Goldman, A., Toker, L. and Silman, I. (1991). Atomic structure of acetylcholinesterase from Torpedo califirnica: a prototypic acetylcholine-binding protein. Science. **253**, 872-879.

Sveistrup, H., Chan, R.Y. and Jasmin, B.J. (1995). Chronic enhancement of neuromuscular activity increases acetylcholinesterase gene expression in skeletal muscle. Am. J. Physiol. (Cell Physiol. 38), C856-C862.

Takeuchi, N. (1963). Some properties of conductance changes at the endplate membrane during the action of acetylcholine. J. Physiol. (Lond.) **167**, 128-140.

Taylor, P. and Radic, Z. (1994). The cholinesterases: from genes to proteins. Annu. Rev. Pharmacol. Toxicol. 34, 281-320.

Tennyson, V.M., Brzin, M. and Kremzner, L.T. (1973). Acetylcholinesterase activity in the myotube and muscle satallite cell of the fetal rabbit. An electron microscopic, cytochemical and biochemical study. J. Histochem. Cytochem. **21**, 634-652.

Teravainen, H. (1967). Electron microscopic localisation of cholinesterases in the rat myoneural junction. Histochemie. **10**, 266-271.

Tiedt, T.N., Albuquerque, C. S. Hudson, C. S. and Rash, J. E. (1978). Neostigmine-induced alterations at the mammalian neuromuscular junction. I. Muscle contraction and electrophysiology. J. Pharm. Exp. Thera. **205**, 326-339.

Torres, J.C., Behrens, M.I and Inestrosa, N.C. (1983). Neural 16S acetylcholinesterase is solubilized by heparin. Biochem. J. **215**, 201-204.

Torres, J.C. and Inestrosa, N.C. (1983). Heparin solubilzes asymmetric acetylcholinesterase from rat neuromuscular junction. FEBS. Lett. **154**, 265-268.

Townsend, H. (1988). The toxic effects of anticholinesterases on muscle. PhD Thesis, University of Aston in Birmingham.

Tsim, K.W.K., Greenberg, I., Rimer, M., Randall, W.R. and Salpeter., M.M. (1992). Transcripts for AChR and AChE show distribution differences in cultured muscle cells. J. Chem. Biol. **118**, 1201-1212.

Tsuji, S., Reiger F. and Peltre, G. (1973). La localisation immunologique de l'acetylcholinesterase. In: La Transmission Cholinergique de l'excitation. Paris, INSERM. 129-130.

Velan, B., Grosfeld, H., Kronman, C., Leitner, M., Gozes, Y., Lazar, A., Flashner, Y., Marcus, D., Cohen, S. and Shafferman, A. (1991). The effect of elimination of intersubunit disulfide bonds on the activity, assembly and secretion of recombinant human acetylcholinesterase. Expression of acetylcholinesterase cys-580-Ala mutant. J. Biol. Chem. **266**, 23977-23984.

Vallette-F-M., De La Porte, S., Koenig, J., Massoulie, J. and Vigny, M (1990). Acetylcholinesterase in cocultures of rat myotubes and spinal cord neurons: effects of collagenase and cis-hydroxyproine on molecular forms, intra- and extracellular distribution, and formation of patches at neuromuscular contacts. J. Neurochem. **54**, 915-923.

Van Dongen, C. J., Valkenburg, P. W. and Van Helden, H. P. (1988). Contribution of de novo synthesis of acetylcholinesterase to spontaneous recovery of neuromuscular transmission following soman intoxication. J. Pharmacol. **149**, 381-384.

Van Dongen, C.J. and Wolthuis, O.L. (1989). On the development of behavioral tolerance to organophosphates I: Behavioural and biochemical aspects. Pharmacol Biochem and Behav. **34**, 473-481.

Vigny, M., Gisiger, V. and Massoulie, J. (1978). "Nonspecific" cholinesterase and acetylcholinesterase in rat tissues: molecular forms, structural and catalytic properties and significance of the two enzyme systems. Proc. Natl. Acad. Sci. USA. **75**, 2588-2592.

Viratelle, O.M. and Bernhard, S.A. (1980). Major component of acetylcholinesterase in *Torpedo* electroplax is not basal lamina associated. Biochemistry. **19**, 4999-5007.

von Bredow, J., Corcoron, K., Maitland, G., Kaminskis, A., Adams, N. and Wade, J. (1991). Efficacy of physostigmine and anticholinergic adjucts as a pre-treatment for nerve agent intoxication. Fund. Appl. Toxicol. **17**, 782-789.

Wake, K. (1976). Formation of myoneural and myotendenous junctions in the chick embryo. Cell. Tissue. Res. 173, 383-400.

Wallace, B.G. (1989). Agrin-induced specializations contain cytoplasmic, membrane, and extracellular matrix-associated components of the postsynaptic apparatus. J. Neurosci. **9**, 1294-1302.

Wallace, B. and Gillon, J.W. (1982). Characterisation of acetylcholinesterase in individual neurons in the leech central nervous system. J. Neurosci. **2**, 1106-1118.

Walker, C.R. and Wilson, B.W. (1976). Regulation of acetylcholinesterase in chick muscle cultures after treatment with diisopropylphosphoro-fluoridate: Ribonuscleic acid and protein synthesis. Neuroscience. **1**, 509-513.

Waser, P. G. and Reller, J. (1965). Bestimmung der Zahl aktiver Zentren der Acetylcholinesterse in motorischen Endplatten. Experimentia. **21**, 402-403.

Wecker, L., Laskowski, M. B. and Dettbarn, W. D. (1978a). Neuromuscular disfunction induced by acetylcholinesterase inhibition. Animal Models in Neuromuscular Diseases. Fed. Proc. Vol. 37, No. 14.

Wecker, L., Kiautu, T. and Dettbarn, W. D. (1978b). Relationships between acetylcholinesterase inhibition and the development of myopathy. J Pharmacol. Expt. Therp. 97-104.

Weeds, A.G., Trentham, D.R., Kean, C.J.C. and Buller, A.J. (1974). Myosin from cross-reinnervated cat muscle. Nature, **247**, 135-139.

Wetherell, J. (1994). Continuous administration of low dose rate of physostigmine and hyosine to guinea-pigs prevents the toxicity and reduced the incapitation produced by soman poisoning. J. Pharm. Pharmacol. **46**, 1023-1028.

Wetherell, J. and French, M.C. (1985). The hydrolysis of succinyldithiocholine and related thiocholine esters by human plasma and purified cholinesterase. Biochem. Pharmacol. **35**, 939-945.

Weinberg, C.B and Hall, Z.W. (1979). Junctional forms of acetylcholinesterase restored at nerve-free endplates. Dev. Biol. **68**, 631-635.

Weinberg, C.B., Sanes, J.R. and Hall, Z.W. (1981). Formation of neuromuscular junctions in adult rats: Accumulation of acetylcholine receptors, acetylcholinesterase, and components of synaptic basal lamina. Dev. Biol. **84**, 255-266.

Wills, J. H. (1972). The measurement of significance of changes in the cholinesterase activities of erythrocytes and plasma in man and animals. Crit Rev. Toxicol. **1**, 153-201.

Wilson, I. B. (1971). The possibility of conformational changes in acetylcholinesterase. In: Triggle, D. J., Moran, J. F. and Barnard, E. A. (ed.) Cholinergic Ligand Interactions. New York, Academic Press.

Wilson, I. B. and Harrison, M. A. (1961). Turnover number of acetylcholinesterase from human erythrocytes. J. of Biol. Chem. **236**, 2292-2295.

Wilson, I. B., Harrison, M. A. and Ginsburg, S. (1960). Carbamyl derivatives of acetylcholinesterase. J. Biol. Chem. **236**, 1498-1500.

Wilson, B.W., Neiberg, P.S., Walker, C.R., Linkhart, T.A. and Fry, D.M. (1973). Production and release of acetylcholinesterase by cultured chick embryo muscle. Dev. Biol. **33**, 285-299.

Wilson, B.W. and Walker, C.R. (1974). Regulation of newly synthesised acetylcholinesterase in muscle cultures treated with diisopropylflourophosphate. Proc. Natl. Acad. Sci. USA. **71**, 3194-3198.

Wolfe, A. D., Rush, R. S., Doctor, B. P., Koplovitz, I., and Jones, D. (1982). Acetylcholinesterase prophylaxis against organophosphate toxicity. Fundam. Appli. Toxicol. **9**, 266-270.

Wolfgang, W.J. and Forte, W.A. (1989). Expression of acetylcholinesterase during visual system development in Drosophila. Dev. Biol. **131**, 321-330.

Wright, D. L and Plummer, D. T. (1973). Multiple forms of acetylcholinesterase from human erythrocytes. Biochemical Journal. **133**, 521-527.

Wrogemann, K. and Pena, S.D.J. (1976). Mitochondrial calcium overload; A general mechanism for cell necrosis in muscle diseases. Lancet. March, **27**. 672-674.

Younkin, S.G., Brett, R.S., Davy, B. and Younkin, L.H. (1978). Substances moved by axonal transport and released by nerve stimulation have an innervation-like effect on muscle. Science. N.Y. **200**, 1292-1295.

Younkin, S. G., Rosenstein, C., Collins, P. L., Rosenberry, T. L. (1982). Cellular localisation of the molecular forms of acetylcholinesterase in rat diaphragm. J. Biol. Chem. **257**, 13630-13637.

Younkin, S. G and Younkin, L.H. (1988). Trophic regulation of skeletal muscle acetylcholinesterase. In: "Nerve-Muscle Cell Trophic Communication". Fernandez, Douso, (eds). 41-59.